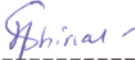


**PHOSPHOACETYLATION OF HISTONES DURING CELLULAR
TRANSFORMATION IN MAMMALIAN CELLS**

Homi Bhabha National Institute

Recommendations of the Viva Voce Committee

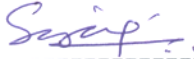
As members of the Viva Voce Committee, we certify that we have read the dissertation prepared by Mr Ramchandra V Amnekar, entitled “**Phosphoacetylation of histones during cellular transformation in mammalian cells**” and recommend that it may be accepted as fulfilling the thesis requirement for the award of Degree of Doctor of Philosophy.



Chairperson – Dr. Neelam Shirsat

8/2/2021

Date:



Guide/Convener – Dr. Sanjay Gupta

08/02/2021

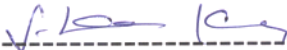
Date:



External Examiner – Prof. M.R.S. Rao

04/02/2021

Date:



Member – Dr. Santosh Kumar

04/02/2021

Date:



Member -Dr. Rukmini Govekar

04/02/2021

Date:

Final approval and acceptance of this thesis is contingent upon the candidate's submission of the final copies of the thesis to HBNI.

I hereby certify that I have read this thesis prepared under my direction and recommend that it may be accepted as fulfilling the thesis requirement.

Date: 26/02/2021

Place: Navi Mumbai


Dr. Sanjay Gupta
Guide

STATEMENT BY AUTHOR

This dissertation has been submitted in partial fulfillment of requirements for an advanced degree at Homi Bhabha National Institute (HBNI) and is deposited in the Library to be made available to borrowers under rules of the HBNI.

Brief quotations from this dissertation are allowable without special permission, provided that accurate acknowledgement of source is made. Requests for permission for extended quotation from or reproduction of this manuscript in whole or in part may be granted by the Competent Authority of HBNI when in his or her judgment the proposed use of the material is in the interests of scholarship. In all other instances, however, permission must be obtained from the author.



Mr. Ramchandra V Amnekar

DECLARATION

I, hereby declare that the investigation presented in the thesis has been carried out by me.
The work is original and has not been submitted earlier as a whole or in part for a degree
/ diploma at this or any other Institution / University.

A handwritten signature in blue ink, appearing to read 'Ramchandra V Amnekar', with a horizontal line underneath the name.

Mr. Ramchandra V Amnekar

List of Publications arising from the thesis

Journal

- 1) **Ramchandra Vijay Amnekar**, Shafqat Ali Khan, Mudasir Rashid, Bharat Khade, Rahul Thorat, Poonam Gera, Shailesh V Shrikhande, Duane T Smoot, Hassan Ashktorab, Sanjay Gupta. Histone deacetylase inhibitor pre-treatment enhances the efficacy of DNA-interacting chemotherapeutic drugs in gastric cancer. *World J Gastroenterol* 2020 February 14; 26(6): 598-613. DOI: 10.3748/wjg.v26.i6.598
- 2) Shafqat Ali Khan, **Ramchandra Amnekar**, Bharat Khade¹, Savio George Barreto, Mukta Ramadwar, Shailesh V. Shrikhande and Sanjay Gupta. p38-MAPK/MSK1 mediated overexpression of histone H3 serine 10 phosphorylation defines distance-dependent prognostic value of negative resection margin in gastric cancer. *Clinical Epigenetics* (2016) 8:88 . DOI 10.1186/s13148-016-0255-9

Chapters in books and lectures notes

1. Asmita Sharda, **Ramchandra Vijay Amnekar**, Abhiram Natu, Sukanya, Sanjay Gupta. Histone posttranslational modifications: Potential role in diagnosis, prognosis, and therapeutics of cancer. *Prognostic Epigenetics. Vol.15, Translational Epigenetics. Academic Press, London:351-373, 2019.*

Conferences

1. 16th Asian Forum of Chromosome and Chromatin Biology, CCMB Hyderabad, 2017. Poster presented entitled “Phosphoacetylation of histones in gastric cancer and their clinical relevance”.

-
2. 4th Annual Conference of Environmental Mutagen Society of India, BARC, Mumbai, 2018. Poster presented entitled “Epigenetic alterations during cellular transformation of gastric epithelial cells “.
 3. “Chromatin Dynamics and Nuclear Organization in Genome Maintenance”, EMBO Workshop, Illkirch, France in 2018. Poster presented entitled “Chromatin Dynamics at the interface of cellular transformation”*
 4. 17th Asian Forum of Chromatin and Chromosome Biology, JNCASR Bangalore, 2018. Poster presented entitled “Chromatin Dynamics at the interface of cellular transformation”.

Others

1. **Ramchandra V Amnekar** and Sanjay Gupta. HDAC Inhibitors in Solid Tumors: An Incomplete Story. Journal of Clinical Epigenetics (2018) 4; 2:8. DOI: 10.21767/2472-1158.100093



Mr. Ramchandra V Amnekar

ACKNOWLEDGEMENTS

Firstly I would like to express my heartfelt gratitude to my PhD advisor/ mentor Dr. Sanjay Gupta, for his undaunted faith in my work and for guiding me not only with my experiments or presentation skills but molding me with a temper that would help me address future scientific explorations. Thank you Sir, for your patience, kindness and imbuing vigor. The best thing that I would cherish about you is your unceasing positivity, resourcefulness and the humility with which you treat every person. I owe my gratitude to you and mam, Mrs. Julie Gupta for your generosity and warmth which you had for all of us during the house parties.

“Research is formalized Curiosity” as said by Zora Neale Hurston. I take this opportunity to thank all my school teachers from St Joseph’s High School, Kurla and all teachers from KJ Somaiya College of Science & Commerce, especially Microbiology department who have laid the foundation of my academic life and gave wings and flight to my curiosity. I am indebted to Mr. Anna Prabhudesai for having faith in me.

ACTREC had been a great workplace with its scenic landscape and updated academic and scientific infrastructure which has been possible because of Dr. Sudeep Gupta (Director, ACTREC), Dr. Rajiv Sarin and Dr. S.V. Chiplunkar (Ex-Directors, ACTREC) and Dr. Prasanna Venkatraman (Deputy-Director, CRI). I thank you all for your efforts especially, Dr V Prasanna for being kind and approachable to students. I also thank ACTREC for fellowship and project funding. I would like to acknowledge my doctoral committee members, Dr. Neelam Shirsat (Chairperson), Dr. Santosh Kumar (BARC) and Dr. Rukmini Govekar for their critic and guidance that helped us to do and think better.

Gupta lab had been a great place to learn and cherish for life. I would like to thank my wonderful seniors Ajit, Monica, Shafkat, Saikat, Divya for introducing me to the field of epigenetics and research. Whatever I have learnt in my PhD right from holding a pipette to execution of an experiment is through their guidance. Next I would like to express my gratitude to our lab manager Mr Bharat Khade, and technicians Mr Santosh Mithbavkar and Mr Arun Kole who actually keeps our lab working. A great deal of work present in this thesis is a cumulative hard work of my wonderful trainees. Thank you, Neha Maurya,

Janhavi Devrukhkar, Kanchan Hariramani, Kajal Dalvi, Soumita Banerjee and Narendra aka “Bahubali” for your support and dedication. This PhD has been a turbulent journey and it has been a great pleasure to sail through with my batch-mate and lab partner Asmita Sharda. No words can express my feelings for you; thank you for being there in thick and thin!!! Thank you to my wonderful juniors Sanket, Mudasir Tripti, Abhiram, Sukanya for the lively lab environment especially Tripti and Sukanya whom I have troubled a lot :>. A special mention goes to our new member Anjali who has helped me with my experiments lately. Thank you and all the best dreamer; you will shine!!!.

This research work would not have been possible without the help and expertise of so many people. I would like to thank Mr. Uday Dandekar, Mr Anish and all other CIR staff members. I thank Mr. Panchal from workshop for being there to help out with any repairing work. I would also like to thank Ms. Rekha, Ms. Shyamal, Mr. Ravi and Mr. Prashant (Flow Cytometry), Ms. Vaishali, Ms. Tanuja, Mr. Jayaraj and (Microscopy), Ms. Sharda (DNA sequencing), Ms. Sharda Sawant and Ms. Siddhi (Electron Microscopy) for their expertise and assistance. I would also like to thank Dr. A. Ingle, Mr. Rahul Thorat, Maheshji and Shashiji of the Laboratory Animal Facility for their help. Thank you to Madanji, Shishirji and late Arunji from ACDSF for their technical help. My heartfelt thanks to Dr. Pradip Chaudhari and Dr. Kiran Bendale for being there for all my dogs and cats whenever needed. I also thank Mr. Anand (IT facility), Mr. Munnoli, Ms. Swati and Ms. Mughda (Library), Ms. Aparna Bagwe, Ms. Ojaswini and Ms. Prema (SCOPE) for their assistance.

This PhD tenure was a beautiful and memorable journey; thanks to the wonderful people of Batch 2013. Thank you all for your support and wish you a good health and success. No words can express my gratitude to Burhan who has been like a loving, caring elder brother and who helped me increase my endurance. I would like to thank all members of Waghmare and Shirsat lab for their help especially Shalaka and Sister Raikamal. Sorab lab members have been a second family in ACTREC. I would like to thank Sorab, Shrikanto, Sarika, Nazia, Monica, Amol, Bhagyashree, Rahul and Pawar kaka for all the wonderful interactions coffee break, planning treks (which someday will come into

reality), our discussion on politics and science. I would like to express my gratitude to Sonali and Abha who had been a great emotional support and friend for life. I hope you achieve great success in life. Another wonderful friend to cherish for life is Sayoni Roy.

A big thank you and love to all my furry angels who gave reasons to come back to lab again after a gloomy day and night. Thank you Gajji, Gajjo, Bow bow, White Brown, Mausiji, Girl, Smarty Bownie, Tinny my Bae Chikki, Tikki, Feistie, Whitie; Dukkar and Pappu. Thank you to Mani, Rani, Golu, Maalu, Cherry, Blossom, Bajrangi, Bhujang, Tiger, Chou and Mouw. Wish I could have you all.

Finally I am indebted to my parents (Mr Vijay Amnekar and Mrs Vidhya Amnekar) for the unceasing support. Thank you to my sister Vedangi my friend Kedar, Prafulla Kaka & Shubhangi Kaki. I hope to cherish and emulate whatever good I have learnt from you.



Mr. Ramchandra V Amnekar

Contents

1.0 Synopsis	1
2.0 List of Figures	19
3.0 List of Tables	23
4.0 List of Abbreviations	25
5.0 Chapter 1 Overview of the thesis	29
1.1 Layout of the thesis	31
6.0 Chapter 2 Review of Literature	34
2.1 Epigenetics and Chromatin: Definition and concept	35
2.2 Epigenetic mechanisms	37
2.2.1 DNA methylation/demethylation	38
2.2.2 RNA interference	39
2.2.3 Histone Post-Translational Modification	39
2.3 Enzymes involved in Post translational modification of histones	41
2.3.1 Histone phosphorylation	41
2.3.2 Histone acetylation	42
2.3.3 Histone methylation	44
2.3.4 Other modifications	46
2.4 Histone modifications – Role in diverse biological processes	46
2.4.1 Histone modifications and transcriptional regulation:	47
2.4.2 Histone modifications in regulation of cell cycle:	48
2.4.3 DNA damage repair and apoptosis:	50
2.4.4 Role in maintenance of chromatin integrity	51
2.5 Histone code and crosstalk	52
2.6 Histone PTMs in cellular transformation and carcinogenesis	54
2.7 H3S10ph and cellular transformation	57
2.8 Therapeutic relevance of histone modifications and modifying enzymes in cancer	60
2.9 Gastric cancer	64
2.10 Prevalence, incidence and mortality	65

2.11	Classification of gastric cancer.....	66
2.11.1	Laurens classification:	67
2.11.2	WHO classification:.....	68
2.11.3	Anatomical classification:	68
2.11.4	Molecular classification of gastric tumors	69
2.12	Etiological factors for gastric cancer development	70
2.12.1	Dietary factors:	70
2.12.2	H pylori:	71
2.12.3	Nitroso compounds:.....	71
2.12.4	Genetics.....	71
2.13	Gastric carcinogenesis:	72
2.14	Epigenetics and gastric carcinogenesis	73
2.15	Alterations in histone PTMs and modifying enzymes in gastric cancer.....	76
7.0	Chapter 3 Aims and Objectives	80
3.1	Statement of purpose	81
3.2	Hypothesis.....	81
3.3	Objective	82
3.4	Work-plan	82
8.0	Materials and Methods	86
4.1	Cell Culture	87
4.1.1	Cell Lines	87
4.1.2	Trypsinization, sub-culturing and maintenance	87
4.1.3	Freeze stock preparation and cell line revival.	88
4.1.4	Cell synchronization	88
4.1.5	Cell cycle analysis	89
4.2	Genetic manipulation.....	89
4.2.1	MSK1 shRNA cloning	89
4.2.2	Transfection of MSK1	90
4.3	Tissue samples.....	90

4.3.1	Tissue collection and inclusion/exclusion criteria	90
4.3.2	Preparation of tissue section slides.....	91
4.3.3	Hematoxylin and eosin staining.....	91
4.4	Immunohistochemical staining	92
4.4.1	Immunohistochemistry:	92
4.5	Transformation model	93
4.5.1	Generation of a transformed gastric cell line.....	93
4.5.2	Development of explants cultures.....	94
4.6	In-vivo experiments.....	94
4.6.1	Development of xenograft mouse model system:	94
4.6.2	Tissue block preparation.....	95
4.6.3	In-vivo therapeutic utility of chemotherapeutic drug and epi-drug	95
4.6.4	Tumor growth	96
4.7	Phenotypic assays.....	96
4.7.1	Short term proliferation assay	96
4.7.2	Proliferation assay by cell counting	97
4.7.3	Long term survival assay:.....	97
4.7.4	Soft agar colony formation assay.....	97
4.8	Biochemical inhibition Assays	98
4.9	Chromatin organization assay.....	98
4.9.1	Micrococcal nuclease digestion assay	98
4.9.2	MNase – Salt fractionation protocol	99
4.9.3	Chromatin Immunoprecipitation or ChIP assay	100
4.10	Protein lysate preparation and visualization	101
4.10.1	Nucleo-cytosolic and chromatin fractionation, and histone extraction	101
4.10.2	Whole cell and cytoplasmic lysate preparation, and nuclear fractionation	101
4.10.3	Sodium dodecyl polyacrylamide gel electrophoresis.....	102
4.10.4	Coomassie staining.....	102
4.10.5	Silver impregnation method.....	103
4.10.6	Western blotting and developing	103
4.11	Immunofluorescence microscopy	104

4.12	RNA extraction and real time PCR	105
4.13	Histone deacetylase assays.	105
4.14	Chemotherapeutic and Epi drug based assays	106
4.14.1	Drug-DNA interaction assay	106
4.14.2	Fraction-affected curve analysis	107
4.14.3	Median effect plot analysis	107
4.15	<i>In silico</i> analysis of The Cancer Genome Atlas for gastric cancer	107
4.16	Statistical analysis	108

9.0 Chapter 5 Results. 109

5.1	To study the alterations in histone post-translational modifications and the associated modifiers upon cellular transformation.....	110
5.1.1	Epigenetic alterations with transient N-methyl-N-nitrosourea treatment and DNA damage response.....	110
5.1.2	Cellular transformation of HFE-145 cell line.....	111
5.1.3	Alteration in phenotypic properties during cellular transformation and development of explant cultures.....	112
5.1.4	Alterations in histone post translational modification post transformation.	114
5.1.5	H3S10phK14ac distribution in chromatin.....	117
5.1.6	Alteration in epigenetic modifiers associated with histone hypoacetylation and increased phosphoacetylation.	119
5.2	To define the role of MSK1 in regulating phosphorylation of histone H3 and its potential importance in acetylation of neighbouring lysine residues in gastric cancer cell line.....	123
5.2.1	Effect of MSK1 in survival of transformed gastric epithelial cells	123
5.2.2	Regulation of H3S10phK14ac by MSK1	125
5.2.3	Crosstalk between H3S10ph and H3K14ac	128
5.2.4	Mechanism of cross talk between H3S10ph and neighbouring H3K14ac... ..	131
5.2.5	MSK mediated regulation of HDAC1 in gastric carcinogenesis.....	134
5.2.6	Level of HDAC1 in gastric cancer.....	137

5.3	To define the role of MSK1 mediated phosphorylation of H3S10 and H3S28 in M phase cells.	139
5.3.1	Levels of MSK1 during the different phases of cell cycle.....	139
5.3.2	Effect of MSK inhibition on histone post-translational modification.....	140
5.3.3	Effect of MSK inhibition on mitotic exit and entry into G1 phase.....	142
5.3.4	Effect of AURKB and MSK inhibition on histone PTM post-release from M phase.....	146
5.3.5	Pathway regulating MSK-mediated H3S10ph, H3S28ph and H3K14ac.....	148
5.4	To study the significance of global histone hypoacetylation in altering the efficacy of chemotherapeutic drug in gastric cancer cell lines and pre-clinical model.....	151
5.4.1	Expression of class I HDAC's and HDAC activity in gastric cancer patients.....	151
5.4.2	Expression of HDAC's, HDAC activity and histone acetylation in gastric cancer cell lines... ..	152
5.4.3	Sequence specific effect of HDACi on the binding of chemotherapeutic drugs.....	153
5.4.4	HDACi and the dose of chemotherapeutic drugs to attain maximum efficacy	155
5.4.5	Synergistic interactions of combinatorial HDACi and chemotherapeutic drug treatments depend on regime.....	158
5.4.6	Effect of HDACi pretreatment on histone PTMs, cell cycle and chromatin organization.....	160
5.4.7	Therapeutic potential of the pre-treatment regime in GC xenograft	162
10.0	Chapter 6 Discussion	165
11.0	Chapter 7 Summary and conclusion.	178
7.1	Summary and conclusion.....	180
7.2	Salient findings.....	178
12.0	Chapter 8 Future directions.	184
13.0	Chapter 9 References.	186

14.0 Chapter 10.0 Appendix

206

10.1 APPENDIX –I Clinicopathological data of patients used in the study .207

10.2 APPENDIX-II – Buffer compositions, list of antibodies and primer
sequence.....208

List of Figures

Sr No	Figure No & Title	Page No
<i>Chapter 2 Review of Literature</i>		
1	2.1 Organization of chromatin and epigenetic mechanism.	36
2	2.2 Euchromatin Vs Heterochromatin.	37
3	2.3 Sites of post translational modifications on the N-terminal tails of histone and their specific association with the chromatin states.	40
4	2.4 Mechanism of transcriptional regulation by histone post translational modification.	47
5	2.5 H3S10ph levels during cell cycle progression.	50
6	2.6 Cross talk between H3S10ph and H4K16ac on FOSL1 enhancer.	53
7	2.7 Cross talk regulating expression of PRC regulated genes.	54
8	2.8 Interplay between misregulated epigenetic and genetic events in the development of cancer.	55
9	2.9 Histone onco-modifications and their functional consequences in cancer	56
10	2.10 MAPK-MSK mediated regulation of immediate early gene expression	58
11	2.11 DEN induced transformation of hepatocytes involves H3S10ph mediated regulation of Pol III gene expression.	59
12	2.12 Anatomy of stomach and stomach wall.	64
13	2.13 Incidence and mortality of different cancers.	65
14	2.14 Laurens classification.	68
15	2.15 Molecular features of the four subgroups classified on the basis of gastric adenocarcinoma dataset of TCGA.	69
16	2.16 Etiological factors associated with development of gastric cancer.	70
17	2.17 Proposed model depicting the multistep process of gastric carcinogenesis (Correa's model).	72
18	2.18 Epigenetic alterations in gastric cancer.	74

Chapter 4 Materials & Methods

19	4.1	Schematic diagram depicting the protocol for carcinogen induced transformation of HFE145 cell line.	93
20	4.2	Schematic diagram depicting the schedule of chemotherapeutic drug and HDAC inhibitor administration.	96

Chapter 5 Results

21	5.1	Dose determination for methylnitrosourea treatment and its effects on histone PTMs.	110
22	5.2	Cellular transformation of HFE145 cell line.	111
23	5.3	Alteration in phenotypic properties associated with transformation of HFE 145	113
24	5.4	In vivo tumorigenic potential of MNU V cell line and development of explants.	114
25	5.5	Histone post translational modification in transformed. and explants cell line	115
26	5.6	Histone post translational modification in transformed. and explants cell line.	116
27	5.7	Chromatin fractionation and the level of H3S10pK14ac.	117
28	5.8	Epigenetic modifiers associated with histone hypoacetylation and increased phosphoacetylation..	120
29	5.9	MAPK pathway associated with H3S10phK14ac.	121
30	5.10	Effect of MSK1 knockdown on AGS cell line.	124
31	5.11	MSK 1 enzyme is crucial for survival of transformed gastric epithelial cells.	125
32	5.12	MSK1 regulates H3S10phK14ac in response to serum induction.	126
33	5.13	MSK regulates EGF induced H3S10phK14ac.	127
34	5.14	Effect of serum induction and inhibitor treatments on MAPK pathway activation.	129
35	5.15	MSK mediated cross talk between H3S10ph and H3K14ac.	130
36	5.16	Regulation of H3S10phK14ac crosstalk in absence of serum starvation	131
37	5.17	Regulatory mechanism of cross talk between H3S10ph and neighbouring H3K14ac in absence of serum starvation.	133

38	5.18	MSK1 mediated regulation of HDAC1 in gastric cancer cell lines and tumor samples.	134
39	5.19	Association of H3S10ph and H3K14ac on HDAC1 promoter.	136
40	5.20	HDAC1 levels in Indian cohort of gastric cancer patients.	137
41	5.21	MSK1 and phMSK1 levels during mitosis.	139
42	5.22	Effect of MSK1 inhibition on mitotic H3 phosphorylation and acetylation.	141
43	5.23	Effect of MSK1 inhibition on mitotic exit/ entry into G1 and cyclin levels.	143
44	5.24	Effect of MSK or Aurora B kinase inhibition on the levels of cyclins.	145
45	5.25	Effect of AURKB and MSK inhibition on histone PTM post mitotic release..	147
46	5.26	Pathway regulating MSK mediated H3 phosphorylation in M phase.	149
47	5.27	Expression of HDAC's (HDAC 1 &2) and HDAC activity is variable within gastric cancer patients.	152
48	5.28	Gastric cancer cell lines reflect the histone acetylation status and HDAC levels of gastric tumors.	153
49	5.29	Pre-treatment regime with histone deacetylase inhibitor enhances binding of chemotherapeutic drugs to chromatin.	154
50	5.30	HDAC inhibitor-dependent sensitization of GC cells decreases the dose of chemotherapeutic drugs to attain maximum efficacy.	156
51	5.31	Median effect plot analysis for drug combinations (chemotherapeutic drugs and histone deacetylase inhibitors).	159
52	5.32	Pre-treatment regime is associated with chromatin relaxation and enhanced DNA damage.	160
53	5.33	Pre-treatment combination leads to cell cycle arrest and re-expression of tumor suppressors.	161
54	5.34	Valproic sensitizes AGS cell xenograft to cisplatin in an in vivo mice model.	163

Models

55	5.1	Alteration associated with gastric cell transformation	122
56	5.2	MSK mediated regulation of HDAC transcription	138

57	5.3	Mitosis specific differential regulation of histone phosphorylation and acetylation by MSK	163
58	5.4	HDAC inhibitor as a sensitizer for chemotherapeutic drugs in a group of patients with high HDAC activity or levels	183

List of Tables

Sr No	Table Name	Page No
<i>Chapter 2 Review of Literature</i>		
1	2.1 Writers and erasers of histone phosphorylation	42
2	2.2 Writers and erasers of histone acetylation	43
3	2.3 Writers and erasers of histone methylation	45
4	2.4 Writers and erasers of histone ubiquitination, citrullination and ribosylation	46
5	2.5 Histone post translational modification and modifying enzymes in cancer	61
6	2.6 Epi-drugs for cancer therapy	62
7	2.7 Differential characteristics of the major types of Laurens classification	67
8	2.8 Histone modification and modifiers altered in gastric cancer	78
<i>Chapter 5 Results</i>		
9	5.1 Regime specific synergistic, additive or antagonistic effect of chemotherapy drugs and HDAC inhibitor	155
<i>Chapter 10 Appendix</i>		
10	10.1 Clinicopathological characteristics of gastric cancer patients used in the study	209

11	10.2 Composition of MNase digestion buffer	211
12	10.3 Composition of Salt fractionation buffer	211
13	10.4 Composition of MKK lysis buffer	212
14	10.5 Composition of Nuclei isolation buffer	212
15	10.6 Composition of gel prepared	213
16	10.7 Composition of SDS-PAGE running buffer	214
17	10.8 Composition of Transfer buffer	214
18	10.9 Composition of NP-40 buffer	214
19	10.10 List of antibodies and their conditions	215
18	10.11 List of primers used in the study	217
19	10.12 Dose for combinatorial treatment of chemotherapy drugs and HDAC inhibitors in fixed constant ratio.	218

Chapter 7
Summary & Conclusion

7.1 Summary and conclusion

Histone post-translational modifications majorly occurring on the N-terminal tails governs DNA accessibility and thus are important in regulating fundamental cellular processes viz; transcription, replication and fidelity of the genome. Any breach in these modifications may lead to deregulation and development of cancer. In consonant, a number of histone PTMs are known to be altered in cancer and so, they have been explored for their utility in better management of cancer. In the current study we investigated the early alteration in histone H3 phosphorylation, acetylation, the cross talk between the two and the associated regulatory mechanism during carcinogen-induced gastric carcinogenesis. Moreover, to best of our knowledge a novel role of MSK kinase in regulating H3 phosphorylation during mitosis was revealed. Further, the global hypoacetylation was exploited by utilizing HDAC inhibitors in combination with chemotherapeutic drug in a pre-clinical model better therapeutic outcome.

7.2 Salient Findings

1) Alteration in histone H3 phosphorylation and acetylation during cellular transformation and the associated modifiers.

- i. *Transformation of gastric epithelial cells with methyl-nitrosourea was achieved after treatment with a non-lethal dose. The transformed cell line, MNUV exhibited higher clonogenic potential without change in cellular proliferation. The tumors developed in vivo recapitulated the human gastric cancer histology, with glandular adenocarcinoma and well to poorly differentiated cell types.*

- ii. *Site-specific histone hypo-acetylations along with increased H3S10ph and H3S10phK14ac were observed post-transformation. The increased enrichment of H3S10phK14ac was found to be on euchromatin.*
 - iii. *p38-mediated increase in phMSK1 levels was observed in transformed cells and was responsible for the increased H3S10phK14ac. Interestingly, the levels of phMSK1 were sequentially increasing during cancer development. The histone hypoacetylation observed is potentially an outcome of increased HDAC1 and decreased level of PCAF.*
- 2) MSK1 is essential for the survival of transformed gastric cancer cells, regulates H3S10phK14ac and HDAC1 expression.**
- i. *MSK1 is essential for the proliferation and clonogenic potential of gastric cancer cells. Further, MSK-mediated H3S10ph and H3S28ph were found to be associated with H3K9ac, H3K14ac and H3K27ac in a context-dependent manner.*
 - ii. *HDAC inhibitor treatment leads to an increase in phosphoacetylation H3S10phK14ac and was dependent on H3S10ph by MSK1. Further, MSK1 partly regulate HDAC1 occupancy at certain sites in chromatin depending on H3S10ph status.*
 - iii. *MSK-mediated H3S10ph is important for transcription of HDAC1. Occupancy of H3S10ph and H3K14ac on HDAC1 promoter regulates its transcription.*
 - iv. *HDAC1 levels are upregulated in Indian cohort of gastric cancer patient samples. This could be attributed to the increased phMSK levels.*

3) Mitogen and Stress activated protein kinase partly regulates H3S10ph and particularly H3S28ph in mitosis via JNK pathway

- i. *MSK1 mediate a part of H3S10ph and H3S28ph in mitosis. However, H3S28 is predominantly phosphorylated compared to H3S10.*
- ii. *The mitotic histone phosphorylation is associated with regulation of the neighboring acetylation marks.*
- iii. *Decrease in H3S10ph and H3S28ph in mitosis was associated with increased H3K9ac and H3K27ac.*
- iv. *Inhibition of MSK by H89 hinders entry of mitotic cells in G1 phase of the cell cycle. However, epigenetic profiling and level of cyclins suggests a G1 like histone modification landscape.*
- v. *MSK-mediated H3 phosphorylation in mitosis is regulated by JNK pathway.*

4) Pre-treatment of histone deacetylase inhibitor enhances the efficacy of DNA-interacting chemotherapeutic drugs in gastric cancer.

- i. *An increased level of Class I HDAC's mediates histone hypoacetylation in gastric cancer which can be reversed by treatment with HDAC inhibitor. The increased histone acetylation alters chromatin architecture.*
- ii. *Pretreatment with HDACi results in opening of chromatin which favours enhanced drug binding and thus it sensitizes gastric cancer cells to chemotherapeutic drugs leading to more cell kill in vitro and in vivo preclinical model.*

- iii. *Valproic acid followed by cisplatin or oxaliplatin is the best possible combinatorial regime for gastric cancer patients with reduced chemotherapeutic drug related toxicity.*
- iv. *Treatment with cisplatin arrests cells in G2/M phase which is overridden with a HDACi pre-treatment. G1 arrest by HDACi further enhances increased cisplatin binding.*
- v. *HDACi treatment also leads to de-repression of tumor suppressor gene expression thus further enhancing cell kill.*
- vi. *HDAC activity assay suggests heterogeneity in HDAC levels between different patients. There is a need to stratify patients based on HDAC activity levels before administering HDAC inhibitors for sensible use and for reducing the drug toxicity.*

To summarize, the present study highlights the significant role played by histone modifications and their dysregulation through chromatin modifiers during cellular transformation which could be explored for therapeutic intervention in combination with chemotherapy drugs. A specific context-dependent crosstalk between histone H3S10 phosphorylation and H3K14 acetylation, regulated by an intricate balance between MSK1, HDAC and HATs, was observed upon cellular transformation. MSK-mediated HDAC1 expression alongwith PCAF downregulation led to hypoacetylation of histones. This together with increased phosphoacetylation constitutes a code that at least in part determines epigenetic landscape of transformed cells. Importantly, translating the epigenetic alterations into useful therapeutic potential by inhibition of HDAC's provides a new strategy for better management of gastric cancer.

Thesis Abstract:

Name : Mr. Ramchandra V Amnekar

Enrollment Number: LIFE09201304005

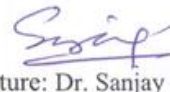
Thesis Title: Phosphoacetylation of histones during cellular transformation in mammalian cells

Histone post-translational modifications (PTMs) dynamically regulate the chromatin organization and thus govern fundamental physiological processes like transcription and replication. Our previous study has shown that H3S10ph levels of the normal resected margins correlate with patients' survival depending on its distance from tumor. This supports the notion that initiated cells with altered histone PTMs are critical in the process of gastric carcinogenesis. In light of the above background, we were interested to study the early histone PTM (phosphorylation and acetylation) alterations during gastric carcinogenesis; particularly the H3 phospho-acetylation crosstalk.

The present work highlights MSK1 as a key player in regulating the transformed phenotype and imparts an altered cancer specific chromatin landscape. This consists of increased phosphoacetylation, H3S10phK14ac and site-specific histone H3 deacetylation mediated by the increased HDAC1 levels. Interestingly, an inverse association between H3 phosphorylation and acetylation was also found to be partly regulated by MSK in mitosis and was essential for immaculate completion of cell division. Further, modulation of cancer specific chromatin landscape i.e global histone hypoacetylation, by HDACi was found to make chromatin more accessible to chemotherapeutic drugs at non-toxic doses; thus, improving therapy response.


08/02/2021

Signature: Mr. Ramchandra V Amnekar


08/02/2021

Signature: Dr. Sanjay Gupta

Forwarded through:


Dr. Sorab N. Dalal, 20/2/2021
Chairperson, Academic &
Training Programme, ACTREC

(Dr. Sorab N. Dalal)
Chairperson, Academic & Training Programme
Tata Memorial Center, ACTREC,
Kharghar, Navi Mumbai - 410210


5/3/21
Dr. S. D. Banavali,
Dean (Academics)
T.M.C.
PROF. S. D. BANAVALI, MD
DEAN (ACADEMICS)
TATA MEMORIAL CENTRE
MUMBAI - 400 012.

Chapter 1

Overview of the thesis

Aberrant gene expression involving inactivation of tumor suppressors and activation of oncogenes is a key preliminary event in the multistep process of carcinogenesis. Recent advancement in molecular biology has reinforced the contribution of epigenetics along with genetic alterations in the development of cancer. The revelations from DNA methylation studies have shifted the notion of cancer being a predominant disease of genetic alterations; particularly the role of DNA methylation as a mechanism of tumor suppressor inactivation has been widely studied. Also, global profiling studies in various cancers have established the association of epigenetic events like histone Post Translational Modifications (PTMs) and modifying enzymes with the different hallmarks of cancers [1]. However, most of these histone PTM alterations like loss of H4K16ac, H4K20me3 and increased H3S10ph are studied in advanced stage cancer – the diagnosis being late.

Gastric Cancer (GC) is a debilitating disease ranking 5th in term of incidence and 3rd in terms of mortality [2]. Gastric carcinogenesis is a complex multifactorial process involving a complex interplay between host related factors and the environment. Many studies have reported alteration in a wide repertoire of epigenetic modifiers (kinases, phosphatases, acetyltransferases, deacetylases, methyltransferases, demethylases and the associated reader proteins) which could be an outcome of genetic or non-genetic events. Interestingly, in our previous study high H3S10ph levels of both, the tumor samples and the histo-pathologically normal resected margins, correlated with poor prognosis of gastric cancer patients. The altered epigenetic profile of the so-called normal gastric cells may in turn deregulate gene expression, increasing uncontrolled proliferation eventually leading to cancer.

Therefore, this warrants the need to study the development and importance of epigenetic alteration in the sequential process of carcinogenesis. This is particularly important since epigenetic events being reversible; detection of early changes could have a greater diagnostic and therapeutic utility, impeding cancer progression or its aggressiveness. However, studies involving mechanistic association of epigenetic alterations with pathogenesis have not been explored in-depth.

In this study the aim is to understand the role of histone post translational modifications, particularly histone H3 phosphorylation and acetylation, and the cross talk between them if any, during the development of gastric cancer. To address this, a sequential *in vitro* carcinogen induced cellular transformation model of gastric cancer was developed. Further, the clinical utility of the alterations was explored by studying their association in gastric cancer patients and the putative alterations were tested for their therapeutic potential.

1.1 Layout of thesis

The basic theme of the entire project is to understand mechanistic links between altered levels of histone PTMs, especially H3S10 phosphorylation and cellular transformation in gastric epithelial cells. The thesis is divided into following chapters.

Briefly,

Chapter 1 describes the background of the study and the layout of thesis for preview.

Chapter 2 starts with review of literature; that describes epigenetics, its mechanism the repertoire of key histone PTM, their role in normal and diseased physiology and their

clinical utility in gastric cancer. Further, the epidemiology, clinical & biological aspects of gastric cancer with emphasis on epigenetics and gastric carcinogenesis is discussed.

Chapter 3 lists the ‘Aims and Objectives’ of the thesis

Chapter 4 describes the methods used in the study under section ‘Materials and Methods’

Chapter 5 highlights the results obtained and is further divided into four parts based on aim of the proposed study and the leads obtained.

- *Describes the development of carcinogen-induced model of gastric cancer and its validation by in vitro and in vivo experiments. The alterations in histone PTMs, the associated modifying enzymes and pathways have been explored.*
- *Role of histone phosphoacetylation and Mitogen & Stress Activated Kinase 1 (MSK1) in survival of the transformed cells is described. The relevance of these alterations viz; increased H3S10phK14ac and Histone Deacetylase1 (HDAC1) in gastric cancer patients along with its association with MSK has been established. Further, the Mitogen-Activated Protein Kinase (MAPK) signaling pathway involved has been explored and the mechanism of cross-talk between H3S10ph and H3K14ac is studied.*
- *Importance of MSK1 as a histone H3 kinase in the mitotic phase of cell cycle and its associations with mitotic exit has been studied.*
- *HDAC inhibitor as a therapeutic target or sensitizer was explored to alter the observed global histone hypo-acetylation using in vitro and in vivo systems in GC*

Chapter 6 discusses the obtained results in context of ongoing research and relevance.

Chapter 7 summarizes the salient findings of the study.

Chapter 8 discusses the directions for future explorations of current findings in-depth.

Chapter 9 en-lists the literature used in the study.

Chapter 10 includes tables related to composition of reagents, primers, antibodies and clinico-pathological parameters of patients.

Chapter 2
Review of Literature

2.1 Epigenetics and Chromatin: Definition and concept

A unique feature of multicellular organism is diversity at structural, physiological and functional level even though they are genetically homogenous. This diversity is achieved in each cell type by virtue of substantially different gene expression profile which is regulated by a specialized mechanism. The mechanism is now known as *Epigenetics* (epigenesis + genetics) and has been derived from the Greek word “*epigenesis*” by Conrad Hal Waddington in 1942 to describe the causal interplay between genes, their products and the resulting phenotype during embryogenesis [3]. According to the contemporary definition proposed in 1970, it is the heritable regulatory mechanism that modulates gene expression without a change in DNA sequence [4].

The mechanisms include reversible modification on DNA, regulation by non-coding RNA or post-translational modifications (PTM) on histone proteins that forms the primary framework for packing the ~2 meter long DNA into the micron scale nucleus (Figure 2.1). These events take place on nucleosomes which are the fundamental unit of DNA packaging in eukaryotes. The electrostatic force of attraction between the negatively charged DNA and positively charged histones plays an important role in the formation of nucleosomes. Each nucleosome consists of an octameric core made up of two molecules each of histone proteins H2A, H2B, H3 and H4, onto which ~147 bp of DNA is wound. Nucleosome formation is catalyzed by a group of chaperone protein complexes and remodellers which in a sequential manner regulates the docking of two H2A-H2B dimers onto a H3-H4 tetramer such that N-terminal tails of histones protrude out [5]. An array of nucleosomes called chromatin further undergoes condensation by linker histone H1 and other non-histone proteins like HMG (High Mobility Group

proteins) at different levels to generate a hierarchy of structures with modular functionalities.

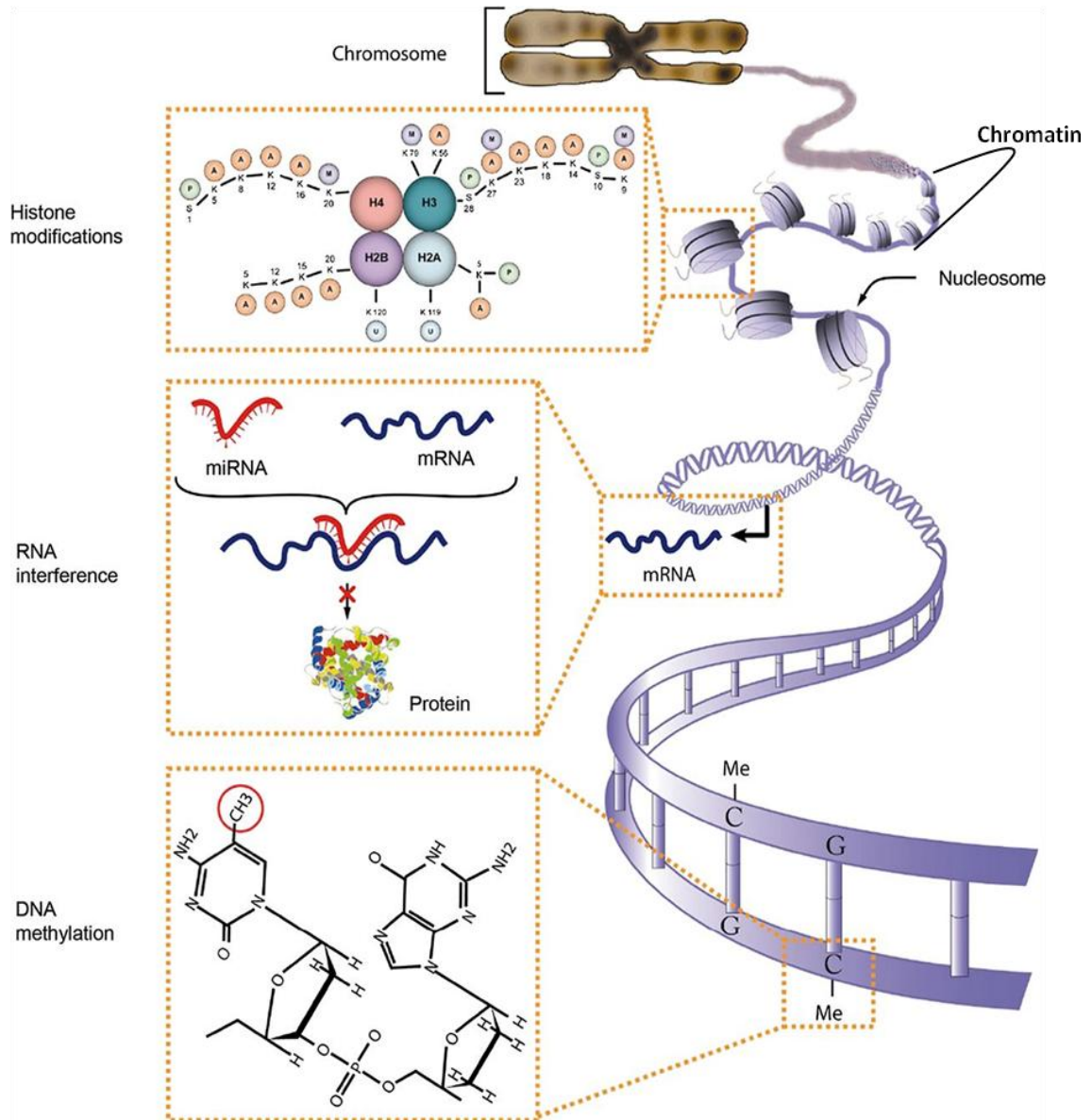


Figure 2.1 Organization of chromatin and epigenetic mechanism. The eukaryotic DNA is wrapped onto an octameric core of histone proteins to form nucleosome, which together with histone H1 forms the chromatosome which undergoes further compaction at different levels, giving rise to mitotic chromosome [6].

The chromatin is thus dynamic, being able to modulate between an open-state chromatin called euchromatin (less condensed) and the closed-state called heterochromatin (more

condensed state) depending on the upstream signal and functional requirements (Figure 2.2) [7].

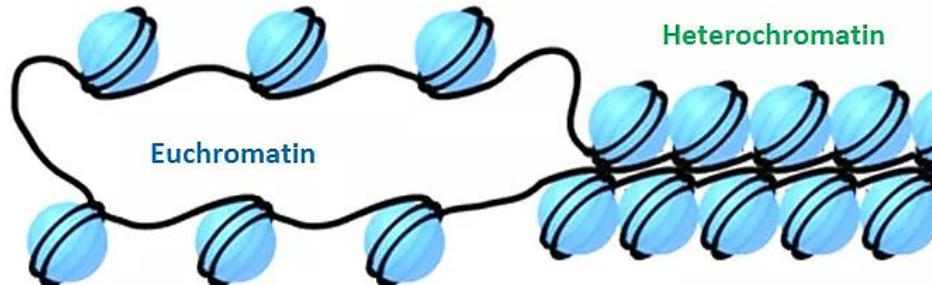


Figure 2.2 Euchromatin Vs Heterochromatin. Chromatin could be organized into a tightly wound, closed state called heterochromatin or it could dynamically reform into the loose, open state called euchromatin (adapted. from <https://vivadifferences.com/euchromatin-vs-heterochromatin/>)

Epigenetics alterations being at the interface of signal reception and outcome are the primary respondents to a wide variety of extracellular stimulus and environmental changes through alteration in different physiological pathways. The local (gene level) and global (genome level) epigenetic state which is a sum of the DNA methylation profile, characteristic levels and specific occupancy of histone PTMs and the miRNA (micro-RNA) present together, constitute the *epigenome*, which could be a tissue or cell-type specific. It is the epigenome that imparts the true structural and functional identity of a cell by regulating gene expression [8].

2.2 Epigenetic mechanisms

Epigenetic events are mainly of three types viz; a) DNA methylation b) Histone post translational modification and c) RNA interference and function at the DNA and protein level. They operate during transcription, replication or post-transcriptionally and

translationally through specific enzymes and chromatin remodelling complexes as discussed below.

2.2.1 DNA methylation/demethylation

It involves transfer of a methyl group from S-adenosylmethionine to the cytosine residues (C-5) of DNA template. The reaction is catalyzed by a group of enzymes called DNA Methyltransferases (DNMT's) viz; DNMT1, DNMT3a and DNMT3b. DNMT1 is involved in methylation of the newly synthesized strand of DNA during replications using the old hemimethylated DNA strand as reference, therefore called as maintenance DNA methyltransferases [9]. It is important for maintaining the tissue specific gene expression pattern during successive rounds of division. DNMT3a and 3b, called as *de novo* methyltransferases are involved in *de novo* DNA methylation of the genome during embryo implantation state and thus are important in embryonic development. The reversal of methylation i.e. demethylation is catalyzed by a group of enzymes called Ten Eleven Translocase (TET) in a highly co-ordinated three step process requiring vitamin-C as a co-factor [9]. In mammals, DNA methylation is globally distributed on CpG sequences with a less density at CpG islands in promoter regions under normal conditions. Methylation of DNA leads to docking of Methyl Binding Proteins (MBP's) and HDAC's resulting in heterochromatization and gene repression. It plays a vital role in regulating gene expression, cellular differentiation, imprinting, X-chromosome inactivation and maintenance of genome stability. In cancer promoter-specific hypermethylation is observed leading to repression of tumor suppressor genes [10].

2.2.2 RNA interference

The non-coding RNA's depending on the length (range from 19-200 bp), structure, processing and mechanism of action are classified as siRNA, miRNA, piRNA and long non-coding or lncRNA. Short sequences of RNA (19-24 nucleotides), called micro RNA (miRNA), post-transcriptionally bind to homologous mRNA leading to interference in their translation. The process involves a RNA Induced Silencing Complex (RISC) consisting of specialized RNA binding and cleavage proteins which includes Dicer, Drosha and Argonaute [11]. The targets of these miRNA's could be genes that are involved in DNA methylation and histone PTM as well, pinning their role in control of other epigenetic processes [12–14]. Non-coding RNA could regulate expression at gene and chromosome level by organizing heterochromatin structures in association with chromatin remodellers and Polycomb Group Proteins (PCG's). A centromeric heterochromatin organization is characterized by repressive modification H3K9me3 and a RNA component, thereby preventing transcription of repetitive elements. Also, X-chromosome inactivation by lncRNA Xist and genome imprinting are regulated by RNA interference [11]. Thus, it plays an important role in preventing genome instability and epigenome maintenance.

2.2.3 Histone Post-Translational Modification

Histones, primarily on their N-terminal tail and to a lesser extent on the C-terminal tail and globular domains are decorated by a variety of post-translational modifications (PTMs) like acetylation, phosphorylation, methylation, sumoylation, ubiquitination etc (Figure 2.3). The key metabolites of cells viz Adenosine triphosphate (ATP), acetyl CoA and S-adenosylmethionine (SAM) act as donors for PTMs. These modifications take

place on specific amino acid residues at specific positions. Predominantly, serine and threonine in histones undergo phosphorylation whereas lysine and arginine can undergo acetylation or methylation [15] like lysine at position 9 of histone H3 can undergo acetylation to form H3K9ac or methylation to form H3K9me/me2/me3.

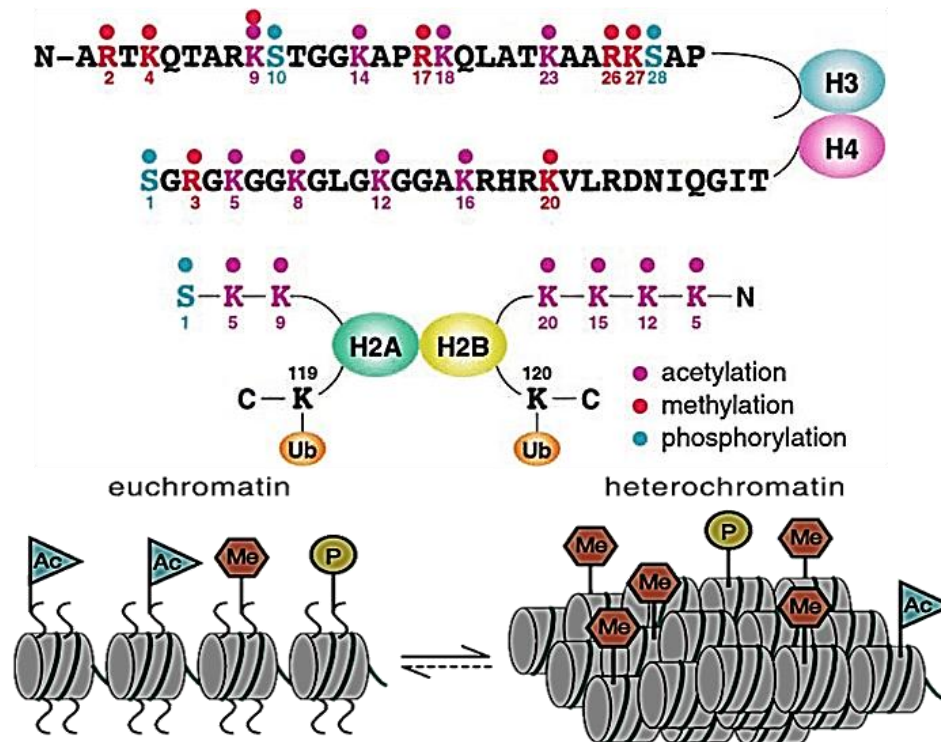


Figure 2.3 Sites of post translational modifications on the N-terminal tails of histone and their specific association with the chromatin states. The modifications depicted include acetylation (pink), methylation (red), phosphorylation (blue) and ubiquitination (orange) [15]. Of these, phosphorylation and acetylation are associated with euchromatin and methylation with heterochromatin [16]

Histone PTMs are key events that regulate important cellular processes like gene expression, replication, DNA repair and cell division by modulating the accessibility of DNA to the different cellular machineries. This demands the need of a complex and dynamic spacio-temporal regulatory mechanisms which is an orchestrated event of ‘writers’ (add modifications), ‘readers’ (recognize the modification) and ‘erasers’

(remove the modifications) [17]. Further, these histone PTMs are known to regulate the modifications at neighbouring as well as distant sites of histones. PTMs like H3K9ac, H3K27ac, H3K4me3 which positively favour transcription are called ‘active marks’ and PTMs like H3K9me3, H3K27me3, H4K20me3 which are associated with repression are called ‘inactive marks’. The histone PTMs are recognized by reader proteins which bring about the downstream effect by altering accessibility of chromatin [18]. Their roles in regulating different physiological processes have been discussed in section 2.4.

2.3 *Enzymes involved in Post translational modification of histones.*

The histone modifications are established by writers, their maintenance and removal is an orchestrated event and follows a systematic relay based system wherein upstream stimuli (growth factor, stress, environmental agents) are translated into physiological downstream effects via chromatin/epigenetic based machinery.

2.3.1 Histone phosphorylation

This modification takes place on serine, threonine, tyrosine and histidine residues on histones and involves transfer of phosphate group from ATP. The enzymes involved (mostly serine/threonine kinases) are highly specific for the residue involved and position in the N or C-terminal tail of histones. They are regulated by different signaling pathways depending on the context involved viz; growth factor stimulation, cytokines, angiogenic factors, DNA damage, cell cycle changes and stress responses. In response to growth factors like epidermal growth factor (EGF), serum or stressors like anisomycin or Lipopolysaccharide (LPS), the MAPK pathway kinases MSK1, MSK2 or Ribosomal protein S-6 Kinase (RSK's) mediates phosphorylation of H3S10 & H3S28, whereas the same modifications are brought about by Cdc-7-INCEP (Inner centromere) or activated

Aurora kinase B (AURKB) in mitosis. The reader protein involved is 14-3-3 ζ in case of H3S10ph and the key phosphatases involved are PP1(Protein phosphatase 1), PP2a and MKP1(Mitogen-activated protein kinase (MAPK) phosphatase) [19].

Table 2.1 Writers and erasers of histone phosphorylation [19]

Modification	Writer	Eraser	Role
H3S10p	MSK1,MSK2,PIM1,	PP1	Transcription
	IKKB, Aurora B		Chromosome condensation
H3S28p	MSK1 and MSK2	PP1	Transcription
	Aurora B		Chromosome Condensation
H3T3p	Haspin		
H3T6p	PKC β 1		Androgen induced transcription
H3T11p	Dlk/Zip		CPC attachment to centromeres
	PRK1		Androgen induced transcription
H2BS14p	MST1		DNA damage repair
			Apoptosis
H2BS32p	Protein kinase C		Apoptosis
γH2AX	ATM/ATR	Wip1	DNA damage repair
	and DNA-PK		Apoptosis
H4S1	Casein Kinase II		Transcription and mitosis

2.3.2 Histone acetylation

Histone acetylation and deacetylation occurs on ϵ -amino nitrogen of lysine residues and is mediated by histone acetyltransferases (HAT's) and histone deacetylases / sirtuins (HDAC/SIRT) respectively. Based on the catalytic domain HAT's can be classified into three families viz p300/CBP (CREB binding protein); Gcn5 N-acetyltransferases or GNATs (including Gcn5, PCAF, Hat1 etc) and the MYST family HATs (MOZ/Morf, Ybf2/Sas2, Tip60 etc) all of which work in multiprotein complexes like SWI-SNF (Switch Sucrose Non fermentable) and SAGA (Spt-Ada-Gcn5 acetyltransferase) [20].

The target residues (in term of position) and histone (H3 or H4) for acetylation may vary from being general to highly site specific. Eg: The MYST family is involved in acetylation of H4 histone at K4, K8, K12 with MYST1 specifically acetylating H4K16 whereas KAT2B (PCAF- p300/CBP associating factor) can bring about H3K9, H3K14, H3K56 and H4K5, H4K8, H4K12 acetylation [20]. HDACs are Zn⁺²-dependent enzymes, whereas sirtuins are NAD⁺-dependent enzymes, catalyzing the removal of acetyl group from histones and non-histone proteins. They form part of co-repressor complexes NCoR/SMRT (Nuclear Co-repressor/ Silencing Mediator for Retinoid and Thyroid hormone receptor) through which their chromatin recruitment is regulated.

Table 2.2 Writers and erasers of histone acetylation [21,22]

Modification	Writer	Eraser	Role
H3K9ac	GCN5,PCAF,CBP, p300, MOZ, MORF	Class I &II HDAC, SIRT	Transcription
H3K14ac	GCN5,PCAF,CBP, p300, MOZ, MORF	Class I &II HDAC	Transcription
H3K18ac	GCN5,PCAF,CBP, p300, MOZ, MORF	SIRT Class I &II HDAC	Hormone stimulated transcription, Maintenance of pericentromeric chromatin
H3K27ac	GCN5,PCAF,CBP, p300, MOZ, MORF	Class I &II HDAC	Transcription
H4K5/12ac	HAT1, HBO1	Class I &II HDAC	Transcription Histone deposition
H4K16ac	TIP60, MOF	Class I &II HDAC	Transcription, Prevents higher order chromatin formation Replication, DNA repair

HDACs are classified into four classes. These are class I (HDAC1–HDAC3 and HDAC8) and class II (HDAC4–HDAC7, HDAC9, and HDAC10). Class II is subdivided into IIa (HDACs 4, 5, 7, and 9) and IIb (HDACs 6 and 10). Class III comprises NAD-dependent Sirtuins (SIRT1–SIRT8) and class IV has only HDAC11. Of these, class I and class II b is localized in nucleus and cytoplasm, respectively. Class II a, class III, and class IV have localization in both nucleus and cytoplasm [17]. The reader proteins involve a bromodomain or Bromodomain and Extra Terminal domain (BET) which recognizes the acetyl group and many of the acetyltransferases and chromatin remodelers have such domains.

2.3.3 Histone methylation

Histone methylation occurs on arginine (R) or lysine (K) residues of histones, utilizing S-adenosyl methionine (SAM) as methyl donor. These residues have the propensity to undergo mono, di, or trimethylation, which may be symmetric or asymmetric in case of arginine methylation [23]. Methylation on specific lysine residues of histones is carried out by lysine methyltransferases like SET1 (Su(var) 3-9, Enhancer-of-zeste and Trithorax), MLL1 (Mixed Lineage Leukemia), MLL2, MLL3, and MLL4. Protein arginine methyltransferase (PRMT) enzymes catalyze the transfer of methyl group onto arginine residues of histones. The reader proteins have specific recognition domains viz; chromodomains, chromoshadow domains, tandem Tudor domains, plant homeodomain (PHD) fingers, tryptophan aspartate rich (WD-40) repeats and malignant brain tumor (MBT) repeats. These reader proteins add an additional level to methyl lysine signaling owing to their ability to differentiate between the different degrees of methylation [24].

Table 2.3 Writers and erasers of histone lysine methylation [24]

Modification	Writer	Eraser	Role
H3K4me1/2/3	SET 1	me1/2- KDM1A-B	Transcription activation
	MLL 1	me2- KDM5D me3- KDM2B, KDM5A-D	Bivalent modification
H3K9 me1/2/3	SETDB1 (me1/2)	me1/2- JMJD1C, KDM1A, KDM3A-B	Maintenance of <i>de novo</i> methylation
	SUV39H1/2 (me3)	me2- KDM4E, PHF2, PHF8	Transcriptional repression
	EZH1 or G9a (me1/2/3)	me3- KDM4A-E	Maintenance of constitutive heterochromatin
H3K27me1/2/3	EZH1/2	me1- KDM7A	Transcriptional silencing
		me2/3- KDM6A-C	X-chromosome inactivation Bivalent modification
H3K36me1/2/3	SETD2 (me3)	me1/2- KDM2A-B	Prevention of cryptic transcription
	NSD1-3	me2- KDM8 me3- KDM4A, KDM4C	DNA DSB repair
H3K79me2/3	Dot1	KDM2B	Position effect variegation in telomeres and subtelomeric regions
			Transcription elongation
H4K20me1/2/3	SET8 (me1)	me1- PHF8 me3- KDM4A	ORC recruitment
	SUV420H1/2 (me2/3)		DNA damage repair Chromosome condensation Regulation of cell cycle and quiescence

2.3.4 Other modifications

Other than these major modifications, histones undergo ubiquitination (ub), citrullination, sumoylation and ribosylation. The histone residues which undergo these modifications, the associated chromatin modifiers and their functional role is been tabulated in Table 2.4

Table 2.4 Writers and erasers of histone ubiquitination, citrullination and ribosylation [25–27]

Modification	Writer	Eraser	Role
H3 citrullination	PAD2/PAD4		Transcription activation
	(<u>P</u> eptidyl <u>l</u> arginine deiminase)	-	Neutrophil activation Inflammation
H3R26 citrullination	PAD2/PAD4 (<u>P</u> eptidyl <u>l</u> arginine deiminase)	-	Transcription
H3S10 and H3S28 PARylation	PARP1(<u>P</u> oly [<u>A</u> DP- ribose] polymerase 1)	-	DNA Repair
H2AK119ub	RNF2- BMI		
	(<u>R</u> ing <u>f</u> inger protein 2- <u>B</u> cell-specific <u>M</u> oloney murine leukemia_virus <u>i</u> ntegration site 1)	USP3/16 Ubiquitin- specific protease	Transcription repression X chromosome inactivation
H2BK120ub	RNF20/RNF40	USP3/16	Transcription activation

2.4 Histone modifications – Role in diverse biological processes

Accessibility to DNA is a prerequisite for any cellular machinery to function work and this is partly achieved by modulation of chromatin organization through histone post-translational modifications. These modifications play important role in diverse processes

like transcription, replication, DNA repair, maintenance of pluripotency, cell death and development by regulating the opening and closing of chromatin and/or recruitment or removal of diverse proteins involved in these cellular processes.

2.4.1 Histone modifications and transcriptional regulation

Allfrey *et al* in 1964, first established the role of histone acetylation and methylation in RNA biogenesis and paved the way for exploration of the functional and regulatory contribution of PTMs on histones [28]. The acetyl group neutralizes the positive charge of histones that weakens their electrostatic interaction with negatively charged DNA, resulting in decondensation of chromatin. Chromatin relaxation (on *cis*-regulatory regions like enhancers and promoters) and remodelling facilitates access of transcriptional machinery to underlying DNA and enables transcription [29] (Figure 2.4).

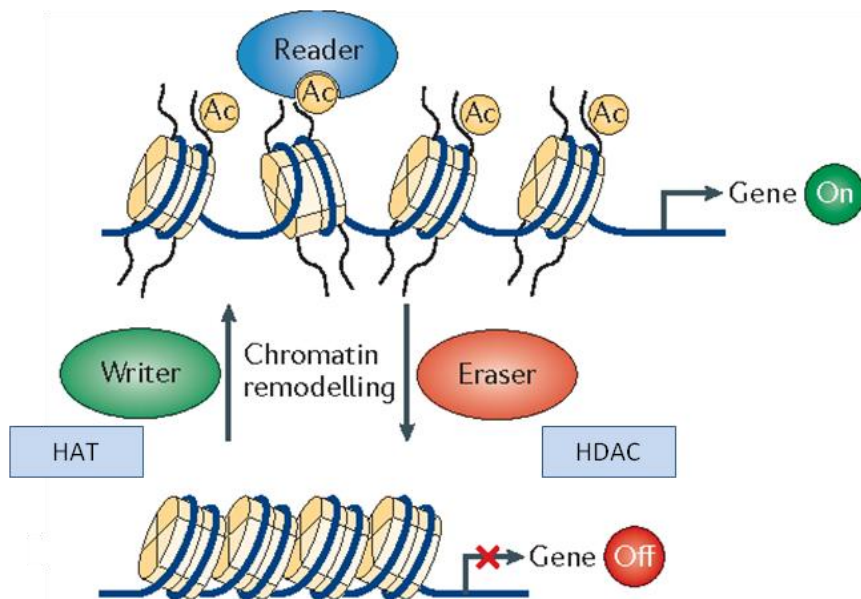


Figure 2.4 Mechanism of transcriptional regulation by histone post translational modification. Histone acetylation mediated by histone acetyltransferases (HAT) leads to decondensation of chromatin via chromatin remodelers, allowing transcription factors and co-activators to gain access to the DNA resulting in gene expression. The repressed or condensed chromatin state is achieved post transcription by deacetylation of histones mediated by HDAC's [30].

Phosphorylation of histone H3 at the serine 10 residue along with acetylation of histones at H3K9, H3K14, H3K27 and H4K16 position has been associated with release of paused RNA polymerase II for transcription of immediate early genes like *c-fos*, *c-jun* and *c-myc* [31–33]. In contrast to acetylation, histone methylation could lead to activation or repression depending on position of the residue involved or the degree of methylation. For example, trimethylation at H3K9 and H3K27 position is associated with transcription repression, whereas monomethylation at this position is associated with active transcription. In case of H3K4, H3K36, and H3K79, both mono- and trimethylation are associated with active transcription [24]. H3K36me₃ which occurs on the coding region during transcription elongation imparts transcriptional precision by preventing cryptic transcription and increases life span in yeast [34]. Histone ubiquitination is another modification that plays an important role in transcriptional elongation. The histone mark H2AK119ub1 play a role in the polycomb-mediated transcriptional repression [35] whereas H2BK123ub1 positively regulates transcriptional elongation [36].

2.4.2 Histone modifications in regulation of cell cycle

The different phases of cell cycle viz G₁, S and G₂M are regulated spatio-temporally with dynamic changes in the organization of chromatin. Histone PTM H4K20me₂ plays an important role during the initiation stage of replication. H2AZ mediated H4K20me₂ at the origin of replication leads to deposition of Origin Recognition Complex proteins (ORC1 and ORC2) resulting in licensing and activation of origin-firing. Also, loss of H2AZ or methyltransferase SUV10H1 leads to G₁-S arrest [37]. A critical factor during replication is distinguishing between newly synthesized and old histone which is important for faithful transfer of ‘chromatin state’ to the daughter cells with identity

similar to that of parental cells. H4K5ac and H4K12ac marks the newly synthesized histones for incorporation during S phase and are found on nascent chromatin [38,39]. During chromatin maturation phase, these modifications are removed by HDAC1&2 which is essential for remodelling of the newly synthesized chromatin resulting in progression of replication fork [40]. Inheritance of chromatin state alongwith copy of DNA is achieved in part by maintenance DNA methylation during replication which involves UHRF1 (U**bi**quitin-like, containing **PHD** and **RING** finger domains 1) mediated H3K18ub that leads to the recruitment of DNMT1 [41].

Overall, G2/M phase has low H3K9ac, H3K18, H3K27ac and H4K16ac levels and high H3K14ac compared to G1 phase [42,43]. H3S10ph and H3S28ph are two interesting modification with contrasting functions across the two distinct phase of cell cycle. In the G1 phase it is associated with open chromatin for transcription whereas in the G2/M it is associated with condensed chromatin. The reduced acetylation state in the G2 /M phase mediated by HDAC3 favors the loading of Aurora B kinase which brings about phosphorylation of H3 at S10 and S28 positions in mammals [44]. Phosphorylation at these sites results in deposition of condensin proteins resulting in condensation of the newly synthesized chromatin and progression to M phase [45,46] (Figure 2.5). Spatial regulation of histone phosphorylation at H3T11 residue mediated by **D**ual **l**eucine **z**ipper **k**inase (Dlk/ZIP) at the centromeres is essential for kinetochore attachment and proper segregation of chromosomes [47].

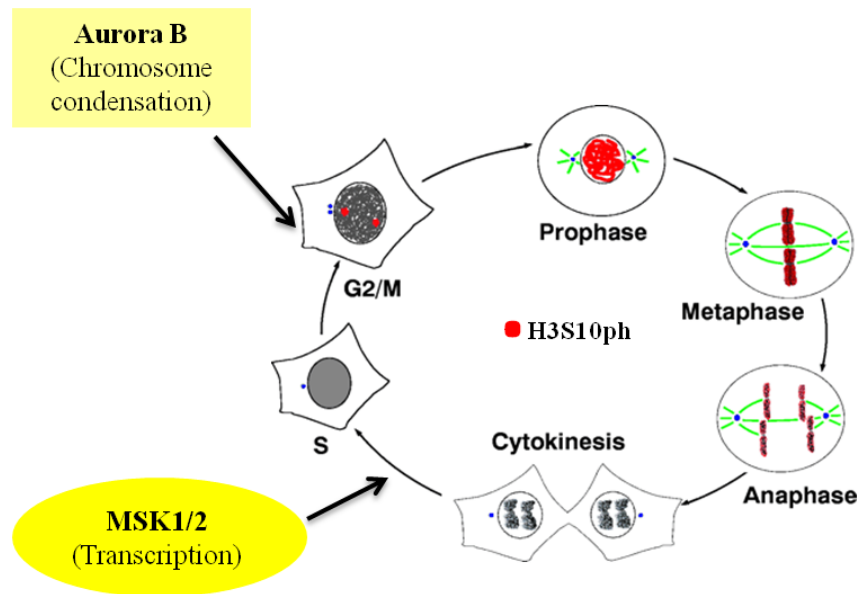


Figure 2.5 H3S10ph levels during cell cycle progression. In interphase, the levels of H3S10ph catalyzed by MSK1/2 kinases are low and associated with transcription. It begins to increase during late G2 phase catalyzed by Aurora kinase B, peaks at metaphase and begins to decrease during anaphase and mitotic exit. In mitosis H3S10ph is associated with chromosome condensation [48].

2.4.3 DNA damage repair and apoptosis

Efficient repair of DNA lesions is imperative for cell viability and genome integrity. In response to IR mediated double stranded breaks (DSB), activation of ATM (Ataxia telangiectasia mutated protein), ATR (Ataxia telangiectasia and Rad3-related protein) or DNA-PK (DNA-dependent protein kinase) kinase leads to increased levels of phosphorylated H2A at S139 (γ H2AX). This modification extends upto mega bases bi-directionally from the site of single or double stranded break. It alongwith H2BS14p helps to establish a heterochromatic foci that enhances recruitment, concentration and retention of DNA repair machinery proteins [49,50]. This induction of γ H2AX at the site of DNA damage is associated with loss of H3S10ph in a G1-specific manner upon IR (Ionizing radiation), suggesting that different codes of histone PTMs regulate the repair

kinetics depending on the cell cycle phase [51]. Indeed, cells in G2/M are more sensitive to IR compared to G1 and S phase cells, owing to the homologous recombination (HR) pathway operating in S phase and the accessibility of chromatin to DNA repair machinery [52]. In case of Non Homologous End Joining (NHEJ), PR-Set7 and Suv4-20 methyltransferase mediated methylation of H4K20 and H3K79 is required for the initial recruitment of 53BP1 (p53 Binding protein), which takes place even in absence of γ H2AX and is essential for proficient repair[53]. In case of acetylation, increased H3K56ac and H4K16ac at site of DSB results in an open chromatin state favoring accessibility of DNA repair proteins [50]. Thus, histone PTMs set the platform for efficient recruitment of repair proteins. When the damage to DNA is irreparable, apoptosis sets in to induce cell death. The condensation of chromatin and digestion into oligonucleosomal units are the chromatin hallmarks of apoptosis [18]. Phosphorylation of histone H2B at the 14th residue of serine is an epigenetic marker for apoptosis that is mediated by the MST1 (Macrophage-stimulating) kinases [54]. Histone modifications like H4K16ac by hMOF and H3T45ph by PKC- δ (Protein Kinase C) promote apoptosis by increasing fragmentation of DNA and the accessibility to DNA damaging agents [55].

2.4.4 Role in maintenance of chromatin integrity

The integrity of chromatin should be maintained both in terms of sequence and structural organization for normal functioning of genome and faithful inheritance. Any breach due to mutations, duplications, breaks or translocations may compromise with the fidelity of genome thereby leading to altered gene expression and diseases like cancer. The histone PTM does maintain the stability by regulating the accessibility of DNA for cellular processes. Aberrant DNA methylation of DNA repair genes like MINT (Munc18-1-

interacting protein 1) and MLH1 (MutL homolog 1) leads to genome wide errors in DNA sequence, which if not rectified increases the frequency of mutation and their accumulation. Under normal conditions the promoters of tumor suppressor genes are enriched in active transcription marks like H3K4me3, H3K9ac, H3K27ac and H4K16ac. Whereas, repetitive elements like satellite regions, Long interspersed nuclear elements (LINE) and Alu sequences are hyper-methylated and enriched in repressive marks like H3K9me3, H3K27me3 and H4K20me3 [56]. This ensures efficient prevention of transposition events and the subsequent instability in genome. H4K16ac mark prevents higher order chromatin compaction and thereby prevents encroaching of nearby repressive marks in transcriptionally competent regions [57]. Loss of repressive marks such as H4K20me3 and H3K27me3 from repetitive satellite regions leads to Chromosome instability (CIN) or Microsatellite instability (MSI) in the genome.

2.5 Histone code and crosstalk

One of the interesting features of histone PTMs is the ability to influence the occurrence, retention or removal of another modification via the recruitment of chromatin associated proteins. This process called 'Histone Crosstalk' could be *cis-acting* (H3-H3 interaction on same tail) or *trans-acting* (H3-H4 or H3-H2A interaction). These crosstalks are mostly dynamic, local events occurring at sites like promoters or enhancers on a fraction of genes and the chromatin modifying complexes involved may have more than one distinct enzymatic activity [58]. Two of the widely studied crosstalks in the cell is the phospho-acetyl and phospho-methyl switch. In response to growth factor stimulus, phosphorylation of H3S10 leads to docking of 14-3-3 ζ proteins which are associated with acetyltransferases CBP/p300. This leads to acetylation of neighboring residues

H3K9 and H3K14, resulting in activation of transcription [59,60]. A similar crosstalk was shown to exist between PIM1 mediated H3S10ph and H4K16ac at the enhancer of c-fos gene where the recruitment of MOF was found to be H3S10ph dependent [32,61] (Figure 2.6).

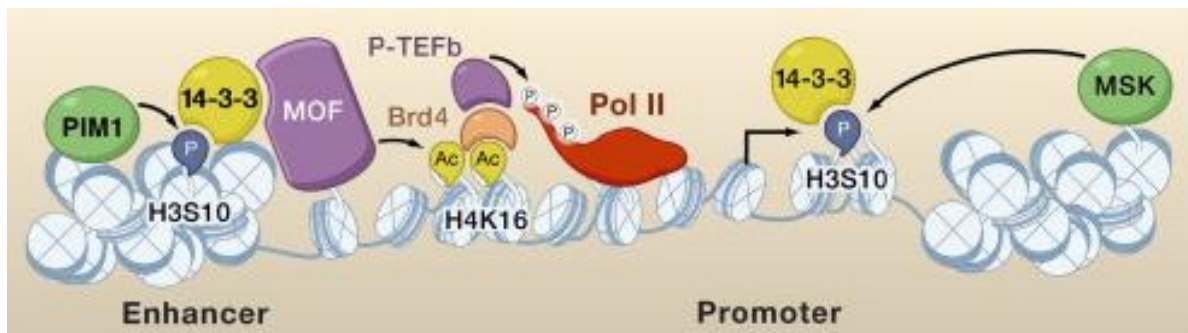


Figure 2.6 Cross talk between H3S10ph and H4K16ac on FOSL1 enhancer. PIM1 mediated H3S10ph on c-fos enhancer leads to recruitment of acetyltransferase MOF via 14-3-3, resulting in H4K16ac. This in turn signals the recruitment of P-TEFb releasing the paused polymerase II for FOSL1 transcription [61]

Similarly a crosstalk exists during establishment of heterochromatin, wherein PRC1 mediated H3K27me3 leads to H2AK119ub1 via the EED (Embryonic ectoderm development) complex of transcriptional repression [62]. Histones in general undergo multiple PTMs, each of them being associated with a specific and contextual output. The different permutations and combinations achieved with crosstalk further add on to the diverse possibilities of functional output that could be achieved. This is important because it adds another level of regulation when PTMs are functionally linked. This is being exemplified by the H3S28ph-H3K27me3 crosstalk, wherein MSK mediated H3S28ph overrides polycomb mediated silencing [63,64] (Figure 2.7).

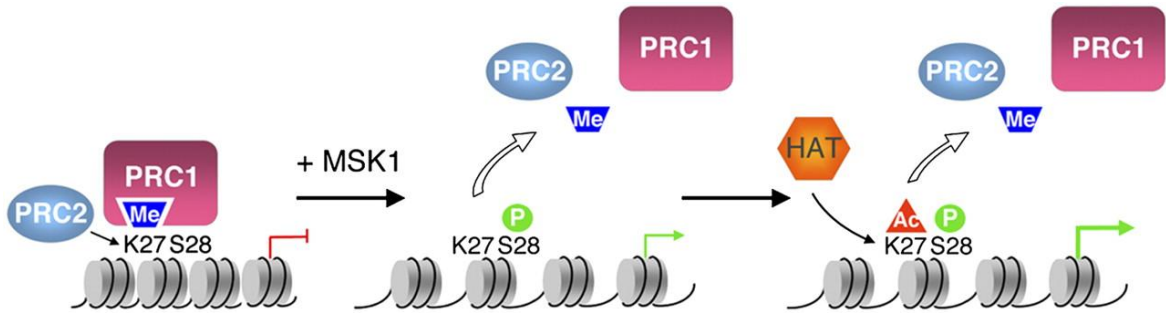


Figure 2.7 Cross talk regulating expression of PRC regulated genes. PRC1 mediated H3K27me3 represses gene expression. During differentiation few genes undergoes MSK1 mediated phosphorylation at H3S28, leading to displacement of PRC complex and recruitment of HAT by the H3S28ph signal. This facilitates H3K27ac and expression of differentiation associated genes [64].

The crosstalk between histone modifications has given rise to the Histone Code Hypothesis proposed by C.D Allis. According to this hypothesis distinct modification on one or more tail act sequentially or in a combination to form a histone code that is read by other proteins to bring about distinct downstream events [16]. The question whether histone phosphorylation precedes acetylation, or established concomitantly or *vice versa* is still debatable in the field as it is highly cell type and context dependent. Also, most of the global histone PTM studies involve profiling of individual histone PTMs and no cancer-specific crosstalk has been explored. This caveat is important to explore because histone PTMs do not work in isolation but in combination to generate a functional output for cellular processes.

2.6 Histone PTMs in cellular transformation and carcinogenesis

As described above various histone modifications dynamically regulates physiological process and thus their normal functioning is imperative for coherence between cellular and organismal homeostasis. These modifications regulate the euchromatic and

heterochromatic state of chromatin and so any imbalance may influence the gene expression and mutation rate. On the other hand, changes in epigenetic modifiers could also result in imbalance of histone modifications. Together these perturbation also sets aberrant gene expression leading to altered cellular phenotype leading to cancer development [65] (Figure 2.8).

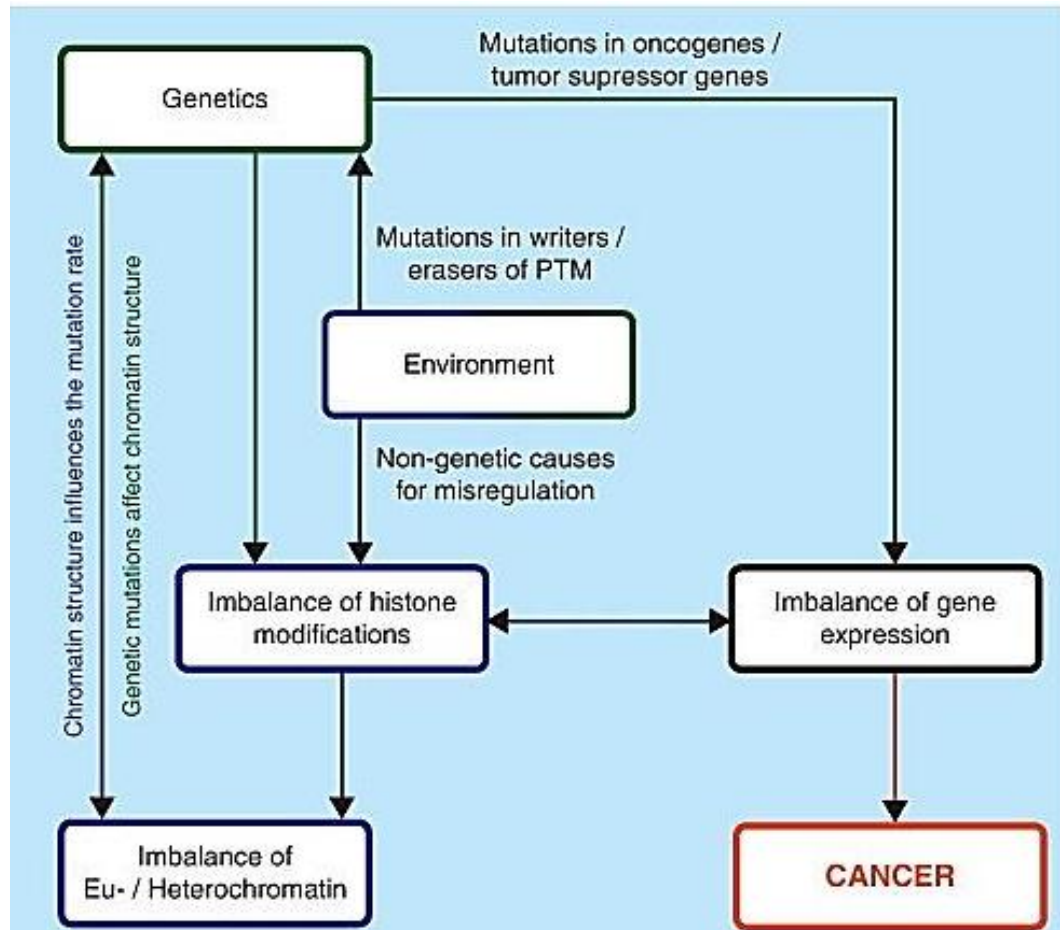


Figure 2.8 Interplay between misregulated epigenetic and genetic events in the development of cancer [65]. The model depicts how genetic and epigenetic events could regulate each other via perturbation of chromatin, eventually leading to cancer. The imbalance of histone modifications is central to this interplay.

Carcinogenesis thus is a complex interplay between epigenetic and genetic events which are influenced by multiple host related factors like age, genetics, sex, diet, metabolism, immune system, lifestyle and various environmental agents which influences epigenetic

processes. The loss of H4K16ac and H4K20me3 are found in multiple cancers making them as the hallmark of cancer [66]. The prominence of these two alterations in different cancers suggests a central role of these modifications in cancer development. During last two decades there has been a surge in reports suggesting the association of specific histone PTM changes with the oncogenic phenotypes observed in cancer (Figure 2.9). This has led to a new term called 'Histone Onco-modification' [1].

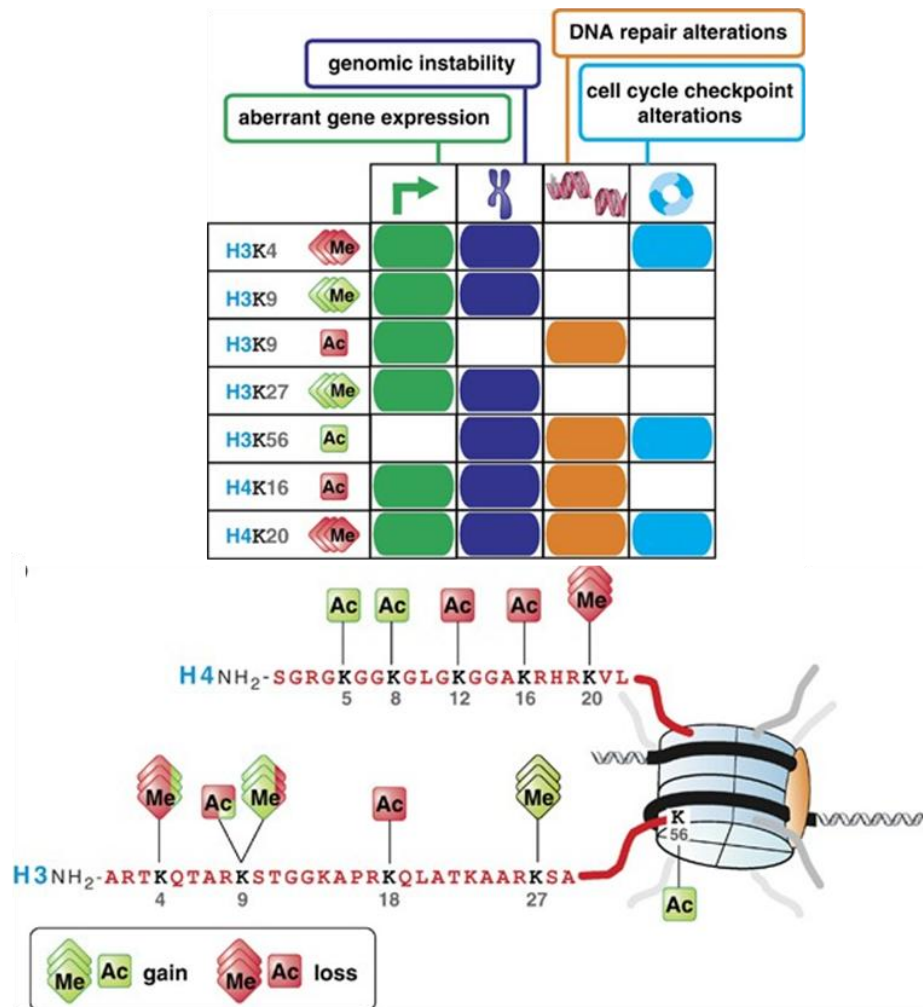


Figure 2.9 Histone onco-modifications and their functional consequences in cancer. Role of altered histone PTM with cancer specific aberrations is tabulated. Site specific histone post translational modification that are increased (green) or decreased (red) in cancer are associated with clinicopathological characteristics are highlighted. [1].

Histone PTMs have been shown to play diverse role in cancer development right from proliferation to metastasis and drug resistance. However, unlike genetic alterations, advancement and association of histone PTMs during the sequential process of carcinogenesis has been poorly explored and the role of H3S10ph in cellular transformation is emerging.

2.7 H3S10ph and cellular transformation

Earlier studies on c-Ha-*ras*^{Val12} oncogene transformed rat fibroblast displayed alteration in chromatin compaction upon transformation with increased MNase sensitivity [67]. This was further observed in rat fibroblasts transformed with various oncogenes viz; *raf*, *fes*, *mos* and *myc* which impacts the Mitogen Activated Protein Kinase or MAPK pathway. The constitutively activated MAP kinase pathway plays a part in oncogenesis through increased H1 phosphorylation via CDK2/cyclin and decreased chromatin compaction as phosphorylation tend to reduce H1 binding to chromatin [68–70].

MAPK pathway activation by various oncogenes, growth factor and stressors was known to increase H3 phosphorylation and so the quest to study the role of H3 phosphorylation with transformation initiated [71]. In 1998, mice fibroblast transformed with oncogenic *RAS* showed a cell cycle independent up-regulation of H3S10ph which mediated the increased transcription of oncogenes, *c-fos*, *c-jun*, *c-myc* [72]. The kinase responsible for increased phosphorylation was found to be mitogen and stress activated protein kinase 1 or 2 (MSK1/2). These kinases were found to be activated by the upstream MAPK signaling kinases viz ERK1/2 or p38 depending on the upstream signals or stimulus involved [73–77] (Figure 2.10).

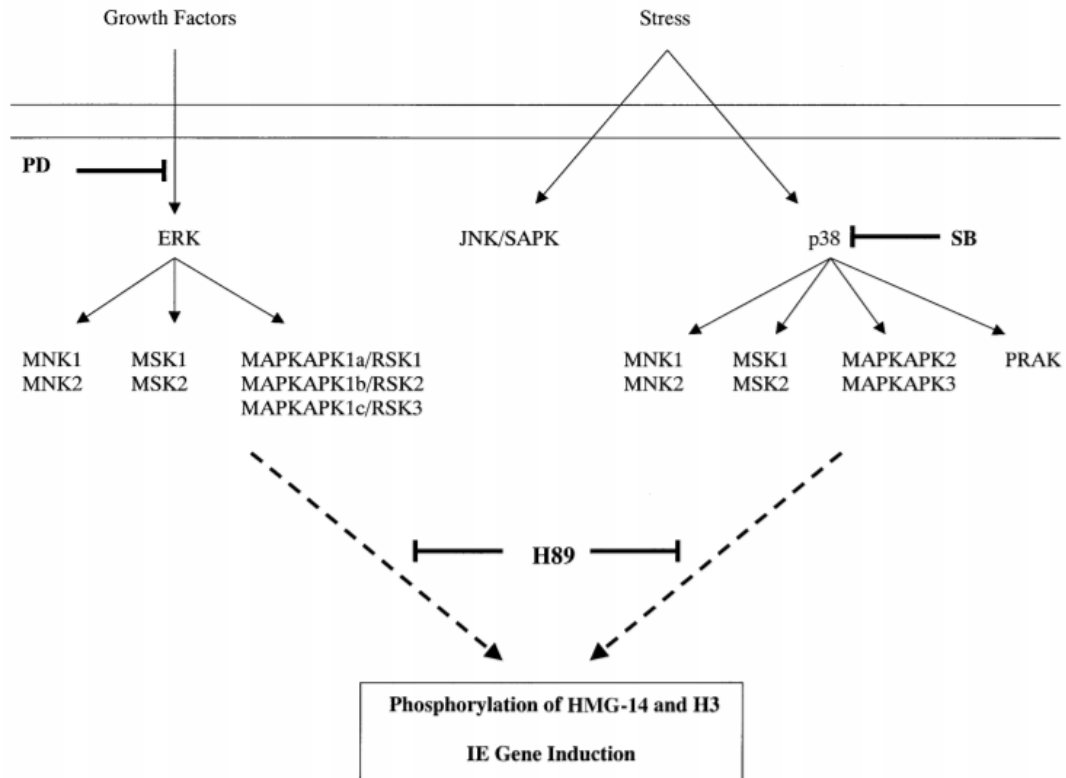


Figure 2.10 MAPK-MSK mediated regulation of immediate early gene expression The ERK1/2 and p38 kinase regulated by the upstream MAPK pathway activates MSK1/2 in response to growth factor stimulus and stress respectively. The activated MSK's regulate the transcription of immediate early genes viz; *c-fos* and *c-jun* via H3S10ph which could be inhibited by the respective inhibitors of MAPK pathway (PD and SB) or MSK (H89) [74].

Moving beyond association, the active role of H3S10ph in the transformation process was demonstrated using shRNA against histone H3 and overexpression of mutant H3S10A in mouse epidermal cells. In this, H3S10ph was found to be indispensable for EGF mediated anchorage-independent growth of cells [78]. Similarly, another study highlighted the crucial role of MSK1 in EGF and TPA induced transformation [79]. Interestingly, in both the studies induction of *c-fos* and *c-jun* were key factors connecting MSK mediated H3S10ph with transformation [78,79]. In a similar study, EGF induced H3S28ph increased transcription of RNA Pol III and TFIIB genes, promoting cell

proliferation and transformation [80]. Further, in an *in vivo* model of skin carcinogenesis, knockout of MSK1/2 was shown to have a tumor suppressive role as the incidence decreases [81]. In a similar study of UV induced skin cancer, MSK and RSK inhibition resulting in decreased H3S10ph was found to have protective effect [82]. In 2013, Zhong *et al* had demonstrated that DEN (Diethylnitrosamine) induced H3S10ph mediate Brf1 expression and Brf1-dependent Pol-III genes. Up-regulation of these genes was found to increase proliferation and mediated transformation of hepatocytes [83].

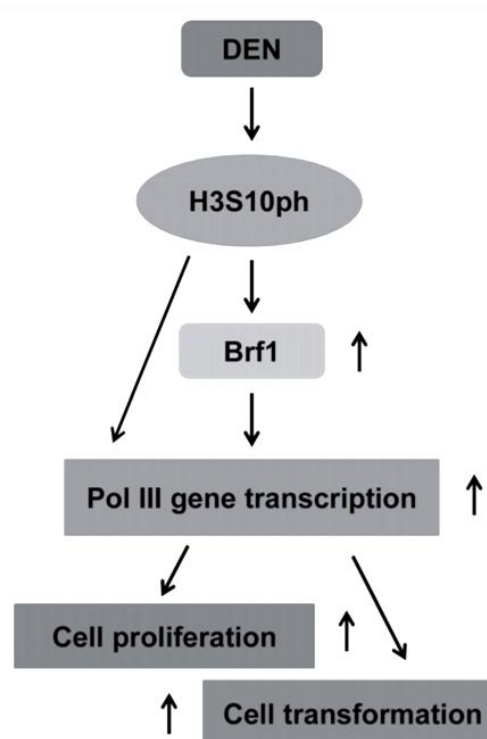


Figure 2.11 *DEN induced transformation of hepatocytes involves H3S10ph mediated regulation of Pol III gene expression. Diethylnitrosamine induced H3S10ph enhances transcription of Brf1 which in turn increases the transcription of Pol III gene. The increase in Pol II genes drives cellular proliferation and transformation [83].*

Likewise, in case of breast cancer, MSK1 mediated H3S10ph was found to be important for expression of progesterone and estrogen target genes, and cell proliferation [84,85]. In contrast to this understanding, a high level of MSK1 was found to be associated with

better survival of HER2 negative and basal like breast cancer patients; mirroring its role in differentiation of luminal type breast cancers, thereby promoting terminal differentiation and preventing metastasis [86,87].

H3S10ph thus plays a crucial role in cellular transformation and cancer progression. Supporting this, immunohistochemical studies in ovarian, melanoma, oesophageal squamous cell carcinoma, glioblastoma, gastric cancer and nasopharyngeal cancer have demonstrated the association of aberrant H3 phosphorylations with clinicopathological characteristics [88–93].

2.8 Therapeutic relevance of histone modifications and modifying enzymes in cancer

It is now well established that deregulated epigenetic mechanisms govern cellular pathways and determine the fate of cancer cells right from proliferation, metastasis to drug resistance. Epigenetic alterations being reversible; understanding the early driver epigenetic events during progression could aid in early detection, therapeutic intervention and disease outcome through therapy. In 2005, Fraga *et al*, demonstrated the loss of H4K16ac and H4K20me3 in multiple cancers, suggesting it to be a hallmark of cancer [66]. After this, a series of global histone PTM studies have highlighted the prognostic utility of studying alterations in histone PTM and the associated epigenetic modifiers in cancer. The following key points highlight their importance.

- *A fundamental association between global histone modification levels and tumor aggressiveness, regardless of cancer tissue of origin suggest their importance and relevance in prediction of disease prognosis.*

Table 2.5 Histone post translational modification and modifying enzymes in cancer [25]

Histone PTM	Writer	Eraser	Cancer Prognosis
H3S10ph	MSK1/2, Aurora kinase B	PP1, MKP1	Stomach
H3K9ac	GCN 5	HDAC1, HDAC2, HDAC3, SIRT-1,6	Lung, ovarian, breast
H3K18ac	CBP/p300	SIRT-6	Lung, prostate, breast, oesophagus
H4K5ac	CBP/P300, HAT1	-	Lung
H4K8ac	TIP60, HB01	-	Lung
H4K16ac	TIP60, hMOF	HDAC1, HDAC2	Lung, breast
H3K4me2	SETD1A, SETD1B, MLL1	KDM1A, KDM1B, KDM5A, KDM5B, KDM5C	Prostate, kidney
H3K4me3	SETD1A, SETD1B, ASH1L	KDM2B, KDM5A, KDM5B, KDM5C	Prostate, liver, kidney
H3K9me3	SUV39H1, SUV39H2, SETDB1	KDM3B, KDM4A, KDM4B, KDM4C, KDM4D	Lung, prostate, breast, leukemia, stomach
H3K27me3	EZH2, EZH1	KDM6A, KDM6B	Breast, ovarian, pancreatic, prostate, oesophagus, stomach
H4K20me3	SUV420H1, SUV420H2	-	Breast, colon, lymphoma, ovarian

➤ *The changes in chromatin organization and modifiers in tumors may help in deciding the utility of epi-drugs and course of therapy.*

As aberrations in epigenome are pharmacologically reversible, epi-drugs as single agents or in combination with standard chemotherapeutic agents are currently envisaged as a new therapeutic strategy in cancer. This would aid to mitigate

Table 2.6 Epidrugs for cancer therapy [94,95]

Class	Compound	Target modifier	Current status
HDAC Inhibitor			
Hydroxamic acid	Vorinostat (SAHA)	HDAC - Class I II IV	FDA approved
	Panobinostat	HDAC - Class I II IV	Phase III Clinical Trial
	Belinostat	HDAC - Class I II IV	Phase II Clinical Trial
	Abexinostat,	HDAC - Class I II	Phase II Clinical Trial
	Pracinostat	HDAC - Class I II	Phase II Clinical Trial
	Dacinostat	HDAC - Class I II	Phase I Clinical Trial
Cyclic tetra peptide	Romidepsin	HDAC 1/2	FDA approved
	Apicidin	HDAC 2,3	Phase II Clinical Trial
	Trapoxin A	HDAC 1,4,11	-
Benzamide	Mocetinostat	HDAC 1, 2, 11	Phase II Clinical Trial
	Entinostat	HDAC 1, 9, 11	Phase II Clinical Trial
	Rocilinostat	HDAC 6	Phase II Clinical Trial
Aliphatic acid	Valproic acid (VPA)	HDAC - Class I	Phase III Clinical Trial
	Pivanex	ND	Phase II Clinical Trial
	Butyrate	HDAC - Class I IIa	Phase II Clinical Trial
Methyltransferase Inhibitor			
Not defined	Tazemetostat	EZH2	Phase I/II Clinical Trial
	E-7438		
	Pinometostat EPZ-5676	DOT1L	Phase I Clinical Trial
Bromo domain inhibitors			
Not defined	GSK525762	BET	Phase I Clinical Trial
	RVX208		Phase II Clinical Trial
	OTX015		Phase I Clinical Trial

limitations of current treatments like drug resistance and toxicity [94]. DNMT inhibitors were the first epi drugs to be used for cancer therapy. HDAC inhibitors are the second most promising epi-drugs with successful outcomes for hematological malignancies. US FDA approved the HDAC inhibitors suberoylanilide hydroxamic acid (SAHA, vorinostat, in 2006) and romidepsin (depsipeptide, in 2009) for the treatment of patients with progressive, persistent or recurrent cutaneous T-cell lymphoma [94]. Further in 2015, FDA approved panobinostat in combination with bortezomib and dexamethasone for the treatment of patients with multiple myeloma and belinostat for the treatment of patients with peripheral T-cell lymphoma (PTCL) [95]. Further, combination treatments of epi-drugs have proved to be a new effective strategy [96,97].

- *The differential PTMs in tumor tissues compared to resection margins (histopathologically normal) can serve biomarker for defining true cut margins.*

This has been demonstrated in case of prostate cancer (PCA) where the malignant and normal tissues could be differentiated based on their H3ac and H3K9me2 levels [98]. Similarly, H3S10ph levels of R0 resected margins could serve as a potential molecular marker for predicting prognosis of R0 resected GC patients [91]

- *Alteration in histone PTMs during the course of therapeutic interventions may in predicting response to different treatment modalities.*

In case of PCA, hormone refractory prostate cancer patients have high levels H3K4me1, H3K4me2, and H3K4me3 marks and so these could be used to stratify patients for androgen based hormone therapy [98].

2.9 Gastric cancer

Gastric cancer is a multistep and multifactorial disease that involves accumulation of tumor cells in the lining of the stomach. The complex disease arises from a precursor or *de novo* lesion in the mucosa (the inner lining of the stomach) that continuous to grow slowly in the other underlying layers viz; a) Mucosa b) Sub-mucosa c) Muscularis and d) Serosa of the stomach (Figure 2.9).

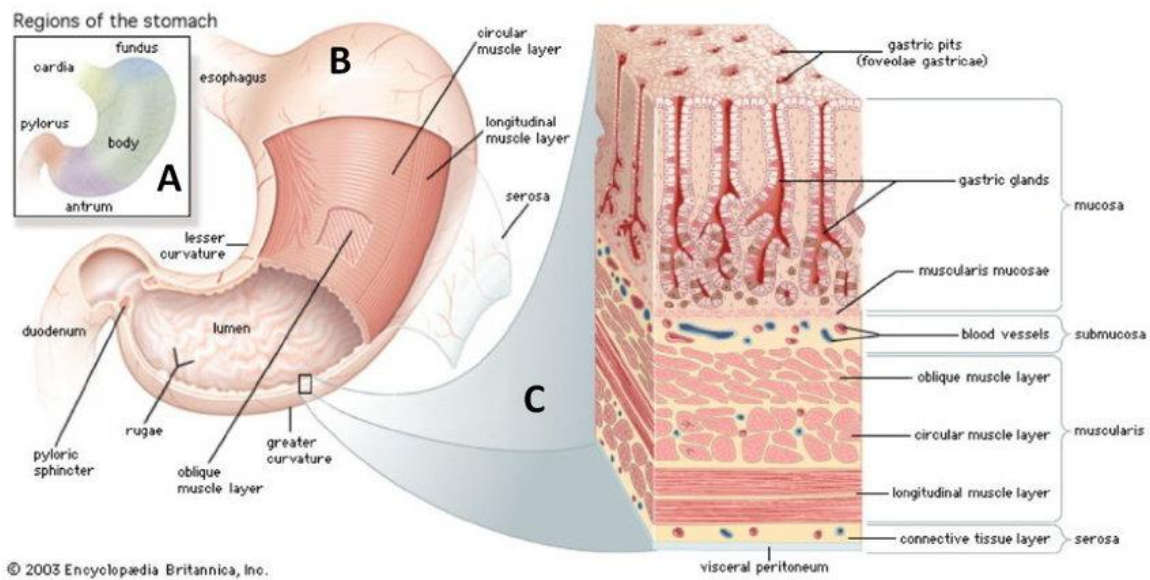


Figure 2.12 Anatomy of stomach and stomach wall Stomach is divided into proximal (cardia, fundus, corpus or body) & distal stomach (antrum and pylorus) Source- Britannica Encyclopedia

Ultimately in about 10% of the cases the gastric dysplasia formed may lead to the generation of a fully grown adenocarcinoma which is predominantly observed in gastric cancer. The tumor cells can metastasize and infiltrate the neighboring lymph nodes, lining the gastrointestinal tract. It is only in the advanced stage of the cancer, where it has the potential to spread to distant organs like peritoneum, liver and bones.

2.10 Prevalence, incidence and mortality

According to GLOBOCON-2018, worldwide a million new cases and around 7 lakh deaths were accounted by gastric cancer. Gastric cancer (GC) is the 3rd leading cause of cancer deaths, 5th in terms of incidence in the world, and the most lethal cancer in Asia.

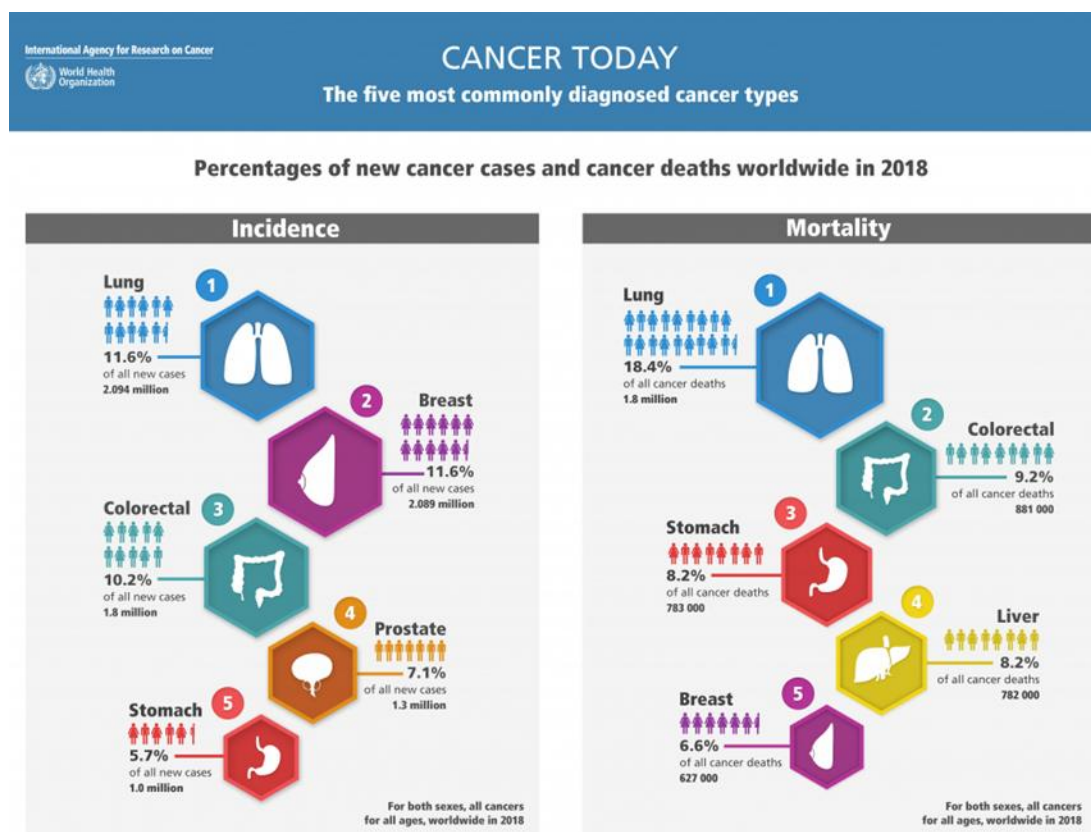


Figure 2.13-Incidence and mortality of different cancers. Dataset depicting the percentage of cancer incidence and mortality as per GLOBOCON-2018 study. Gastric cancer ranked 5th and 3rd in terms of incidence and mortality worldwide. (Source-<https://gco.iarc.fr/>)

The incidence rates vary geographically with East Asia (South Korea with the highest rate) having the highest incidence rate, whereas Northern America, Europe and Africa have the lowest. Males are twice more susceptible than females [2]. Overall, a decrease in global age standardized incidence has been observed over the past few decades especially

in the non cardia type (distal region of stomach) of GC. This has been attributed to control of *H pylori* infection, improved hygiene, antioxidant rich diet and advanced diagnostic methods. However, the surge in cardia type cancers continues [99,100]. The ~5 year survival rate is around 20% and has improved over the last few decades with rates as high as 71.59% in South Korea, due to advancement in early diagnostic methods [101]. The survival rate has a positive relation with early detection [100].

In India, GC is one of the most aggressive cancers, ranking 5th in terms of incidence and mortality [2]. According to the Global Burden of Disease Study 1990–2016, the age standardized incidence rate of stomach cancer in India has decreased across all states since 1990, yet it is responsible for the high proportion of cancer DALY (Disability Adjusted Life Years) (over 9% of the total cancer DALYs). Similarly to global risk factors, the decrease is due to improved life style and diet, reduced consumption of salty food, reduced smoking, but not associated with *H. pylori* as the prevalence of infection is persistent [99,102]

2.11 Classification of gastric cancer

The histological classification system employed is based on pathohistological (microscopic morphology, tissue architecture and cell type) manifestations in the cancer and its correlation with pathophysiological characteristics of the patient and overall outcome [103]. Recently the heterogeneity in gastric cancer has been molecularly classified into four important subtypes based on gene expression based molecular markers [104].

2.11.1 Laurens classification:

The lesions are classified into one of the three major types viz; (i) intestinal (54%) (ii) diffuse (32%) and (iii) intermediate or mixed type containing equal features of the first two types (15%). It takes into consideration the natural history of gastric carcinoma in association with environmental factors, changes in incidence, carcinogenesis, cell differentiation and predisposers [103,105]. The differences have been tabulated in Table 2.7 and the histological features are depicted in Figure 2.14.

**Table 2.7 Differential characteristics of the major types of
Lauren's classification**

Characteristics	Intestinal type	Diffuse type
Gross morphology	Exophytic	Ulcerating, diffuse
Microscopy	Glandular	Single cells, signet-ring cells
Main co-existing precancer condition	Atrophic gastritis, intestinal metaplasia	Non-atrophic gastritis'
Precancer lesion	Adenoma, dysplasia; Correa sequence	Foveolar hyperplasia?
Age	Old age	Young age, all age group
Sex	Males > females	Equal
Prevailing site	Antrum and angulus	Corpus, whole stomach
Metastasis	Lymph nodes, liver	Lymph nodes,
Biology	Oestrogen protects?	Neuroendocrine differentiation?
Prior or co-existing	Common by serology (>80e90%)	Common (>90%)
<i>H. pylori</i>	False-negative results frequent with breath test, antigen stool test biopsy-based urease test, or by microscopy,	All tests are reliable

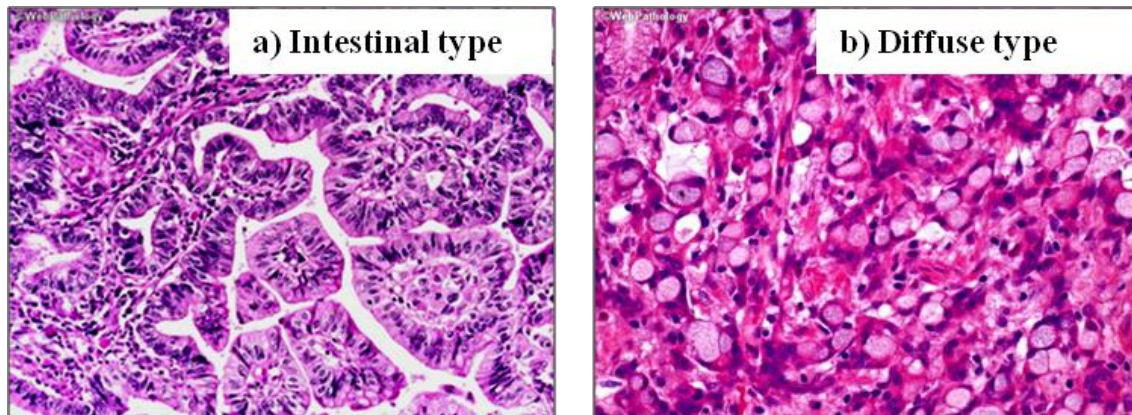


Figure 2.14 Lauren's classification - a) Intestinal type - Tubulo-papillary structure; b) Diffuse type – Cells with large intracytoplasmic vacuoles and peripheral nuclei, a feature of Signet Ring Carcinoma. *Source- Webpathology.com.*

2.11.2 WHO classification:

It classifies gastric cancer based on type of cells involved and histological features viz; epithelial and non-epithelial (sarcomas), majority of which are epithelial. Of the epithelial type almost 90% are adenocarcinomas and are classified into 4 major types, viz tubular, papillary, mucinous and poorly cohesive (includes signet ring carcinoma, SRC and non-signet ring tumor cells). Besides these, uncommon histological variants do exist [103,106].

2.11.3 Anatomical Classification:

Based on the location, the tumor are classified as Cardia (tumors arising in proximal region) and Non Cardia (tumors arising in distal region). Non-cardia gastric cancer accounts for the majority of the cases worldwide and is the predominant type in high-risk areas.

2.11.4 Molecular classification of gastric tumors

As a part of The Cancer Genome Atlas (TCGA), the gastric cancer genome, epigenome and transcriptome has been widely studied and based on common gene signatures, DNA methylation pattern and mutational status; four molecular subtypes have been proposed.

This includes i) EBV – Epstein bar virus positive ii) CIN-Chromosome instability iii) MSI- Microsatellite instable and iv) GS –genome stable group. As the classification is based of molecular alterations, stratification of patients for the subtype specific relevant targeted therapy could be achieved [104]. The salient features of this group are graphically presented in Figure 2. 15

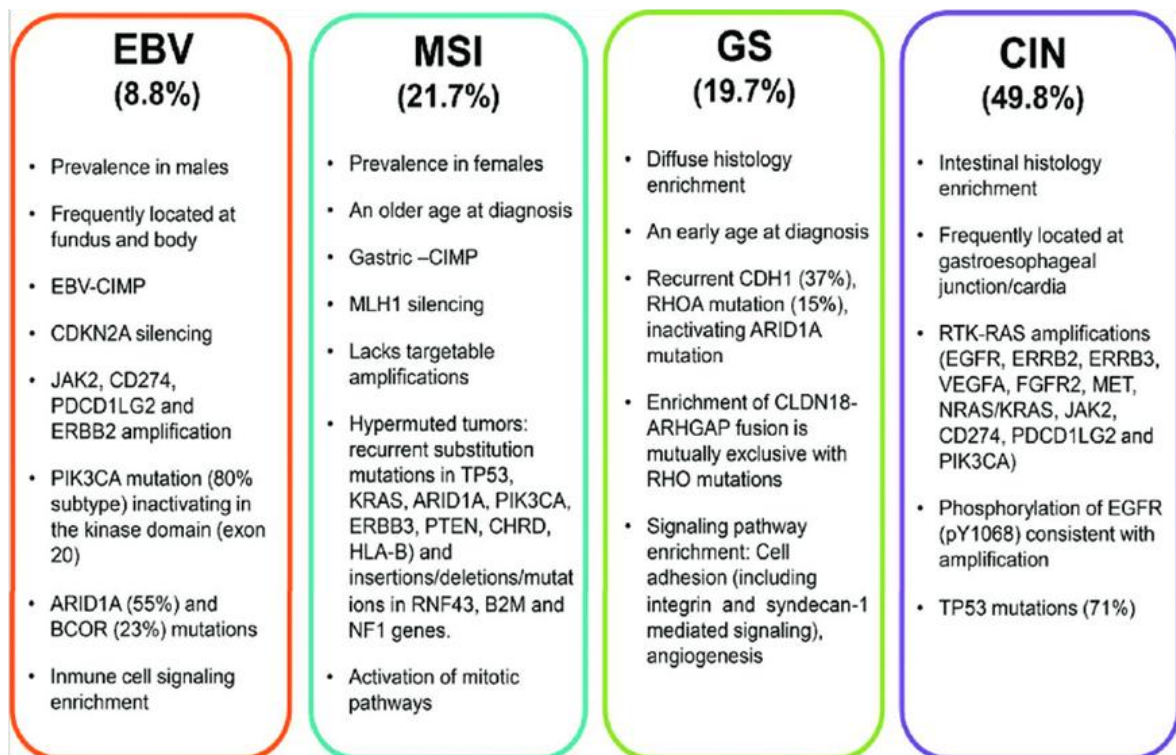


Figure 2.15 Molecular features of the four subgroups classified on the basis of gastric adenocarcinoma dataset of TCGA It includes Epstein Bar virus positive (EBV), Microsatellite instable (MSI), Genome stable (GS) and Chromosome instability (CIN) group [104]

2.12 Etiological Factor for gastric cancer development

Gastric carcinogenesis being multifactorial and cancer a number of environmental and host related factor are implicated in its pathogenesis. A few of the major etiological factors have been discussed as follows and summarized in Figure 2.16

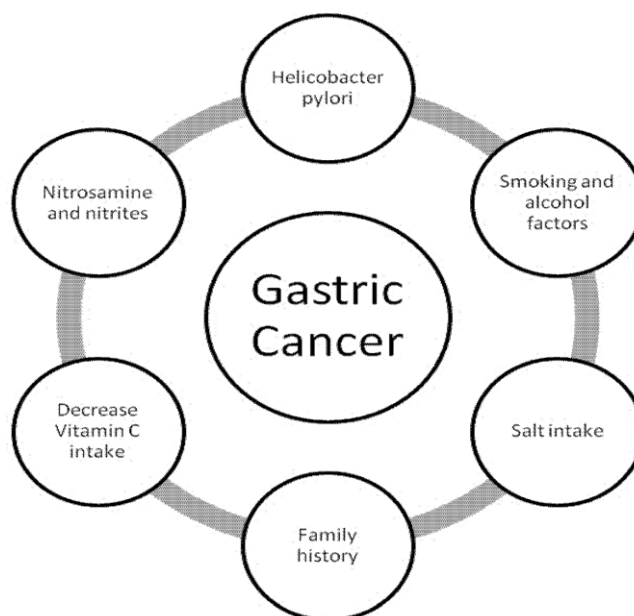


Figure 2.16 Etiological factors associated with development of gastric cancer. Host related factors like diet, genetics and behavioral practices like smoking or alcohol and environmental factors like *H pylori*, nitrosamine pollutants together contribute to development of gastric cancer [107].

2.12.1 Dietary factors

Consumption of high salt, smoked meat, pickled and processed food has been associated with gastric cancer development as they could be the source of nitroso compounds. Salt is an irritant and causes inflammation in gastric mucosa which is a prime event in carcinogenesis. On the other hand, diet rich in antioxidants, Vitamin C and short chain fatty acids has a counteractive effect [100,108].

2.12.2 *H pylori*

One of the predisposing factor of gastric cancer is *Helicobacter pylori* infection which has been classified as a type I carcinogen. The effects of *H. pylori* infection on gastric cancer appear multifactorial, involving host and environmental factors. The inflammatory response mounted and the CagA protein secreted by *H pylori* that causes aberrant Wnt pathway activation, are key mechanisms associated with pathogenesis of GC. *H pylori* is involved in both intestinal and diffuse type cancers and mostly affect the non cardia region of stomach [100,108].

2.12.3 Nitroso compounds

Nitroso compounds like NDMA and methylnitrosourea are known to induce mutations via DNA adduct formations like O⁶methylguanine adducts that can give rise to G to A transition mutations and also to sister chromatin exchange in a dose and exposure dependent manner [109]. Besides genetic, nitroso compounds could also alter the epigenome via histone PTMs, DNA methylation, and chromatin remodelling [83,110]. The sources of nitroso compounds could be dietary; via occupational exposure or endogenously derived through nitrosation of amino acids in the stomach and colon [100].

2.12.4 Genetics

Around 1-3% of GC's have a hereditary predisposition that is grouped into three syndromes: gastric adenocarcinoma and proximal polyposis of the stomach (GAPPS), hereditary diffuse gastric cancer (HDGC) and familial intestinal GC. HDGC have germline mutations in tumor suppressors CDH1, CTNNA1, BRCA2 and STK11. Besides these people suffering from Li-Fraumeni syndrome (germline mutation of TP53), Peutz-Jeghers syndrome (frameshift mutation in STK11), hereditary nonpolyposis

colorectal cancer (mutation in mismatch repair genes) and familial adenomatous polyposis (germline APC mutation) are susceptible to GC [107].

2.13 Gastric carcinogenesis

Development of gastric cancer is a gradual process wherein continuous insult of the gastric tissue, together by interaction with the host related factors leads to accumulation of molecular and phenotypic alteration resulting in pre-neoplastic and neoplastic lesions [111]. Based on epidemiological and pathological evidence, Correa proposed a multistep model of gastric carcinogenesis for the intestinal type of gastric cancer (Figure 2.17).

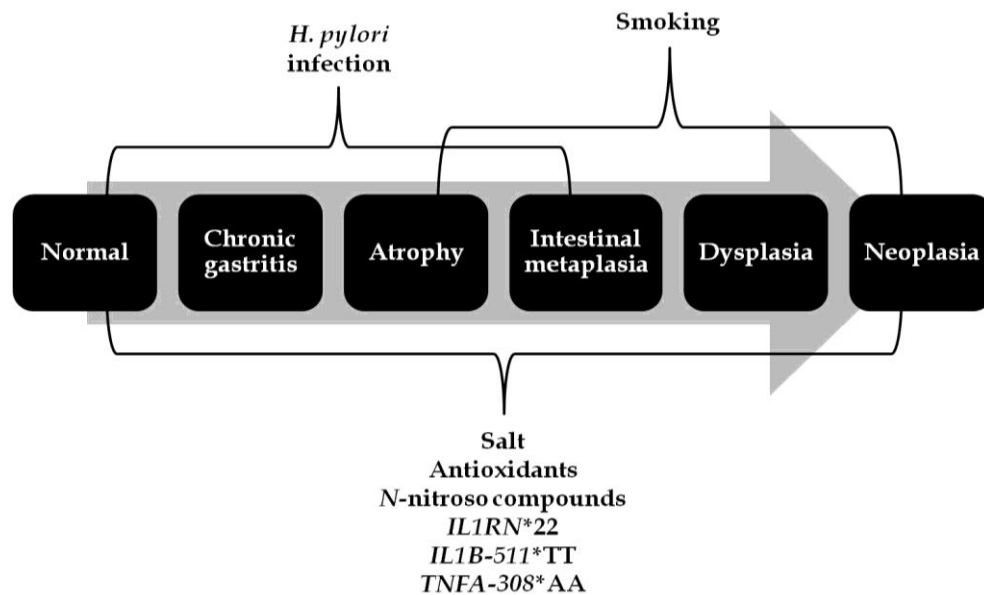


Figure 2.17 Proposed model depicting the multistep process of gastric carcinogenesis (Correa's model). Host related factors like gene polymorphisms and diet together with environmental factors like nitroso compounds and *H. pylori* play key roles during the early steps of the process which are reversible. Accumulation of *de novo* mutations occurs at a later stage, transmuting the pre-neoplastic lesions to neoplastic ones [112].

The first stage of **chronic gastritis** sets with inflammation of gastric mucosa which becomes less conspicuous with age. Following this stage, progressive **atrophy** results wherein there is loss of glandular activity (chronic atrophic gastritis) and is characterized

by cell differentiation resulting in **intestinal metaplasia** with mucous secreting intestinal cells [113,114]. These stages are aggravated by irritants like salts, spice and consumption of diet poor in antioxidants and vitamins [112]. Excessive salt damages gastric mucosa, which stimulates increased cell proliferation so as to regenerate the withered mucosal epithelium. This together with *H pylori* infections sets chronic inflammation, leading to increased inflammatory response by immune cells generating ROS. The ROS generated together with the nitroso compounds produced in the gastric lumen causes DNA damage and acquirement of mutations. With loss of regulation these cell undergoes multiple rounds of proliferation giving rise to pre neoplastic lesions which breaches the gastric tissue organization, resulting in dysplasia which eventually progresses to a full blown adenocarcinoma [111]. In contrast, diffuse type of gastric cancer has an early onset and do not follow a multistep pattern. However, their development is associated with *H pylori* and chronic inflammation [115]. Interestingly, based on molecular classification of GC, a very few genetic driver events are associated with gastric carcinogenesis and almost 20% of the tumors show modest genetic alteration (GS genome stable type), impinging the role of epigenetic events evolving simultaneously during the process [104].

2.14 Epigenetics and Gastric Carcinogenesis

Gastric carcinogenesis involves molecular alterations at DNA, RNA and epigenetic levels (Figure 2.18). DNA methylation studies of gastric tumors have highlighted the progressive methylation of genes from atrophy to intestinal metaplasia to adenocarcinoma stage. A number of genes associated with cell cycle regulation (p16, p14), tumor suppression (SFRP,TFF1,CHD5), cell adhesion (CDH1) and DNA repair (hMLH1, MINT) are downregulated in GC due to CpG island hypermethylation which

contributes to genome instability and survival [116–119]. The presence of this methylation phenotype during the early stage of carcinogenesis, suggests the presence of a field which is conducive for accumulation and selection of genetic aberration. Corroborating this, in the MSI group of GC, DNA methylation of the mismatch repair gene hMLH1 has been attributed to its microsatellite unstable genome [119]. Infact, in a MNU induced gastric carcinogenesis model of mice, treatment with a DNMT inhibitor

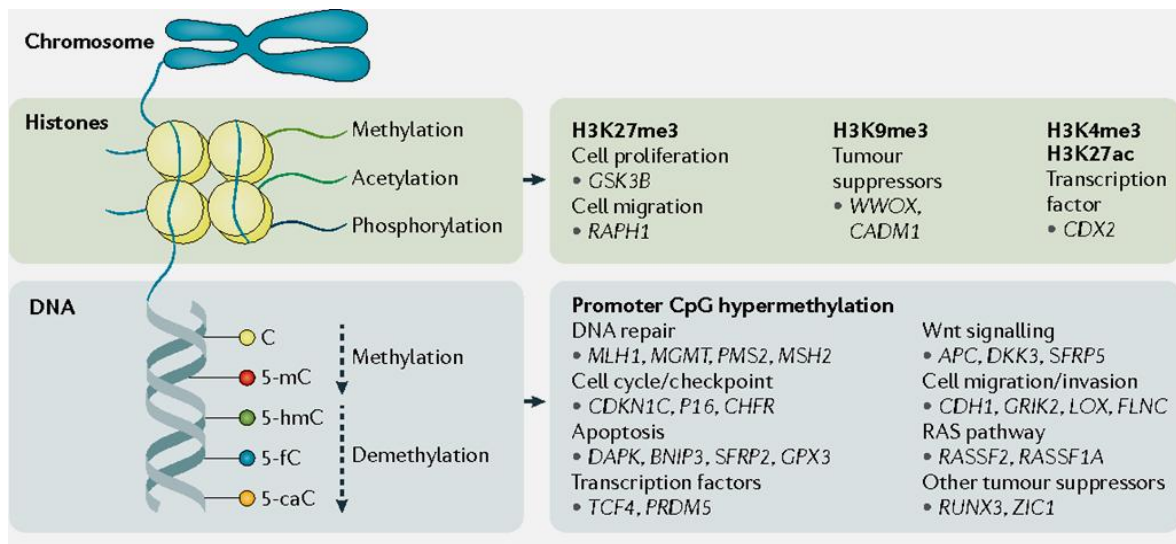


Figure 2.18 Epigenetic alterations in gastric cancer. Development of gastric cancer involves alterations in the three epigenetic process viz DNA methylation, histone modifications and miRNA profile. These alterations lead to aberrant silencing of tumor suppressors involved in cell cycle regulation, control of apoptosis, cell migration and aberrant activation of signaling pathways like Wnt [104].

was shown to prevent the development of cancer, consolidating the role of aberrant DNA methylation in the early steps of gastric carcinogenesis [120]. In a Mongolian gerbil model system the role of *H pylori* induced inflammatory response in causing DNA methylation was established [121]. The treatment of *H pylori* infection was found to reverse methylation of CDH1 (Cadherin1), MGMT (Methylguanine DNA methyltransferase) and COX2 (Cyclooxygenase2) and treatment with anti-inflammatory

drugs reduced DNA methylation and the subsequent development of gastric cancer. Unlike *H pylori*, hypermethylation mediated by EBV (Epstein bar virus) does not involve role of inflammation but a modulation in DNMT levels and loss of TET expression. The EBV group of gastric cancer exhibits the highest level of DNA methylation referred as the CIMP or CpG island methylator phenotype [119,122]. Like DNA hypermethylation, global DNA hypomethylation especially in repetitive elements LINE1 and ALU were also found to parallel the transition from chronic gastritis to intestinal metaplasia and further to adenocarcinoma and correlated with poor prognosis in GC [123,124]. Thus, aberrant DNA hypermethylation and hypomethylation, both could act as an epimutation, driving GC.

DNA methylation is known to occur simultaneously with histone PTM. ChIP sequence coupled with DNA methylation profiling has demonstrated the association of H3K27me3 with repression of promoter hypermethylated genes in gastric cancer [125,126]. This is consistent with the progressive increase in H3K27me3 levels with the pathology of GC [127]. Similarly, in an IHC based investigation, H3S10ph and γ H2AX was found to progressively increase during the course of gastric carcinogenesis from non atrophic gastritis to adenocarcinoma; with relatively high level in *H pylori* group [128,129]. The progressive increase in H3S10ph could be interphase associated as there was no correlation with Ki67 staining. Interestingly, the H3S10ph labeling progressed positionally with the pathology of disease from the bottom antral to the top corpus region [128]. A recent report on *H pylori* and MNU induced gastric carcinogenesis has further supported the role of increased H3S10ph. In this model; inflammation mediated STAT3 (Signal Transducer and Activator of Transcription) activation was found to be the cause

of aberrant MSK activation and increased H3S10ph levels which led to expression of oncogenes like NFATC (Nuclear factor of activated T-cells) and genes associated with inflammatory response that mediate cancer progression [130].

2.15 Alterations in histone PTMs and modifying enzymes in Gastric Cancer

Alterations in global histone PTM changes and their correlation with clinicopathological characteristics of patients have been well documented in gastric cancer. Some of these key alterations and modifiers have been further validated in cell lines and animal models to elucidate the mechanism. Few of these alterations studied in gastric cancer have been listed below and summarized in Table 2.8

- a) One of the earliest histone modifications to be investigated in gastric cancer was H4 acetylation (H4ac), which was found to be downregulated in gastric carcinomas and adenomas compared to adjacent non neoplastic mucosa. This downregulation of H4ac significantly correlated with advanced stage, depth of tumor invasion and lymph node metastasis. Further, the decreased levels were also observed in some areas of intestinal metaplasia, suggesting its association with development and progression of gastric cancer [131].
- b) Park *et al.* reported high levels of the heterochromatic mark H3K9me3 in gastric cancer and addressed its strong correlation with tissue invasion, lymphovascular invasion, and tumor recurrence, resulting in poor prognosis. Further they found that the methylation dominant group (H3K9me3) had poor prognosis and survival compared to the acetylation (H3K9ac and H4K16ac) dominant group [132]. Similar association of H3K9me2 and H3K9me3 with survival was supported by another independent study [133].

- c) He *et al.* demonstrated increased EZH2 and the subsequent H3K27me3 expression in gastric cancer tissues. Its strong association with the tumor stage and lymph node metastasis established this mark as a potent prognostic marker for survival and tumor aggressiveness [127,133]. The aberration was targetable as the increased expression of EZH2 was found to be regulated by STAT3 signaling and a combinatorial treatment with si-STAT3 and EZH2-specific inhibitor, 3-deazaneplanocin A (DZNEP) was found to increase apoptosis in GC cell lines [134].
- d) PRMT-6 (Protein arginine methyltransferase 6) mediated asymmetric (as) dimethylation of H3R2 (H3R2me2as) is another methylation mark with high prognostic value. A strong correlation between increased PRMT6 and H3R2me2as was observed in GC patients and it resulted in poor survival outcome. Interestingly, knockdown of PRMT6, restored the expression of tumor suppressor PCDH7 (Protocadherin 7), affecting the proliferation and invasiveness of gastric cancer cells [135]
- e) Loss of H4K16ac is also reported in gastric cancer and was found to be a result of downregulation of hMOF. This decreased hMOF levels correlated with clinicopathological characteristics like T-stage, lymph node metastasis and distant metastasis [91,132,136]
- f) H2B mono-ubiquitination was found to be an independent prognostic marker for GC due to its strong association with tumor differentiation, lymph node metastasis, TNM stage and overall survival. Loss of this mark correlated with progression of cancer, from the well differentiated intestinal phenotype to poor differentiation type of Lauren's classification [137].

g) Multiple studies have highlighted the aberrant overexpression of HDAC's in gastric cancer. In a retrospective analysis, either all three or one of the 3 Class I HDACs were found to be highly upregulated in GC [138]. Further, this high expression correlated with lymph node metastasis and poor survival of patients. High levels of HDAC1 & 2 were also validated by Mutze *et al* who proposed their role in chemoresistance [139]

Table 2.8 Histone modification and modifiers altered in gastric cancer [25,91]

Histone Modifications		
	Level	Correlation with
H3K9me3	High	Lymphovascular invasion, tumor stage, survival and recurrence
H3K27me3	High	Lymph node metastasis
γH2AX	High	Invasiveness, differentiation, lymph node metastasis and <i>Helicobacter pylori</i> positive intestinal metaplasia and dysplasia
H3S10ph	High	Survival
H3R2me2 (asymmetric)	High	Survival
H2B mono-ubiquitination	Low	Tumor differentiation, lymph node metastasis, TNM stage and overall survival
Epigenetic Modifier		
HDAC 1	High	Poor survival
HDAC 2	High	Nodal state and tumor grade
PCAF	Low	Tumor invasion, size, stage and survival
EZH2	High	Tumor stage, lymph node metastasis and survival
PRMT 6	High	Tumor invasiveness and survival

H3 phosphorylation is another modification that has been studied in gastric cancer [128,129,140]. In Indian cohort, our group has reported significant loss of H4K16ac, H4K20me3 and gain of H3S10ph in gastric cancer tissues compared to histopathologically normal resection margin. This increased H3S10ph was found to be p38-MAPK and MSK dependent. Interestingly, with respect to distance from the site of tumor, higher H3S10ph levels were observed in the negative resected margins which had a direct association with clinicopathological characteristics. This suggests the possibility of field cancerization wherein, presence of initiated cells with molecular alterations like H3S10ph may seed for loco-regional recurrence which is observed in GC. Thus, MSK mediated H3S10ph has a prognostic utility in predicting survival and defining the true negative resection margin in gastric cancer [91].

H3S10ph has been found to be upregulated in pre-neoplastic lesions of GC and in coherence with histone acetylation it mediates transcription of immediate early genes during cellular transformation. Therefore, the importance of crosstalk between H3S10ph and neighboring histone acetylation marks is envisaged in the proposed study. Further, mechanism of histone phosphoacetylation during gastric carcinogenesis is studied in-depth in G1 phase of cell cycle. This would help us in understanding the mechanistic role of pathways active during the early stages of gastric cancer that could be targeted, making timely intervention possible.

Chapter 3
Aims & Objectives

3.1 Statement of purpose

Multiple studies have highlighted alteration in histone post translational modifications, modifying enzymes and their association with clinicopathological parameters in gastric cancer. Our lab has also established the prognostic utility of increased H3S10ph of tumor tissues with survival, in Indian cohort of GC. Interestingly, with respect to distance from the site of tumor, high H3S10ph levels in the histopathologically normal adjacent or disease free margins correlated with the clinicopathological characteristics and poor survival. This suggests that initiated cells with altered epigenetics marks are key events in the early steps of carcinogenesis. The increased H3S10ph may drive the process towards neoplasia considering its role in transcription of oncogenes and its association with transformation. Therefore, it becomes imperative to understand the early driver epigenetic events during the process of carcinogenesis. Epigenetic alterations being reversible, such study could aid in early detection and disease outcome through therapy

3.2 Hypothesis

Previous work in the lab has led to the identification of differentially expressing histone post translational modifications in gastric cancer patients. A p38 stimulated and MSK mediated increased H3S10ph alongwith hypoacetylation of histone H3 and H4K16ac, has been observed in tumour compared to their normal resected margin. H3S10ph and neighbouring histone acetylation (H4K9ac, H3K14ac, and H4K16ac) has been shown to works in combination leading to a particular cellular function.

Therefore, we hypothesize that understanding the cross-talk between acetylation and phosphorylation of histones and its mechanism will provide important information involved in the process of gastric carcinogenesis. In the present study, we are interested

to understand and delineate the early alteration in histone phosphorylation and acetylation, and the associated cross-talk that might re-programme the gene expression pattern favouring cancer development. This will also help us to explore the targetable epigenetic events which could be used for early prediction and therapy.

3.3 Objective

In light of this background, the objective of the present study is

‘To study the association between phosphorylation and acetylation of histone H3 and the modifying enzymes involved in cellular transformation’

To address the objective the following questions have been formulated:

- 1) To study the alterations in histone post-translational modifications and the associated modifiers upon cellular transformation.*
- 2) To define the role of MSK1 in regulating phosphorylation of histone H3 and its potential importance in acetylation of neighboring lysine residues in gastric cancer cells*
- 3) To define the role of MSK1 mediated phosphorylation of H3S10 and H3S28 in mitotic cells.*
- 4) To study the significance of global histone hypoacetylation in altering the efficacy of chemotherapeutic drug in gastric cancer cell lines and pre-clinical model.*

3.4 Work-plan

- 1) To study the alterations in histone post-translational modifications and the associated modifiers upon transformation**

- a) Generation of transformed cell line by treating untransformed gastric cell line, HFE145 with methylnitrosourea.
 - b) *In vitro* and *in vivo* validation of malignant transformation by soft agar assay and tumorigenicity in NOD-SCID mice.
 - c) *Ex vivo* tissue explant preparation and culture of cell lines E3.2 and E2.1.
 - d) Phenotypic characterization of transformed cell line by assessing clonogenic potential, ploidy changes by flow cytometry and proliferation by MTT assay.
 - e) Investigation of alterations in histone PTMs H3S10ph, H3S28ph, H3S10phK14ac, site specific H3 acetylation and the associated chromatin modifiers (MSK1, Histone deacetylase 1 HDAC1 and histone acetyl transferases, GCN5 and PCAF).
 - f) MAPK pathway assessment in histone PTM regulation by using specific inhibitors.
 - g) Investigating the enrichment of H3S10phK14ac phosphoacetylation mark in euchromatin or heterochromatin by partial Micrococcal Nuclease (MNase) digestion followed by salt fractionation.
- 2) **To define the role of MSK1 in regulating phosphorylation of histone H3 and its potential importance in acetylation of neighboring lysine residues in gastric cancer cell line.**
- a) Effect of MSK knockdown on histone PTMs and physiological parameters like proliferation, anchorage independent growth and clonogenic potential.

- b) Identifying the regulatory mechanism for phosphoacetylation of histones using MSK inhibitor, H89 and HDAC inhibitor, valproic acid
 - c) Assessment of chromatin occupancy of respective epigenetic modifier by cell fractionation.
 - d) Assessment of MSK inhibition on HDAC1 expression by real time PCR and western blotting.
 - e) Biological significance of association between phMSK1 and HDAC1 by serial transplanted xenograft tissues.
 - f) Occupancy of H3S10ph and H3K14ac on HDAC1 promoter and MSK binding site analyzed by ChIP qPCR.
 - g) Level of HDAC1 and its association with survival analyzed by immunohistochemistry on samples obtained from an Indian cohort of gastric cancer patients.
- 3) To define the role of MSK1 mediated phosphorylation of H3S10 and H3S28 in M phase cells.**
- a) Levels of MSK1 and phMSK1 in asynchronous, G₁ phase and mitotic cells assessed by western blotting and cell fractionation.
 - b) Role of MSK in mitotic H3 phosphorylation and acetylation studied by inhibition with specific inhibitor H89.
 - c) Effect of MSK and Aurora kinase B inhibition on mitotic exit of cells analyzed by flow cytometry and western blotting.

- d) Pathway regulating MSK mediated mitotic H3 phosphorylation studied by using MAPK inhibitors.
- 4) **To study the significance of global histone hypoacetylation in altering the efficacy of chemotherapeutic drug in gastric cancer cell lines and pre-clinical model.**
- a) Histone acetylation and histone deacetylase (/HDAC) activity in gastric tumor tissues and cell lines assessed by western blotting and colorimetric assays, respectively.
- b) Analysis of data present at The Cancer Genome Atlas (TCGA) to study transcript level heterogeneity of class I HDACs and validation in human gastric tumor tissue samples and cell lines by real time PCR.
- c) Identifying regimes for enhancing drug binding to DNA by combinatorial treatment of HDAC inhibitors with chemotherapeutic drugs in different regimes followed by drug binding assay.
- d) Identification of most potential combinatorial regime of HDACi and chemotherapy drugs by MTT assay, fraction affected curve analysis and median plot analysis.
- e) Assessing alterations of histone acetylation, chromatin remodelling, cell cycle arrest and transcription associated with pre-treatment regime.
- f) *In vivo* assessment of potential effectiveness of pre-treatment regime with valproic acid and cisplatin in NOD-SCID mice.

Chapter 4
Materials & Methods

4.1 Cell Culture

4.1.1 Cell Lines

Gastric cancer cell line, AGS (ATCC® Number: CRL-1739™, moderately differentiated), the normal immortalized cell line HFE145 (SV40T-antigen and hTERT), MNU treated cell lines viz MNUI, MNUIII, MNUV and the explants cell lines E3.2 and E2.1 were used in the study. All cell lines were maintained in RPMI medium (Invitrogen) supplemented with sodium bicarbonate, L-glutamine and non essential amino acids. The cells were grown at 37°C in 5% CO₂ supplemented with 10% FBS (Gibco-South American origin), 100units/ml penicillin and 100mg/ml streptomycin (Hi-Media). Fresh medium was added every alternate day.

4.1.2 Trypsinization, sub-culturing and maintenance

The cells were trypsinized and sub cultured as per the experiment using the standard protocol with slight modifications [141]. For trypsinization, a 90% confluent 90mm dish (5 X 10⁶ cells) was washed with 3ml of 1X PBS (Phosphate Buffered Saline), pH 7.2-7.4 (137mM NaCl, 2.7mM KCl, 8mM Na₂HPO₄, and 2mM KH₂PO₄) followed by treatment with 1ml trypsin/EDTA (0.25% w/v trypsin, 0.2% EDTA in 1X PBS) solution. The trypsin was aspirated after 60 seconds and cells were incubated at room temperature for 3 minutes. Cells were harvested in 3ml of complete RPMI medium and sub-cultured with a split ratio of 1:4 or counted as per the experimental requirement. Cells were counted on hemocytometer using Erichrome B staining method and number of viable cells/ml was calculated using the following formula.

No. of cells/ml = average number of cells per WBC chamber × dilution factor (2) × 10⁴.

4.1.3 Freeze stock preparation and cell line revival.

A 90% confluent 90mm dish was used to make freeze stocks for storage. Following trypsinization as mentioned above the harvested cells were centrifuged for 5 minutes at 3000 rpm. The supernatant was aspirated and the cells were resuspended in 1ml of freezing media (90% serum and 10% DMSO). The identity of cell line with respect to name, passage number and date of preparation were recorded on the vials. The cells were gradually frozen at -20°C for 2 hours and -80°C overnight before transferring them to liquid nitrogen for long term storage.

For reviving the cell lines, the freeze vials were thawed by immersion in 37°C water bath for 3 minutes. The thawed suspension was aseptically transferred to a sterile 15ml tube containing 5ml culture medium and centrifuged for 5 minutes at 3000 rpm. The cell pellet was resuspended in fresh media and plated in a T-25 flask containing media with 20% serum. Cells were allowed to attach overnight (37°C, 5% CO₂) before media was replaced and cells were passaged or sub-cultured as described above.

4.1.4 Cell cycle synchronization

Cell cycle synchronization was done by serum starvation method, double thymidine block or using nocodazole as per the experiment. Serum starvation protocol- Cells at 40-45% confluency (90mm plate) were washed with 1X PBS twice for 60 seconds. This was followed by incubation in 4ml of 1X PBS for 15 minutes. The cells were grown in incomplete RPMI for 48 hours with addition of fresh media after every 24 hours. Double thymidine block was employed for G1 arrest. The cells at 40% confluency were incubated in 4mM thymidine (Sigma) for 15 hours followed by a 12 hours release period in complete RPMI without thymidine post thorough 1X PBS washing. This was repeated

and 14 hours post 2nd release the cells were enriched in G1 phase. For M phase synchronization, cells at 70-80% confluency were treated with 0.03µg/ml of Nocodazole for 16 hours. The mitotic cells were collected by mitotic shake off method.

4.1.5 Cell cycle analysis

Cell cycle phase was analysed by flow cytometry using propidium iodide staining method. Briefly cells were washed twice with 1X PBS, resuspended in 200µl of 1X PBS and fixed by adding 70% chilled ethanol dropwise while vortexing. The cells were fixed overnight at -20^oC. Post fixation, cells were washed with 1X PBS to remove alcohol, resuspended in 500µl of PBS containing 0.1% Triton X-100 and 100µg/ml of RNase A for permeabilization and RNase inactivation respectively. Post incubation for 15 minutes at 37^oC, 25µg/ml of propidium iodide (Sigma) was added, mixed and the suspension was further incubated at 37^oC for 15 minutes. The DNA content was analyzed on a FACS Calibur flow cytometer (BD Biosciences, USA). Mod-FIT software was used for analyzing the data. For ploidy determination, human lymphocyte from healthy individual was used as a diploid control and the DNA Index was calculated by dividing the G0/G1 channel of test cellline by G0/G1 channel value of diploid lymphocytes [142].

4.2 Genetic Manipulation

4.2.1 MSK1 shRNA cloning

To understand the role of MSK1 in phosphoacetylation of histones, it was knocked-down in AGS and MNUV cell line. For the knockdown approach MSK1 (Genbank-AF074393) shRNA sequence was obtained from the TRC portal of Broad's Institute and it was cloned in pLKO.1-EGFP-f puro vector using restriction sites for AgeI and EcoRI.

Positive clones as selected by restriction enzyme digestion were validated by DNA sequencing.

4.2.2 Transfection of MSK1

Transfection in AGS and MNUV cell line was carried out by Fugene HD (Promega) or Turbofect (Thermoscientific) transfection reagent as per the manufacturer's protocol. Briefly, the cells were grown at 50% confluency in 30mm plate in complete DMEM medium. 2µg of plasmid was diluted in 200µl of media to which 6µl of transfection reagent (ratio of 1:3) was added and incubated at room temperature for 20 minutes to form complexes. The mixture was overlaid on the cells dropwise and was incubated for 24 hours at 37⁰C in 5% CO₂. The selection was under 200ng/ml of Puromycin (Hi-Media).

4.3 Tissue Samples

4.3.1 Tissue collection and inclusion/exclusion criteria

Paired freshly resected frozen (FRF) tissues samples from normal adjacent gastric mucosa (negative resection margin) and tumor samples and formalin-fixed paraffin-embedded (FFPE) tissues blocks (N=25) were earlier collected from GC patients through ICMR-tumor tissue repository of Tata Memorial Hospital, Mumbai, India. The protocol was earlier reviewed and approved by institutional review board and ethics committee (Project No 466). The tissue samples were utilized in the present project. Around seven inclusion criteria- *Adenocarcinoma (type of cancer)*, *Curative surgery (intent of surgery)*, *Indian (domicile of the patient)*, *HBV infection negative*, *HCV infection negative*, *HIV infection negative* and *Igm (tissue weight, only for FRF tissues)* were followed and

written informed consent was undertaken earlier from all the patients. Based on histopathological analysis, the tumor content was found to be >60% in all tumor samples and no tumor cell was found in the negative resection margins. All the patients were operated between 2009 and 2012 at Tata Memorial Hospital, Mumbai, India. The FRF tissues were frozen immediately in liquid nitrogen, and stored at -80°C until required for experimental use. The clinicopathological characteristics of the patient are tabulated in Table 10.1.

4.3.2 Preparation of tissue section slides

The FFPE tissue blocks were processed on a microtome (*Leica*) and $4\mu\text{m}$ thick sections were prepared. Tissue sections were then transferred to clean poly-L Lysine coated slides and incubated overnight at 37°C . These tissue slides were then stored at room temperature until required for experimental use [143].

4.3.3 Hematoxylin and eosin staining

The staining was done on poly-L lysine coated glass tissues slides as per the standard protocol. The FFPE tissue sections slides were deparaffinized by incubating at 65°C overnight. The molten paraffin was washed off by two xylene treatments for 10 minutes each and then treated with 100% ethanol twice for 5 minutes each. After air drying for 30 min at 37°C the FFPE and FRF tissues slides were stained with 0.1% Mayer's hematoxylin (Sigma) for 10 minutes, rinsed in running tap water for 5 minutes and then dipped in 0.5% eosin for 10 times, each lasting for 1-2 seconds. The excess stain was removed by dipping in distilled water until the eosin stops streaking, followed by 5 minutes washes in 50, 70 and 100% graded ethanol solutions. In the end, slides were cleaned by washing in xylene and mounted with DPX mountant (Qualigens) [144]. The

H&E stained tissue sections were used for histopathological analysis to confirm the identity of the tissues and the tumor content.

4.4 Immunohistochemical staining

4.4.1 Immunohistochemistry

Immunohistochemical staining was performed using VECTASTAIN® ABC kit (Vector Lab). Formalin-fixed paraffin-embedded tissue blocks were sectioned at a thickness of 4µm and mounted on poly-L-lysine coated glass slides. The sections were deparaffinized through a graded series of xylene and rehydrated through a graded series of absolute alcohol to distilled water. The endogenous peroxidase activity was quenched with 3% hydrogen peroxide in methanol at room temperature for 30 minutes in dark. The antigen retrieval was carried out in cooker with 1M Tris buffer (pH 4.0). The primary antibody was used at a dilution of 1:100 (HDAC1; Sigma) and the slides were incubated overnight in a humidified chamber. The developing was done with diaminobenzidine (DAB; Sigma) staining for 5 minutes. The sections were washed under flowing tap water and counterstained with Harris's hematoxylin. The slides were then dehydrated with a graded series of absolute alcohol to xylene and mounted with DPX mountant. The control slides consisted of sections without primary antibody treatment [145]. The nuclear immunohistochemical staining was scored using H-score which is based on intensity of staining (ranges zero to three) and percentage of stained cells using the formula,

H-score= [(0 x % of cells with staining intensity of zero) + (1 x % of cells with staining intensity of one) + (2 x % of cells with staining intensity two) + (3 x % of cells with staining intensity three)].

The immunohistochemical staining was analyzed by pathologist, Dr Poonam Gera at TMC-ACTREC.

4.5 Transformation model

4.5.1 Generation of a transformed gastric cell line

The transformation process was carried out using N-methyl-N-nitrosourea (MNU), as a source of nitroso compound with few modifications [146,147]. A non-lethal dose (25µg/ml) was selected for the study after screening a series of doses (25µg/ml-200µg/ml) for their effects on cell morphology and proliferation for 48 hours. Around 3×10^5 cells were treated for 1 hour at 37°C in a 60mm plate. Post-treatment two washes of 1X PBS were treated to remove residual MNU, fresh media was added and the cells were allowed to grow for 48 hours. The cells were then sub-cultured for next round of treatment. Five rounds of treatment were given and freeze vials were prepared after 1st, 3rd and 5th treatment, resulting in cell lines MNUI, MNUIII and MNUV (Figure 4.1). The transformation was validated by performing soft agar assay and subcutaneous injection of the cells in NOD-SCID mice.

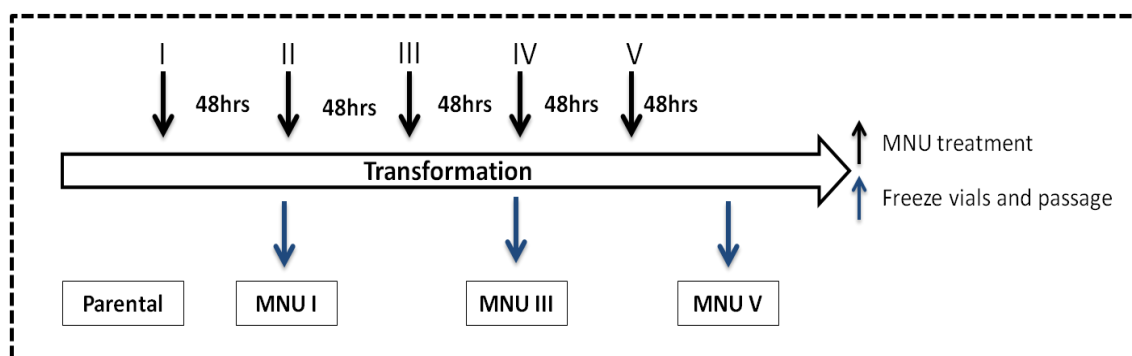


Figure 4.1- Schematic diagram depicting the protocol for methylnitrosourea induced transformation of HFE145 cell line. Cells were treated with 25µg/ml of MNU for 1hour.

4.5.2 Development of explants cultures

Around 8 million MNUV cells were subcutaneously injected into the right hind flanks of 6-8 week old NOD-SCID mice. The tumors developed post 3 months were aseptically removed in a petri dish and washed multiple times with sterile 1X PBS containing 100units/ml penicillin and 100mg/ml streptomycin. It was then minced into small pieces, washed thoroughly with 1X PBS and slices of around 2mm thickness from the core were placed in sterile 30mm plates (1piece per plate). The slices were submerged with RPMI media supplemented with 10% FBS, 100units/ml penicillin, 100mg/ml streptomycin and 2mM L-glutamine. The medium was changed twice a week and post 20 days, the single clone explant cultures of MNUV cell line developed. Two cell lines MNU E3.2 and MNU E2.1 were derived.

4.6 *In vivo experiments*

4.6.1 Development of xenograft mouse model system:

All animal experiments were performed under Institutional Animal Ethics Committee–approved protocol and institutional guidelines for the same (Proposal No 05/2014). Xenograft mouse models were developed with AGS and the MNU transformed MNUV cell line. MNUV cell line was injected to determine its tumorigenicity and AGS cell line was used to study the *in vivo* therapeutic potential of chemotherapeutic drug (Cisplatin) and epi-drug (Valproic acid). NOD-SCID strain (non-obese diabetic and severe combined immunodeficiency) of immune-compromised mice was obtained from ACTREC animal house facility and were maintained in ventilated caging. About 3-8 million AGS and MNUV cells were subcutaneously injected into the right hind flanks of 6-8 week old NOD-SCID mice. The growth of the tumor was monitored over a period of 3 months

around which tumor induction was observed. After 3 months when the tumors reached a length of around 12mm; the mice were sacrificed in a CO₂ chamber and the tumors were excised.

4.6.2 Tissue block preparation

A part of the xenograft tumor was frozen in liquid nitrogen and stored at -80⁰C and the other part was used for paraffin block preparation. The tissue was fixed in 10% formalin in 1X PBS overnight, washed with water to remove excess formalin and dehydrated with 70% ethanol overnight. Blocks were prepared and sectioned from the fixed tissue as described in 4.3.2 using standard procedure for histopathological examination. [143].

4.6.3 *In vivo* therapeutic utility of chemotherapeutic drug and epi-drug

To study the *in vivo* therapeutic potential of a combination therapy of VPA and cisplatin a xenograft model with AGS cell line was developed. About 3 million AGS cells were subcutaneously injected in four- to six-week old NOD-SCID mice. Post 3 months of injection, when the tumor reached a length of ~12mm, it was transplanted subcutaneously in multiple mice. Tumors with a size of ~5mm were then divided in the following cohorts: saline only, VPA only, cisplatin only and VPA followed by cisplatin (pre-treatment group). VPA and cisplatin were administered intraperitoneally at a dose 300mg/kg/d and 2mg/kg/d twice a week for 5 weeks with an interval of 2 days from the last doses as shown in Figure 4.2. After tumor development and the respective treatment regimes, the animals were sacrificed by exposing to a carbon dioxide saturated atmosphere. The tumor tissues were collected; tissue blocks were prepared and sectioned for H&E staining.

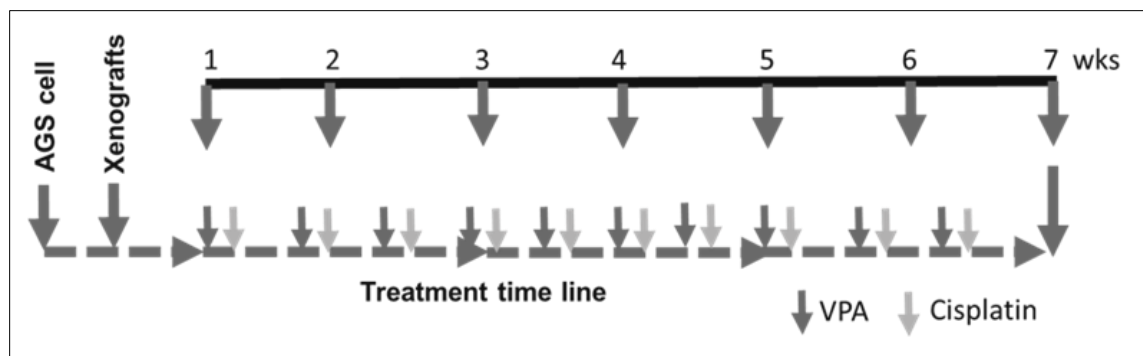


Figure 4.2- Schematic diagram depicting the schedule of chemotherapeutic drug and HDAC inhibitor administration. VPA (300mg/kg/d) and Cisplatin (2mg/kg/d) were administered intraperitoneally twice a week for 5 weeks.

4.6.4 Tumor growth

Tumor growth was monitored once per week by measuring two perpendicular tumor diameters with a caliper. Post-drug treatment animals were monitored for 5-6 weeks and sacrificed when the largest tumor diameter reached 12mm. Tumor volume was calculated as $V = \pi / 6 \times \text{length} \times \text{width}^2$.

4.7 Phenotypic Assays

4.7.1 Short term proliferation assay

Cellular proliferation was quantified by the ability of viable cells to reduce tetrazolium salt 3-(4,5-dimethylthiazol-2-yl)-2, 5-diphenyl tetrasodium bromide (MTT) to a colored formazan product. Around 2000 cells per 100 μ l of media were plated in triplicates on a microtiter plate. After 24 hours intervals, 20 μ l MTT solutions (5mg/ml in PBS) was added to the wells and incubated further for 4 hours. Then, 100 μ l solubilization buffer (10% SDS, 0.1% HCl and 1% iso-propanol) was added to each plate and incubated overnight for 12 hours. The absorbance was measured at 570nm with Spectrostar Nano-

Biotek, Lab Tech plate reader and a graph of absorbance against number of days was plotted. The proliferation was assayed for 4-5 days [141].

4.7.2 Proliferation assay by cell counting

Around 25,000 cells were seeded in triplicates in 6 well plates and at an interval of 24 hours upto 96 hours the cells were harvested and counted by Erythrosin B staining [148]. Briefly 100µl of diluted cell suspension was mixed with 100µl of 0.5% Erythrosin B stain and was counted using a hemocytometer. Average of the triplicate readings at the respective time point was plotted against number of days.

4.7.3 Long term survival assay:

The clonogenic potential of cells was assessed by plating 1000-2000 cells in a 60mm plate in triplicates. The media was changed at regular time intervals and after 14 days the plates was stained. For this the colonies were first fixed with 4% paraformaldehyde for 30 minutes followed by staining with 0.5% crystal violet in 50% methanol for 1hour. The excess stain was removed by washing the plates in water and colonies with more than 50 cells were counted under a light microscope [149].

4.7.4 Soft agar colony formation assay

Confluent cell lines were harvested in their respective media, stained with trypan blue and the viable cells were counted using a hemocytometer. About 1000 cells were mixed in 0.4% top agar and seeded onto a 0.8% bottom agar layer in a 6 well plate. 100µl of complete medium was added thrice a week to prevent drying of surface and colonies were counted after 14 days under a light microscope (20X magnification) [150] for the respective cell lines and number of colonies were plotted.

4.8 Biochemical inhibition assays

Cells at 40% confluency were serum starved with incomplete RPMI for 48 hours to synchronize the cells and reduce the MAPK activity. The MSK specific inhibitor, H89 (Cell Signaling) and HDAC inhibitor, valproic acid was used in the study at 15 μ M and 4mM concentration, respectively. Sub-confluent cell cultures was pretreated with 15 μ M H89, 4mM VPA or DMSO as vehicle control for 30 minutes and then stimulated with 20ng/ml EGF (Sigma) or serum for 20 and 90 minutes, respectively. The ERK1/2, p38 and JNK inhibitor viz; PD98059 (Calbiochem), SB203580 (Calbiochem) and SP600125 (Calbiochem) were used at 10 μ M concentration for 1 to 3 hours on asynchronous or mitotic cells depending on the experiment. Whole cell lysates were prepared at the respective timepoints. AGS cells (70-80% confluency) were treated with 0.03 μ g/ml of nocodazole for 16 hours for mitotic synchronization. The mitotic cells were collected by shake off method and treated with the respective inhibitors viz; 15 μ M H89 and/or 0.2 μ M of aurora kinase B specific inhibitor AZD-1152 HQPA for 60 minutes. To understand the role of MSK in M-phase exit and entry into G1, the treated mitotic cells were centrifuged at 3000 rpm for 5 minutes. The cells pellets were then washed with complete media to remove nocodazole and H89 or AZD-1152 HQPA. The cells were replated in complete RPMI media with and without H89 or AZD-1152 HQPA for the indicated time periods.

4.9 Chromatin Organization assay

4.9.1 Micrococcal nuclease digestion assay

Around 6 X 10⁶ cells post trypsinization were washed with 1X PBS and resuspended in 400 μ l of chilled MNase digestion buffer (Table 10.3.1). The cells suspension was incubated on ice for 10 minutes and centrifuged at 4000 rpm for 5 minutes at 4^oC.

Purified nuclear pellet was resuspended in MNase digestion buffer with 2mM CaCl₂ and 50U MNase/mg of DNA. The concentration of the nuclei was estimated on Nanodrop at 260nm and adjusted to 1µg/µl. About 50µg of chromatin was used per timepoint and was incubated for 0, 2.5 and 5 minutes in 37⁰C water bath. The reaction was stopped by adding 2X lysis buffer (0.6M NaCl, 20mM EDTA, 20mM Tris–Cl, pH 7.5, 1% SDS and 150µg/ml RNase A) and incubated for 30 minutes at 37⁰C followed by Proteinase K (80 µg/mg DNA) treatment for 2 hours at 50⁰C. DNA was recovered by phenol–chloroform extraction followed by overnight ethanol precipitation at –20⁰C. The precipitated DNA was dissolved in 50µl TE buffer and concentration was determined by A260/A280 absorbance. MNase-digested samples were resolved on 1.8% 1 X TAE agarose gel and visualized by ethidium bromide staining.

4.9.2 MNase – Salt fractionation protocol

To explore the enrichment of H3S10phK14ac in euchromatic and heterochromatic nucleosomes a time dependent MNase followed by differential salt fractionation was performed. Modified Sanders method was used for the same [151–153]. Around 8×10⁶ cells were resuspended in chilled MNase buffer for 8 min on ice. The nuclei pellet was centrifuged at 3500 rpm for 5 minutes at 4⁰C. The concentration of nuclei was adjusted to 1µg/µl and around 250µg of nuclei was used. The nuclei were resuspended in MNase buffer and MNase was carried out using 2mM CaCl₂ and 50U MNase/mg of chromatin. The reaction was carried out in 37⁰C water bath for only 2.5 and 7.5 minutes and was stopped with 5mM EGTA solution. The partial MNase treatment is crucial for the release of euchromatin or more open chromatin associated nucleosome. The digested nuclei were then centrifuged at 4000 rpm for 5 minutes. The supernatant was collected and labeled as

S1. The nuclei pellet was resuspended in 200µl of fractionation buffer (Table 10.3.2) containing 100mM NaCl, and incubated on a 2D orbital platform at minimum speed for 1 hour at 4⁰C. It was then centrifuged at 4000 rpm for 5 minutes at 4⁰C to get the supernatant labeled as S2. The nuclei pellet was resuspended in 400mM fractionation buffer and again incubated as above followed by centrifugation to get the supernatant fraction S3 and the pellet P containing the insoluble chromatin fraction. The pellet was resuspended in 400mM fractionation buffer. From all the fractions, 1/3rd part was processed for DNA extraction and the remaining was used for protein lysate.

4.9.3 Chromatin Immunoprecipitation or ChIP assay

Around 1.2×10^7 asynchronously growing AGS cells were used for ChIP. Mononucleosome isolation was done in MNase digestion buffer containing 10mM CaCl₂ and was prepared by incubating 1mg chromatin with 150 units of MNase for 30 minutes at 37°C followed by inactivation of MNase by 5mM EGTA. The nuclei were resuspended in ChIP dilution buffer (Table 10.3.3) and 100 µg of chromatin was incubated with 1µg of anti- H3K14ac, anti- H3S10ph and IgG antibodies. 20µl of magnetic DYNA beads (Thermo Fischer) were added to chromatin-antibody mixture and incubated for 16 hours on a rotating platform. Separation of antibody-nucleosome complex and washing of bound complex was done using magnetic rack. The DNA was eluted in TE buffer and qPCR was carried out using 2X Taq Master Mix and a set of primers listed in (Table 10.3.12) [145].

4.10 Protein Lysate preparation and visualization

4.10.1 Nucleo-cytosolic and chromatin fractionation, and histone extraction

Around 6×10^6 cells were directly harvested in 500 μ l ice cold MKK lysis buffer (Table 10.3.4) and incubated for 30 minutes on ice with intermittent mixing. The cell lysate was centrifuged at 17,000 rpm for 20 minutes at 4⁰C to separate nucleo-cytosolic (supernatant) and chromatin pellet fraction. Histones were extracted from the chromatin pellets by acid extraction method [154]. Briefly, the chromatin pellet suspended in 0.2M H₂SO₄ was sonicated for 10 seconds at 10% amplitude, vortexed for 2 hours followed by centrifugation at 17,000 rpm for 20 minutes at 4⁰C. The acid soluble histones from the supernatant were precipitated overnight in acetone at -20⁰C. The histone pellets obtained after centrifugation at 17,000 rpm for 20 minutes at 4⁰C were washed with acidified acetone (containing 50mM HCl), acetone, dried in speedevap and then reconstituted in 0.1% β ME. Nucleo-cytosolic and histones/ chromatin fraction were resolved on 15% Sodium dodecyl- polyacrylamide gel electrophoresis (SDS-PAGE) respectively.

4.10.2 Whole cell and cytoplasmic lysate preparation, and nuclear fractionation

To prepare whole cell lysate, cells were washed with 1X PBS, resuspended in Nuclei extraction buffer (without spermine and spermidine) (Table 10.3.5) and incubated on ice for 10 minutes. Post incubation it was briefly sonicated at 20% amplitude for 10-15 seconds (to lyse the nuclei and shear chromatin) and centrifuged at 17,000 rpm for 10 minutes. The supernatant was taken as whole cell lysate and stored in -80⁰C till further use. For nuclear fractionation the cells post washing with 1X PBS were resuspended in Nuclei extraction buffer and incubated on ice for 10 minutes. The cells were centrifuged at 5000 rpm for 5 minutes and the supernatant was taken as cytoplasmic fraction. The

nuclear pellet was washed with nuclei extraction buffer, centrifuged and the supernatant was mixed with the cytoplasmic fraction. The nuclear pellet was resuspended in the nuclear extraction buffer until further use.

4.10.3 Sodium dodecyl polyacrylamide gel electrophoresis

Whole cell lysates and histone were separated on 10% and 15-18% sodium dodecyl sulphate polyacrylamide gels or SDS-PAGE; using Tris-Glycine buffer (25mM Tris-Cl, 250mM Glycine and 0.1% SDS; pH 8.3) (Table 10.3.6 and 10.3.7). The protein estimation was performed by Folin Lowry method and the protein samples for gel loading were made in 2X SDS-loading buffer (50mM Tris-Cl pH 6.8, 20% v/v glycerol, 4% SDS, 2% β -Mercaptoethanol and bromophenol blue), boiled for 10 minutes and stored at -20°C until further use.

The electrophoresis was carried out at a constant current of 15 mA in the stacking gel and 25 mA in the resolving gel until the tracking dye bromophenol blue reached the bottom or it was over run in case of histones. The gels were then subjected to staining by coomassie or silver impregnation method or transferred onto PVDF (Polyvinylidene difluoride) membrane for western blotting.

4.10.4 Coomassie Staining

Post electrophoresis the gels were transferred to a tray containing Coomassie Brilliant Blue R-250 (CBBR) staining solution (0.1% w/v CBBR, 10% acetic acid and 50% methanol in water). After staining for 5 hours to overnight, the gel was destained with a solution of 50% methanol and 10% acetic acid in water, with several changes until clear protein bands were visible [155].

4.10.5 Silver Impregnation method

In case of histone the protein visualisation was done by ammonical silver nitrate method. Post electrophoresis the gel was washed three times in 50% methanol with shaking for 5 hours to overnight to remove excess SDS. It was then gently washed in MQ and immersed in silver stain solution which was prepared by dropwise addition of silver nitrate solution (0.8% final) in ammonical sodium hydroxide (0.38%) solution in water until the dark precipitate becomes invisible. Post 30 minutes incubation on a rotating platform, the solution is decanted and a MQ wash for 5 minutes is given, followed by developing with a developer (0.15ml formaldehyde and 15mg citric acid in 100 ml D/W) until the bands appear. The reaction is stopped with detainer solution (50% methanol and 10% acetic acid in MilliQ) [156].

4.10.6 Western Blotting and Developing

The proteins (50-70 μ g for WCL and 8-10 μ g for pure histones) from the SDS-PAGE gels were transferred onto 0.05 μ M PVDF membrane which was preactivated in absolute methanol for 60 seconds followed by MilliQ. The gel equilibrated in 1X transfer buffer (Table 10.3.8) was sandwiched between 3 sheets of Whatman filter; inserted in the transfer assembly tank (Trans-Blot Cell, Bio-Rad) and the transfer was carried out at 300 mA for 4 hours under cold conditions. The transfer of proteins was verified by staining the membrane with Fast green dye (0.05% in destainer solution) followed by destaining until clear band appears. This was followed by water washes and the membrane was scanned and stored in MilliQ at around 10⁰C. The proteins transferred onto PVDF membrane were probed using specific antibody conditions as listed in (Table 10.3.10). Briefly the membrane was blocked in 'blocking buffer' i.e. 5% BSA or skimmed milk in

1X TBS-T (Tris-buffered saline with Tween-20) for 1 hour at room temperature on orbital shaker. The membrane was then treated with primary antibody prepared in 1-5% BSA in TBST using the recommended and standardized dilution for 1 hour to overnight incubation at 4⁰C on an orbital shaker. The membrane was thoroughly washed three times with 1X TBS-T for 10 minutes each at room temperature. The membrane was then incubated with the horse radish peroxidase (HRPO) conjugated secondary antibody in 5% BSA in 1X TBS-T for 1 hour at room temperature on orbital shaker. Post incubation the membrane was washed vigorously three times with 1X TBS-T at room temperature and developed using ECL-Plus chemiluminescence kit (Millipore) or Bio Rad's Clarity Max. The signal was detected and captured in Biorad's Chemidoc analyser using the Image Lab 6.0 software for processing.

4.11 Immunofluorescence Microscopy

Cells were seeded over sterilized glass coverslips in 30mm tissue culture dishes. The cover slips containing cells were washed twice with 1X PBS and fixed with 4% paraformaldehyde (Sigma) for 20 minutes. The fixative was washed off twice with 1X PBS and cells were permeabilised using 0.2% Triton X-100 in 1X PBS for 10 minutes. Cells were washed twice with 1X PBS and placed in primary antibody dilution (Table no 10.3.10) at 4°C overnight. Next day, the cells were washed three times each, with 1X PBS and 0.1% NP-40 containing 1X PBS, and placed in fluorophore conjugated secondary antibody (Invitrogen) dilution for two hours in dark conditions. All the subsequent steps were performed in dark. Excess secondary antibody was washed with 1X PBS and 0.1% NP-40 containing 1X PBS and coverslips were DAPI stained (0.1µg/µl) for 5 minutes and excess stain was washed with 1X PBS. Mounting medium

for fluorescence was added on clean glass slides and coverslips were carefully placed on the glass slides and imaged using Zeiss 510 Meta-confocal imaging system. Image analysis was performed using Image J or FIJI software.

4.12 RNA extraction and real time PCR

RNA was extracted by TRIZol method (Invitrogen 5596026) as per the manufacturer protocol. The integrity of the RNA was checked on standard MOPS gel and cDNA was synthesized using ThermoScientific Revert-Aid cDNA synthesis kit as per the manufacturer's protocol using random primers (Fermentas, K1632). cDNA was subjected to real-time (SYBERgreen, AgilentTech) PCR for the analysis of respective chromatin modifier genes. RT-PCR amplification was done using specific primers with initial denaturation at 95°C for 2 minutes; followed by 30 cycles of denaturation at 95°C for 30 seconds, primer annealing at 60°C for 30 seconds, primer extension at 72°C for 1 minute and a final extension at 72°C for 10 minutes. The data analysis was performed using the $\Delta\Delta C_t$ based calculations and fold change was plotted. In case of semi-quantitative PCR Dream-Taq 2X Master mixes (New England Biolab) was used using the same conditions. The amplified products were resolved on 1.5% agarose gels and visualized by Ethidium bromide staining. The list of primers used in the study is tabulated in (Table 10.3.11).

4.13 Histone deacetylase assays.

Assays were performed using the colorimetric HDAC activity assay kit from BioVision (BioVision Research Products, USA) as per manufacturer instructions. Around 100 μ g of whole cell lysate prepared using modified NP-40 buffer (Table 10.3.9) was used for the assay. Briefly, the lysates were incubated with HDAC colorimetric substrate (acetylated lysine side chain) at 37°C for the deacetylation reaction. Post 2 hours incubation, the

lysine developer was added which generates a chromophore with the deacetylated lysines; the levels of which correlates with the HDAC activity. Lysates with 1mM VPA served as the negative control. The absorbance was measured at 405nm wavelength and the average absorbance of duplicates was plotted.

4.14 Chemotherapeutic and Epi drug based assays

4.14.1 Drug-DNA interaction assay

AGS cells were treated with chemotherapeutic drugs viz cisplatin, oxaliplatin or epirubicin with or without HDAC inhibitors (HDACi) viz VPA, TSA and SAHA in three different combinations [a) Pre-treatment HDACi → chemo drug; b) Concurrent HDACi & chemo drug together and c) Post-treatment Chemo drug → HDACi]. The IC-50 concentrations were previously determined in the lab and post 24 hours treatment the cells were washed and nuclei was isolated as described in section 4.10.2. To estimate the DNA concentration at 260nm, a part of the nuclear pellet obtained was lysed in nuclei lysis buffer (200µl 5mM urea-2mM NaCl) and the DNA concentration was adjusted to 1µg/ml. An equal volume was taken to measure the concentration of DNA-bound cisplatin, oxaliplatin and epirubicin at 220, 205 and 254nm, respectively, as per European Pharmacopoeia 5.5 and previous research works [157]. The average absorbance of three independent experiments was plotted for each of the chemotherapeutic drugs and the absorbance was considered to be directly proportional to the amount of DNA bound to drug.

4.14.2 Fraction-affected curve analysis

Fraction-affected (FA) curves is a method to analyze growth inhibition using multiple drugs and involves analyzing the growth inhibition with drug concentration above and below the IC-50 values of the individual drugs keeping a fixed ratio of the two drugs (Table 10.3.12). Using this method MTT assays were carried out and the cell survival percentage values obtained from three independent experiments was plotted. The fraction-affected values that represent the percentages of cell death were calculated using the following formula: FA value = $1 - (\% \text{ cell survival}/100)$. FA values ranged from 0.01 to 0.99 with value 1 denoting complete cell death. The readings and calculations were interpreted using CompuSyn software, which is based on the Chao Tally's algorithm [158,159]. FA values and respective combined doses of the drugs were used to generate the FA curves.

4.14.3 Median effect plot analysis

The median effect plot helps us understand the nature of interaction between two drugs with respect to growth inhibition. It shows the combination index (CI) on the Y-axis and FA values on the X-axis. CI values for a particular FA value range from 0 to 1 with CI < 0.8, CI = 0.8- 1.2, and CI > 1.2 representing the synergistic, additive or antagonistic nature of drug combinations, respectively. were used to generate The median effect plots were generated from the FA values and total doses of drug combinations (chemotherapeutic drugs and HDACi) with the help of CompuSyn software [158,159].

4.15 *In silico analysis of The Cancer Genome Atlas for gastric cancer*

To analyze the expression levels of HDAC1, HDAC2 and HDAC3 in normal and tumor samples of pan cancer, TCGA PANCAN normalized RSEM counts were obtained from

UCSC cancer genome browser. p-value was determined using Wilcoxon-Mann-Whitney test analysis.

4.16 Statistical analysis

All data are expressed as average obtained \pm standard deviation (SD) from n=3 experiments. Statistical significance was determined by conducting an un-paired student's *t*-test. All p values were two-sided, and $p < 0.05$ was considered significant. The graphs were plotted using GraphPad Prism 6 software.

Chapter 5

Results

5.1 To study the alterations in histone post-translational modifications and the associated modifiers upon cellular transformation

5.1.1 Epigenetic alterations with transient N-methyl-N-nitrosourea treatment and DNA damage response

According to Correa's model, nitroso compounds and the damage caused by them is one of the factors contributing to gastric carcinogenesis. So, N-methyl-N-nitrosourea (MNU) was chosen as a source of nitroso compound to develop the *in vitro* gastric carcinogenesis model. MNU being unstable at ambient temperature and acidic pH, a 1 hour exposure was given as per the protocol developed by Rhim *et al* [147]. A non-lethal dose of the carcinogen was determined by treating sub-confluent HFE145 cells (normal immortalized) with increasing doses of MNU for 1 hour and performing MTT assay after 24 and 48 hours (Figure 5.1 A).

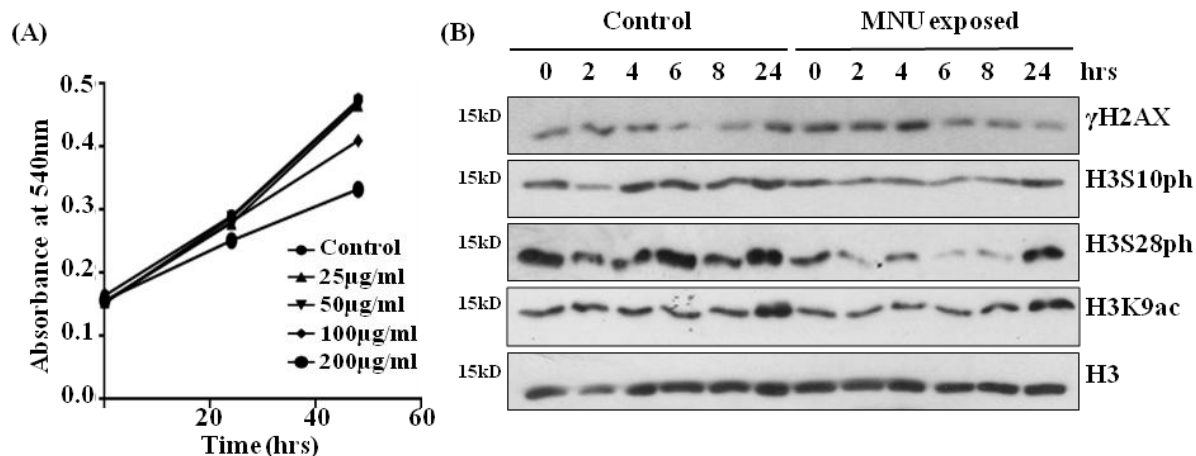


Figure 5.1 Dose determinations for methylnitrosourea treatment for development of *in vitro* gastric carcinogenesis model and its effects on histone PTMs (A) Graphical representation of MTT assay to find the non-lethal dose of MNU. HFE145 cells were treated with 25-200 µg/ml concentrations of MNU for 1 hour (B) Western blots showing the kinetics of histone post translational modification, viz induction of γ H2AX and loss of H3S10ph, H3S28ph and H3K9ac post DNA damage by MNU treatment (25 µg/ml for 1 hour). The basal levels were recovered within 24 hours suggesting recovery post damage. hrs- hours

A dose of 25 μ g/ml and 50 μ g/ml did not show any significant cell death and therefore was used for further experiment. The potency of 25 μ g/ml dose to induce DNA damage and repair was studied by checking its effect on histone modification. The data suggested an increase in γ H2AX levels indicating DNA damage post 1 hour treatment which was restored to its normal level within 24 hours in MNU treated cells. Interestingly, a decrease in H3S10ph, H3S28ph and H3K9ac was also observed post-MNU exposure which was recovered within 24 hours (Figure 5.1 B). This is consistent with earlier report from our lab wherein a decrease in H3S10ph and H3K9ac was observed post-DNA damage by IR radiation [51]. Thus, the dose of MNU used for the model development had a functional effect on chromatin dynamics and was non-lethal.

5.1.2 Cellular transformation of HFE-145 cell line

The transformation model of gastric cancer was developed by five rounds of MNU treatment (25 μ g/ml) to HFE145 cell line (Figure 5.2 A).

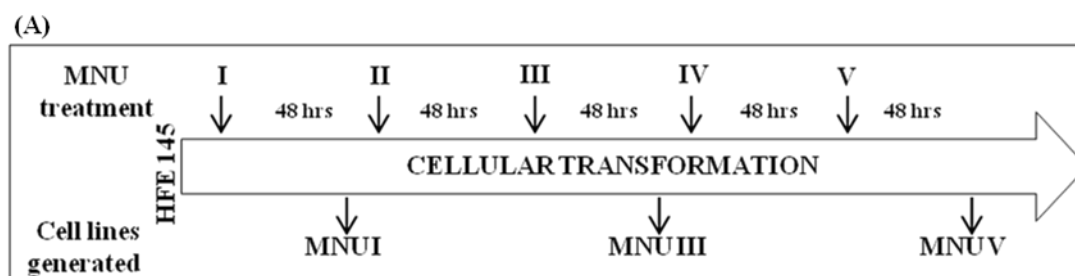


Figure 5.2 Cellular transformation of HFE145 cell line. (A) Schematic workflow for transformation of HFE145 cell line using methyl nitrosourea (MNU). Briefly 3×10^5 cells were treated with a non-lethal dose of MNU for 1 hour followed by washing and recovery of cell. Post 48 hours the next round of treatment was given. Five rounds of treatments were given and cell lines were generated at 1st, 3rd and 5th treatment; viz, MNUI, MNUIII and MNUV. hrs- hours

The cell lines derived viz, MNUI, MNUIII and MNUV showed no morphological alterations under light microscopy (Figure 5.2 B). The cellular transformation was

confirmed by the anchorage independent growth employing the soft agar assay. The colonies were observed only in MNUV cell line (Figure 5.2 C, left panel). The colonies were counted and represented graphically (Figure 5.2 C, right panel). This suggested that MNUV cell line is transformed; anchorage independent growth being the property of transformed cells.

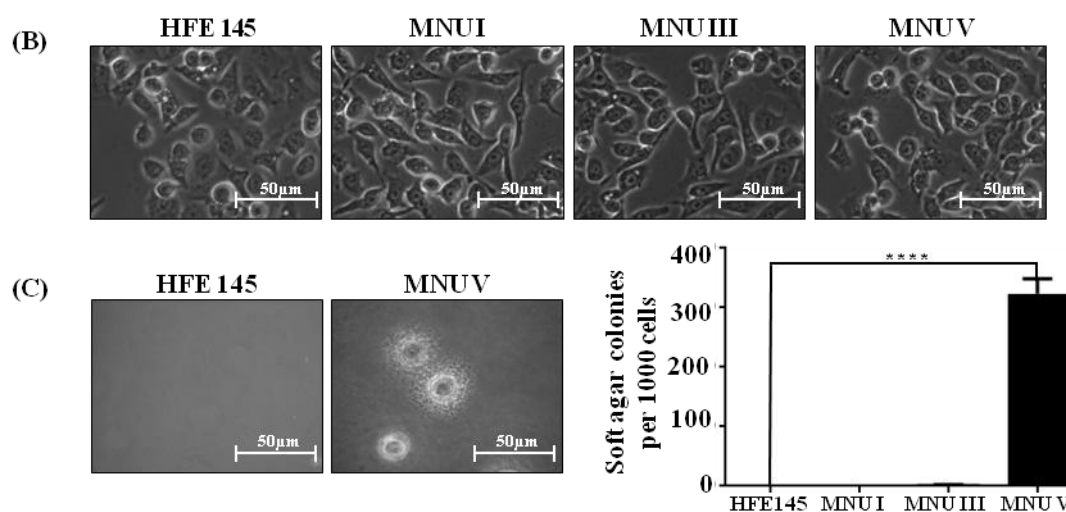


Figure 5.2 Cellular transformation of HFE145 cell line. (B) Light microscopic images showing morphological features of the cell lines generated (Scale -40X). (C) Soft agar assay showing colonies formed by MNUV cell line (left panel) and the number of soft agar clones observed (right panel). Unpaired student's t-test applied for statistical analysis **** $p < 0.0005$.

5.1.3 Alteration in phenotypic properties during cellular transformation and development of explant cultures

After *in vitro* validation of cellular transformation of MNUV cell line, the alteration in proliferation and clonogenic potential was studied and compared to parental HFE145 cell line. The data showed that there is no significant change in cell proliferation (Figure 5.3 A); however, a significant increase in clonogenic potential was observed in MNUV cell line (Figure 5.2 B&C). Further, no significant alteration in cell ploidy was observed upon transformation as assessed by flow cytometry using lymphocyte control (Figure 5.2 D).

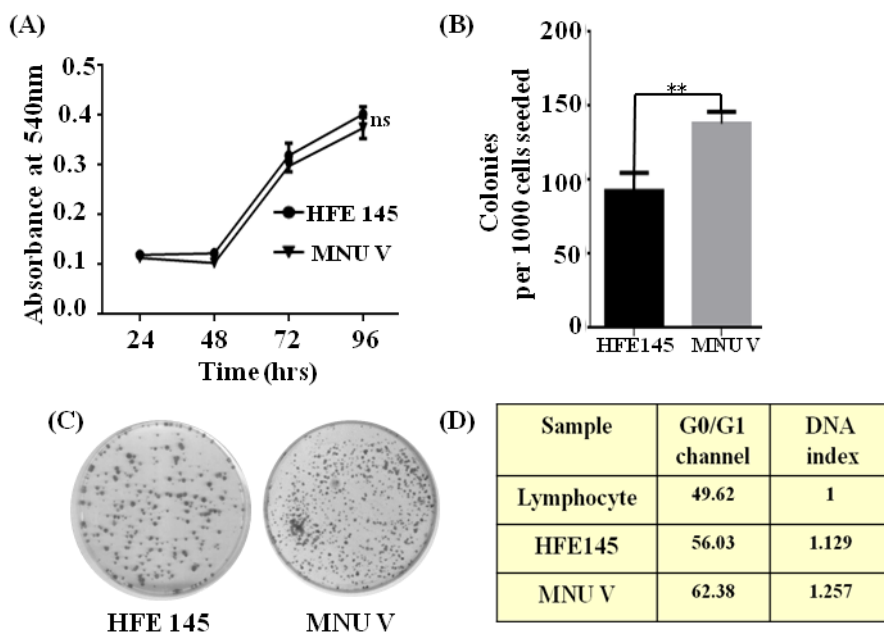


Figure 5.3 Alteration in phenotypic properties associated with transformation of HFE145 (A) MTT assay carried out to assess the change in proliferation during transformation. (B&C) The clonogenic potential was assessed and a significant increase in the percentage of colonies formed was observed in MNUV cell line. Unpaired student's t-test applied for statistical analysis. $**p < 0.005$; hrs- hours.(D) Ploidy changes was studied by flow cytometry using lymphocytes as diploid control. DNA index = Sample G0/G1 channel / Lymphocyte G0/G1 channel.

The tumorigenic potential was validated *in vivo* by subcutaneous injection of 10 million MNUV cells in NSG mice (Figure 5.4 A). Tumors (12mm in length) were observed post 3 months of injection and grew successfully post two subcutaneous serial transplantation in NOD-SCID mice. To understand the pathology of tumor, H&E stained sections of tumor were subjected to histopathological examination. Glandular growth of tumors with well to poorly differentiated cell types, characteristic of adenocarcinoma of stomach were observed (Figure 5.4 B). Thus, the tumor developed from the transformed cell line mimicked the pathology of gastric tumors *in vivo* (Figure 5.4 C). Further, to understand the alteration in histone PTMs from the initial transformed state (MNUV) to the progressive state, explants cultures were established from the tumors as MNUE3.2 and MNUE2.1 cell lines (Figure 5.4 D).

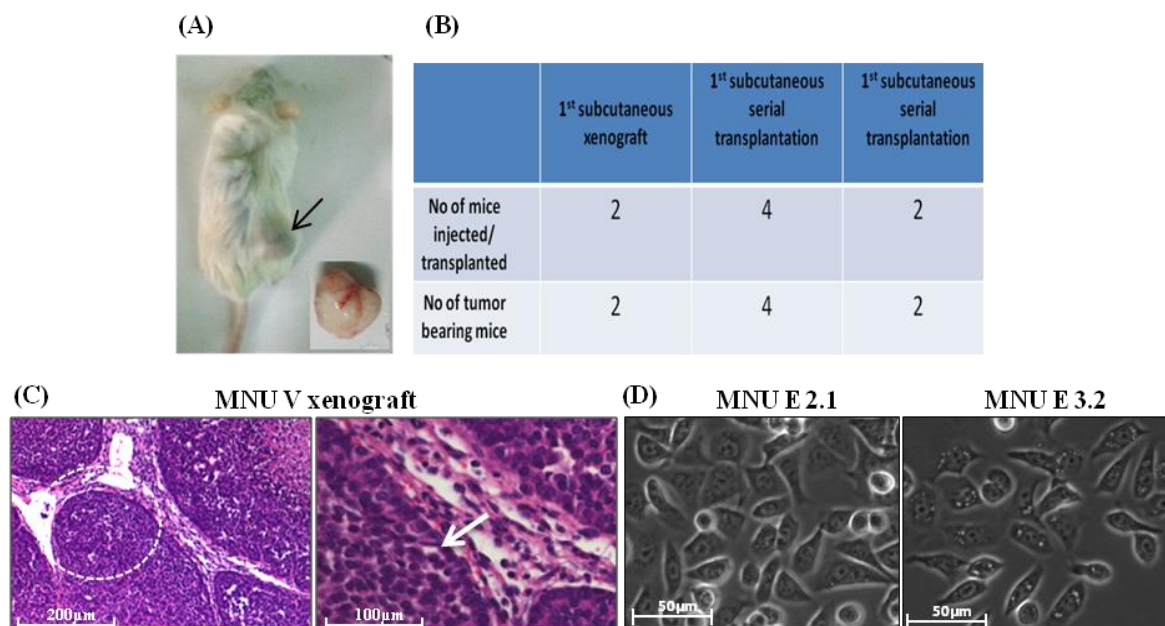


Figure 5.4 *In vivo* tumorigenic potential of MNUV cell line and development of explants. (A) Images of tumor induced in NSG mice post subcutaneous injection of MNUV cells. (B) Table representing the serial transplantation in NOD-SCID mice (C) H&E staining of tumors obtained from MNUV xenograft exhibiting glandular growth (marked in white circle) and moderately to poorly transformed cells (marked in arrow). (D) Light microscopic image of explants cell lines E3.2 and E2.1 developed from MNUV xenograft tumors. Scale -40X.

5.1.4 Alterations in histone post translational modification post transformation.

Transformation of HFE145 cell line to MNUV was associated with alteration in phenotypic properties. To understand the role of histone phosphorylation and acetylation during this process, their global levels were profiled by western blotting. As histone PTMs are dynamic and cell cycle specific, the cell cycle phase was determined by flow cytometry (Figure 5.5 A). The profile showed no significant change in the distribution of cell population in the different phases of cell cycle. With sequential transformation of HFE145 to MNUV, a decrease in site-specific histone acetylation viz, H3K9 and H3K14 was observed with no major change in other histone modifications (Figure 5.5 B).

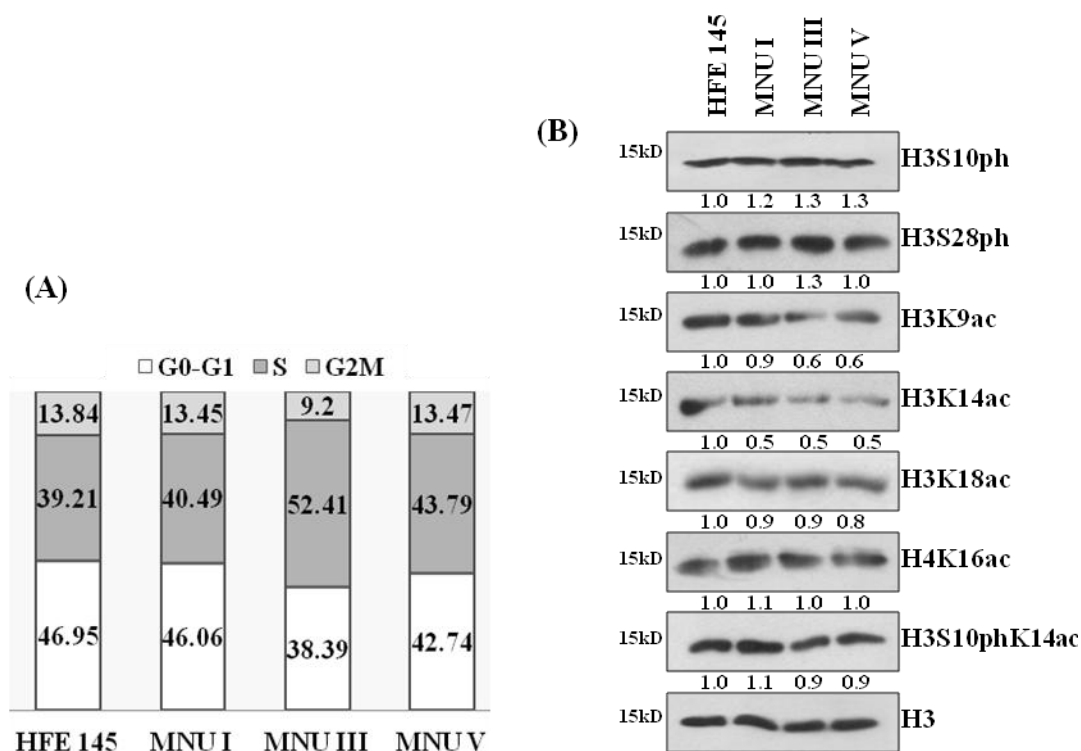


Figure 5.5 Histone post translational modification during sequential transformation of HFE145 cell line (A) Cell cycle profile of cells used for histone extraction; showing no significant difference in the distribution of cells. (B) Western blots showing differential levels of histone post translational modifications during sequential transformation of HFE145 to MNU V.

Further, the site-specific histone modifications in the untransformed (HFE145), transformed (MNUV) and explants tumor derived cell lines (E3.2 and E2.1) were studied. The cell cycle profile showed no significant change in the distribution of cells (Figure 5.6 A). In continuation with earlier sequential transformation results, a sequential decrease in H3K9ac, H3K14ac, H3K18ac, H3K27ac and H3K56ac was observed. Interestingly, a subtle increase in H3S10ph alongwith a significant increase in the dual modification, H3S10phK14ac was observed in the explants cell lines (Figure 5.6 B). Earlier study from lab has reported increased H3S10ph levels in Indian cohort of gastric cancer patients, so the levels of histone phosphoacetylation in gastric tumors and their adjacent normal resected margins was explored [91]. Western blotting showed that 3 of the 7 gastric

tumors had high levels of H3S10phK14ac suggesting a tumor heterogeneity in context of epigenetic alterations (Figure 5.6 C). Thus, the data suggests that gastric carcinogenesis is associated with decreased histone H3 acetylation and increased H3S10ph and H3S10phK14ac.

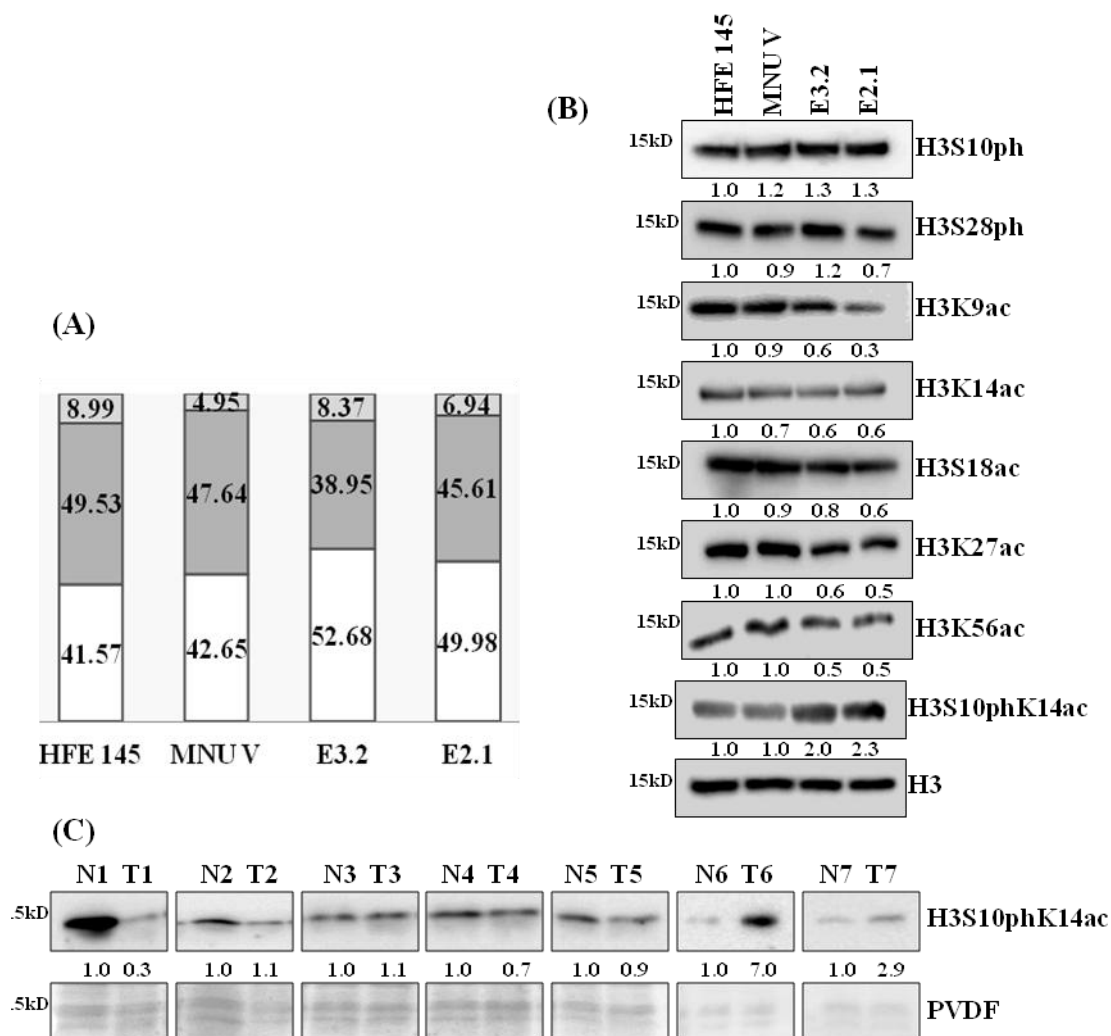


Figure 5.6 Histone post translational modification in transformed and explants cell line. (A) Cell cycle profile of cells used for histone extraction; showing no significant difference in the distribution of cells. (B) Western blots showing differential levels of histone post translational modifications post transformation in HFE145, MNUV, E3.2 and E2.1 cell lines. (C) Western blots showing the differential levels of H3S10phK14ac levels in Indian cohort of gastric cancer patients. Histones were extracted from tumor (T) and adjacent normal resected margins (N) (n=7). PVDF membrane serves as loading control.

5.1.5 H3S10phK14ac distribution in chromatin

Chromatin organization is a functionally important component of gene expression which is governed by the different histone PTMs. The phosphoacetylation mark H3S10phK14ac, is a mark of active transcription associated with open and closed chromatin during the G1 and M phase respectively. To explore the chromatin distribution of H3S10phK14ac, partial MNase digestion followed by salt fractionation was carried out for enrichment of nucleosomes and histone PTMs associated with open chromatin, at lower salt concentrations. The tightly bound nucleosomes in heterochromatin would require higher salt concentrations for elution. Around 8×10^6 asynchronous, E3.2 and AGS cells were digested with MNase for 2.5 and 7.5 minutes. The nuclei collected post-MNase inactivation were sequentially fractionated with 100mM and 400mM NaCl to obtain S1, S2, S3 fractions and insoluble chromatin pellet, P (detailed in figure legend). As shown in Figure 5.7 A, the fractions showed sequential increase in the amount of higher molecular weight DNA with decrease in mono-, di- nucleosomes from S1 to P corresponding to the elution of histones of nucleosomes from euchromatic to heterochromatic regions (Figure 5.7 A upper and lower panel).

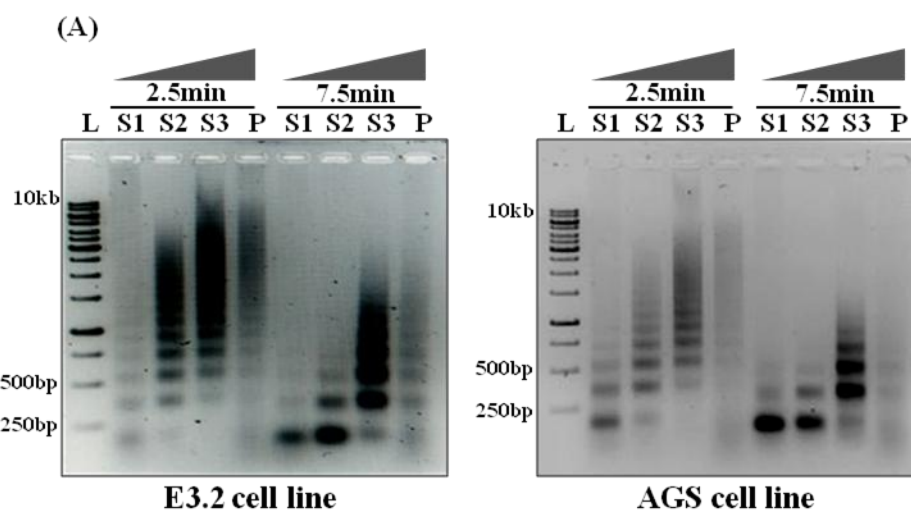


Figure 5.7 Chromatin fractionation and level of H3S10phK14ac. The differential occupancy of H3S10phK14ac mark depending on extent of chromatin compaction was assessed by partial MNase digestion followed by sequential salt fractionation of nuclei with 100mM and 400mM NaCl. S1, S2, S3 and P corresponds to supernatant fractions post MNase inactivation, treatment with 100mM NaCl, treatment with 400mM NaCl and finally the insoluble chromatin pellet respectively. (A) Agarose gel electrophoresis of DNA fragments extracted from the different fractions, exhibiting a gradual increase in higher molecular weight DNA from S1 to P. bp-base pairs, kb-kilo base pairs and ▲ indicates sequential increase in molecular weight of DNA with increase in salt concentration, 1- mono-nucleosome, 2-di-nucleosome. L – 1kb DNA ladder

Further, enrichment of histone PTMs was verified by profiling the levels of H3K9ac and H3K9me3 associated with open and closed chromatin, respectively. H3K9ac showed a sequential decrease, whereas H3K9me3 showed an increase from fraction S1 to P. Surprisingly, H3S10phK14ac was found to be highly enriched in S1 fraction containing nucleosomes which are associated with open chromatin (Figure 5.7 B upper and lower panel). The enrichment of H3S10phK14ac substantially decreases from fraction S2 to S3, and was almost absent in fraction P, reflecting an inverse relation with DNA fragment length viz; euchromatin to heterochromatin. Similar distribution pattern of H3S10phK14ac was also observed in AGS gastric adenocarcinoma cell line (Fig 5.7 B).

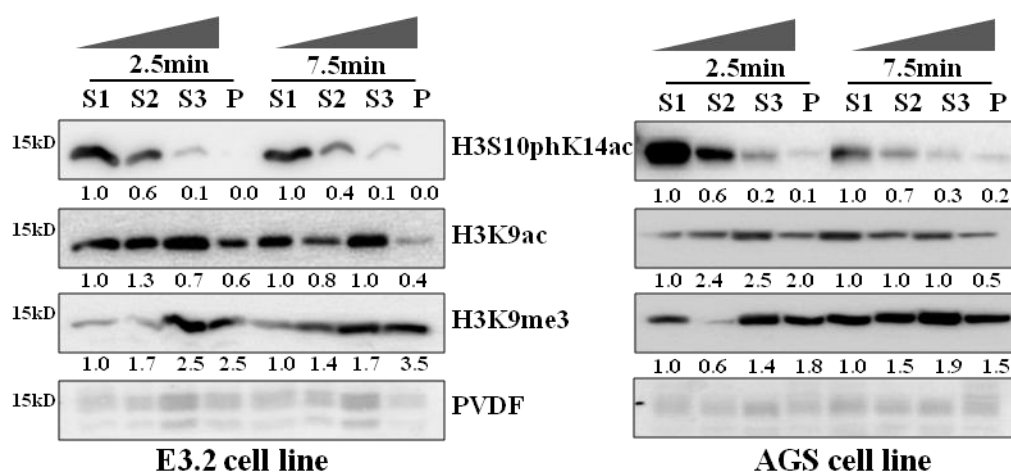


Figure 5.7 Chromatin fractionation and the level of H3S10phK14ac (B) Western blots showing the distribution of euchromatic (H3K9ac), heterochromatic (H3K9me3) and phosphoacetylation mark H3S10phK14ac across the different fractions. PVDF membrane serves as loading control.

Thus, the increased H3S10phK14ac levels associated with cancer progression is distributed in euchromatic regions and possibly associates with transcriptionally active regions of chromatin.

5.1.6 Alteration in epigenetic modifiers associated with histone hypoacetylation and increased phosphoacetylation.

To understand the mechanism behind histone hypoacetylation and increased phosphoacetylation, the levels of the associated kinases, histone acetyltransferases and histone deacetylases were profiled in the model cell lines. Since, H3 phosphoacetylation is known to be associated with MAPK activation and was found to be associated with open chromatin, the levels of activated mitogen and stress activated protein kinase1 (MSK1) which is known to mediate phosphorylation at H3S10 and H3S28 was profiled . A sequential increase in the levels of activated form of MSK1 viz phMSK1 was observed in MNUV and E3.2 and E2.1 cell lines (Figure 5.8 A).

Interestingly, phMSK1 levels were also found to be sequentially upregulated in another N-nitrosodiethylamine (NDEA) induced sequential hepatocellular carcinoma (HCC) model system (Figure 5.8 B) [160]. The levels surged from dysplastic stage (8 weeks), advanced neoplastic stage (12 weeks) upto HCC (16 weeks). The levels of *K-Ras* (Kirsten Rat Sarcoma Viral Oncogene Homolog) was also higher in the transformed cell line, MNUV and the explants cell lines, in coherence with its association with deregulated MAPK pathway that is observed in different cancers (Figure 5.8 B). The overall HDAC activity remains unchanged in different transformed gastric cell lines compared to HFE145, although an increase in HDAC1 level was observed. (Figure 5.8 A&C). Of the known HAT's, the levels of PCAF/KAT2B was found to be significantly

reduced in the explants cell lines viz; E3.2 and E2.1 in accordance with earlier reports in gastric cancer (Figure 5.8 A) [161–163].

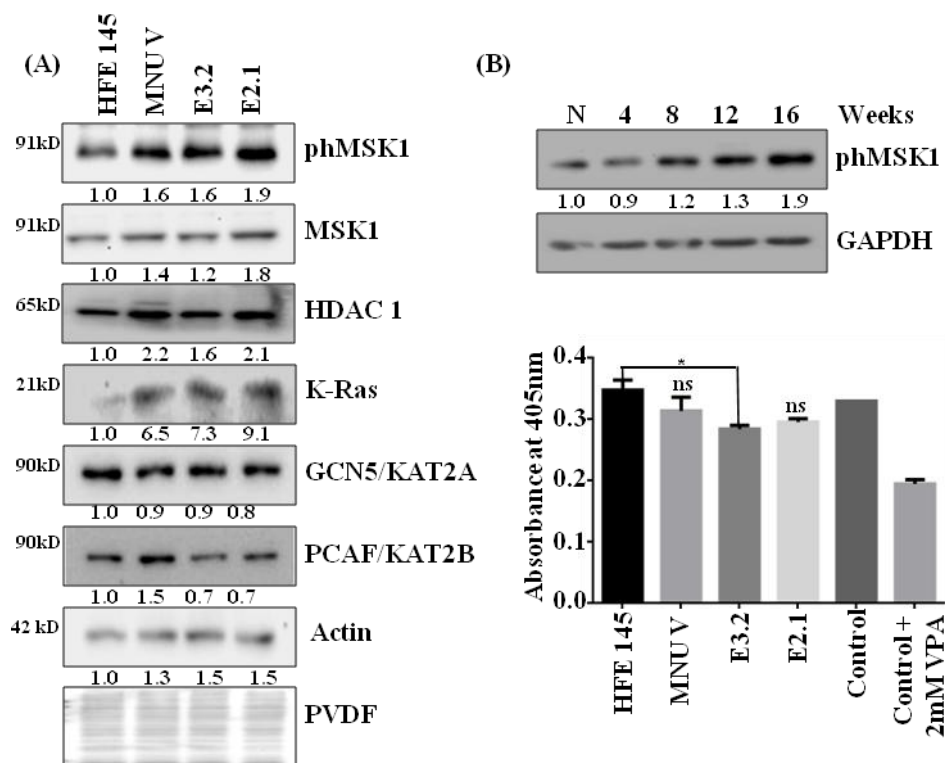


Figure 5.8 Epigenetic modifiers associated with histone hypoacetylation and increased phosphoacetylation (A) Western blots showing the levels of phMSK1, HDAC1, K-Ras and histone acetyltransferases, PCAF and GCN5 post transformation in HFE145, MNUV, E3.2 and E2.1 cell lines. (B) Western blots showing increased levels of phMSK1 in N-nitrosodiethylamine (NDEA) induced sequential rat hepatocellular carcinoma (HCC) model system. (C) HDAC activity measured in the above mentioned cell lines were assessed by in vitro calorimetric assay using whole cell lysates Unpaired student's t-test applied for statistical analysis for n = 2 experiments. *p < 0.05; ns- non significant

The transformation process was associated with increased levels of phMSK1 which is activated by ERK1/2 or p38 pathway in response to growth factors, cytokines or stress [77]. To seek the upstream kinase responsible for increased phMSK1 level, E3.2 cells were treated with inhibitors, SB203580 and PD98059 for p38 and ERK1/2 respectively. The p38 inhibitor treatment showed a significant decrease in phMSK level post 1 hour

treatment, highlighting the role of p38 pathway in activation of MSK1 kinase during transformation (Figure 5.9 A). Interestingly, H3S10phK14ac was significantly downregulated with both the inhibitors independently, and the effect was more pronounced when cells were treated with both inhibitors together suggesting contribution of both ERK and p38 pathway in its regulation. However, no significant change in H3S10ph or H3K14ac was observed with either of the inhibitors. This suggests that, only a fraction of global H3S10ph and H3K14ac constitutes the phosphoacetyl mark (H3S10phK14ac) which is possibly associated with transcription and regulated by the ERK/p38 pathway (Figure 5.9 B).

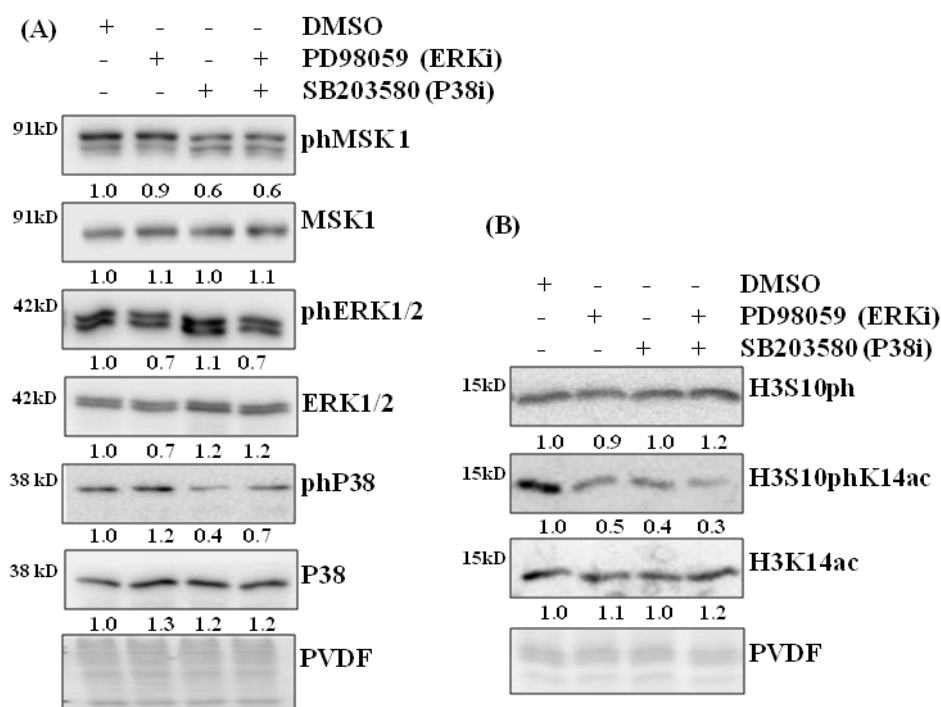
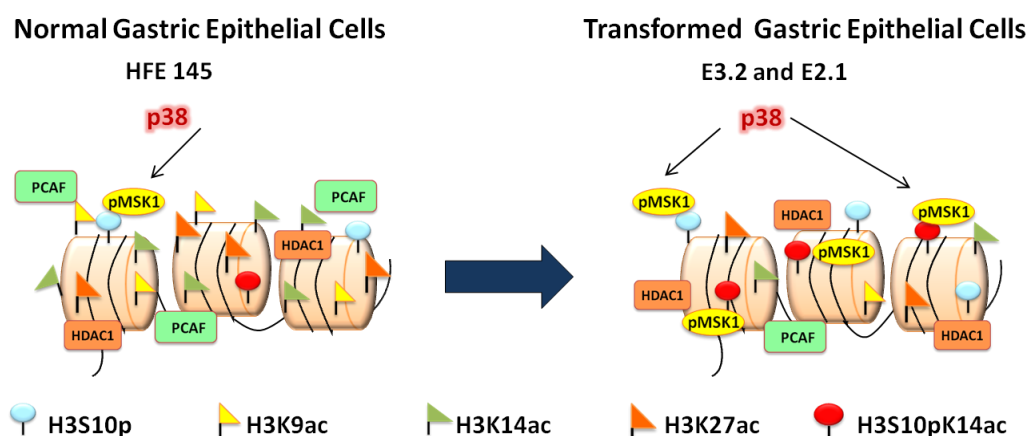


Figure 5.9 MAPK pathway associated with increased H3S10phK14ac levels. The putative upstream MAP kinase pathway responsible for increased pMSK1 levels was validated by treating E3.2 cells with ERK1/2 (PD98059) and p38 (SB203580) inhibitor. (A) Western blots suggesting that MSK is activated by the p38 MAPK pathway. (B) Western blots suggesting that the p38-MSK1 axis regulates the increased H3S10phK14ac levels. PVDF membrane serves as the loading control.

Thus, during gastric carcinogenesis, the p38 mediated increase in pMSK1 might regulate the increased H3S10phK14ac and the upregulation of HDAC1 and downregulation of PCAF/KAT2B may contribute to the observed H3 hypoacetylation.

Result Summary 5.1

To study the alterations in histone post-translational modifications and the associated modifiers upon cellular transformation



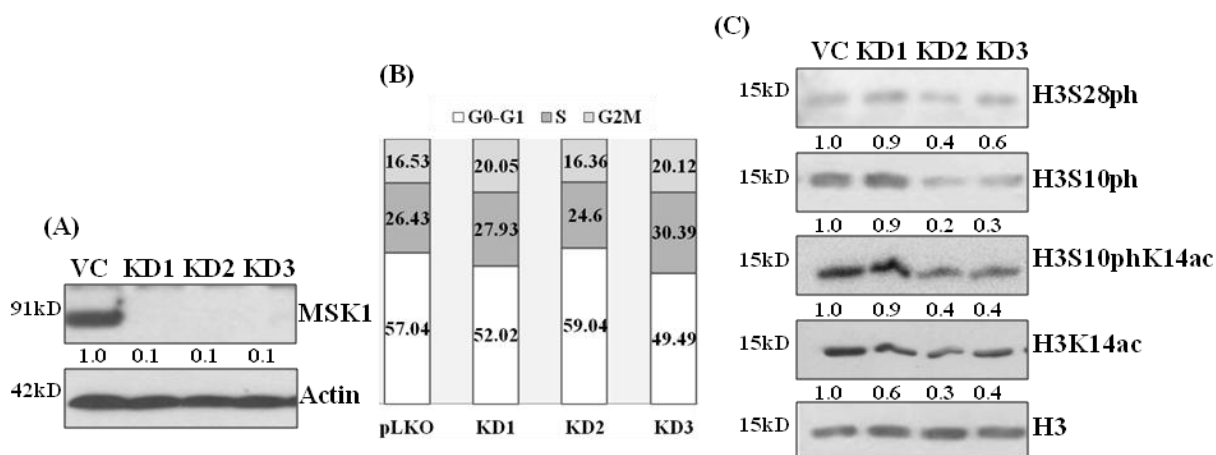
Model 5.1- Alteration associated with gastric cell transformation. Transformation of gastric epithelial cell is associated with MSK1 mediated increased H3S10ph and H3S10phK14ac, and the site specific hypoacetylation observed is an outcome of increased HDAC1 and decreased PCAF levels.

After exploring the histone PTM alteration post transformation, the role of MSK kinase in the survival and regulation of phosphoacetylation in GC was explored in the next aim of objective.

5.2 To define the role of MSK1 in regulating phosphorylation of histone H3 and its potential importance in acetylation of neighbouring lysine residues in gastric cancer cell line.

5.2.1 Effect of MSK1 in survival of transformed gastric epithelial cells

Earlier models of cellular transformation in fibroblasts and keratinocytes have demonstrated the importance of MSK1 in regulating the expression of oncogenes promoting the transformation process [82,164]. However, the role of MSK1 in survival of transformation of gastric epithelial cells has not been studied. To understand this phenotypic assay were carried out after MSK1 knockdown in MNUV and AGS cell line. Three knockdown clones were selected and the knockdown efficiency of around 80 to 90% was confirmed at protein level in AGS cellline (Figure 5.10 A). The cells were serum starved for 48 hours (Figure 5.10 B). Two of the three MSK1 knockdown clones showed a significant decrease in H3S10ph, H3S28ph and H3S10phK14ac post 4 hours serum induction (Figure 5.10 C). The two clones showing similar pattern were taken ahead for further studies.



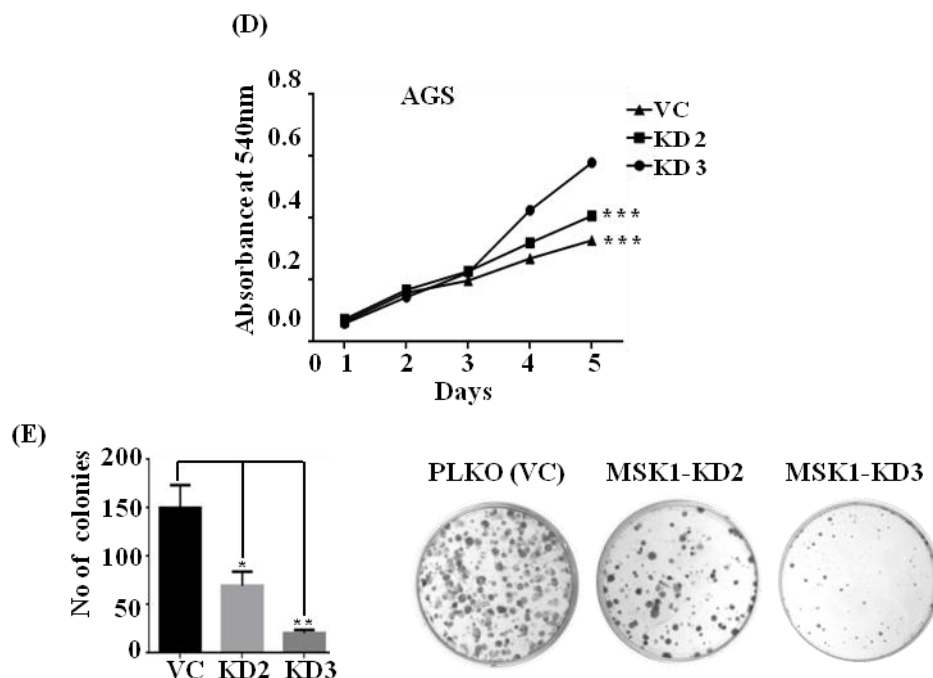


Figure 5.10 Effect of MSK1 knockdown on AGS cell line. (A) Western blot analysis validating MSK1 knockdown in AGS cell line. (B) Histogram depicting percentage of MSK1 KD AGS cells in different phases of cell cycle post serum release (C) Western blots showing effect of MSK1 KD on histone PTM in AGS cells. (D) MTT assay AGS cell line, shows a decrease in proliferation upon MSK1 KD $n^{***}p < 0.0005$. (E) Clonogenic assay showing decrease in clonogenic potential upon MSK1KD in AGS cell line (left panel) $*p < 0.03$, $**p < 0.005$. Representative images of clonogenic assay (right panel). Unpaired student's *t*-test applied for statistical analysis. VC-Vector control and KD-Knockdown

MSK1 knockdown significantly inhibited cell proliferation as assessed by MTT assay in different clones of AGS cell line (Figure 5.10 D). Further, the clonogenic potential of AGS clones (Figure 5.10 E left and right panel) was also decreased post MSK1 knockdown. Similar studies were also carried out in MSK1 knockdown clone of MNUV cell line. The data showed inhibition of cell proliferation, anchorage independent growth and clonogenic potential as earlier observed in AGS knockdown clones (Figure 5.11). Thus, MSK1 mediated gene expression plays an important role in the proliferation, anchorage independent growth and survival of transformed gastric cells.

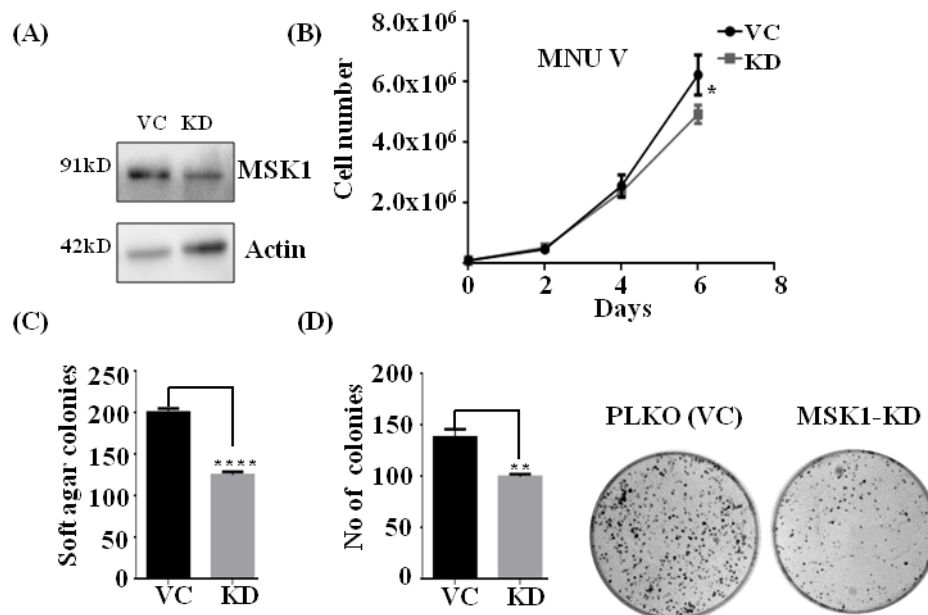


Figure 5.11 MSK1 is crucial for survival of transformed MNUV cells. (A) Western blot analysis validating MSK1 KD in MNUV cell line. (B) Proliferation assays by doubling time calculation shows a decrease in proliferation upon MSK1 KD *p < 0.03. (C) Soft agar assay exhibiting a decrease in anchorage independent growth upon MSK1 KD, ****p < 0.00003. (D) Clonogenic assay showing decrease in clonogenic potential upon MSK1 KD (left panel) **p < 0.005. Representative images of clonogenic assay (right panel). VC-Vector control and KD-Knockdown

5.2.2 Regulation of H3S10phK14ac by MSK1

To understand the importance of MSK1 in histone H3 phosphorylation and cross-talk with neighbouring H3K14 acetylation, the catalytic activity of MSK was inhibited with inhibitor H89 in E3.2 and AGS cell line. Since MSK mediated H3S10ph is known to be a G1 phase and a transcription associated phenomenon mediated by MAPK signaling, the cells were serum starved for 48 hours. Post serum starvation E3.2 cells were pretreated with $15 \mu\text{M}$ H89 for 30 minutes followed by 10% serum induction for 90 minutes. In case of E3.2 cell line dampening of the MAPK signaling was observed post-serum starvation as suggested by decrease in phMSK1 level (lane 2) compared to no starvation control (No SS) (Figure 5.12 A). On serum induction, the MAPK pathway was activated with

increased levels of phMSK1 (lane 3), however a very mild decrease in pMSK1 level was observed by H89 (lane 4) as it affects the catalytic activity and not the activation of MSK. A significant decrease in H3K9ac, H3K27ac and H3S10phK14ac was observed with more or less consistent level of H3S10ph and H3K14ac post serum starvation (lane 2). This decreased acetylation and phosphoacetylation is possibly the result of reduced proliferation and transcription upon serum starvation [165,166]. The cell cycle profile indeed suggests a decreased S-phase population upon serum starvation (Figure 5.12 B).

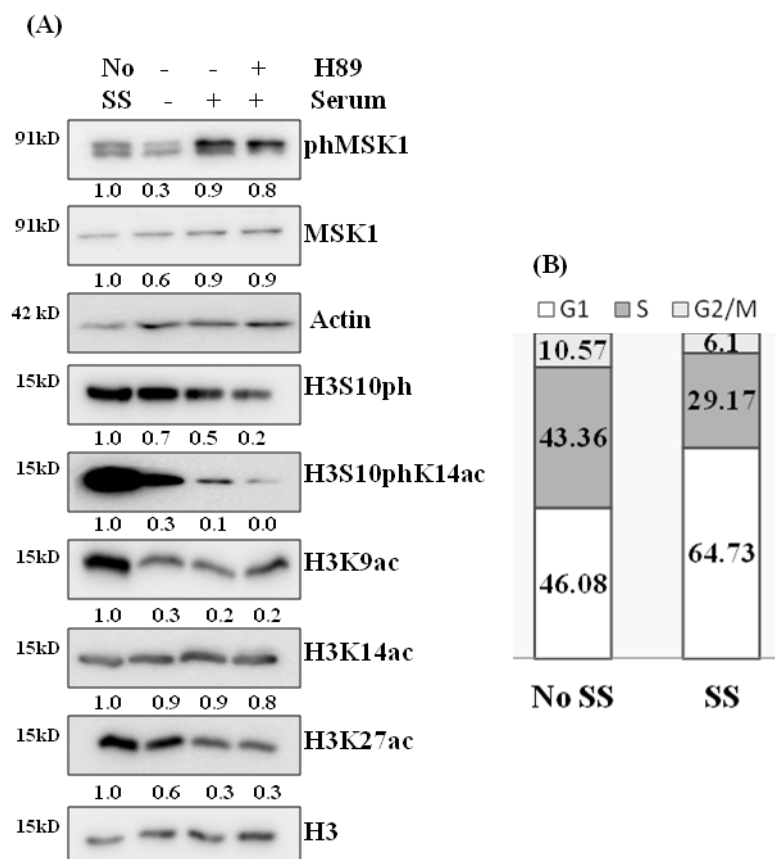


Figure 5.12 MSK regulates H3S10phK14ac in response to serum induction. (A) Western blot depicting alterations in histone PTMs upon serum induction and MSK inhibition in E3.2 cell line. The cells were serum starved for 48hrs, pretreated with DMSO (vehicle control) or 15 μ M H89 for 30 minutes followed with 10% serum induction for 90 minutes. (B) Histogram depicting alteration in cell cycle phase upon serum starvation. SS- Serum starvation and No SS- No serum starvation.

Interestingly post-serum induction H3S10ph and H3S10phK14ac decreased further (lane 3), however, both these marks were significantly decreased with the phosphoacetylation mark almost absent when MSK was inhibited (lane 4), suggesting the role of MSK kinase in H3 phosphorylation and phosphoacetylation in the G1 phase. However, no decrease in the levels of H3K9ac, H3K14ac and H3K27ac was observed (lane 4) (Figure 5.12).

In case of AGS cell line, post-serum starvation the cells were stimulated with EGF (20 ng/ml) for 20 minutes, as EGF signalling mediated MAPK activation is known to stimulate growth. An increase in pMSK1 levels with increased H3S10ph levels was observed post-EGF induction (Figure 5.13 A). However, in presence of H89 a significant decrease in H3S10ph, H3S28ph and the phosphoacetylation mark, H3S10phK14ac was observed. Interestingly, unlike E3.2 a marked decrease in acetylation on H3K9, H3K14 and H3K27 was observed (Figure 5.13 B).

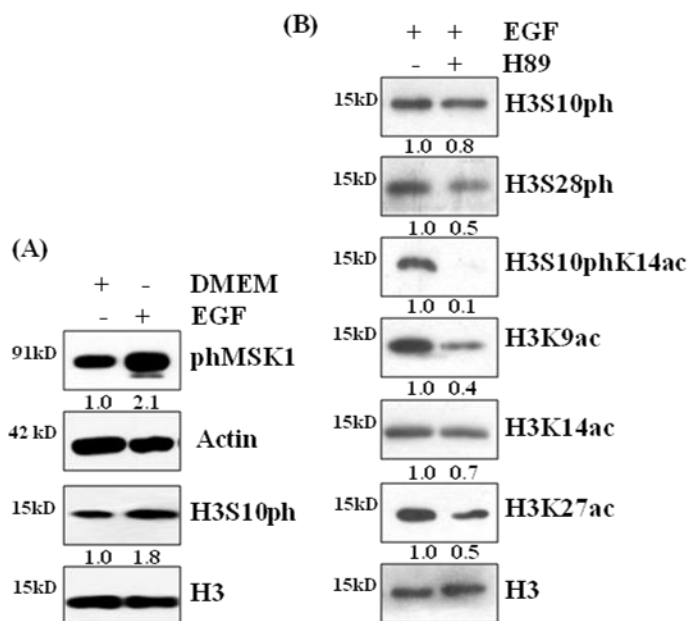


Figure 5.13 MSK regulates EGF induced H3S10phK14ac (A) Western blot depicting activation of MAPK pathway (phMSK1) and induction of H3S10ph after stimulating AGS cells with 20 ng/ml of EGF for 20 minutes (B) Western blot depicting alterations in H3S10 & H3S28

phosphorylation and neighbouring histone acetylation post MSK inhibition with H89 during EGF stimulation.

This data suggests EGF-mediated alteration in H3K9ac, H3K14ac and H3K27ac in AGS cell line. Thus, MSK mediates alteration in H3S10ph, H3S28ph and H3S10phK14ac in the G1 phase and its influence on neighbouring histone H3 acetylation is a context-dependent phenomenon.

5.2.3 Crosstalk between H3S10ph and H3K14ac

Our previous observation suggested that MSK's regulate H3S10phK14ac levels in cells post-serum induction. Histone modifications undergo cross-talk wherein H3 phosphorylation may predispose the neighbouring lysine residues to acetylation by influencing the recruitment of HAT's and HDAC's [60]. Thus, the earlier observed decrease of H3S10phK14ac post-H89 treatment might be a consequence of decreased HAT recruitment due to absence of H3S10ph (Figure 5.14 A). Studies have shown that inhibition of histone deacetylase increases acetylation of histones by shifting the balance of acetylation-deacetylation towards HAT's [167] (Figure 5.14 A). This increased acetylation is a H3 phosphorylation dependent phenomenon?

To delineate this interesting question, a pre-treatment of H89 and HDACi valproic acid (VPA) was given independently or together for 30 minutes post-serum starvation followed by 10% serum induction for 90 minutes in both E3.2 and AGS cell line. Western blot analysis showed activation of ERK1/2, p38 and MSK1 after induction by serum in all the groups. (Figure 5.14 B).

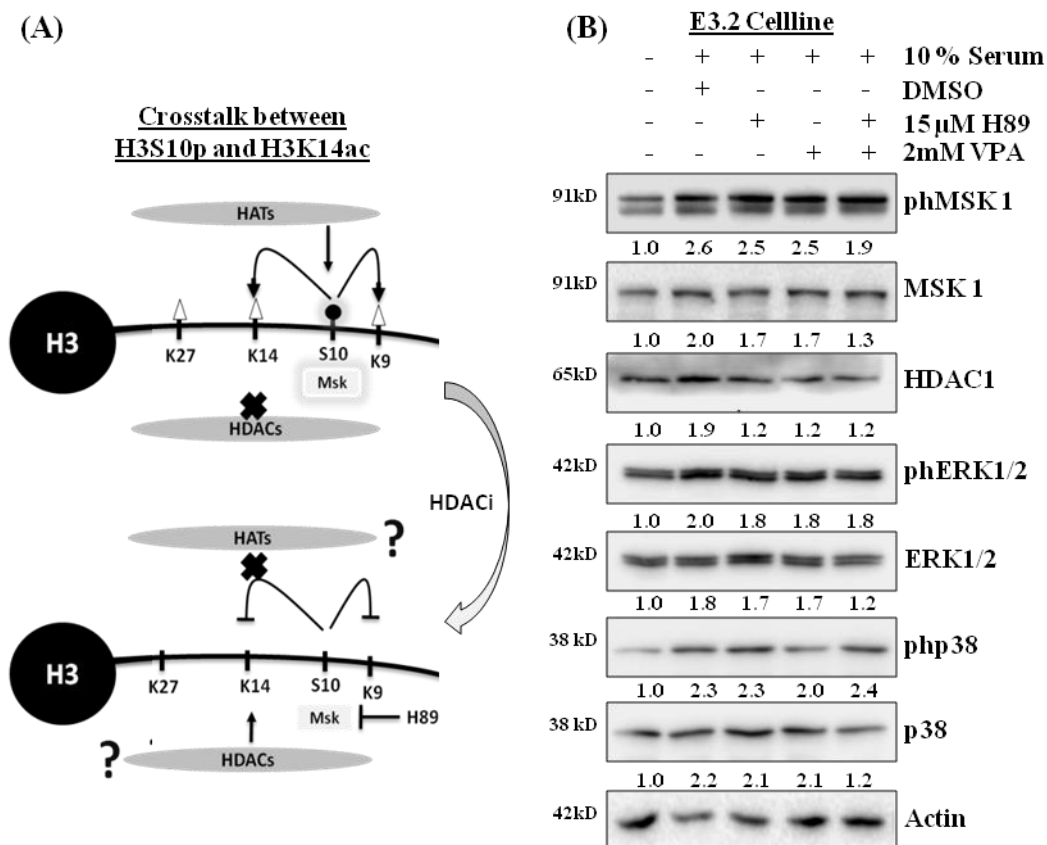


Figure 5.14 Effect of serum induction and inhibitor treatments on MAPK pathway activation. (A) Schematic diagram proposing the role of H3S10ph in inducing H3K14ac- MSK mediated H3S10ph might be regulating HAT recruitment and H3K14ac, leading to H3S10ph K14ac. If acetylation is indeed phosphorylation dependent then induction of phosphoacetylation would be hampered, post a combinatorial treatment of H89 and HDAC inhibitor, valproic acid (VPA). (B) Western blots suggesting the activation of p38 and ERK1/2 pathway upon serum induction in E3.2 cell line.

Further, the histone modifications were profiled in E3.2 and AGS cell lines and the data suggested an increase in global H3K9ac, H3K14ac and H3K27ac in case of only VPA (lane 4) or VPA+H89 (lane 5) treated cells, in accordance with inactivation of HDAC's (Figure 5.15). Interestingly, H3S28ph was found to be upregulated post-VPA treatment and this increase was MSK-dependent as the phosphorylation was absent in VPA+H89 treated cells (lane 5). Surprisingly, an increase in phosphoacetylation mark H3S10phK14ac was also observed post -VPA treatment, (lane 4) which was absent in

VPA+H89 treated cells (lane 5). The decrease in H3S10phK14ac levels in the VPA+H89 lane was almost equal to that of H89 (lane 3) (Figure 5.15). This suggests that majority of histone acetylation is independent of MSK mediated H3S10ph; however, H3S10ph possibly regulate HAT recruitment and acetylation at few local sites. Pertinently, HDACi mediated increased H3S28ph and H3S10phK14ac phosphoacetylation is MSK-mediated and H3S10ph dependent phenomenon.

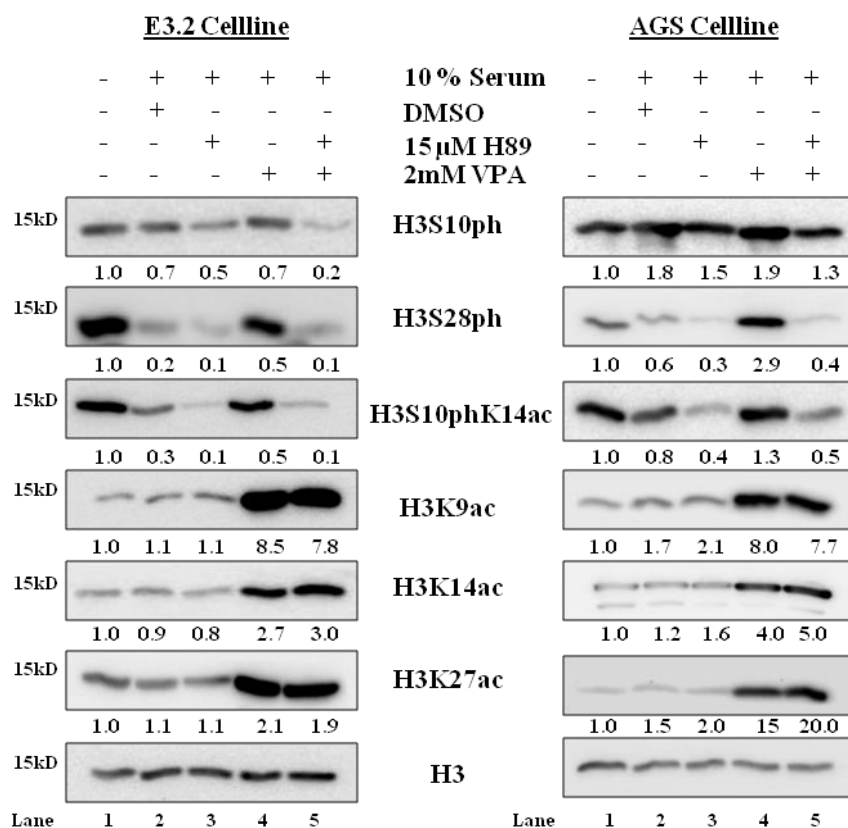


Figure 5.15 MSK mediated cross talk between H3S10ph and H3K14ac To understand the role of MSK mediated H3S10ph in influencing neighbouring acetylation; the effect of H89 on phosphoacetylation in presence of HDAC inhibitor, VPA was studied. Western blots showing the effect of H89 and VPA on histone phosphorylation, acetylation and phosphoacetylation.

Interestingly, the experiments carried out without serum starvation showed no dependence on MSK mediated H3S10ph. The increased phosphoacetylation,

H3S10phK14ac persisted even upon MSK inhibition by H89 (lane 4&8 compared to lane 3&7) (Figure 5.16). The possible explanation for this could be ERK mediated regulation of H3S10phK14ac which is independent of MSK1 as suggested in section 5.1.6. No change in H3S10ph level was observed upon MSK inhibition in this case.

Thus, the same crosstalk could be mediated via different upstream signalling pathway and that is dependent on the cellular environment or context involved.

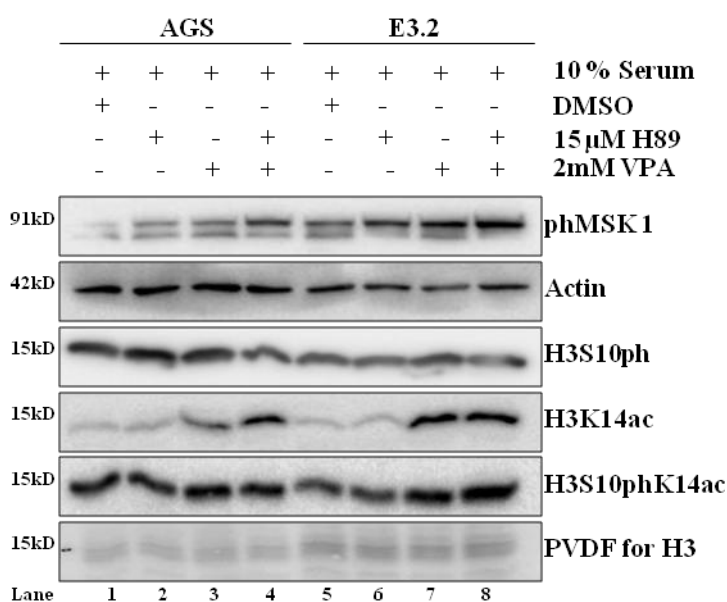


Figure 5.16 Regulation of H3S10phK14ac crosstalk in absence of serum starvation. To understand the role of MSK mediated H3S10ph in influencing neighbouring acetylation in absence of serum starvation AGS and E3.2 cells were treated with H89 in presence and absence of HDAC inhibitor, VPA. Western blots showing the induction of MSK independent histone phosphoacetylation in response to VPA and absence of serum starvation.

5.2.4 Mechanism of cross talk between H3S10ph and neighbouring H3K14ac

To understand the interplay between chromatin modifiers associated with H3 phosphorylation and acetylation in regulating the H3S10phK14ac crosstalk, the chromatin occupancy of kinases, phosphatases, acetyltransferases and deacetylase post

inhibitor treatment was studied (Figure 5.17). E3.2 cells post-serum induction and inhibitor treatment were fractionated into nucleocytoplasmic (NC) and chromatin (C) fraction, and subjected to western blotting. The fractionation was validated with α -tubulin and lamin B for cytoplasmic and nuclear fractions, respectively. Further, western blots showed a decrease in H3S10ph, H3S10phK14ac in H89 treated cells (lane 6) and increased level of H3S10phK14ac in VPA treated cells (lane 7). This validated the efficient inhibition of MSK's and HDAC's. In case of kinases, MSK1 was predominantly present in the nucleocytoplasmic fraction and the chromatin occupancy of active MSK1 (phMSK1) was increased in all the inhibitor treated cells (lane 6-8) (Figure 5.17).

The increased chromatin occupancy of MSK1 upon VPA (lane 7) and VPA+H89 (lane 8) treatment suggests that enhanced phosphorylation at H3S10 and H3S28 position takes place in response to HDAC inhibition. Interestingly, the chromatin occupancy of HDAC1 increased upon MSK inhibition (lane 6) suggesting that absence of H3S10ph might favour HDAC recruitment. Further, HDAC1 chromatin occupancy also increased after VPA treatment (lane 7).

In case of phosphatases, no difference in occupancy of MKP1 was observed while PP1 phosphatase was found to be decreased in both the fractions in H89 treated cells (lane 6). Conversely, PP1 levels post-VPA treatment was found to be increased in both the fractions. The adapter protein, 14-3-3 ζ which is known to have a high binding affinity for phosphoacetylation mark was found to have no differential occupancy post-inhibitor treatment [168]. Also, no alteration in differential occupancy of HAT's, PCAF and GCN5 were observed (Figure 5.17) Together, the data suggests that MSK1-mediated

H3S10ph could influence the recruitment of HDAC's and thus affect the neighbouring H3K14 acetylation; especially in response to HDAC inhibitor, VPA.

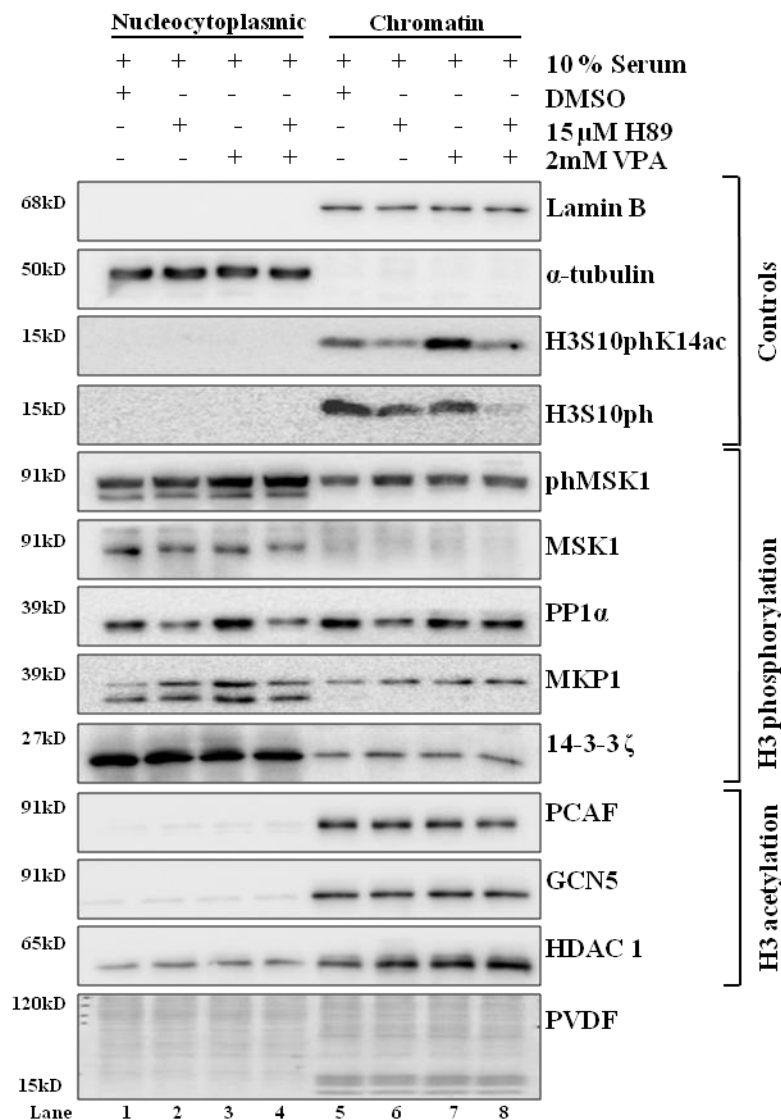


Figure 5.17 Regulatory mechanism of cross talk between H3S10ph and neighbouring H3K14ac To understand the mechanism of cross talk between H3S10ph and H3K14ac, E3.2 cells were fractionated into nucleocytoplasmic and chromatin fraction and the occupancy/enrichment of epigenetic modifiers associated with histone phosphorylation and histone acetylation were studied. Western blots depict the increased chromatin occupancy of phMSK1 and HDAC1, post-H89 or VPA treatment either singly or in combination. No differential chromatin occupancy of HAT's was observed.

5.2.5 MSK mediated regulation of HDAC1 in gastric carcinogenesis

HDAC1 and 2 are immediate early genes, their expression being regulated by MAPK pathway in response to growth factor stimuli [169]. The earlier data showed an upregulation of active MSK1 and HDAC1 upon cellular transformation. Thus, MSK1 might be responsible for the observed increased levels of HDAC1. MSK-mediated histone phosphoacetylation has been implicated in expression of immediate early genes, like *c-fos*, *c-jun*, *c-myc* and ribosomal RNA genes which are known to be upregulated in cancer [76,83]. Therefore, the transcripts of immediate early genes, *c-fos*, *c-jun*, *c-myc*, *cox2*, HDAC1 and HDAC2 were explored in H89 treated AGS cells. The expression of *c-jun*, HDAC1 and HDAC2 were found to be decreased after H89 treatment (Figure 5.18 A). An increase in HDAC1 was observed upon cellular transformation (in earlier section 5.1.6), so the level was studied in MSK1 knockdown AGS and MNUV cell lines. A significant decrease in HDAC1 protein levels was observed upon MSK1 depletion (Figure 5.18 B).

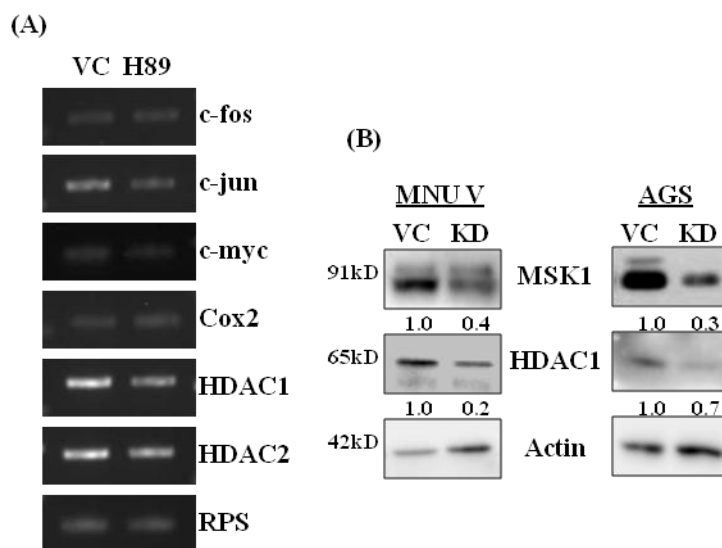


Figure 5.18 MSK1 mediated regulation of HDAC1 in gastric cancer cell lines and tumor samples. (A) 48 hours serum starved AGS cells were treated with 15 μ M H89 or DMSO as vehicle control upon serum induction for 1 hour and the levels of immediate early genes was studied by qPCR. (B) Western blots depicting the decrease in HDAC1 levels post MSK1 knockdown in MNUV and AGS cellline.

Further, the relation between MSK1 with HDAC1 was studied serial transplanted xenograft tumor tissues of MNUV cell line. The data suggested that along with serial transplantation there is increased activation of pMSK1 and this correlated with HDAC1 level (Figure 5.18 C). Overall the data suggests that MSK mediated positive regulation of HDAC1 could be the possible reason for high expression of HDAC1 in gastric cancer.

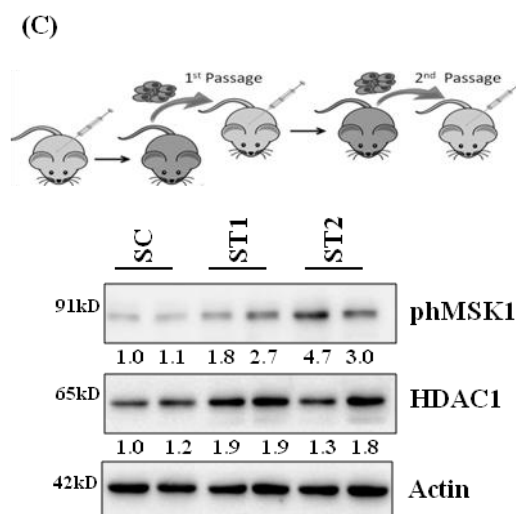


Figure 5.18 (C) MSK1 mediated regulation of HDAC1 in gastric cancer cell lines and tumor samples. Western blots suggesting a correlation between pMSK1 and HDAC 1 in serial transplanted MNU xenograft tumor tissue. SC-Tumor with MNUV cell line; ST1-Serial transplant 1; ST2-Serial transplant 2

MSK1 mediated increase of transcription involves phosphorylation of histone H3 at S10 and S28 position in chromatin. These post-translational modifications take place on the promoters of MSK target genes and favoring the recruitment of chromatin remodeler, SWI-SNF [170,171]. This result in increased histone acetylation at H3K9 and H3K14, thereby increasing the gene transcription.

To investigate whether H3S10ph and H3K14ac is involved in increased level of HDAC1 the recruitment of H3S10ph and H3K14ac on HDAC1 promoter was studied. The mono-nucleosomal ChIP with antibodies against H3S10ph and H3K14ac was performed on MNase digested chromatin of AGS cell line (Figure 5.19). The phenol-chloroform extracted DNA was subjected to qPCR, using primers for specific *cis-acting* elements of HDAC1 promoter. These *cis-acting* elements are recognized by the putative transcription factors known to be associated with complexes containing MSK1/2 as depicted in the HDAC1 promoter sequence (Figure 5.19 A). ChIP qPCR data showed enrichment over the IgG control lane for H3S10ph and H3K14ac at the FOS, CREB3, CREB3B/D and FOS-L1 sites (Figure 5.19 B right panel). Therefore, the H3S10ph and H3S28ph modifications observed at the promoter of HDAC1 gene correlates with activation of transcription. This data further suggest the role of MSK1-mediated H3S10ph and associated H3K14ac in the enhanced transcription of HDAC1 gene.

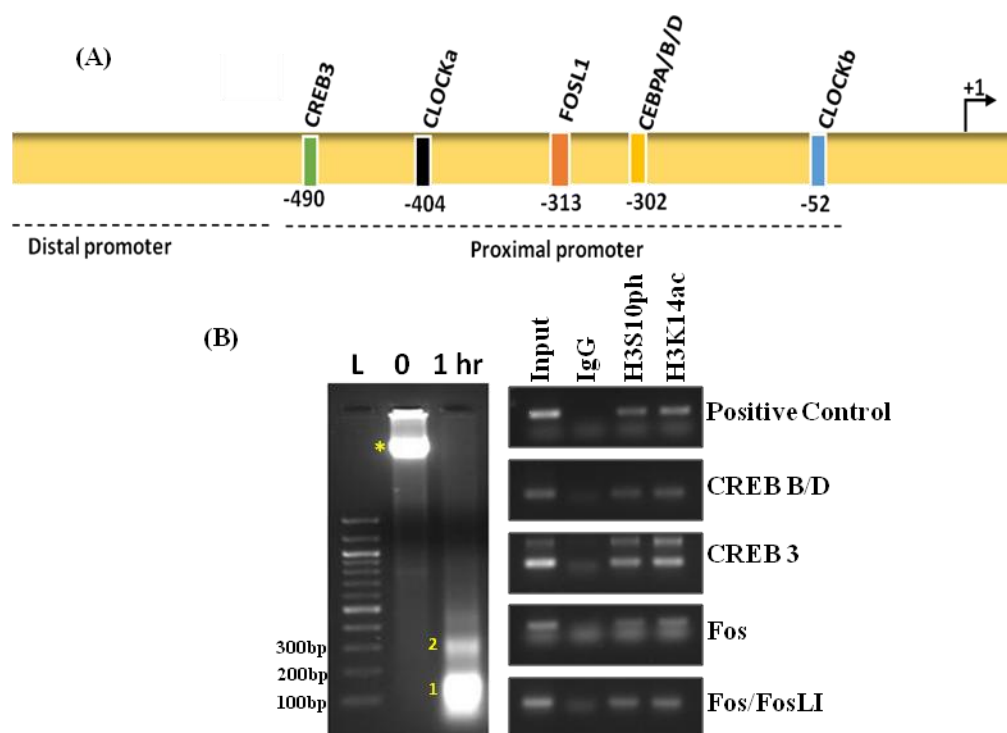


Figure 5.19 Association of H3S10ph and H3K14ac on HDAC1 promoter (A) Schematic diagram of possible MSK1 binding sites on HDAC1 promoter (B) Purity of mono-nucleosome generated for ChIP was assessed by 1.8% agarose gel electrophoresis (left panel). H3S10ph and H3K9ac occupancy on HDAC1 promoter as assessed by ChIP qPCR (right panel). bp-base pairs, * indicates undigested higher molecular weight DNA, 1- mono-nucleosome, 2- di-nucleosome and L – 100bp DNA ladder.

5.2.6 Level of HDAC1 in gastric cancer

HDAC 1 protein levels were studied in paired gastric cancer tissue samples of Indian cohort by immunohistochemistry. Earlier in the same samples an up-regulation of p38 mediated phMSK1 and H3S10ph levels have been reported [91].

Histopathology of adenocarcinomas from stomach revealed malignant cells arranged in loosely cohesive glands, tubules or small sheets with high N: C ratio. The level of HDAC1 was significantly increased ($p < 0.0001$) in the gastric tumor (T) tissues compared to their adjoining normal resected margins (Figure 5.20 A & B). The results were quantitatively estimated in the form of H-score which takes into account the intensity of staining and the percent population associated.

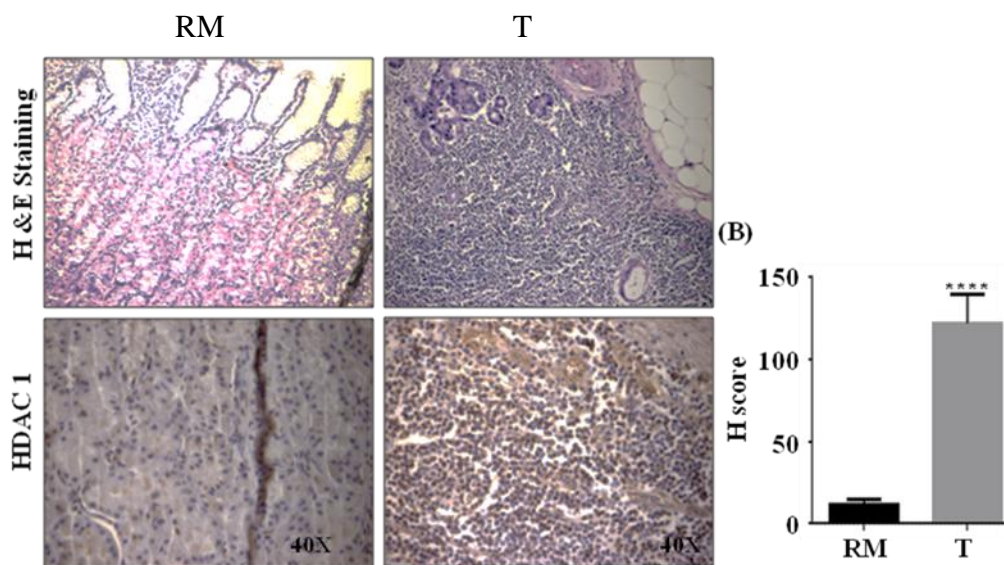
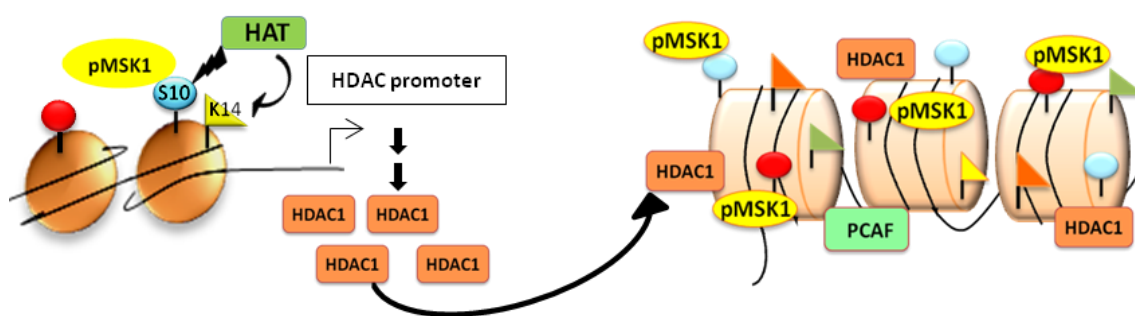


Figure 5.20 HDAC1 levels in Indian cohort of gastric cancer patients. (A) Hematoxylin & Eosin and immunostaining of HDAC1 in paired tumor (T) and resection margin (RM) tissues (n=24) 40X. (B) Comparing mean H-score of HDAC1 immunostaining revealed high HDAC1 expression in tumor samples compared to normal resected margins. *** $p < 0.0005$.

Result Summary 5.2.

To define the role of MSK1 in regulating phosphorylation of histone H3 and its potential importance in acetylation of neighbouring lysine residues in gastric cancer cell line.



Model 5.2 MSK1 mediated regulation of HDAC 1 levels in gastric cancer. Gastric carcinogenesis was found to be associated with MSK mediated increased phosphoacetylation of histone H3 at S10 and K14. At the HDAC1 promoter, this increased phosphoacetylation results in increased HDAC1 transcription with increase in HDAC1 protein, which together with decreased PCAF levels contributes to the global histone hypoacetylation.

A characteristic feature of H3S10 and H3S28 phosphorylation is their spatio-temporal regulation with contrasting functional roles depending on the cell cycle phase [172]. Interestingly with respect to regulation, the pathways and the kinases involved in phosphorylation of H3S10 and H3S28 during the G1 and M phase also differ. In the G1 phase, ERK1/2 and p38 MAPK kinase pathway mediated phosphorylation of mitogen and stress activated protein kinase MSK, predominantly catalyses the phosphorylation, whereas in M phase, JNK pathway mediated activation of Aurora B kinase (AURKB).

In present study with MSK1, the active level of MSK1 was found to be present in the M phase of cell cycle. In an earlier study by Shawn et al, MSK1/2 levels were detected in M

phase, however their functional implications in mitosis have not been studied [173]. Further, Aurora B kinase is the only kinase proposed to mediate H3S10ph and H3S28ph in mitosis. Thus, the presence of MSK and the unknown functional relevance associated in mitosis led us to explore its role in H3 phosphorylation during mitosis in gastric cancer.

5.3 To define the role of MSK1 mediated phosphorylation of H3S10 and H3S28 in M phase cells.

5.3.1 Levels of MSK 1 during the different phases of cell cycle

To understand the role of MSK in mitosis, its protein level and functionally activated form, pMSK was analyzed in the G1 and M phase of the cell cycle. AGS cells were synchronized in the G1 and M phase and the cell cycle phases were validated by flow cytometry. The enrichment of ~70% and ~75 % were found in the G1 and M phase, respectively (Figure 5.21 A).

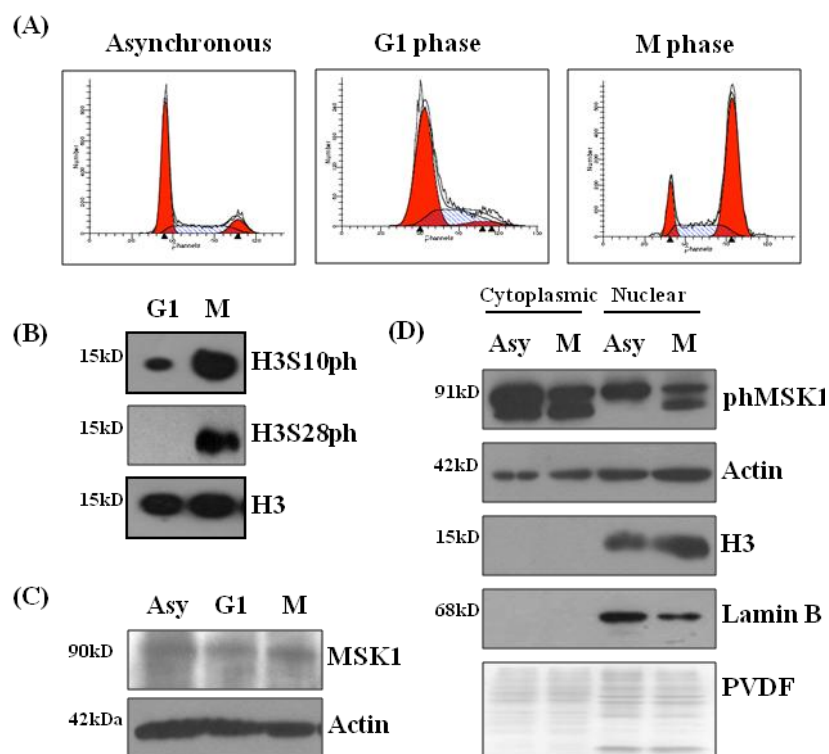


Figure 5.21 MSK1 and phMSK1 levels during mitosis AGS cells were synchronized in G1 phase and M phase by double thymidine block and nocodazole treatment respectively. (A) The cell cycle profile of the arrested cells was confirmed by flow cytometry. (B) High H3S10ph and H3S28ph in M phase compared to G1 phase was validated by western blotting. (C) The levels of MSK1, through the cell cycle were studied by western blotting. (D) Western blots showing the presence of active MSK1 viz phMSK1 in the nuclear fraction during mitosis.

Western blotting data showed high levels of H3S10ph and H3S28ph in the mitotic population compared to G1 cells; further, validating the cell cycle observation (Figure 5.21 B). Interestingly, the MSK1 levels were found to be similar in the G1 and M phase cells (Figure 5.21 C). However, the levels of phMSK1 (S370ph) was found to be higher in the cytosolic fraction in both the cell cycle phases; however in of nuclear fraction, phMSK1 was found to persist to a relatively low level in M phase compared to G1 phase (Figure 5.21 D). The data suggests that MSK1 is present in both the cell cycle phases and might have some functional role to play in mitosis.

5.3.2 Effect of MSK inhibition on histone post-translational modification

To delineate the role of MSK1 in regulating mitotic phosphorylation and acetylation, mitotic cells were treated with MSK inhibitor, H89 for 60 minutes and the histone modifications were profiled. The data showed increased levels of H3S10ph, H3S28ph and H3K14ac with decrease in H3K9ac and H3K18ac in the mitotic population as compared to asynchronous AGS cells (Figure 5.22A). Surprisingly on MSK inhibition, a decrease in H3S10ph, H3S28ph and H3K14ac was observed; whereas the neighboring acetylation marks, H3K9ac and H3K27ac was found to be increased (Figure 5.22 C). This alteration in histone PTM was not an outcome of different cell cycle phase as confirmed by flow cytometry (Figure 5.22 C). The decrease in histone phosphorylation was more profound at H3S28 position suggesting a preferential site by MSK during mitosis. Further, immuno-fluorescence of mitotic cells validated the decrease in H3S28ph

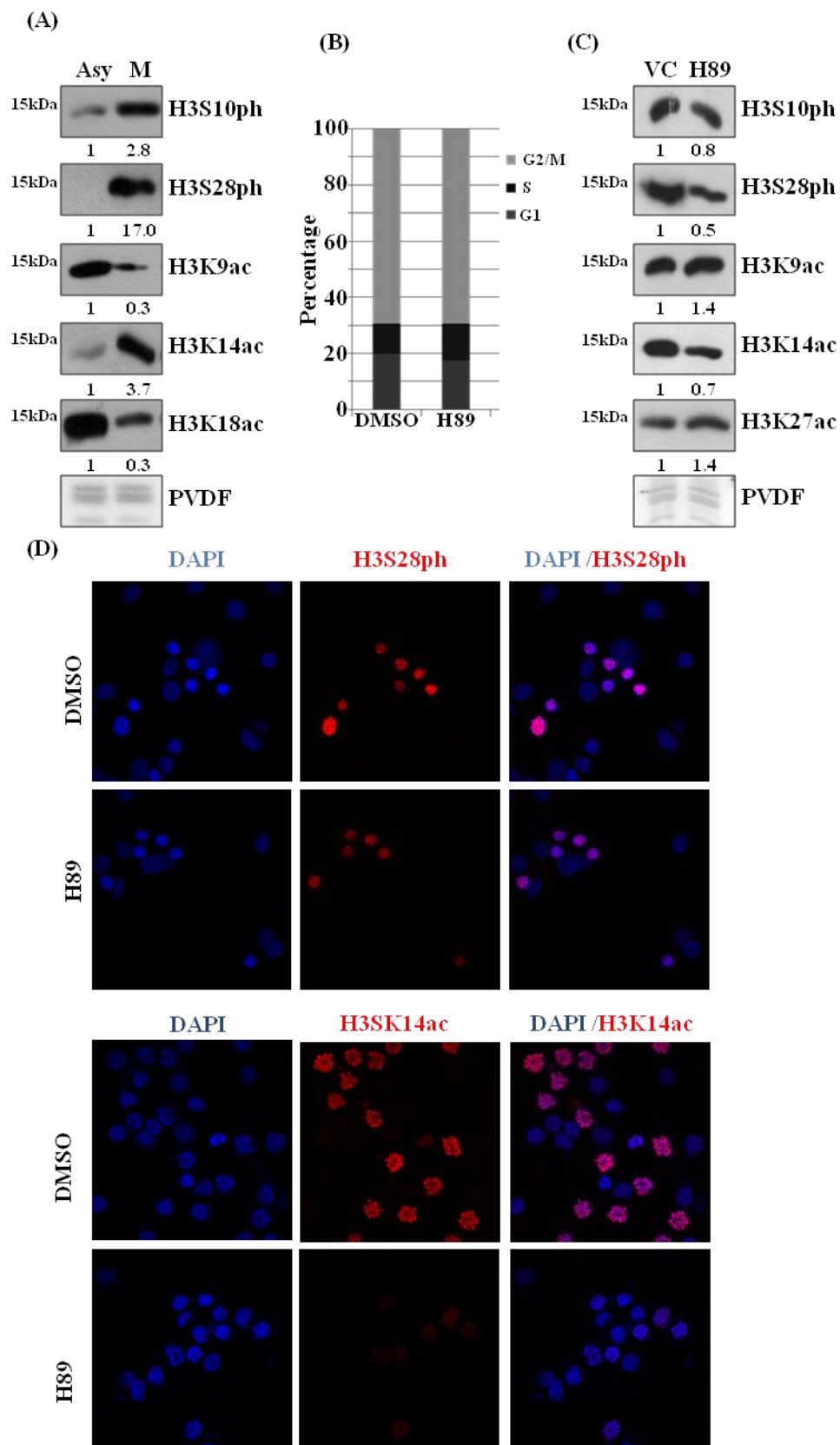


Figure 5.22. Effect of MSK1 inhibition on mitotic H3 phosphorylation and acetylation. AGS cells synchronized in M phase by 16 hours nocodazole treatment. MSK were inhibited by 15 μ M H89 treatment for 60 minutes in presence of nocodazole. (A) Western blots depicting the high H3S10ph/H3S28ph and low H3K9ac and H3K27ac in M phase compared to G1 phase (B) The cell cycle profile of the mitotic cells post MSK inhibition was studied by flow cytometry. (C) Western blots depicting the effect of MSK1 inhibition on mitotic H3. MSK inhibition leads to partial decrease in H3S10ph, predominant decrease in H3S28ph, H3K14ac and increase in H3K9ac and H3K27ac. PVDF serves as the loading control. (D) Immunofluorescence analysis of mitotic cells validating the decrease in H3S28ph and H3K14ac foci upon MSK inhibition.

and H3K14ac post-MSK inhibition. Thus, MSK kinase has partial influence on mitotic histone H3 phosphorylation alongwith Aurora kinase B (AURKB) which is responsible for the majority of histone H3 phosphorylation (Figure 5.22 D).

5.3.3 Effect of MSK inhibition on mitotic exit and entry into G1 phase

To understand whether the altered histone PTMs observed upon MSK inhibition has some functional implication in M phase; its effect post-release from nocodazole was checked by allowing the cell to progress from the mitotic phase (Figure 5.23 A). The mitotic cells were treated with H89 for 60 minutes, washed and reseeded in complete RPMI (Set I). In another set, the H89 treated cells after washing were again treated with H89 containing media to know whether MSK inhibition affects mitotic exit (Set II). The cell cycle profile of the cells in the above two sets was chased for 24 hours. In the first case, the cells either in the DMSO or H89 group progressed similarly through the cell cycle (Figure 5.23 B). In set II, MSK inhibition post-nocodazole release showed a delayed progression of cells with ~70% cells arrested in mitotic phase compared to ~48% in DMSO group post one hour release (Figure 5.23 C). After 24 hours, ~45% of the H89 treated cells were found to be in M phase as opposed to ~29% in DMSO control group. This suggested that MSK mediated mitotic H3 phosphorylation and the associated regulation of mitosis specific neighbouring histone acetylation might be important for

proper mitotic exit and re-entry into G1 phase.

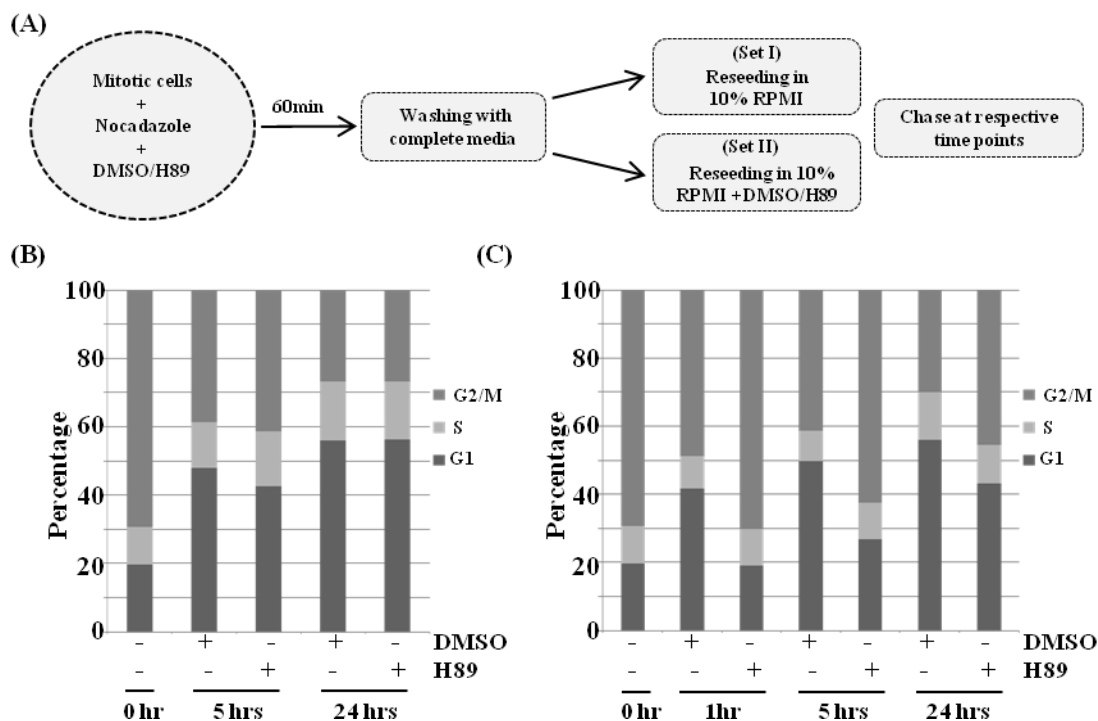


Figure 5.23 *Effect of MSK1 inhibition on mitotic exit/ entry into G1 phase.* AGS cells were synchronized in M phase by 16 hours nocodazole treatment. MSK was inhibited by 15 μ M H89 and the cell cycle profile was analyzed (A) Schematic diagram depicting the protocol of study. (B) Effect of MSK inhibition on mitotic exit upon reseeding in absence of MSK inhibitor (Set I) (C) Effect of MSK inhibition on mitotic exit upon reseeding in presence of MSK inhibitor (Set II).

Further, this observation was tested by immunofluorescence. For this, the mitotic cells either treated with H89 for 1hour or post release in presence of H89 were fixed and immuno-stained for alpha tubulin and lamin A (Figure 5.23 D). The number of mitotic (DAPI intense and Lamin A negative), dividing (Lamin A negative cells in anaphase and cytokinesis) and interphase (Lamin A positive) cells were quantified and their percentage was plotted graphically (Figure 5.23 E). Posts mitotic release the number of interphasic and cells undergoing division increased in the DMSO control group; however in the H89 treated group the number of mitotic cells was high. Thus, the flow cytometry data was complemented by immunofluorescence.

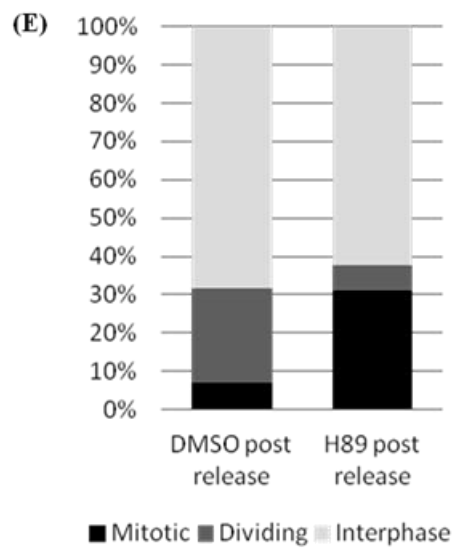
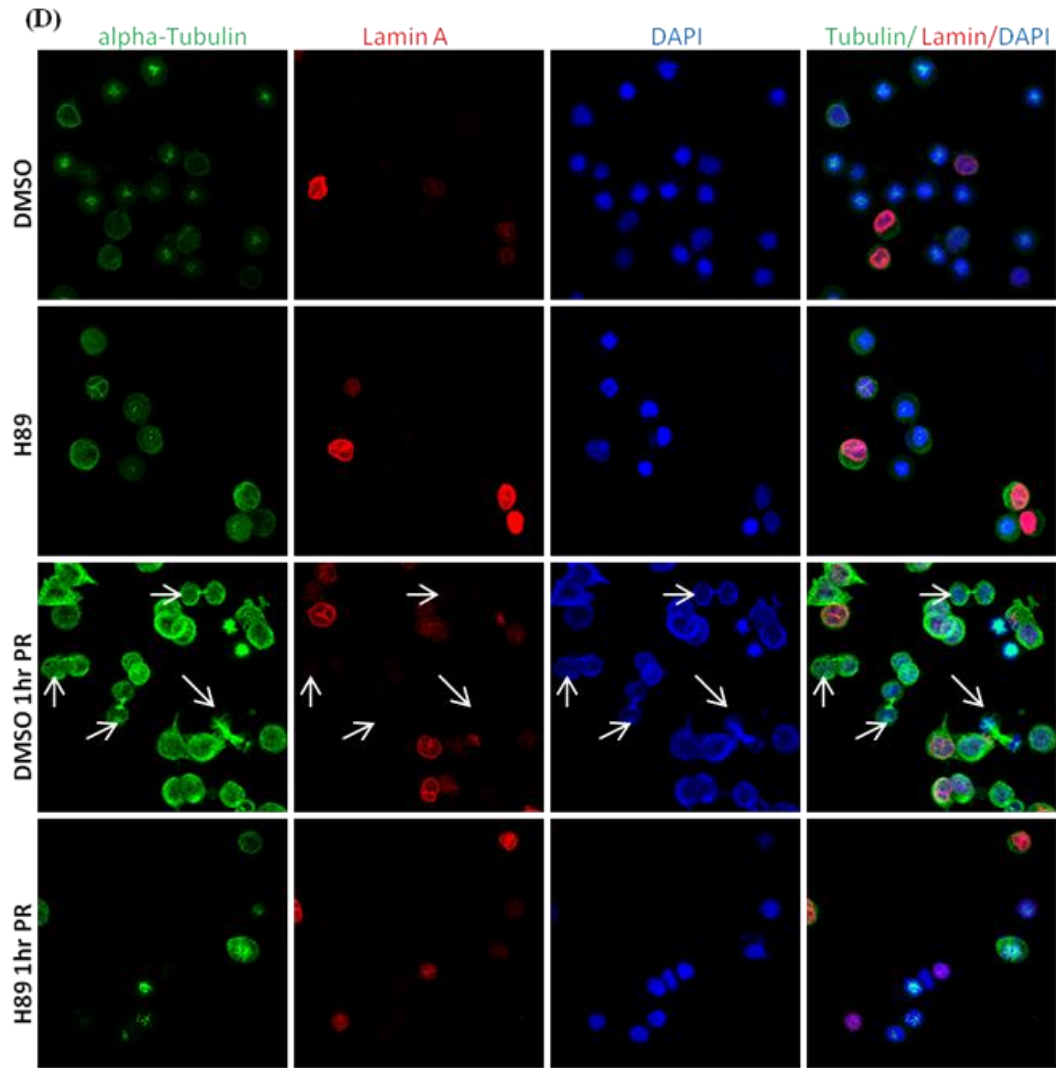


Figure 5.23 Effect of MSK1 inhibition on mitotic exit/ entry into G1 phase. AGS cells were synchronized in M phase by 16 hours nocodazole treatment. MSK was inhibited by 15 μ M H89 and post treatment release in presence or absence of H89, the fixed cells were immuno-stained for alpha tubulin and lamin A (D) Immunofluorescence of mitotic cells exhibited three type of cell populations a) Mitotic (condensed chromatin with intense DAPI staining and absence of Lamin A), b) dividing (Lamin A negative cells in anaphase and cytokinesis highlighted by arrow) and interphase (Lamin A positive). (E) Histogram depicting the percentage of the three cell populations post 1hr release. Around 40-50 cells were counted.

Since, the mitotic exit was affected with an arrest in M phase; the levels of specific cyclins were analyzed. The effect of MSK inhibition on cyclin levels was studied and compared with Aurora kinase B inhibition by 0.2 μ M AZD-1152 HQA. To address this, the mitotic cells were treated with competitive inhibitors of Aurora kinase B and MSK for 60 minutes and the lysates prepared were subjected to western blotting (Figure 5.24).

On AURK B inhibition, a decrease in mitotic specific cyclin B with increase of Cyclin D was observed which is characteristic of cells that have entered G1 phase. Surprisingly, MSK inhibition was also associated with cyclin D increase; however, without a change in cyclin B levels compared to DMSO control (Figure 5.24).

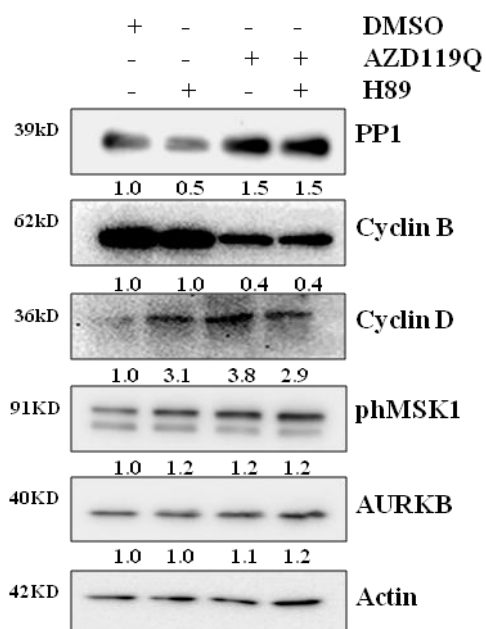


Figure 5.24 Effect of MSK or Aurora B kinase inhibition on the levels of cyclins Western blot showing up regulation of cyclin D and decrease in cyclin B levels upon Aurora kinase B inhibition. No decrease in cyclin B was observed upon MSK inhibition.

Aurora kinase B (AURKB) is known to regulate the protein levels of Protein Phosphatase 1 gamma (PP1 γ) during mitosis with a decrease in AURKB leading to upregulation of PP1 γ and the subsequent H3 dephosphorylation associated with mitotic exit [174,175]. Earlier studies from lab have also reported PP1 α as a phosphatase for H3S10ph during G1 phase. So, the level of PP1 α was explored during mitosis upon MSK and AURKB inhibition. Interestingly, AURKB inhibition led to increase in PP1 α but this increase was not observed upon MSK inhibition (Figure 5.23). Taken together this data suggests that like AURKB, MSK mediated H3 phosphorylation and the associated regulation of histone acetylation is essential for proper mitotic exit; however, the underlying mechanism is different.

5.3.4 Effect of AURKB and MSK inhibition on histone PTM post-release from M phase

MSK regulated mitotic histone PTM is important for mitotic exit as demonstrated by cell cycle kinetics post-mitotic release. To understand the molecular regulation, the levels of histone PTMs, associated kinases and HAT's were profiled during mitosis and post-mitotic release. As observed in previous data by flow cytometry, an arrest of cells in G2/M was evident post-release; and post 1 hour mitotic release a substantial number of cells entered in G1 phase of cell cycle in the DMSO control group (Figure 5.25 A). H3S10ph and H3S28ph levels decreased post AURKB inhibition and decreased levels persisted post mitotic-release (Figure 5.25 B lane 2 &5). However, upon MSK inhibition

H3S28ph levels were predominantly decreased in mitosis; and decreased further post-mitotic release, thus, mimicking the G1-state (Figure 5.25 B lane 3&6).

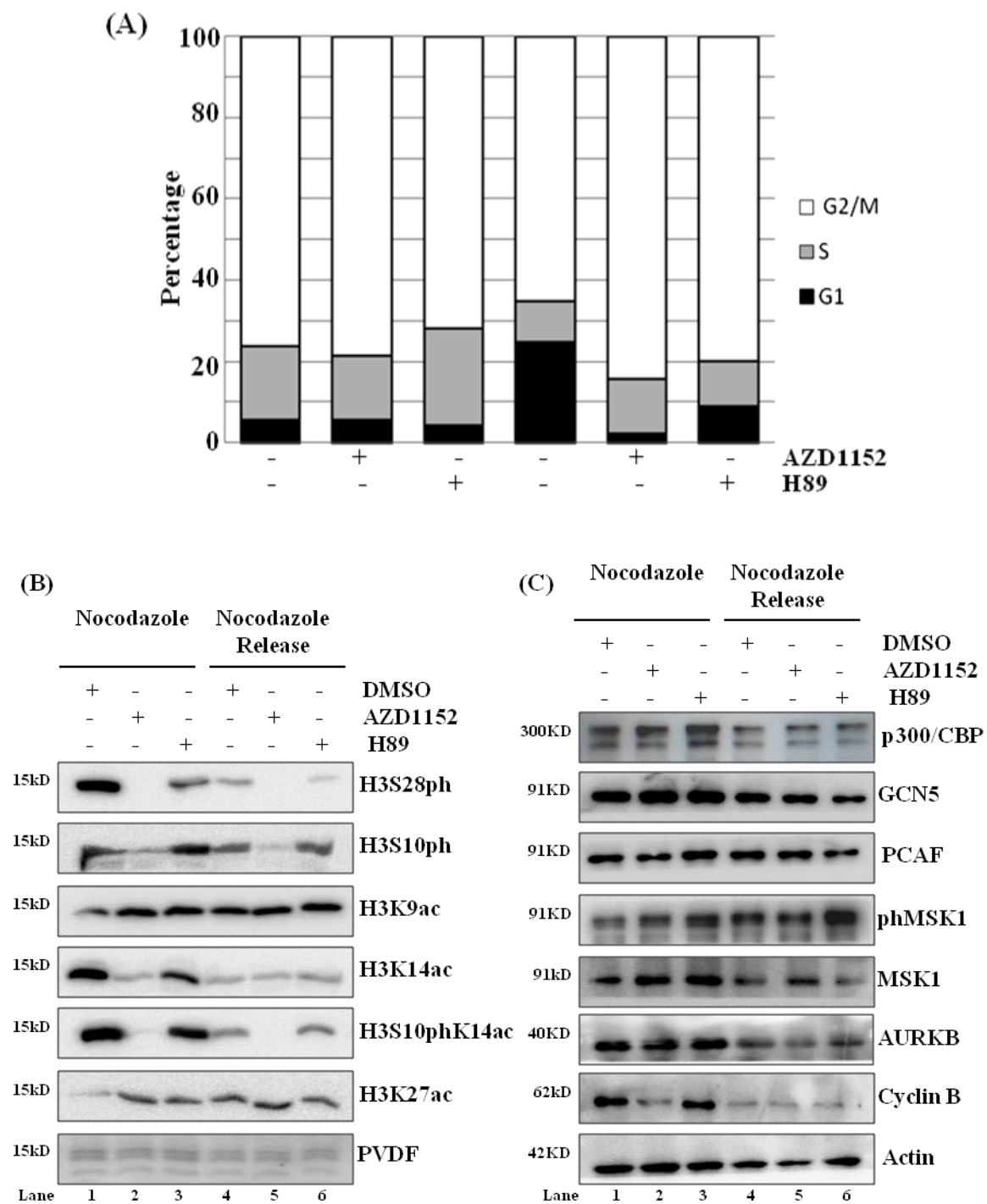


Figure 5.25 Effect of AURKB and MSK inhibition on histone PTM post mitotic release. (A) Cell cycle profiles of AGS cells inhibited by MSK and AURKB inhibitors in presence and absence of nocodazole. (B) Alteration in histone PTM post release from M phase and inhibition of MSK and AURKB. PVDF serves as the loading control. (C) Alterations in HAT's and kinases associated post release from M phase and inhibition of MSK and AURK.

Interestingly, upon inhibition of MSK and AURKB, the acetylation at the neighbouring H3K9 and H3K27 increased, but decreased at H3K14 residue which is a mitotic specific acetylation mark. The histone PTM levels during mitosis and post release, together suggested that although the flow profile indicated towards a G2/M arrest; however, at the molecular level the cells had acquired an epigenetic state comparable to that of G1 cells (Figure 5.25 A).

The alterations in histone acetylation was not associated with alteration in the levels of respective histone acetyltransferases viz; PCAF, GCN5 or p300/CBP as assessed by western blotting. As observed earlier in figure 5.2, an increase in pMSK1 level upon MSK and AURKB inhibition, and the level of AURKB was found to decrease only after mitotic exit, as expected. The cyclin B levels that decreased upon AURKB inhibition in G2/M phase cells, decreased in the DMSO control and MSK inhibition group only upon mitotic release (Figure 5.25 B). Thus, together the data suggests that MSK and AURKB inhibitions drive the cells into a 2N or G- like epigenetic state at the molecular level even though appears to be arrested in a 4N stage by flow cytometry. This could be due to a defect in anaphase or cytokinesis and needs further investigation.

5.3.5 Pathway regulating MSK-mediated H3S10ph, H3S28ph and H3K14ac

After validating the functional role of MSK-mediated H3 phosphorylation and acetylation in mitosis, the pathway regulating MSK in mitosis was studied. ERK1/2 and p38 pathway is known to regulate MSK in G1 phase, and JNK pathway is known to regulate mitotic

H3S10 and H3S28 phosphorylations, nocodazole arrested mitotic cells were treated with inhibitors for ERK1/2 (PD98059), p38 (SB203580) and JNK (SP-600125) along with MSK (H89) for 1 hour. The data suggested that one hour treatment with inhibitors decreases H3 phosphorylations.

Moreover, alterations in phosphorylation were more pronounced after JNK inhibitor compared to other inhibitors considering the fact that JNK pathway also regulates Aurora B kinase in M phase. The pattern of decrease observed after H89 treatment for H3S10ph, H3S28ph and H3K14ac was similar to that of only with JNK inhibitor. Interestingly, decrease in phMSK level was also observed on JNK inhibition. In case of p38 inhibitor a prominent decrease in H3S10ph was observed but no change in H3S28ph or H3K14ac was observed (Figure 5.26). Thus, JNK-mediated MSK phosphorylation regulates a part of H3S10ph, H3S28ph and H3K14ac in mitosis along with Aurora B kinase.

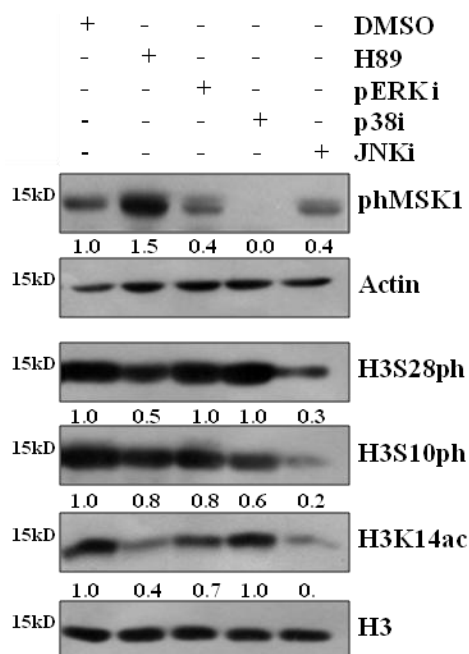
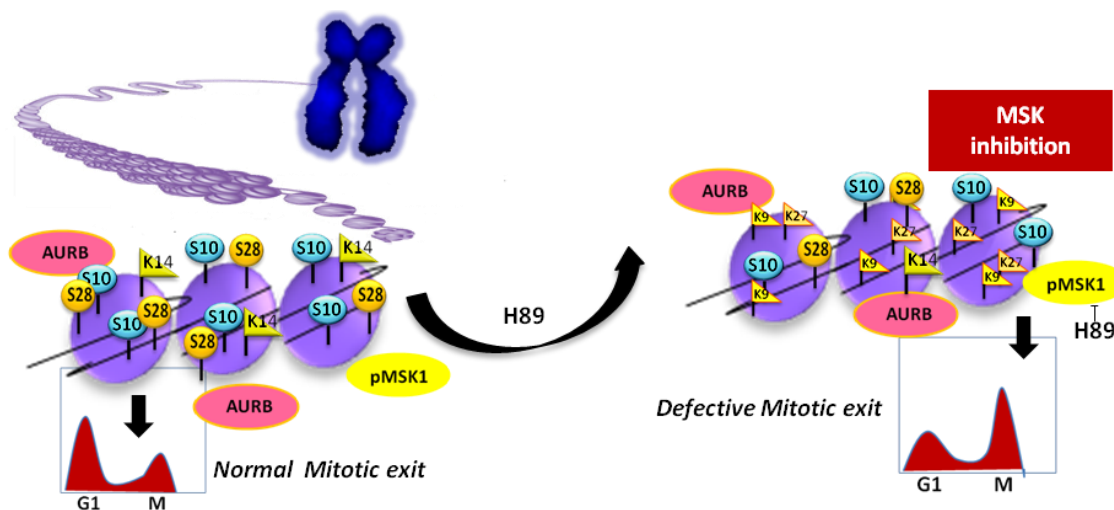


Figure 5.26 Pathway regulating MSK mediated H3 phosphorylation in M phase. AGS cells arrested in mitosis were treated for 1 hour with 10nM ERK, p38 and JNK pathway inhibitors and its effect on histone PTM was profiled by western blotting

Result Summary 5.3

To define the role of MSK1 mediated phosphorylation of H3S10 and H3S28 in M phase cells.



Model 5.3: Mitosis specific regulation of H3 phosphorylation and acetylation by MSK MSK along with Aurora B kinase catalyzes H3S10ph and predominantly H3S28ph during mitosis. Perturbation of this MSK mediated mitotic phosphorylations by H89 results in increased H3K9ac and H3K27ac, suggesting an inverse relation between these two modifications, unlike the positive correlation observed in G1phase. Deregulation of histone acetylation during mitosis was associated with defect in mitotic exit.

Deregulation of histone acetylation during mitosis was associated with error in mitotic exit and this could be lethal. In our earlier study, hypoacetylation of histones at position H3K9ac, H3K14ac, H3K18ac, H3K27ac and H3K56ac was observed during gastric carcinogenesis and this was possibly an outcome of increased HDAC1 which was validated in transformed cell lines and gastric tumors. Thus, by modulating the histone acetylation landscape one could favor pro or anti proliferatory pathways. This could be leveraged by increasing the acetylation using HDACi for treatment of GC. Interestingly, our IHC data suggested that heterogeneity in HDAC levels dictates patient survival. This prompts the potential use of HDAC inhibitors as chemosensitizer for gastric cancer therapy. In the following aim the significance of global histone hypoacetylation in altering the efficacy of chemotherapeutic drug in gastric cancer cell lines and pre-clinical model has been explored.

5.4 To study the significance of global histone hypoacetylation in altering the efficacy of chemotherapeutic drug in gastric cancer cell lines and pre-clinical model.

5.4.1 Expression of class I HDAC's and HDAC activity in gastric cancer patients

Earlier study from our lab has demonstrated low levels of histone H3 and H4 acetylation in the tumor tissues compared to resected margins (RM) tissues in Indian cohort of gastric cancer patients. Further, loss in acetylation was found to be an outcome of higher HDAC activity in tumor tissues as studied by colorimetric HDAC activity assay. Also, a decrease in H3 acetylation was observed at specific position alongwith downregulation of PCAF and up-regulation of HDAC1 in our MNU mediated gastric transformation model. Taken together, the data suggests an inverse correlation between HDAC activity and histone acetylation in GC. HDAC inhibitors (HDACi), a novel class of small molecule therapeutics has shown great promise but resistance to HDACi is often observed alongwith limited success in solid tumors. One of the reasons for HDACi failure in solid tumors may be heterogeneity in expression or activity of class 1 HDACs in patients which is not accounted while administering the dose of HDACi. To understand the need of patient stratification for HDACi therapy, HDAC activity was assessed and was found to be significantly different among GC patients (Figure 5.27 A). Further, the differential expression was validated at transcript level by analyzing TCGA data for the expression of class 1 HDAC viz; HDAC1, HDAC2 and HDAC3 in gastric adenocarcinoma patients ($n = 415$) versus control ($n = 35$), and grouped them into high and low expression based on their Z-score. Around 24% of gastric adenocarcinoma patients showed upregulation in HDAC1, HDAC2 and HDAC3 (Figure 5.27 B).

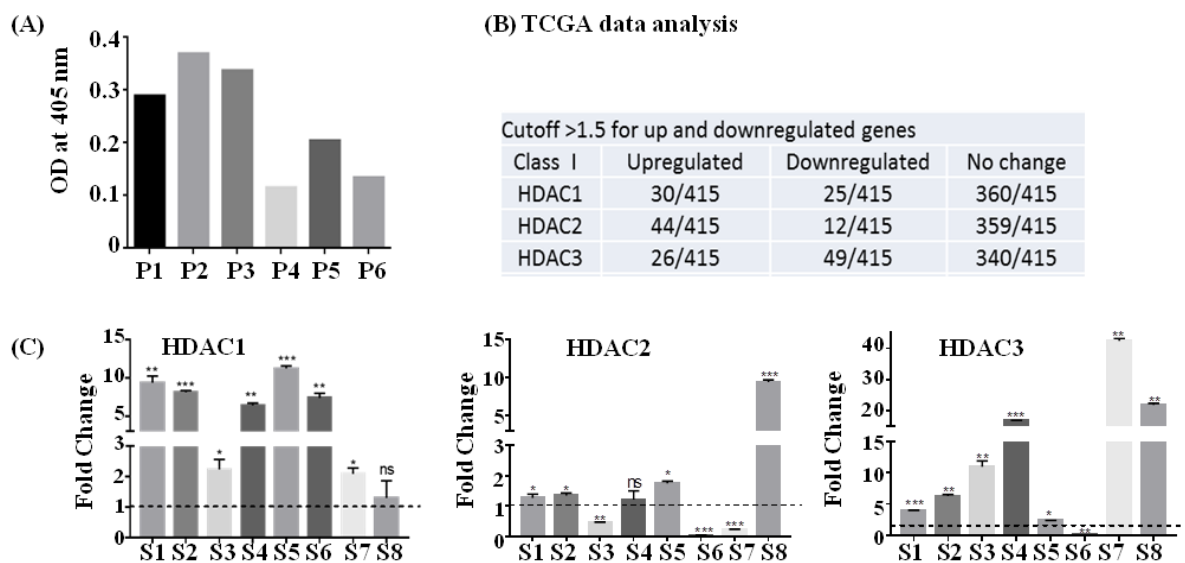


Figure 5.27 Expression of HDAC's (HDAC 1 & 2) and HDAC activity is variable within gastric cancer patients (A) Differential HDAC activity amongst patients was studied calorimetrically. (B) Analysis of The Cancer Genome Atlas data for class I HDAC transcript levels in gastric adenocarcinoma patients. (C) Expression of Class I HDAC viz HDAC1, HDAC2 and HDAC3 in gastric cancer tumors compared to normal tissue (* $P < 0.05$; ** $P < 0.009$; *** $P < 0.0009$).

Like HDAC activity, heterogeneity was also observed in the transcripts levels of class I HDAC's within different patients, as validated by RT-PCR using pooled normal gastric DNA as control (Figure 5.27 C). The data provides evidence for the need of patient stratification and for tailoring the dose of HDACi for sensitizing tumors to the anti-proliferative effects of chemotherapeutic drugs at reduced doses with minimal side effects.

5.4.2 Expression of HDAC's, HDAC activity and histone acetylation in gastric cancer cell lines

Histone acetylation and class I HDAC levels was determined in AGS and HFE145 cell lines. A decrease in site-specific histone acetylation at H3K9ac, H3K18ac, H3K27ac (Figure 5.28 A), along with increased HDAC activity (Figure 5.28 B) was observed in

AGS cell line compared to HFE 145. Further, the transcripts levels of HDAC's showed higher levels of class I HDACs alongwith 7 and 11 (Figure 5.28 C) in transformed AGS cells. The AGS cell line with high HDAC levels and activity, together with low histone acetylation reflected the human gastric tumor status, and was therefore used for studying the potential role of HDACi in sensitizing the anti-cancer effects of chemotherapy drugs both *in vitro* and *in vivo*.

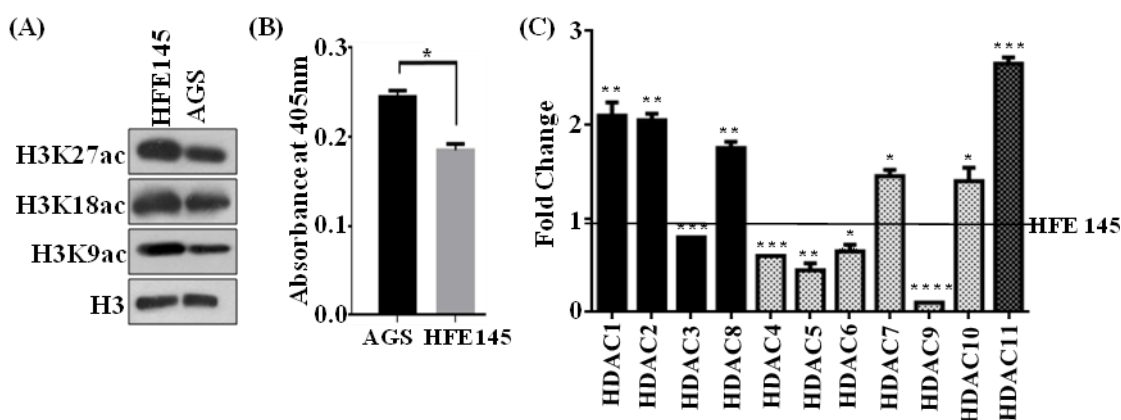


Figure 5.28 Gastric cancer cell lines reflect the histone acetylation status and HDAC levels of gastric tumors. (A) Western blot depicting decreased site specific histone acetylation in transformed AGS cell line compared to untransformed HFE145. (B) HDAC activity in GC cell lines was quantified calorimetrically using whole cell lysate (C) Real time PCR data of Class I to Class IV HDAC levels in the AGS cell line compared to HFE145 (* $P < 0.05$; ** $P < 0.009$, *** $P < 0.0009$).

5.4.3 Sequence specific effect of HDACi on the binding of chemotherapeutic drugs

HDACi mediated hyperacetylation might promote chromatin relaxation, which may in turn enhance the binding of chemotherapeutic drugs bound to DNA. To explore the potent regime for drug administration, AGS cells were treated with HDACi and chemotherapeutic drugs at IC₅₀ values in three different sequence combinations (Figure 5.29 A): (1) Concurrent regime (24 hours HDACi and chemotherapeutic drug together); (2) Pre-treatment regime (24 hours HDACi treatment followed by 24 hours

chemotherapeutic drug treatment); and (3) Post-treatment regime (24 hours chemotherapeutic drug treatment followed by 24 hours HDACi treatment). The inhibitory concentration or IC-50 values for the HDACi's viz; VPA, TSA, SAHA and the chemotherapeutic drugs viz; cisplatin, oxaliplatin and epirubicin were determined for AGS cells previously in the lab by MTT assay. The IC-50 value for cisplatin, oxaliplatin and epirubicin from the dose response curves was found to be 12 μ M, 10 μ M and 0.2 μ M/L, respectively and for the HDAC inhibitors, VPA, TSA and SAHA was 4 mM, 2 μ M and 0.01 μ M, respectively.

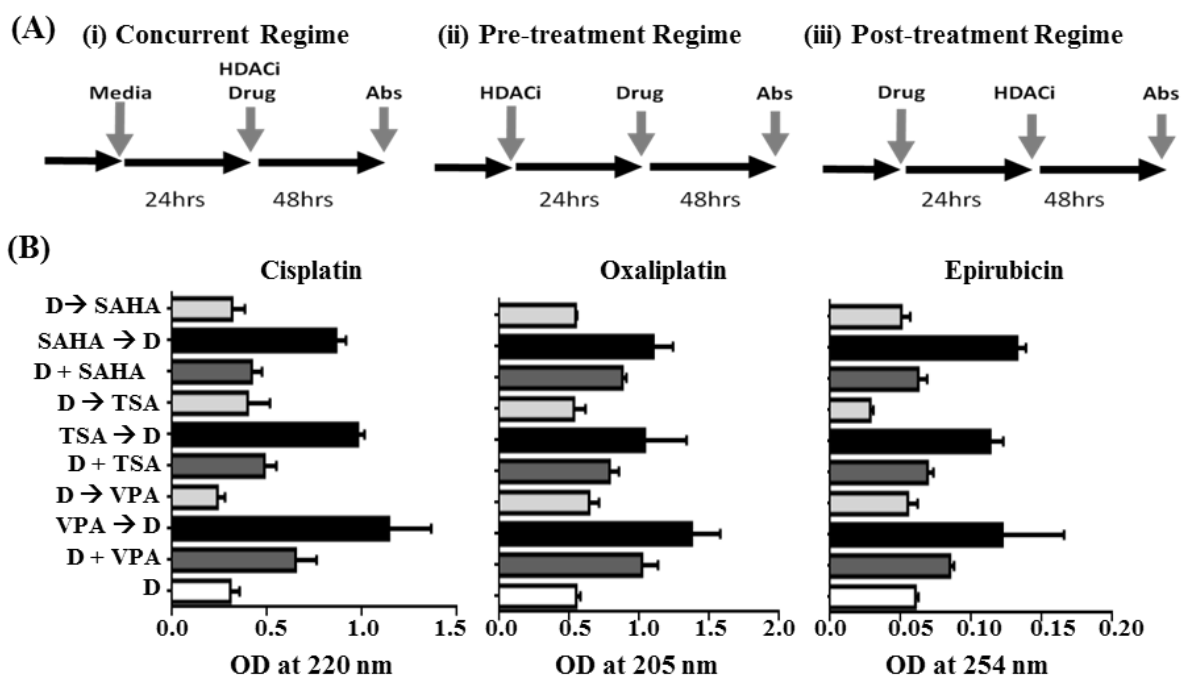


Figure 5.29 Treatment regimens with histone deacetylase inhibitor and binding of chemotherapeutic drugs to chromatin. (A) Schematic representation of three different combination regimes: (i) concurrent [histone deacetylase inhibitor (HDACi) + Drug (D)], (ii) pre- (HDACi followed by Drug) and (iii) post- (Drug followed by HDACi). (B) AGS cells were treated with chemotherapeutic drugs and HDACi at their IC-50 concentration for 24 hours in three different combinations as (A). After the respective treatments, nuclei were extracted from the treated cells, their concentrations were adjusted and the amount of drug bound to DNA was spectrophotometrically estimated. The mean absorbance was plotted against the different drug regimes

The data showed that irrespective of the chemotherapeutic drug or HDACi used, the quantity of DNA-bound chemotherapeutic drugs was increased with pre-treatment regimes followed by concurrent regime. However, post-treatment did not show any increase compared to control for all three HDACi's (Figure 5.29 B). This data suggests that pretreatment with HDACi followed by chemotherapeutic drug could be a more effective regime for a combinatorial therapy.

5.4.4 HDACi and the dose of chemotherapeutic drugs to attain maximum efficacy

The effect of regime-specific combinatorial treatment of HDACi and chemotherapeutic drugs on cell death was studied using fraction affected plot (FA) analysis (Figure 5.30 A) [159]. MTT assays were performed using a fixed constant ratio of chemotherapeutic drugs using three different concentrations below and above the IC-50 value and in three different combination regimes; concurrent, pre- and post- (Table 9.2). The pre-treatment regime with the three HDAC inhibitors led to more cell death compared to concurrent or post-treatment in combination with cisplatin (Figure 5.30 A), oxaliplatin (Figure 5.27 B) and epirubicin (Figure 5.30 C). Further, the combined doses of chemotherapeutic drugs and HDACi required to achieve FA values of 0.5, 0.75 and 0.95 was analyzed and tabulated (Table 5.2). The pre-treatment regime of VPA with cisplatin required lesser combined doses to achieve FA 0.5, 0.75 and 0.95 compared to both concurrent and post-treatment regimes. However, pre-treatment of TSA or SAHA with cisplatin could only attain FA values of 0.5 and 0.75 at a lower combined dose than concurrent or post-treatment combinations. In the case of oxaliplatin, pretreatment with only VPA attained FA values of 0.5, 0.75 and 0.95; whereas, TSA and SAHA achieved only FA values of 0.5 at lower combined doses than the concurrent or post-treatment regimes.

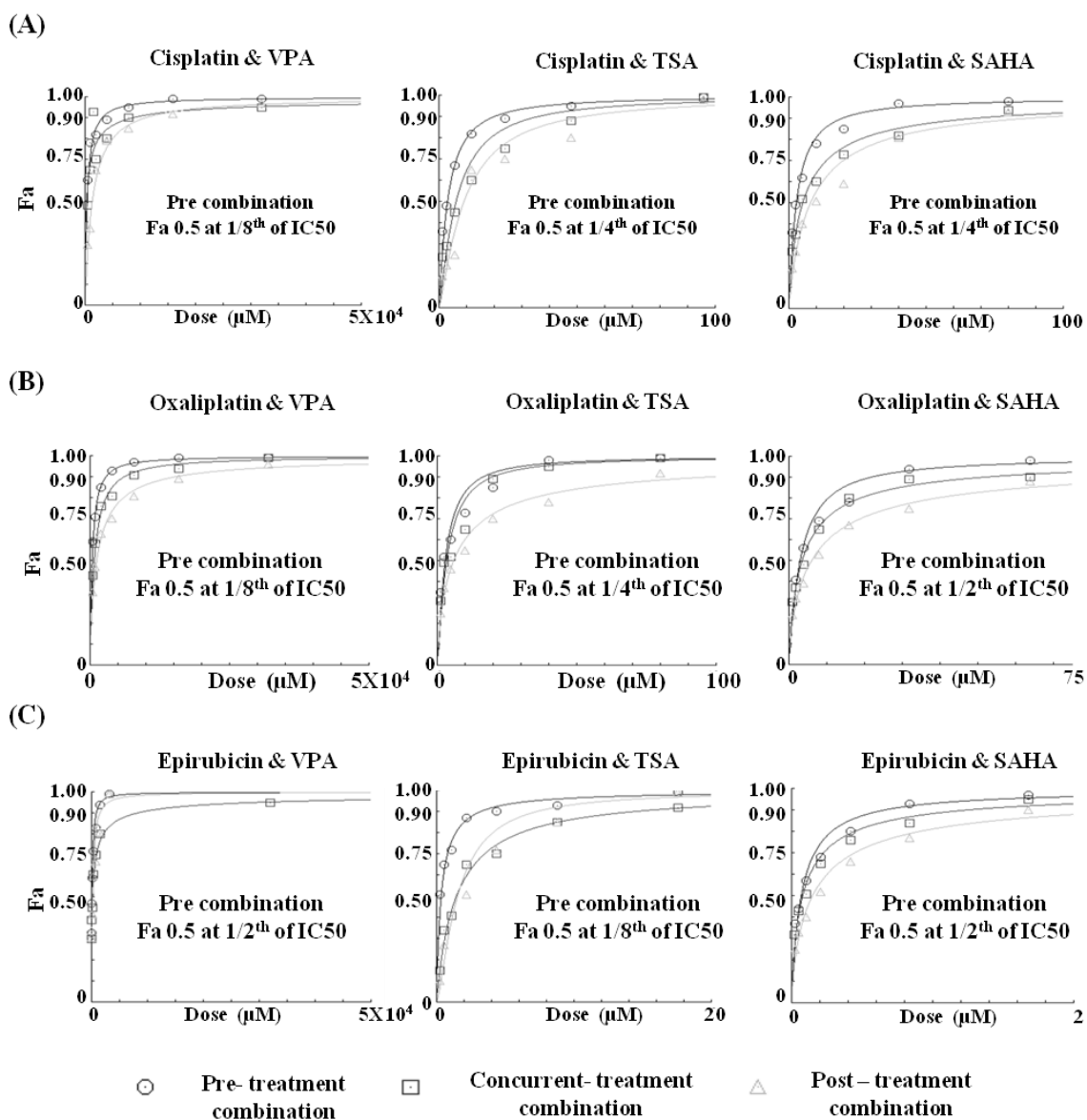


Figure 5.30 HDAC inhibitor-dependent sensitization of GC cells decreases the dose of chemotherapeutic drugs to attain maximum efficacy. AGS cells were treated with chemotherapeutic drugs (cisplatin, oxaliplatin and epirubicin) and HDAC inhibitors (valproic acid (VPA), trichostatin A (TSA) and suberoylanilide hydroxamic acid (SAHA)) for 24 hours each in three different combinations: (i) concurrent (HDACi + Drug), (ii) pre- (HDACi Drug) and (iii) post- (Drug HDACi) at the combined dose (as mentioned in Table 10.2.12), and MTT assays were performed. Fraction-affected dose response curve of (A) Cisplatin; (B) Oxaliplatin; and (C) Epirubicin in different combinations with VPA, TSA or SAHA

In the case of epirubicin, pre-treatment with TSA was found to be most effective, achieving FA values of 0.5 and 0.75 at lesser doses, followed by SAHA. Overall, in the pre-treatment combination regimes, cell death by cisplatin and oxaliplatin is effectively enhanced with VPA, and epirubicin with TSA.

Drugs	Regime and result of FA and median effect plot analysis		Fraction affected (FA)		
			0.5	0.75	0.95
Cisplatin and VPA	Pre	Dose of Cis , VPA (μM)	0.965, 386.359	2.711, 1084.65	15.361, 6144.61
		Combination index (CI)	0.352	0.471	0.784
	Concurrent	Dose of Cis , VPA (μM)	0.705, 282.387	3.874, 1549.74	67.690, 27076.0
		Combination index (CI)	0.257	0.673	3.454
	Post	Dose of Cis , VPA (μM)	3.254, 1301.90	9.362, 3745.16	55.260, 22104.1
		Combination index (CI)	1.188	1.627	2.820
Oxaliplatin and VPA	Pre	Dose of Oxa , VPA (μM)	0.788, 394.469	2.094, 1047.04	10.796, 5398.39
		Combination index (CI)	0.404	0.453	0.552
	Concurrent	Dose of Oxa , VPA (μM)	1.533, 766.633	4.305, 2152.92	24.406, 12203.2
		Combination index (CI)	0.786	0.933	1.249
	Post	Dose of Oxa , VPA (μM)	2.362, 1181.47	8.451, 4225.64	71.917, 35958.6
		Combination index (CI)	1.211	1.83182	3.68265
Epirubicin and TSA	Pre	Combined Dose (μg)	0.030, 0.300	0.093, 0.931	0.623, 6.231
		Combination index (CI)	0.645	0.727	1.222
	Concurrent	Combined Dose (μg)	0.129, 1.299	0.410, 4.105	2.835, 28.356
		Combination index (CI)	2.789	3.207	5.563
	Post	Combined Dose (μg)	0.137, 1.375	0.301, 3.010	1.122, 11.220
		Combination index (CI)	2.952	2.351	2.201

5.4.5 Synergistic interactions of combinatorial HDACi and chemotherapeutic drug treatments depend on regime

To assess which combination regimes of chemotherapeutic drugs and HDACi have a synergistic effect, median effect plot was generated using the FA values and combined doses of drugs. The data was quantitatively analyzed using CI at FA levels of 0.5, 0.75 and 0.95 (Table 5.1 and Figure 5.31).

At an FA value of 0.5, concurrent and pre-combination regimes of VPA with cisplatin or oxaliplatin, pre-combination of TSA or SAHA with cisplatin, and pre-combination of TSA and epirubicin showed synergistic effects, whereas all other combination regimes showed antagonistic effects. In continuation, at an FA value of 0.75, pre-treatment and concurrent combination regimes of VPA or TSA with cisplatin or oxaliplatin showed synergistic effects; however, all other combinations showed additive or antagonistic effects. Further, at an FA level of 0.95, only pre-combination of VPA with cisplatin or oxaliplatin showed synergistic effects; however, all other combinations showed antagonistic effects.

In conclusion, post-treatment with VPA, TSA or SAHA did not have any synergistic effect when combined with cisplatin, oxaliplatin or epirubicin. VPA was found to have a more synergistic effect in the pre-treatment combination regime with cisplatin and oxaliplatin.

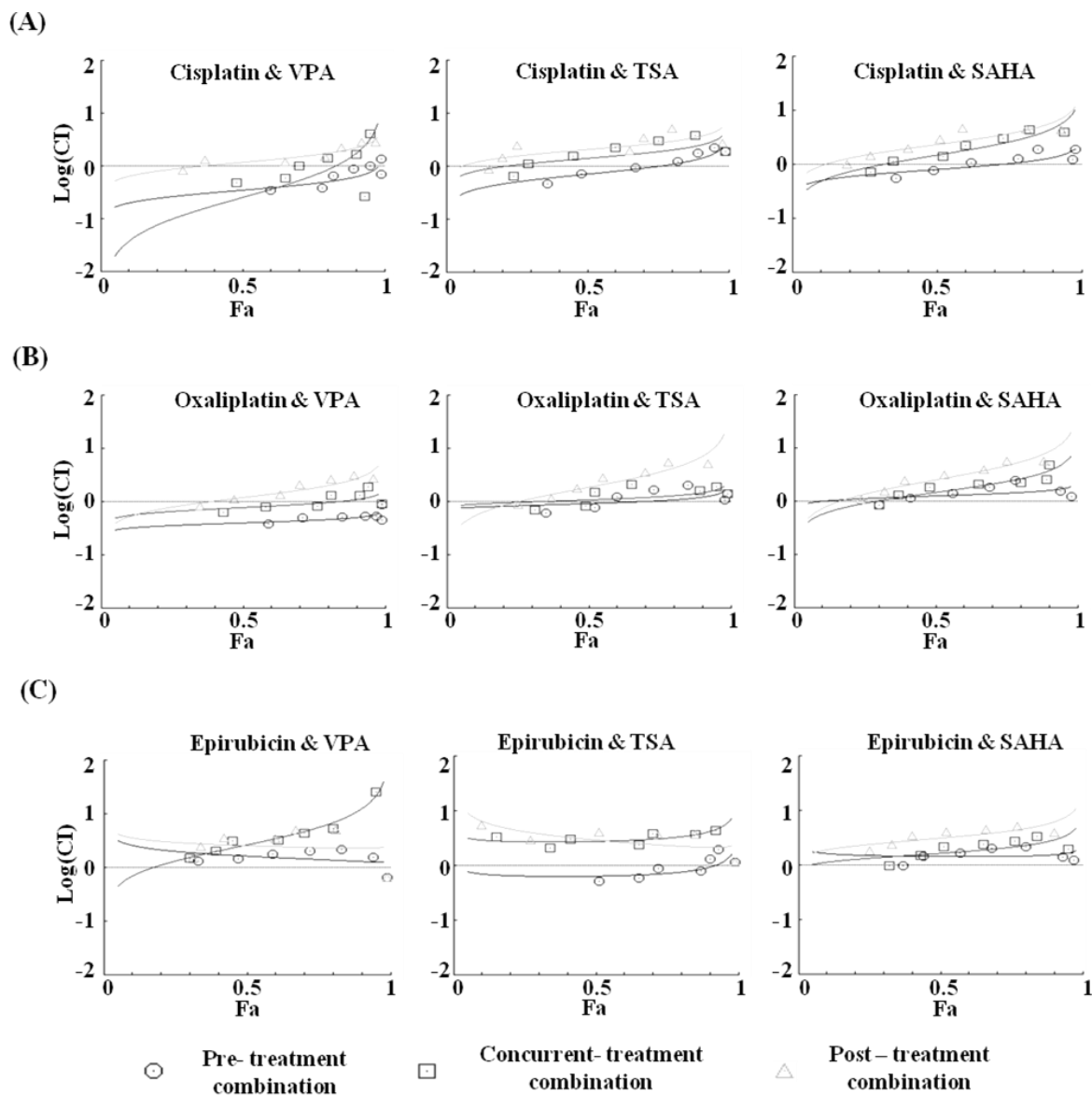


Figure 5.31 Median effect plot analysis for drug combinations (chemotherapeutic drugs and histone deacetylase inhibitors). AGS cells were treated with chemotherapeutic drugs (cisplatin, oxaliplatin and epirubicin) and HDAC inhibitors [valproic acid (VPA), trichostatin A (TSA) and suberoylanilide hydroxamic acid (SAHA)] for 24 hours each in three different combinations - concurrent (HDACi + Drug), pre- (HDACi Drug) and post- (Drug HDACi) at the combined dose (as mentioned in Table 6.1), and MTT assay was performed. Median effect plot shows the combination index (CI) on the Y-axis and fraction-affected values on the X-axis; (A) Cisplatin; (B) Oxaliplatin; and (C) Epirubicin in different combinations with VPA (left panel), TSA (middle panel) and SAHA (right panel). For a particular fraction affected value, the combination index values range from 0 to 1; $CI < 0.8$, $CI = 0.8-1.2$, and $CI > 1.2$ represents the synergistic, additive or antagonistic nature of drug combinations, respectively

5.4.6 Effect of HDACi pretreatment on histone PTMs, cell cycle and chromatin organization

Pre-treatment of valproic acid followed by cisplatin was found to be the most potent combinatorial regime for GC cells. So the molecular alteration associated with this combinatorial regime was explored following treatment of AGS cells with IC-25 doses of VPA and cisplatin either alone or in combination. The effect of VPA in inducing chromatin relaxation was validated by performing MNase assay where an increased intensity of mono- and di-nucleosomes, with a decrease in high molecular weight DNA was observed in VPA-treated cells compared to control (Figure 5.32 A). In association, the levels of H3ac and H4K16ac increased after VPA treatment (Figure 5.33 B). H4K16ac is known to prevent higher order chromatin organization and so its increase, further validates chromatin opening post VPA treatment [57].

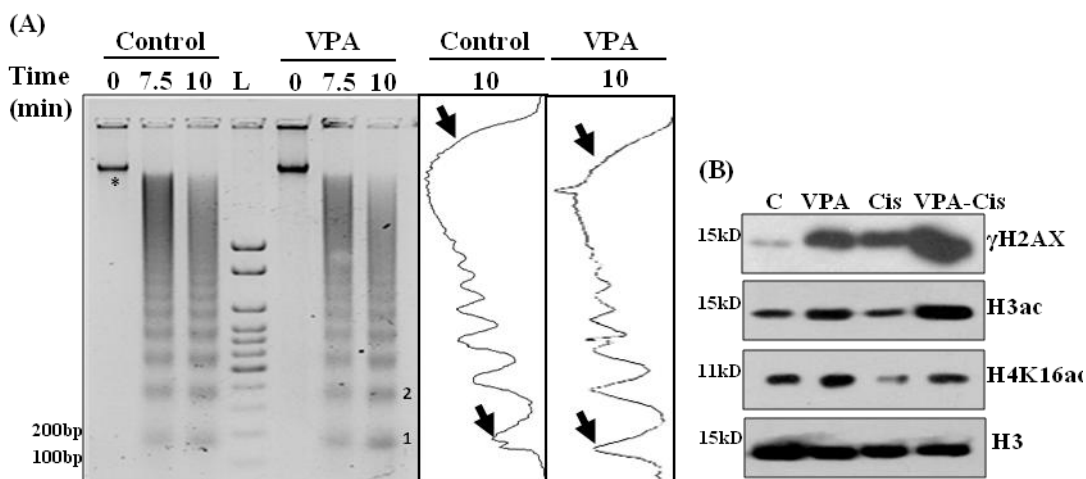


Figure 5.32 Pre-treatment regime is associated with chromatin relaxation and enhanced DNA damage (A) Valproic acid (VPA) (2 mM).mediated increased acetylation leads to chromatin relaxation as analyzed by MNase assay. The time-dependent kinetics was studied following 24 hours treatment of AGS cells with IC-25 concentration of VPA (B) Western blot depicting increased DNA damage with pre treatment regime as suggested by increased levels of γ H2AX. bp-base pairs, * indicates undigested higher molecular weight DNA, 1- mono-nucleosome and 2- di-nucleosome and L – 100bp DNA ladder.

The DNA damage mark γ H2AX was significantly high after combinatorial treatment compared to VPA and cisplatin alone, suggesting increased DNA damage (Figure 5.32 B). H4K16ac was found to be decreased after cisplatin treatment alone, indicating the compaction of chromatin. This was likely an outcome of G2/M arrest post-cisplatin treatment, which may hinder drug binding to chromatin. On the other hand, VPA treatment was found to arrest cells in G1 phase, leading to an open chromatin conformation that favours enhanced drug binding (Figure 5.33 A). In GC, HDAC-mediated repression of tumor suppressor genes has been reported earlier which can be countered by HDAC inhibitors [139,167].

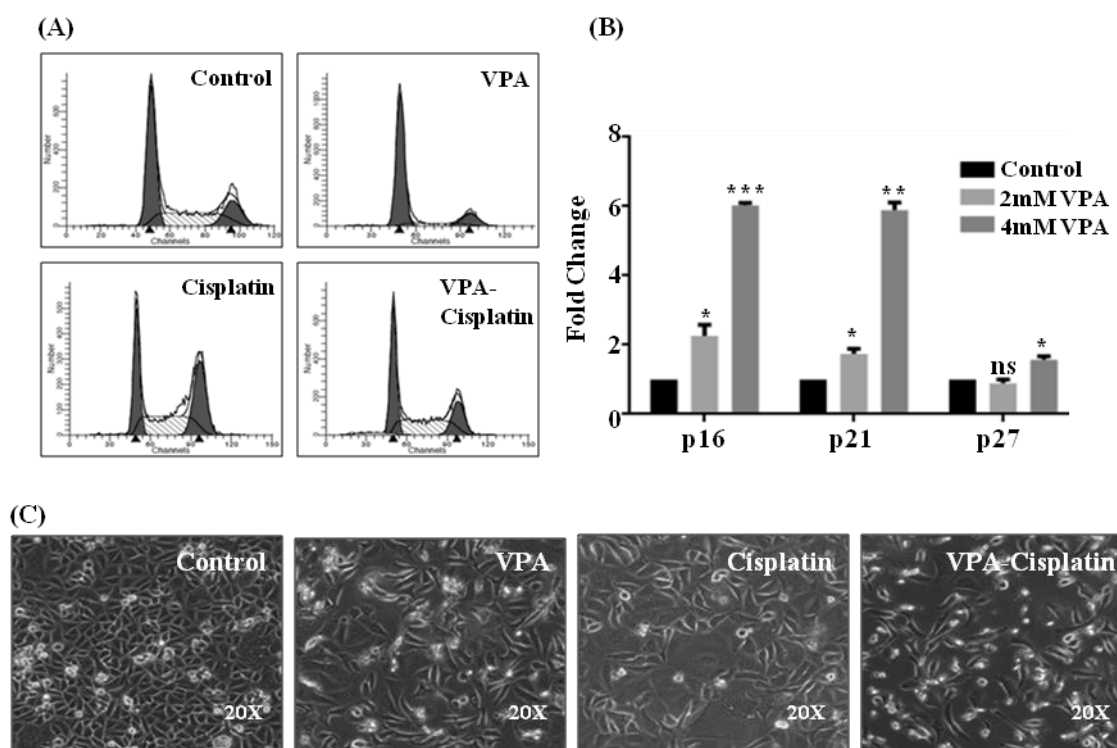


Figure 5.33 Pre-treatment combination leads to cell cycle arrest and re-expression of tumor suppressors. (A) AGS cells treated with VPA/Cisplatin, alone or in combination were arrested in G1 phase by VPA (B) RT-PCR depicting the re-expression of tumor suppressor's p16, p21 and p27 genes post treatment with IC-25 and IC-50 concentration of VPA for 24 hrs. (* $P < 0.02$; ** $P < 0.0009$; *** $P < 0.0001$; ns- non significant)

So, the levels of tumor suppressors were assessed after IC-25 and IC-50 treatment of VPA for 24 hours. A two-fold increase in p16, p21 and p27 was observed (Figure 5.33 B), suggesting the involvement of tumor suppressor-mediated cell cycle arrest and cell death as observed by microscopy (Figure 5.33 C).

Thus, pre-treatment regime of VPA opens chromatin, increases the expression of tumor suppressor genes, and enhances cisplatin binding to chromatin, ultimately leading tumor cell death.

5.4.7 Therapeutic potential of the pre-treatment regime in GC xenograft

The potential of the pre-treatment regime was explored in an *in vivo* xenograft tumor model, developed using AGS cells in NOD-SCID mice. The pre-treatment regime of HDACi, VPA alone or combined with cisplatin was explored for tumor regression (Figure 5.34 A and B). The animals were divided into 4 groups: (i) control, (ii) VPA (300mg/kg/day), (iii) cisplatin (2mg/kg/d), and (iv) combinatorial pre-treatment group (VPA followed by cisplatin with doses as mentioned above) and the animals were treated as depicted in the schematic diagram (Figure 5.34 A).

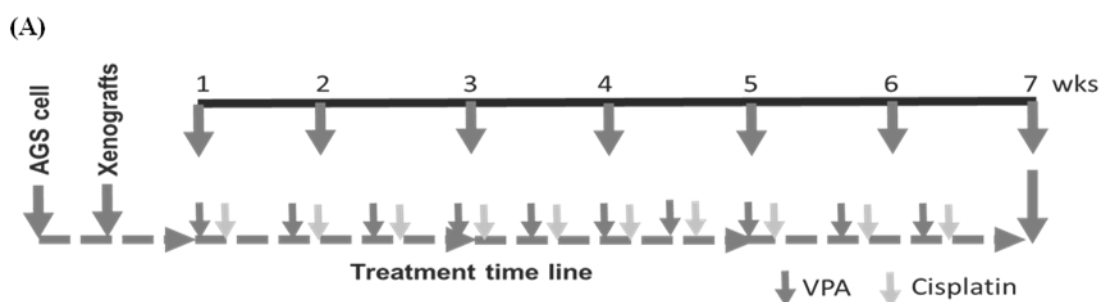


Figure 5.34 Valproic sensitizes AGS cell xenograft to cisplatin in an *in vivo* mice model. (A) Schematic diagram highlighting timeline of *in vivo* drug administration. AGS cells were injected into NOD-SCID mice. After tumors reached approximately 10mm in length mice were divided into four groups ($n = 3$), (1) control, (2) valproic acid (300 mg/kg/d), (3) cisplatin (2 mg/kg/d), and (4) combinatorial treatment of valproic acid followed by cisplatin at the same dose mentioned above.

A change in tumor volume was observed in VPA, cisplatin, and VPA followed by cisplatin-treated groups after 3 weeks of treatment. After 5 weeks of treatment the cisplatin and VPA alone group showed a similar decrease in tumor volume and a 3-fold decrease in tumor volume was observed in the combinatorial treatment group (Figure 5.34 B). Thus, the pre-treatment regime showed a synergistic anti-cancer effect in the pre-clinical model.

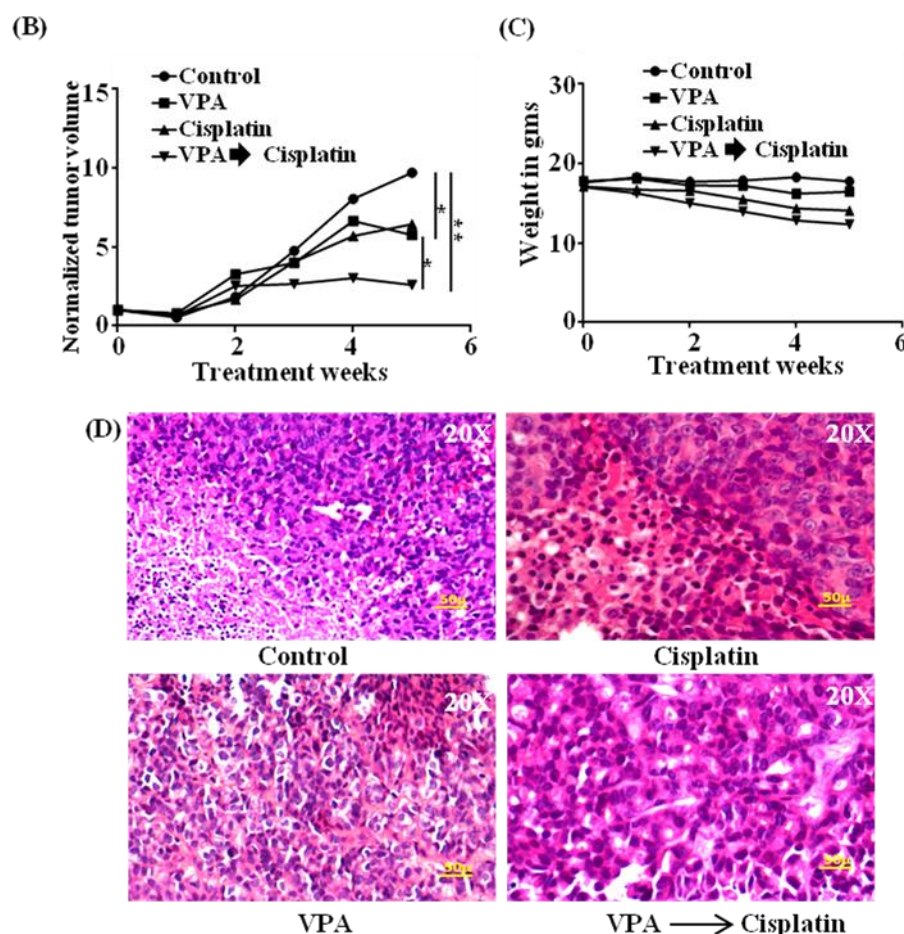


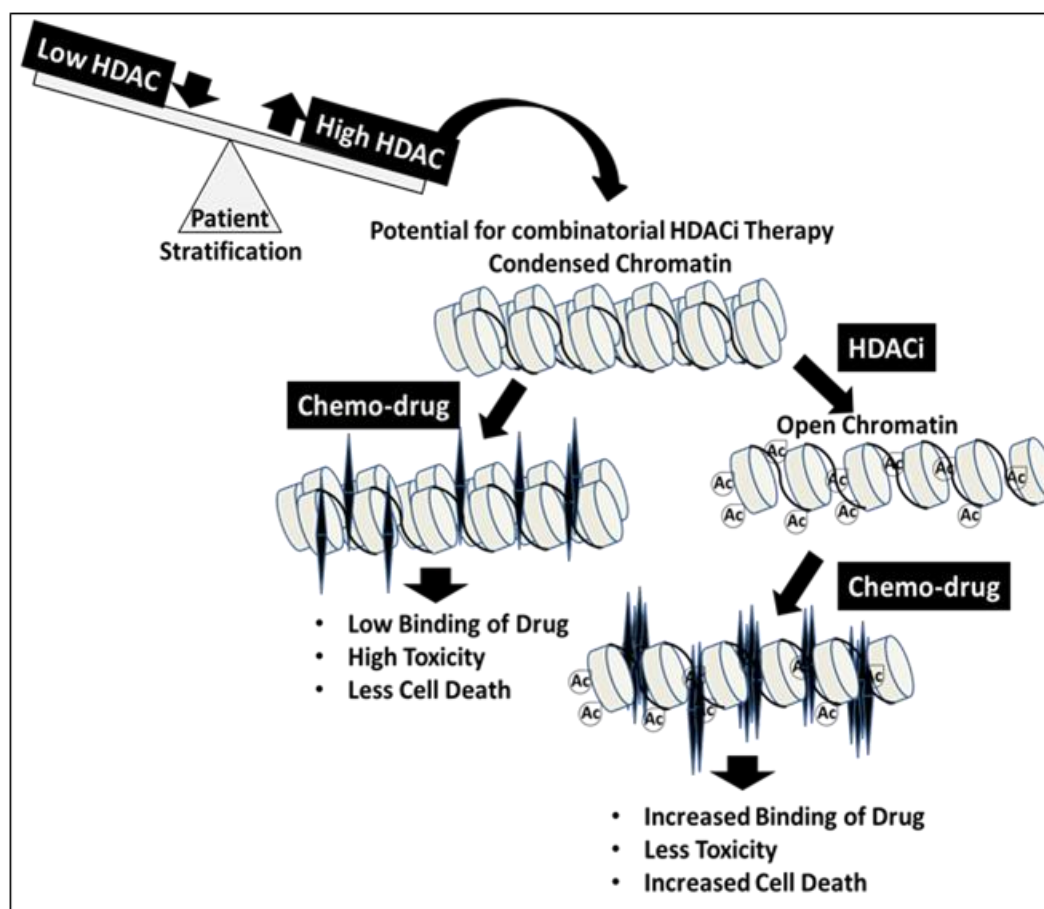
Figure 5.34 Valproic sensitizes AGS cell xenograft to cisplatin in an in vivo mice model. (B) Average tumor volumes of groups normalized to the initial tumor volumes (before treatment) are plotted over a period of 5 wk of drug treatment. The outcome was statistically validated by performing unpaired t-tests (* $P < 0.05$; ** $P < 0.005$). (C) To assess toxicity mean weight of animals in a group was measured over the treatment period. (D) Histopathology of tumor sections from the different groups was studied by hematoxylin and eosin staining following 5 weeks of treatment. Nuclei from the pre-treatment group were large and intensely stained compared to those from control and cisplatin group.

The drug toxicity was assessed by measuring the animal weight weekly and was found to be minimal, with a 15% weight loss in the combination group, suggesting a better drug tolerance (Figure 5.34 C). Histopathological examination of different tumor tissues showed decreased levels of viable cells (20%-55%) in the case of the combinatorial treatment group compared to the control group (70%-90%). Interestingly, infiltration of inflammatory cells was also observed in the combination group. A greater number of mitotic cells were observed in cisplatin alone and the combinatorial group mirroring with the G2/M arrest observed in cisplatin group. Chromatin-associated alterations in the form of pleomorphic, hyper-chromatic nuclei were observed in the combinatorial treated group compared to control after drug treatments. (Figure 5.34 D).

The preclinical study thus proposes the use of the pre-treatment regime in clinical trials after patient stratification for better HDACi therapy success in solid tumors.

Result summary 5.4

To study the significance of global histone hypoacetylation in altering the efficacy of chemotherapeutic drug in gastric cancer cell lines and pre-clinical model.



Model 5.4 HDAC inhibitor acts as a sensitizer for chemotherapeutic drugs in a group of patients with high HDAC activity or levels. A prior treatment of histone deacetylase inhibitors would relax the condensed chromatin of a stratified patient group; making it more accessible and increasing its interaction with chemotherapeutic drugs compared to only first-line chemo treatment. This would enhance the number of cells killed at lower drug concentrations with a decrease in side-effects and toxicity. HDAC: Histone deacetylase; HAT: Histone acetyltransferase

Chapter 6
Discussion

6.1 Discussion

Histone post-translational modifications (PTMs) dynamically regulate the chromatin organization and thus govern fundamental physiological processes like transcription and replication. These changes may also influence the rate of mutation, its fixation, modulating the gene expression and governs key cancer phenotypes. Thus, imbalance in the level of histone PTMs could be early drivers of altered growth in the process of carcinogenesis [8,176]. Our previous study has shown that H3S10ph levels of the normal resected margins correlate with patients' survival depending on its distance from tumor. This supports the notion that initiated cells with altered histone PTMs are critical in the process of gastric carcinogenesis [91]. In light of the above background, we were interested to study the early histone PTM (phosphorylation and acetylation) alterations during gastric carcinogenesis; particularly the H3 phospho-acetylation crosstalk. The translation of the functional output downstream of chromatin is further regulated by a combination of histone PTMs rather than a single PTM. These modifications require co-ordination between different chromatin modifiers in complexes which could be altered in cancer; thus increasing the repertoire of possible targets for therapeutic interventions and the ways to block the pathway.

The present work highlights MSK1 as a key player in regulating the transformed phenotype and imparts an altered cancer specific chromatin landscape. This consists of increased phosphoacetylation, H3S10phK14ac and site-specific histone H3 acetylation mediated by the increased HDAC1 levels. Interestingly, an inverse association between H3 phosphorylation and acetylation was also found to be partly regulated by MSK in mitosis and was essential for immaculate completion of cell division. Further, the

modulation of cancer specific chromatin landscape, global hypoacetylation, by HDACi was found to make chromatin more accessible to chemotherapeutic drugs at non-toxic doses; thus, improving therapy response.

The N- Methylnitrosourea (MNU), implicated in gastric carcinogenesis, at a prolonged non-lethal dose exposure was sufficient enough for cellular transformation. The transformed cell line, MNU-V developed tumors in NOD-SCID mice which exhibited glandular growth with well to poorly differentiated cells characteristic of gastric adenocarcinoma of human; further strengthening our model system. Interestingly, there is no change in proliferation between the normal HFE145 and the transformed MNUV cell line which could be attributed to the genetic background of HFE145 cell line. Immortalization of the cell line has been achieved with expression of SV-40T antigen and hTERT which would already increase the proliferation. This view is further supported by the latest study where transformation of a gastric cell line GES1 (SV-40T antigen and hTERT immortalized) by MNU was associated without a change in proliferation [130]. In another four stage breast cancer model of transformation by SV-40 large T antigen (L), hTERT (T) and H-Ras (R), an increase in proliferation between the primary HMC-p6 and the immortalized HMC-LT cell line was observed; however, the change was less apparent between HMC-LT and the transformed cell line HMC-LTR [177]. The prominent change in clonogenic potential obtained in our transformation model is in coherence with the above mentioned studies, suggesting that transformation preferably enhances the survival of cells than proliferation.

Our data showed alteration in histone PTM during (HFE145 vs MNUV) and upon (HFE145 vs MNUV vs explant cell lines E3.2 and E2.1) transformation. An increase in

H3S10ph and the phosphoacetyl mark, H3S10phK14ac was observed upon transformation which was independent of the cell cycle profile. This is one of the interesting and novel observations of our study which was further validated in gastric cancer tissue samples; where we observed heterogeneity in the H3S10phK14ac levels with ~42% showing high levels. This heterogeneity suggests the possibility of multiple pathways that are associated with development of gastric cancer. Earlier studies on oncogene or nitroso-compound mediated cellular transformation have implicated the role of H3S10ph in transcription of *c-fos*, *c-myc*, Trefoil Factor 1 (TFF1) or Pol III gene expression and this contributes to the proliferation advantage alongwith transformation [72,83]. The increased H3S10phK14ac in present study was found to be enriched in loosely bound nucleosomes or euchromatin; and therefore, influence the altered gene expression profile pertinent to the transformed cell lines, E3.2 and E2.1. The future ChIP sequence analysis of H3S10phK14ac in the normal and transformed cell line would shed more light on the transformation specific gene expression pattern in our system.

The H3S10phK14ac was in turn regulated by MSK1 kinase, whose protein levels and activated form, phMSK1 (S376) was found to be upregulated sequentially during transformation, high in MNUIII and MNUV and persisted upon transformation as well as in explant cultures, E3.2 and E2.1. This was attuned with the increased level of oncogene, K-Ras which is another regulatory protein of the MAPK pathway, known to be constitutively activated in cancer. Whether the MSK mediated H3 phosphorylation is regulated by constitutive activation of the upregulated K-Ras is yet to be explored. Another possibility of increased MSK1 levels could be regulation by mir148b which is known to be downregulated in gastric cancer and negatively regulates MSK1 expression

[178,179]. Upregulation of mir148b in gastric cancer cells mimics the proliferation defect observed post MSK knockdown of the present study. Recently, STAT3 pathway has been shown to positively regulate MSK1 expression during transformation of gastric epithelial cells by MNU [130]. Thus, multiple pathways could regulate the increased MSK1 expression as an early event in gastric carcinogenesis.

In contrast, our inhibitor based study implicates p38 pathway as the upstream kinase for MSK activation and the associated increase of H3S10ph and H3S10phK14ac during gastric carcinogenesis. p38- MAPK pathway has been implicated in angiogenesis, peritoneal dissemination and distant metastasis of gastric cancer alongwith its role in chemoresistance via regulation of epithelial to mesenchymal transition and multidrug resistance genes [164,180–183] Similarly, MSK has been implicated in chemoresistance of prostate cancer cells and myeloma cells via CREB phosphorylation [179,184]. Thus, it is plausible that the p38-MSK axis may be operating the gene expression associated via H3S10pK14ac or phosphorylation of other transcription factors. It is noteworthy that even ERK pathway could regulate the phosphoacetylation via a different kinase. The transformation model of gastric carcinogenesis in the present study thus consolidates earlier studies and our earlier finding where the p38 MAPK-MSK axis was found to mediate the increased H3S10ph observed in Indian cohort of GC patients and proposes it to be one of the earliest events in development of GC [91].

Contrarily to the concept of positive influence of H3S10ph on neighbouring histone acetylation, the increased H3S10ph in our case was associated with decreased H3K9 and H3K14 acetylation. Interestingly, the global levels of H3K18ac, H3K27ac and H3K56ac were also found to be decreased which could be attributed to the sequentially increased

level of HDAC1 during transformation and the decrease in histone acetyltransferase, PCAF/KAT2B. This observations are in consonance with a series of studies that have reported down regulation of PCAF and increased HDACs and the associated histone deacetylation in GC [138,139,161,163,185]. The resulting closed chromatin state due to reduced acetylation may restrict binding of chemotherapeutic drugs leading to chemoresistance like that of 5FU in colorectal cancer upon PCAF downregulation [163]. It may also cause a decrease in expression of tumor suppressor genes. A characteristic example is acetylated p53 mediated transcriptional activation of p21 which is abrogated in gastric cancer [186]. Our observation thus suggests HDAC's as good candidate for GC therapy and the pathways responsible for PCAF downregulation would be worth exploring.

MSK1 mediated H3S10ph has been found to be indispensable for oncogene-induced transformation in fibroblasts [79]. However, the role of MSK in survival and growth of tumor is contentious as it differs depending on cancer type. In case of breast cancer, a high MSK level is known to be associated with better survival. MSK plays a role in differentiation of breast epithelial cells and in its absence cells undergo a state of dormancy; where they are isolated and give rise to distant metastasis at a later stage [86,87] However in hormone dependent breast cancer, MSK1 is crucial for the survival of cancer cells [85]. In contrast, MSK1 has been found to be essential for the survival of cells in gastric, colon and lung cancer [130,187]. Interestingly in our study, a protective role of MSK is observed as its knockdown not only affects the proliferation but also the anchorage-independent growth of the transformed cell. Therefore, it is plausible that

MSK-dependent H3S10phK14ac might be regulating genes associated with transformed phenotypes.

The increased phosphoacetylation suggests towards a positive crosstalk between H3S10 and H3K14 and the possible role of MSK involved were studied in detail. Several studies at gene-specific level and *in vitro* experiments have highlighted the crosstalk [60,188]. H3 phosphorylation is a mitotic mark and therefore to delineate the regulation of low level of H3 phosphorylations in G1 phase by MAPK pathway, it was important to synchronize the cells in G1 phase. Hence, the investigation was carried out after serum starvation and releasing the cells by serum induction. The data suggests two types of chromatin events occurring in the transformed cells. At a global level H3K9, H3K14 and H3K27ac seems to be independent of H3S10ph and H3S28ph, as decrease in these two modifications upon MSK inhibition did not affect their global levels. This is further corroborated with the interesting observation pertaining to the localization of HAT's which were predominantly chromatin bound irrespective of the inhibitor treatment. However, the decrease in the phosphoacetyl mark H3S10phK14ac suggests that H3S10ph might regulate HAT recruitment and H3K14ac at local sites. Interestingly, H3S10ph seems to negatively regulate HDAC1 chromatin recruitment.

HDAC inhibitor mediated stabilization of H3S10ph in presence of anisomycin and induction of H3S28ph in response to TSA has been reported but the underlying mechanism has not been completely elucidated [189]. Here, we experimentally proved that these epigenetic alterations are catalyzed by MSK1. In response to VPA, an increase in MSK1-dependent H3S28ph and H3S10phK14ac was observed which might possibly stimulate stress response genes. Earlier study has shown that H3S28ph is a known to be a

regulator for stimulating stress response genes [190]. A perplexing observation in our study was the differential effect of MSK and HDAC inhibition on phosphoacetylation depending on serum or stress status of the cells. Phosphoacetylation (H3S10phK14ac) increases post-HDAC inhibition seems to be independent of MSK- mediated H3S10ph in absence of serum starvation. This observation is particularly important as a tumor is spatially heterogenous in availability of serum and growth factors. So, VPA will have different outcomes on histone PTMs and thereby underlying gene expression, and in turn may even influence the survival of tumors.

Several studies have reported HDAC up-regulation in gastric cancer; however, the mechanism of HDAC aberrant expression is not reported. Consistent with an earlier study highlighting its regulation by MAPK pathway [169,191]; our MSK inhibitor based and knockdown studies highlight that MSK mediated H3S10phK14ac mediates the increased HDAC1 expression during carcinogenesis. Thus, inhibiting the kinase and HDAC activity may prevent or delay gastric carcinogenesis. This view is further supported by epidemiological study in Mediterranean population where a diet rich in yogurt, high fibre and fish oils has been attributed to low incidence of colon cancer [192,193]. The short chain fatty acids produced with the high fiber diet are potent HDAC inhibitor and thereby controlling the aberrant activity of HDAC's [194,195].

Another novel finding of our study was the elucidation of MSK-mediated H3 phosphorylation during mitosis. To the best of our knowledge Aurora kinase B is the only known mitotic kinase for H3 [45,196]; however, loss of H3S10ph and more specifically H3S28ph upon MSK inhibitions suggests a substantial role of MSK in mitotic H3 phosphorylation. Phosphorylation on Ser-10 occurs in early G2, while phosphorylation

on Ser-28 is detected in early mitosis suggesting different upstream regulatory mechanism for these two phosphorylation events [197]. Infact, several studies have reported the presence of residual H3S28ph after AURKB knockdown [196,198,199]. Interestingly, our study suggests that JNK pathway which regulates AURKB regulates MSK in mitosis. Indeed, the primary sequence of MSK possess the P-x-x-S/T-P motif which are being recognized and phosphorylated by ERK, p38 and JNK MAPK-kinase pathway and the phMSK levels were found to be partly decreased upon JNK inhibition [200]. A perplexing result in our study was the complete loss of H3S10ph and H3S28ph upon AURKB inhibition; where a residual signal phosphorylated by MSK was expected. This could be explained by the decreased cyclin B levels which suggest progression of the cells from metaphase to anaphase. Indeed, AURKB is known to regulate cyclin B transcription in gastric cancer via CREPT protein (cell cycle related and expression elevated protein in tumor) and may even regulate its protein levels [201]. This was in turn associated with increased PP1 α levels. AURKB inhibition is also known to result in cyclin B degradation, recovery of PP1 γ activity and its chromatin recruitment for dephosphorylation of H3 phosphorylation post-metaphase [174,175]. Interestingly, the decrease in cyclin B was not observed upon MSK inhibition, suggesting different downstream mechanisms of H3 phosphorylation regulation although the upstream signal remains the same. This suggest that possibly MSK spatially regulates mitotic H3S28ph and H3 acetylation.

The histone phosphorylation seems to finely regulate H3 acetylation during mitosis. Depletion of H3S10ph, H3S28ph led to upregulation of neighboring acetylation on H3K9 and H3K27 and thus mimicking the acetylation status of interphase cells. However, these

molecular alterations were contrary to the cell cycle profile; which indicated an arrested G2/M population post-nocodazole release and MSK or AURKB inhibition. Indeed, AURKB inhibition or depletion is known to allow cycling of cells with altered ploidy (2N to 8N) with a single large or multi-nuclear morphology arising out of the compromised cytokinesis [202]. The formation of these 4N and 8N state is very important to explore in context of tumor dormancy, reversal of senescence and resistance to chemotherapeutic drugs. Thus, there seems to be an interesting crosstalk, wherein, H3 phosphorylation mediated by AURKB and MSK regulate the H3 acetylation status of mitotic chromatin with different regulatory modules. Nevertheless, this part of study again reiterates the significance of alteration in the H3 acetylation state of cells in modulating growth and cell division, an alternative that could be exploited for cancer treatment.

Earlier part of our present study have shown increased HDAC1 and decreased PCAF levels during gastric carcinogenesis. The histone deacetylation is associated with gene repression; this alteration may lead to selection of initiated cells with repressed tumor suppressor genes. Further, the resulting compact chromatin architecture may limit the accessibility of chromatin to DNA interacting chemotherapeutic drugs and partly contribute to chemoresistance. Thus, modulating the acetylation levels and chromatin organization via HDAC inhibitors would be a suitable strategy for better outcome of therapeutic intervention in GC patients.

Acetylation marks and their modifiers have been widely researched in cancer for their diagnostic, prognostic and therapeutic potential [1]. Even though with potent *in vitro* and pre-clinical studies, clinical application of HDACi in solid tumors has been

disappointing. Some of the confounding factors behind this failure includes the concurrent treatment regime employed, limited combinatorial chemotherapeutic studies, and lack of patient stratification for sensible drug administration. Our study suggest that sensitizing GC cells or *in vivo* xenografts, having increased levels of Class 1 HDACs with pre-HDACi treatment results in histone hyperacetylation and relaxed chromatin organization. The concomitant increased accessibility of chromatin to DNA-interacting drugs induces DNA damage and cell death. A synergistic effect is always preferred and to be achieved in a combinatorial study to be considered for pre-clinical or clinical studies. In our study, pre-treatment combinations of HDACi and chemotherapeutic drugs showed higher percentages of cell death at low combined doses; however, only VPA with oxaliplatin or cisplatin was found to be best as their combination was found to have a synergistic effect across FA values from 0.5 to 0.95. Thus, the pre-treatment approach with HDACi would allow for a low dosage of chemotherapeutic drugs with similar dose-related cytotoxicity. Mutze *et al* had also highlighted the importance of HDACi-SAHA pretreatment to sensitize GC cell lines; however, it was not tested *in vivo* [139]. In our pre clinical study with NOD-SCID mice, the synergistic effect was further recapitulated and a decrease in tumor volume was observed in the pre-treatment group with low toxicity compared to the cisplatin only and VPA groups. Also, VPA alone as a sensitizer had no appreciable side effects in the pre-clinical study as body weight in the VPA-treated group was not altered compared to the VPA/cisplatin-treated group. Moreover, antioxidants like thioredoxin (Trx) play an important role in determining HDACi-induced cell death in cancer cells [203]. Normal cells have relatively higher levels of Trx, and therefore could account, in part, for the low toxicity observed in the pre-clinical protocol. Post-VPA

treatment the cells are arrested in the G1 phase as opposed to the G2/M phase in the case of cisplatin treatment. In the G1 phase the chromatin being more open, favors enhanced cisplatin binding and more cell death as suggested by increased γ H2AX levels. A recent phase II study in GC with vorinostat as a first-line therapy in combination with capecitabine and cisplatin did not meet its expected outcome [96]. In this study, vorinostat was administered concurrent with chemotherapeutic drugs thus vorinostat probably had insufficient time to enforce a chromatin modulatory effect, leading to weak drug binding. The need for changing chromatin organization by HDACi is further strengthened by phase I clinical trials with VPA and the topoisomerase II inhibitor epirubicin [204]. In this study, a pre-exposure of VPA for 48 hours was found to be essential to obtain synergistic outcomes with epirubicin.

Decades of research involving HDACi and chemotherapeutic drugs have failed to take into account the HDAC levels or activity status of patients, resulting in inappropriate and indiscriminate HDACi dose administration. In the ongoing Neck-V-CHANCE trial in head and neck cancer, valproic acid will be administered two week prior to the administration of cisplatin and cetuximab. However, this trial also does not stratify patients based on HDAC activity/levels [205]. Our HDAC activity correlative data that links HDAC expression with histone acetylation, and the presence of heterogeneous HDAC transcript levels and activity in patients, provides sufficient evidence for categorizing patients for HDACi therapy. Weichert *et al* [138] in their IHC based study have showed that approximately 71% (209/293) of GC patients are positive for the expression of either all three or one of the three class 1 HDAC isoforms. Recent publication by Jiang *et al* [206] showed an association between high HDAC1 (60%

patients) with larger tumor size, tumor grade, lymph node metastasis and lymphovascular invasion, making it an independent prognostic factor for GC. Further, our IHC based study has also highlighted increased level of HDAC1 in Indian cohort of gastric cancer patient. However, *in silico* TCGA data analysis suggests that only 24% of GC patients have higher transcript levels of class 1 HDACs. This difference could be attributed to either increased protein stability or the fact that HDAC1 being an immediate early genes, its transcription is rapid and transient with short half lives of transcript; making its detection variable amongst patients and also depending on the cell cycle phase of the bulk tumour. Nevertheless, the heterogeneity observed both at transcript and protein levels highlight the need for prior assessment of class 1 HDAC levels and patient stratification before HDACi therapy. It will also contribute in deciding the dose of HDACi for pre-treatment regimes with DNA-interacting chemotherapeutic drugs for better therapeutic potential.

Overall, the study highlights that early events during transformation and cancer development involves alterations in histone phosphorylation and acetylation. The phosphoacetylation related chromatin signaling is regulated by p38-MSK-MAPK pathway; involves a context-dependent interplay of chromatin modifiers MSK, HDAC's and HAT's. The epigenetic modulators and associated pathways that impact not only the initiation, but also the process of carcinogenesis could be timely reversed or mitigated for healthy life, reduced cancer incidence and better therapeutic outcomes.

Chapter 7
Summary & Conclusion

7.1 Summary and conclusion

Histone post-translational modifications majorly occurring on the N-terminal tails governs DNA accessibility and thus are important in regulating fundamental cellular processes viz; transcription, replication and fidelity of the genome. Any breach in these modifications may lead to deregulation and development of cancer. In consonant, a number of histone PTMs are known to be altered in cancer and so, they have been explored for their utility in better management of cancer. In the current study we investigated the early alteration in histone H3 phosphorylation, acetylation, the cross talk between the two and the associated regulatory mechanism during carcinogen-induced gastric carcinogenesis. Moreover, to best of our knowledge a novel role of MSK kinase in regulating H3 phosphorylation during mitosis was revealed. Further, the global hypoacetylation was exploited by utilizing HDAC inhibitors in combination with chemotherapeutic drug in a pre-clinical model better therapeutic outcome.

7.2 Salient Findings

1) Alteration in histone H3 phosphorylation and acetylation during cellular transformation and the associated modifiers.

- i. *Transformation of gastric epithelial cells with methyl-nitrosourea was achieved after treatment with a non-lethal dose. The transformed cell line, MNUV exhibited higher clonogenic potential without change in cellular proliferation. The tumors developed in vivo recapitulated the human gastric cancer histology, with glandular adenocarcinoma and well to poorly differentiated cell types.*

-
- ii. *Site-specific histone hypo-acetylations along with increased H3S10ph and H3S10phK14ac were observed post-transformation. The increased enrichment of H3S10phK14ac was found to be on euchromatin.*
 - iii. *p38-mediated increase in phMSK1 levels was observed in transformed cells and was responsible for the increased H3S10phK14ac. Interestingly, the levels of phMSK1 were sequentially increasing during cancer development. The histone hypoacetylation observed is potentially an outcome of increased HDAC1 and decreased level of PCAF.*
- 2) MSK1 is essential for the survival of transformed gastric cancer cells, regulates H3S10phK14ac and HDAC1 expression.**
- i. *MSK1 is essential for the proliferation and clonogenic potential of gastric cancer cells. Further, MSK-mediated H3S10ph and H3S28ph were found to be associated with H3K9ac, H3K14ac and H3K27ac in a context-dependent manner.*
 - ii. *HDAC inhibitor treatment leads to an increase in phosphoacetylation H3S10phK14ac and was dependent on H3S10ph by MSK1. Further, MSK1 partly regulate HDAC1 occupancy at certain sites in chromatin depending on H3S10ph status.*
 - iii. *MSK-mediated H3S10ph is important for transcription of HDAC1. Occupancy of H3S10ph and H3K14ac on HDAC1 promoter regulates its transcription.*
 - iv. *HDAC1 levels are upregulated in Indian cohort of gastric cancer patient samples. This could be attributed to the increased phMSK levels.*

3) Mitogen and Stress activated protein kinase partly regulates H3S10ph and particularly H3S28ph in mitosis via JNK pathway

- i. *MSK1 mediate a part of H3S10ph and H3S28ph in mitosis. However, H3S28 is predominantly phosphorylated compared to H3S10.*
- ii. *The mitotic histone phosphorylation is associated with regulation of the neighboring acetylation marks.*
- iii. *Decrease in H3S10ph and H3S28ph in mitosis was associated with increased H3K9ac and H3K27ac.*
- iv. *Inhibition of MSK by H89 hinders entry of mitotic cells in G1 phase of the cell cycle. However, epigenetic profiling and level of cyclins suggests a G1 like histone modification landscape.*
- v. *MSK-mediated H3 phosphorylation in mitosis is regulated by JNK pathway.*

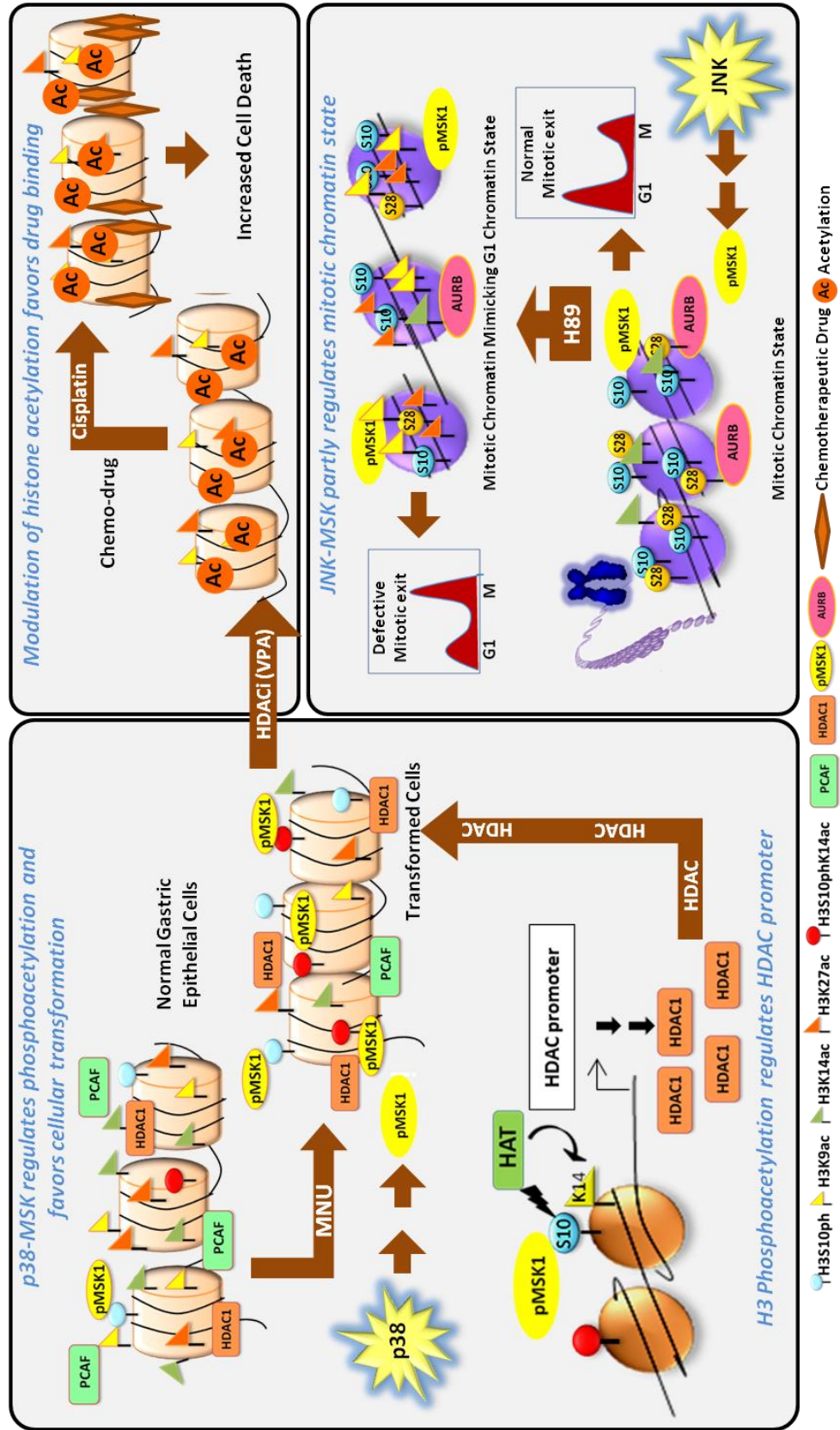
4) Pre-treatment of histone deacetylase inhibitor enhances the efficacy of DNA-interacting chemotherapeutic drugs in gastric cancer.

- i. *An increased level of Class I HDAC's mediates histone hypoacetylation in gastric cancer which can be reversed by treatment with HDAC inhibitor. The increased histone acetylation alters chromatin architecture.*
- ii. *Pretreatment with HDACi results in opening of chromatin which favours enhanced drug binding and thus it sensitizes gastric cancer cells to chemotherapeutic drugs leading to more cell kill in vitro and in vivo preclinical model.*

- iii. *Valproic acid followed by cisplatin or oxaliplatin is the best possible combinatorial regime for gastric cancer patients with reduced chemotherapeutic drug related toxicity.*
- iv. *Treatment with cisplatin arrests cells in G2/M phase which is overridden with a HDACi pre-treatment. G1 arrest by HDACi further enhances increased cisplatin binding.*
- v. *HDACi treatment also leads to de-repression of tumor suppressor gene expression thus further enhancing cell kill.*
- vi. *HDAC activity assay suggests heterogeneity in HDAC levels between different patients. There is a need to stratify patients based on HDAC activity levels before administering HDAC inhibitors for sensible use and for reducing the drug toxicity.*

To summarize, the present study highlights the significant role played by histone modifications and their dysregulation through chromatin modifiers during cellular transformation which could be explored for therapeutic intervention in combination with chemotherapy drugs. A specific context-dependent crosstalk between histone H3S10 phosphorylation and H3K14 acetylation, regulated by an intricate balance between MSK1, HDAC and HATs, was observed upon cellular transformation. MSK-mediated HDAC1 expression alongwith PCAF downregulation led to hypoacetylation of histones. This together with increased phosphoacetylation constitutes a code that at least in part determines epigenetic landscape of transformed cells. Importantly, translating the epigenetic alterations into useful therapeutic potential by inhibition of HDAC's provides a new strategy for better management of gastric cancer.

Phosphoacetylation of histone H3 during cellular transformation



Chapter 8
Future Directions

Future Directions based on the leads obtained from the present study:

- 1) The level of phosphoacetylation H3S10pK14ac could be validated in a large cohort of gastric cancer patients to study its relation with clinicopathological characteristics of patients. (Result 5.1 section 5.1.4)

- 2) ChIP-seq to decipher the genes regulated by H3S10pK14ac in different stages of gastric carcinogenesis. (Result 5.1 section 5.1.4 and 5.2 section 5.2.5)

- 3) The potential of HDACi therapy in combination with standard chemotherapy could be explored in clinics. (Result 5.4)

- 4) Knockdown and ChIP studies of MSK1 and MSK2 to understand the genes regulated by MSK in mitosis and during mitotic exit. Further, to analyze the role of MSK inhibition in aneuploidy. (Result 5.3 section 5.3.2)

Chapter 9
References

-
- [1] J. Füllgrabe, E. Kavanagh, B. Joseph, Histone onco-modifications, *Oncogene*. 30 (2011) 3391.
- [2] F. Bray, J. Ferlay, I. Soerjomataram, R.L. Siegel, L.A. Torre, A. Jemal, Global cancer statistics 2018: GLOBOCAN estimates of incidence and mortality worldwide for 36 cancers in 185 countries, *CA. Cancer J. Clin.* 68 (2018) 394–424. doi:10.3322/caac.21492.
- [3] C.H. Waddington, The epigenotype. 1942., *Int. J. Epidemiol.* (2012). doi:10.1093/ije/dyr184.
- [4] E.J. Richards, Inherited epigenetic variation - Revisiting soft inheritance, *Nat. Rev. Genet.* (2006). doi:10.1038/nrg1834.
- [5] K. Luger, A.W. Mäder, R.K. Richmond, D.F. Sargent, T.J. Richmond, Crystal structure of the nucleosome core particle at 2.8 Å resolution, *Nature*. 389 (1997) 251.
- [6] G.H. Kim, J.J. Ryan, G. Marsboom, S.L. Archer, Epigenetic mechanisms of pulmonary hypertension, *Pulm. Circ.* (2011). doi:10.4103/2045-8932.87300.
- [7] C.L. Woodcock, R.P. Ghosh, Chromatin higher-order structure and dynamics., *Cold Spring Harb. Perspect. Biol.* (2010). doi:10.1101/cshperspect.a000596.
- [8] P.A. Jones, S.B. Baylin, The Epigenomics of Cancer, *Cell.* (2007). doi:10.1016/j.cell.2007.01.029.
- [9] B. Jin, Y. Li, K.D. Robertson, DNA methylation: Superior or subordinate in the epigenetic hierarchy?, *Genes and Cancer*. (2011). doi:10.1177/1947601910393957.
- [10] J.R. Edwards, O. Yarychivska, M. Boulard, T.H. Bestor, DNA methylation and DNA methyltransferases, *Epigenetics Chromatin*. (2017) 1–10. doi:10.1186/s13072-017-0130-8.
- [11] J.W. Wei, K. Huang, C. Yang, C.S. Kang, Non-coding RNAs as regulators in epigenetics (Review), *Oncol. Rep.* (2017). doi:10.3892/or.2016.5236.
- [12] L. Tuddenham, G. Wheeler, S. Ntounia-Fousara, J. Waters, M.K. Hajihosseini, I. Clark, T. Dalmay, The cartilage specific microRNA-140 targets histone deacetylase 4 in mouse cells, *FEBS Lett.* (2006). doi:10.1016/j.febslet.2006.06.080.
- [13] M. Fabbri, R. Garzon, A. Cimmino, Z. Liu, N. Zanesi, E. Callegari, S. Liu, H. Alder, G. Marcucci, G.A. Calin, K. Huebner, C.M. Croce, MicroRNA-29 family reverts aberrant methylation in lung cancer by targeting DNA methyltransferases 3A and 3B, *Proc. Natl. Acad. Sci. U. S. A.* (2007). doi:10.1073/pnas.0707628104.
- [14] L. Sinkkonen, T. Hugenschmidt, P. Berninger, D. Gaidatzis, F. Mohn, C.G. Artus-Revel, M. Zavolan, P. Svoboda, W. Filipowicz, MicroRNAs control de novo DNA methylation through regulation of transcriptional repressors in mouse embryonic stem cells, *Nat. Struct. Mol. Biol.* (2008). doi:10.1038/nsmb.1391.
- [15] Y. Zhang, D. Reinberg, Transcription regulation by histone methylation: Interplay between different covalent modifications of the core histone tails, *Genes Dev.* 15 (2001)

- 2343–2360. doi:10.1101/gad.927301.
- [16] T. Jenuwein, C.D. Allis, Translating the histone code, *Science* (80-.). (2001). doi:10.1126/science.1063127.
- [17] I. Cohen, E. Poręba, K. Kamieniarz, R. Schneider, Histone modifiers in cancer: Friends or foes?, *Genes and Cancer*. 2 (2011) 631–647. doi:10.1177/1947601911417176.
- [18] T. Kouzarides, Chromatin Modifications and Their Function, *Cell*. 128 (2007) 693–705. doi:10.1016/j.cell.2007.02.005.
- [19] T. Banerjee, D. Chakravarti, A Peek into the Complex Realm of Histone Phosphorylation, *Mol. Cell. Biol.* 31 (2011) 4858–4873. doi:10.1128/mcb.05631-11.
- [20] V. Di Cerbo, R. Schneider, Cancers with wrong HATs: The impact of acetylation, *Brief. Funct. Genomics*. 12 (2013) 231–243. doi:10.1093/bfgp/els065.
- [21] X.J. Yang, *Histone Acetyltransferases, Key Writers of the Epigenetic Language*, Elsevier Inc., 2016. doi:10.1016/B978-0-12-802389-1.00001-0.
- [22] X.J. Yang, E. Seto, HATs and HDACs: From structure, function and regulation to novel strategies for therapy and prevention, *Oncogene*. (2007). doi:10.1038/sj.onc.1210599.
- [23] S. Lanouette, J. Haddad, P. Zhang, J.F. Couture, Impacts of Histone Lysine Methylation on Chromatin, *Chromatin Signal. Dis.* (2016) 25–53. doi:10.1016/B978-0-12-802389-1.00002-2.
- [24] J.Y. Cui, Z.D. Fu, J. Dempsey, *The Role of Histone Methylation and Methyltransferases in Gene Regulation*, Elsevier Inc., 2019. doi:10.1016/B978-0-12-812433-8.00002-2.
- [25] A. Sharda, R. V. Amnekar, A. Natu, Sukanya, S. Gupta, *Histone posttranslational modifications: Potential role in diagnosis, prognosis, and therapeutics of cancer*, Elsevier Inc., 2019. doi:10.1016/b978-0-12-814259-2.00014-5.
- [26] J. Fuhrmann, K.W. Clancy, P.R. Thompson, *Chemical Biology of Protein Arginine Modifications in Epigenetic Regulation*, *Chem. Rev.* (2015). doi:10.1021/acs.chemrev.5b00003.
- [27] G. Smeenk, N. Mailand, Writers, readers, and erasers of histone ubiquitylation in DNA double-strand break repair, *Front. Genet.* (2016). doi:10.3389/fgene.2016.00122.
- [28] V.G. Allfrey, R. Faulkner, A.E. Mirsky, ACETYLATION AND METHYLATION OF HISTONES AND THEIR POSSIBLE ROLE IN THE REGULATION OF RNA SYNTHESIS, *Proc. Natl. Acad. Sci.* (1964). doi:10.1073/pnas.51.5.786.
- [29] K. Struhl, Histone acetylation and transcriptional regulatory mechanisms, *Genes Dev.* . 12 (1998) 599–606.
- [30] E. Verdin, M. Ott, 50 years of protein acetylation: From gene regulation to epigenetics, metabolism and beyond, *Nat. Rev. Mol. Cell Biol.* (2015). doi:10.1038/nrm3931.

- [31] A.L. Clayton, S. Rose, M.J. Barratt, L.C. Mahadevan, Phosphoacetylation of histone H3 on c-fos- and c-jun-associated nucleosomes upon gene activation, *EMBO J.* 19 (2000) 3714–3726. doi:10.1093/emboj/19.14.3714.
- [32] A. Zippo, A. De Robertis, R. Serafini, S. Oliviero, PIM1-dependent phosphorylation of histone H3 at serine 10 is required for MYC-dependent transcriptional activation and oncogenic transformation, *Nat. Cell Biol.* 9 (2007) 932–944. doi:10.1038/ncb1618.
- [33] A.L. Clayton, S. Rose, M.J. Barratt, L.C. Mahadevan, Phosphoacetylation of histone H3 on c-fos- and c-jun-associated nucleosomes upon gene activation, *EMBO J.* (2000). doi:10.1093/emboj/19.14.3714.
- [34] P. Sen, W. Dang, G. Donahue, J. Dai, J. Dorsey, X. Cao, W. Liu, K. Cao, R. Perry, J.Y. Lee, B.M. Wasko, D.T. Carr, C. He, B. Robison, J. Wagner, B.D. Gregory, M. Kaeberlein, B.K. Kennedy, J.D. Boeke, S.L. Berger, H3K36 methylation promotes longevity by enhancing transcriptional fidelity, *Genes Dev.* 29 (2015) 1362–1376. doi:10.1101/gad.263707.115.
- [35] W. Zhou, P. Zhu, J. Wang, G. Pascual, K.A. Ohgi, J. Lozach, C.K. Glass, M.G. Rosenfeld, Histone H2A Monoubiquitination Represses Transcription by Inhibiting RNA Polymerase II Transcriptional Elongation, *Mol. Cell.* 29 (2008) 69–80. doi:10.1016/j.molcel.2007.11.002.
- [36] R. Pavri, B. Zhu, G. Li, P. Trojer, S. Mandal, A. Shilatifard, D. Reinberg, Histone H2B Monoubiquitination Functions Cooperatively with FACT to Regulate Elongation by RNA Polymerase II, *Cell.* 125 (2006) 703–717. doi:10.1016/j.cell.2006.04.029.
- [37] H. Long, L. Zhang, M. Lv, Z. Wen, W. Zhang, X. Chen, P. Zhang, T. Li, L. Chang, C. Jin, G. Wu, X. Wang, F. Yang, J. Pei, P. Chen, R. Margueron, H. Deng, M. Zhu, G. Li, H2A.Z facilitates licensing and activation of early replication origins, *Nature.* 577 (2020) 576–581. doi:10.1038/s41586-019-1877-9.
- [38] R.E. Sobel, R.G. Cook, C.A. Perry, A.T. Annunziato, C.D. Allis, Conservation of deposition-related acetylation sites in newly synthesized histones H3 and H4, *Proc. Natl. Acad. Sci. U. S. A.* 92 (1995) 1237–1241. doi:10.1073/pnas.92.4.1237.
- [39] J.A. Mello, G. Almouzni, The ins and outs of nucleosome assembly, *Curr. Opin. Genet. Dev.* 11 (2001) 136–141. doi:10.1016/S0959-437X(00)00170-2.
- [40] S. Bhaskara, V. Jacques, J.R. Rusche, E.N. Olson, B.R. Cairns, M.B. Chandrasekharan, Histone deacetylases 1 and 2 maintain S-phase chromatin and DNA replication fork progression, *Epigenetics and Chromatin.* 6 (2013). doi:10.1186/1756-8935-6-27.
- [41] W. Qin, P. Wolf, N. Liu, S. Link, M. Smets, F. La Mastra, I. Forné, G. Pichler, D. Hörl, K. Fellingner, F. Spada, I.M. Bonapace, A. Imhof, H. Harz, H. Leonhardt, DNA methylation requires a DNMT1 ubiquitin interacting motif (UIM) and histone ubiquitination, *Cell Res.* 25 (2015) 911–929. doi:10.1038/cr.2015.72.
- [42] D. Bonenfant, H. Towbin, M. Coulot, P. Schindler, D.R. Mueller, J. van Oostrum,

- Analysis of dynamic changes in post-translational modifications of human histones during cell cycle by mass spectrometry, *Mol. Cell. Proteomics*. 6 (2007) 1917–1932. doi:10.1074/mcp.M700070-MCP200.
- [43] T.B. Kheir, A.H. Lund, Epigenetic dynamics across the cell cycle, *Essays Biochem.* 48 (2010) 107–120. doi:10.1042/BSE0480107.
- [44] Y. Li, G.D. Kao, B.A. Garcia, J. Shabanowitz, D.F. Hunt, J. Qin, C. Phelan, M.A. Lazar, A novel histone deacetylase pathway regulates mitosis by modulating Aurora B kinase activity, *Genes Dev.* 20 (2006) 2566–2579. doi:10.1101/gad.1455006.
- [45] R. Giet, D.M. Glover, Drosophila Aurora B Kinase Is Required for Histone H3 Phosphorylation and Condensin Recruitment during Chromosome Condensation and to Organize the Central Spindle during Cytokinesis, 152 (2001) 669–681.
- [46] H. Goto, Y. Yasui, E.A. Nigg, M. Inagaki, Aurora-B phosphorylates Histone H3 at serine28 with regard to the mitotic chromosome condensation, *Genes to Cells*. 7 (2002) 11–17. doi:10.1046/j.1356-9597.2001.00498.x.
- [47] H. Cerutti, J.A. Casas-Mallano, Histone H3 phosphorylation: Universal code or lineage specific dialects?, *Epigenetics*. 4 (2009) 71–75. doi:10.4161/epi.4.2.7781.
- [48] C. Prigent, S. Dimitrov, Phosphorylation of serine 10 in histone H3, what for?, *J. Cell Sci.* (2003). doi:10.1242/jcs.00735.
- [49] M. Podhorecka, A. Skladanowski, P. Bozko, H2AX Phosphorylation: Its Role in DNA Damage Response and Cancer Therapy, *J. Nucleic Acids*. 2010 (2010) 920161. doi:10.4061/2010/920161.
- [50] H.T. Van, M.A. Santos, Histone modifications and the DNA double-strand break response, *Cell Cycle*. 17 (2018) 2399–2410. doi:10.1080/15384101.2018.1542899.
- [51] A.K. Sharma, S. Bhattacharya, S.A. Khan, B. Khade, S. Gupta, Dynamic alteration in H3 serine 10 phosphorylation is G1-phase specific during ionization radiation induced DNA damage response in human cells, *Mutat. Res. - Fundam. Mol. Mech. Mutagen.* 773 (2015) 83–91. doi:10.1016/j.mrfmmm.2015.01.017.
- [52] T.M. Pawlik, K. Keyomarsi, Role of cell cycle in mediating sensitivity to radiotherapy, *Int. J. Radiat. Oncol. Biol. Phys.* (2004). doi:10.1016/j.ijrobp.2004.03.005.
- [53] C.T. Tuzon, T. Spektor, X. Kong, L.M. Congdon, S. Wu, G. Schotta, K. Yokomori, J.C. Rice, Concerted Activities of Distinct H4K20 Methyltransferases at DNA Double-Strand Breaks Regulate 53BP1 Nucleation and NHEJ-Directed Repair, *Cell Rep.* 8 (2014) 430–438. doi:10.1016/j.celrep.2014.06.013.
- [54] W.L. Cheung, K. Ajiro, K. Samejima, M. Kloc, P. Cheung, C.A. Mizzen, A. Beeser, L.D. Etkin, J. Chernoff, W.C. Earnshaw, C.D. Allis, Apoptotic phosphorylation of histone H2B is mediated by mammalian sterile twenty kinase, *Cell*. 113 (2003) 507–517. doi:10.1016/S0092-8674(03)00355-6.

- [55] P.J. Hurd, A.J. Bannister, K. Halls, M.A. Dawson, M. Vermeulen, J. V. Olsen, H. Ismail, J. Somers, M. Mann, T. Owen-Hughes, I. Gout, T. Kouzarides, Phosphorylation of histone H3 Thr-45 is linked to apoptosis, *J. Biol. Chem.* (2009). doi:10.1074/jbc.M109.005421.
- [56] S. Jørgensen, G. Schotta, C.S. Sørensen, Histone H4 Lysine 20 methylation: Key player in epigenetic regulation of genomic integrity, *Nucleic Acids Res.* 41 (2013) 2797–2806. doi:10.1093/nar/gkt012.
- [57] M. Shogren-Knaak, H. Ishii, J.-M. Sun, M.J. Pazin, J.R. Davie, C.L. Peterson, Histone H4-K16 Acetylation Controls Chromatin Structure and Protein Interactions, *Science* (80-.). 311 (2006) 844–847. doi:10.1126/science.1124000.
- [58] T. Suganuma, J.L. Workman, Crosstalk among Histone Modifications, *Cell.* 135 (2008) 604–607. doi:10.1016/j.cell.2008.10.036.
- [59] W.S. Lo, R.C. Trievel, J.R. Rojas, L. Duggan, J.Y. Hsu, C.D. Allis, R. Marmorstein, S.L. Berger, Phosphorylation of serine 10 in histone H3 is functionally linked in vitro and in vivo to Gcn5-mediated acetylation at lysine 14, *Mol. Cell.* 5 (2000) 917–926. doi:10.1016/S1097-2765(00)80257-9.
- [60] P. Cheung, K.G. Tanner, W.L. Cheung, P. Sassone-Corsi, J.M. Denu, C.D. Allis, Synergistic coupling of histone H3 phosphorylation and acetylation in response to epidermal growth factor stimulation, *Mol. Cell.* 5 (2000) 905–915. doi:10.1016/S1097-2765(00)80256-7.
- [61] A. Zippo, R. Serafini, M. Rocchigiani, S. Pennacchini, A. Krepelova, S. Oliviero, Histone Crosstalk between H3S10ph and H4K16ac Generates a Histone Code that Mediates Transcription Elongation, *Cell.* 138 (2009) 1122–1136. doi:10.1016/j.cell.2009.07.031.
- [62] P. Cheung, Liu, H. Wang, C. Zhou, Y.Y. Wang, A. Han, F. Ding, R. Chen, P. Kapoor-Vazirani, J.D. Kagey, P.M. Vertino, S.H. Baek, Histone Crosstalk between H2B Monoubiquitination and H3 Methylation Mediated by COMPASS, *Cell.* 131 (2010) 1084–1096. doi:10.1016/j.cell.2007.09.046.
- [63] P.N.I. Lau, P. Cheung, Histone code pathway involving H3 S28 phosphorylation and K27 acetylation activates transcription and antagonizes polycomb silencing, *Proc. Natl. Acad. Sci. U. S. A.* (2011). doi:10.1073/pnas.1012798108.
- [64] S.S. Gehani, S. Agrawal-Singh, N. Dietrich, N.S. Christophersen, K. Helin, K. Hansen, Polycomb group protein displacement and gene activation through MSK-dependent H3K27me3S28 phosphorylation, *Mol. Cell.* 39 (2010) 886–900. doi:10.1016/j.molcel.2010.08.020.
- [65] T. Waldmann, R. Schneider, Targeting histone modifications - epigenetics in cancer, *Curr. Opin. Cell Biol.* 25 (2013) 184–189. doi:10.1016/j.ceb.2013.01.001.
- [66] M.F. Fraga, E. Ballestar, A. Villar-garea, M. Boix-chornet, J. Espada, G. Schotta, T. Bonaldi, C. Haydon, S. Roperio, K. Petrie, N.G. Iyer, E. Calvo, J.A. Lopez, A. Cano, M.J. Calasanz, D. Colomer, N. Ahn, A. Imhof, C. Caldas, T. Jenuwein, M. Esteller, Loss of

- acetylation at Lys16 and trimethylation at Lys20 of histone H4 is a common hallmark of human cancer, *37* (2005) 391–400. doi:10.1038/ng1531.
- [67] J. Laitinen, L. Sistonen, K. Alitalo, E. Hölttä, c-Ha-rasVal 12 oncogene-transformed NIH-3T3 fibroblasts display more decondensed nucleosomal organization than normal fibroblasts, *J. Cell Biol.* 111 (1990) 9–17. doi:10.1083/jcb.111.1.9.
- [68] R.E. Herrera, F. Chen, R.A. Weinberg, Increased histone H1 phosphorylation and relaxed chromatin structure in Rb-deficient fibroblasts, *Proc. Natl. Acad. Sci. U. S. A.* 93 (1996) 11510–11515. doi:10.1073/pnas.93.21.11510.
- [69] L.T. Holth, D.N. Chadee, V.A. Spencer, S.K. Samuel, J.R. Safneck, J.R. Davie, Chromatin, nuclear matrix and the cytoskeleton: Role of cell structure in neoplastic transformation (review), *Int. J. Oncol.* 13 (1998) 827–837. doi:10.3892/ijo.13.4.827.
- [70] Chadee and Davie - Increased phosphorylation of H1 in mouse fibroblasts transformed with oncogenes or constitutively active mitogen activated protein kinase kinase.pdf, (n.d.).
- [71] L.C. Mahadevan, A.C. Willis, M.J. Barratt, Rapid histone H3 phosphorylation in response to growth factors, phorbol esters, okadaic acid, and protein synthesis inhibitors, *Cell.* 65 (1991) 775–783. doi:10.1016/0092-8674(91)90385-C.
- [72] D.N. Chadee, M.J. Hendzel, C.P. Tylicski, C.D. Allis, D.P. Bazett-Jones, J.A. Wright, J.R. Davie, Increased Ser-10 phosphorylation of histone H3 in mitogen-stimulated and oncogene-transformed mouse fibroblasts, *J. Biol. Chem.* 274 (1999) 24914–24920. doi:10.1074/jbc.274.35.24914.
- [73] M. Deak, A.D. Clifton, J.M. Lucocq, D.R. Alessi, Mitogen- and stress-activated protein kinase-1 (MSK1) is directly activated by MAPK and SAPK2/p38, and may mediate activation of CREB, *EMBO J.* 17 (1998) 4426–4441. doi:10.1093/emboj/17.15.4426.
- [74] S. Thomson, A.L. Clayton, C.A. Hazzalin, S. Rose, M.J. Barratt, L.C. Mahadevan, The nucleosomal response associated with immediate-early gene induction is mediated via alternative MAP kinase cascades: MSK1 as a potential histone H3/HMG-14 kinase, *EMBO J.* 18 (1999) 4779–4793. doi:10.1093/emboj/18.17.4779.
- [75] C.E. McCoy, D.G. Campbell, M. Deak, G.B. Bloomberg, J.S.C. Arthur, MSK1 activity is controlled by multiple phosphorylation sites, *Biochem. J.* 387 (2005) 507–517. doi:10.1042/BJ20041501.
- [76] I.S. Strelkov, J.R. Davie, Ser-10 phosphorylation of histone H3 and immediate early gene expression in oncogene-transformed mouse fibroblasts, *Cancer Res.* 62 (2002) 75–78.
- [77] A. Soloaga, S. Thomson, G.R. Wiggin, N. Rampersaud, M.H. Dyson, C.A. Hazzalin, L.C. Mahadevan, J.S.C. Arthur, MSK2 and MSK1 mediate the mitogen- and stress-induced phosphorylation of histone H3 and HMG-14, *EMBO J.* 22 (2003) 2788–2797. doi:10.1093/emboj/cdg273.
- [78] H.S. Choi, B.Y. Choi, Y.-Y.Y. Cho, H. Mizuno, B.S. Kang, A.M. Bode, Z. Dong, Phosphorylation of histone H3 at serine 10 is indispensable for neoplastic cell

- transformation, *Cancer Res.* 65 (2005) 5818–5827. doi:10.1158/0008-5472.CAN-05-0197.
- [79] H.-G. Kim, K.W. Lee, Y.-Y. Cho, N.J. Kang, S.-M. Oh, A.M. Bode, Z. Dong, Mitogen- and stress-activated kinase 1-mediated histone H3 phosphorylation is crucial for cell transformation, *Cancer Res.* 68 (2008) 2538–2547. doi:10.1158/0008-5472.CAN-07-6597.
- [80] Q. Zhang, Q. Zhong, A.G. Evans, D. Levy, S. Zhong, Phosphorylation of histone H3 serine 28 modulates RNA polymerase III-dependent transcription, *Oncogene.* 30 (2011) 3943–3952. doi:10.1038/onc.2011.105.
- [81] T. Bertelsen, L. Iversen, J.L. Riis, J.S.C. Arthur, B.M. Bibby, K. Kragballe, C. Johansen, The role of mitogen- and stress-activated protein kinase 1 and 2 in chronic skin inflammation in mice, *Exp. Dermatol.* 20 (2011) 140–145. doi:10.1111/j.1600-0625.2010.01153.x.
- [82] Z. Dong, K. Yao, H. Chen, K. Liu, A. Langfald, G. Yang, Y. Zhang, D.H. Yu, M.O. Kim, M.H. Lee, H. Li, K.B. Bae, H.G. Kim, W.Y. Ma, A.M. Bode, Z. Dong, Kaempferol targets RSK2 and MSK1 to Suppress UV radiation-induced skin cancer, *Cancer Prev. Res.* (2014). doi:10.1158/1940-6207.CAPR-14-0126.
- [83] Q. Zhong, G. Shi, Q. Zhang, Y. Zhang, D. Levy, S. Zhong, Role of phosphorylated histone H3 serine 10 in DEN-induced deregulation of pol III genes and cell proliferation and transformation, *Carcinogenesis.* 34 (2013) 2460–2469. doi:10.1093/carcin/bgt219.
- [84] G.P. Vicent, C. Ballaré, A.S. Nacht, J. Clausell, A. Subtil-Rodríguez, I. Quiles, A. Jordan, M. Beato, Induction of Progesterone Target Genes Requires Activation of Erk and Msk Kinases and Phosphorylation of Histone H3, *Mol. Cell.* 24 (2006) 367–381. doi:10.1016/j.molcel.2006.10.011.
- [85] D. Reyes, C. Ballaré, G. Castellano, D. Soronellas, J.R. Bagó, J. Blanco, M. Beato, Activation of mitogen- and stress-activated kinase 1 is required for proliferation of breast cancer cells in response to estrogens or progestins, *Oncogene.* 33 (2014) 1570–1580. doi:10.1038/onc.2013.95.
- [86] X. Pu, S.J. Storr, N.S. Ahmad, E.A. Rakha, A.R. Green, I.O. Ellis, S.G. Martin, High nuclear MSK1 is associated with longer survival in breast cancer patients, *J. Cancer Res. Clin. Oncol.* 144 (2018) 509–517. doi:10.1007/s00432-018-2579-7.
- [87] S. Gawrzak, L. Rinaldi, S. Gregorio, E.J. Arenas, F. Salvador, J. Urosevic, C. Saura, J. Arribas, J. Cortes, A. Rovira, M. Muñoz, A. Lluch, V. Serra, J. Albanell, A. Prat, A.R. Nebreda, S.A. Benitah, R.R. Gomis, MSK1 regulates luminal cell differentiation and metastatic dormancy in ER + breast cancer, *Nat. Cell Biol.* 20 (2018) 211–221. doi:10.1038/s41556-017-0021-z.
- [88] A. Sun, W. Zhou, J. Lunceford, P. Strack, L.M. Dauffenbach, C.A. Kerfoot, Level of phosphohistone H3 among various types of human cancers, *BMJ Open.* 2 (2012) e001071. doi:10.1136/bmjopen-2012-001071.
- [89] S. Nakashima, A. Shiozaki, D. Ichikawa, S. Komatsu, H. Konishi, D. Iitaka, T. Kubota, H.

- Fujiwara, K. Okamoto, M. Kishimoto, E. Otsuji, Anti-phosphohistone H3 as an independent prognostic factor in human esophageal squamous cell carcinoma, *Anticancer Res.* (2013).
- [90] R. Pacaud, M. Cheray, A. Nadaradjane, F.M. Vallette, P.F. Cartron, Histone H3 phosphorylation in GBM: A new rationale to guide the use of kinase inhibitors in anti-GBM therapy, *Theranostics.* 5 (2015) 12–22. doi:10.7150/thno.8799.
- [91] S.A. Khan, R. Amnekar, B. Khade, S.G. Barreto, M. Ramadwar, S. V Shrikhande, S. Gupta, p38-MAPK/MSK1-mediated overexpression of histone H3 serine 10 phosphorylation defines distance-dependent prognostic value of negative resection margin in gastric cancer, *Clin. Epigenetics.* 8 (2016) 88. doi:10.1186/s13148-016-0255-9.
- [92] D.S.C. Maggio, S. Coe, P. Atadja, P. Dent, S. Grant, B. Shi, M. Moradzadeh, A. Tabarraei, H.R. Sadeghnia, Valproic acid alters chromatin structure by regulation of chromatin modulation proteins, *Cancer Res.* 7 (2015) 1–13. doi:10.1158/0008-5472.CAN-04-2478.
- [93] B. Zheng, L. Liang, C. Wang, S. Huang, X. Cao, R. Zha, L. Liu, D. Jia, Q. Tian, J. Wu, Y. Ye, Q. Wang, Z. Long, Y. Zhou, C. Du, X. He, Y. Shi, MicroRNA-148a suppresses tumor cell invasion and metastasis by downregulating ROCK1 in gastric cancer, *Clin. Cancer Res.* 17 (2011) 7574–7583. doi:10.1158/1078-0432.CCR-11-1714.
- [94] C.L. Miranda Furtado, M.C. Dos Santos Luciano, R. Da Silva Santos, G.P. Furtado, M.O. Moraes, C. Pessoa, Epidrugs: targeting epigenetic marks in cancer treatment, *Epigenetics.* (2019). doi:10.1080/15592294.2019.1640546.
- [95] M. Mottamal, S. Zheng, T.L. Huang, G. Wang, Histone deacetylase inhibitors in clinical studies as templates for new anticancer agents, *Molecules.* 20 (2015) 3898–3941. doi:10.3390/molecules20033898.
- [96] C. Yoo, M.H. Ryu, Y.S. Na, B.Y. Ryoo, C.W. Lee, Y.K. Kang, Vorinostat in combination with capecitabine plus cisplatin as a first-line chemotherapy for patients with metastatic or unresectable gastric cancer: Phase II study and biomarker analysis, *Br. J. Cancer.* 114 (2016) 1185–1190. doi:10.1038/bjc.2016.125.
- [97] K.K.W. To, W.S. Tong, L. Wu Fu, Reversal of platinum drug resistance by the histone deacetylase inhibitor belinostat, *Lung Cancer.* 103 (2017) 58–65. doi:10.1016/j.lungcan.2016.11.019.
- [98] J. Ellinger, P. Kahl, J. Von Der Gathen, S. Rogenhofer, L.C. Heukamp, I. Gütgemann, B. Walter, F. Hofstädter, R. Büttner, S.C. Müller, P.J. Bastian, A. Von Ruecker, Global levels of histone modifications predict prostate cancer recurrence, *Prostate.* 70 (2010) 61–69. doi:10.1002/pros.21038.
- [99] A. Etemadi, S. Safiri, S.G. Sepanlou, K. Ikuta, C. Bisignano, R. Shakeri, M. Amani, C. Fitzmaurice, M.R. Nixon, N. Abbasi, H. Abolhassani, S.M. Advani, M. Afarideh, T. Akinyemiju, T. Alam, M. Alikhani, V. Alipour, C.A. Allen, A. Almasi-Hashiani, J. Arabloo, R. Assadi, S. Atique, A. Awasthi, A. Bakhtiari, M. Behzadifar, K. Berhe, N. A.

- Zarghi, Z.J. Zhang, M. Naghavi, R. Malekzadeh, P. Sajadi, The global, regional, and national burden of stomach cancer in 195 countries, 1990–2017: a systematic analysis for the Global Burden of Disease study 2017, *Lancet Gastroenterol. Hepatol.* 5 (2020) 42–54. doi:10.1016/S2468-1253(19)30328-0.
- [100] P. Rawla, A. Barsouk, Epidemiology of gastric cancer: Global trends, risk factors and prevention, *Prz. Gastroenterol.* 14 (2019) 26–38. doi:10.5114/pg.2018.80001.
- [101] C.M. Oh, Y.J. Won, K.W. Jung, H.J. Kong, H. Cho, J.K. Lee, D.H. Lee, K.H. Lee, C.H. Kim, C.I. Yoo, H. Kim, H.S. Nam, J.S. Huh, J.H. Youm, M.K. Oh, N.S. Hong, S.S. Kweon, W.C. Kim, Y.S. Kang, Cancer statistics in Korea: Incidence, mortality, survival, and prevalence in 2013, *Cancer Res. Treat.* (2016). doi:10.4143/crt.2016.089.
- [102] P.K. Dhillon, P. Mathur, A. Nandakumar, C. Fitzmaurice, G.A. Kumar, R. Mehrotra, P. Gangadharan, E. Dutta, K.S. Reddy, M. Naghavi, C.J.L. Murray, S. Swaminathan, L. Dandona, The burden of cancers and their variations across the states of India: the Global Burden of Disease Study 1990–2016, *Lancet Oncol.* 19 (2018) 1289–1306. doi:10.1016/S1470-2045(18)30447-9.
- [103] B. Hu, N. El Hajj, S. Sittler, N. Lammert, R. Barnes, A. Meloni-Ehrig, Gastric cancer: Classification, histology and application of molecular pathology, *J. Gastrointest. Oncol.* 3 (2012) 251–261. doi:10.3978/j.issn.2078-6891.2012.021.
- [104] A.J. Bass, V. Thorsson, Shaw, R. Tarnuzzer, Z. Wang, L.L. Yang, J.C. Zenklusen, T. Davidsen, C.M. Hutter, H.J. Sofia, R. Burton, S. Chudamani, J. Liu, Comprehensive molecular characterization of gastric adenocarcinoma, *Nature.* 513 (2014) 202–209. doi:10.1038/nature13480.
- [105] J. Ma, H. Shen, L. Kapesa, S. Zeng, Lauren classification and individualized chemotherapy in gastric cancer (Review), *Oncol. Lett.* 11 (2016) 2959–2964. doi:10.3892/ol.2016.4337.
- [106] F. Berlth, E. Bollschweiler, U. Drebber, A.H. Hoelscher, S. Moenig, Pathohistological classification systems in gastric cancer: Diagnostic relevance and prognostic value, *World J. Gastroenterol.* 20 (2014) 5679–5684. doi:10.3748/wjg.v20.i19.5679.
- [107] L. Sosa, E. Rodriguez-Wulff, Topics in Prevention of Diseases in Gastroenterology, in: *Curr. Top. Public Heal.*, 2013. doi:10.5772/55138.
- [108] P. Karimi, F. Islami, S. Anandasabapathy, N.D. Freedman, F. Kamangar, Gastric cancer: Descriptive epidemiology, risk factors, screening, and prevention, *Cancer Epidemiol. Biomarkers Prev.* 23 (2014) 700–713. doi:10.1158/1055-9965.EPI-13-1057.
- [109] A.E. Pegg, Methylation of the o6 position of guanine in DNA is the most likely initiating event in carcinogenesis by methylating agents, *Cancer Invest.* (1984). doi:10.3109/07357908409104376.
- [110] D. Ziech, R. Franco, A. Pappa, V. Malamou-Mitsi, S. Georgakila, A.G. Georgakilas, M.I. Panayiotidis, The role of epigenetics in environmental and occupational carcinogenesis,

- Chem. Biol. Interact. (2010). doi:10.1016/j.cbi.2010.06.012.
- [111] P. Correa, Human Gastric Carcinogenesis: A Multistep and Multifactorial Process- First American Cancer Society Award Lecture on Cancer Epidemiology and Prevention, *Cancer Res.* 52 (1992) 6735–6740.
- [112] B. Peleteiro, N. Lunet, Role of Genetic and Environmental Risk Factors in Gastric Carcinogenesis Pathway, Gastritis Gastric Cancer - New Insights Gastroprotection, *Diagnosis Treat.* (2011). doi:10.5772/23662.
- [113] P. Correa, Y.H. Shiao, Phenotypic and genotypic events in gastric carcinogenesis, *Cancer Res.* 54 (1994) 1941–1944.
- [114] P. Correa, Perspectives in Cancer Research A Human Model of Gastric Carcinogenesis I, *Nutrition.* (1988) 3554–3560.
- [115] A. Meining, A. Morgner, S. Miehle, E. Bayerdörffer, M. Stolte, Atrophy-metaplasia-dysplasia-carcinoma sequence in the stomach: A reality or merely an hypothesis?, *Bailliere's Best Pract. Res. Clin. Gastroenterol.* 15 (2001) 983–998. doi:10.1053/bega.2001.0253.
- [116] J.H. Lee, S.J. Park, S.C. Abraham, J.S. Seo, J.H. Nam, C. Choi, S.W. Juhng, A. Rashid, S.R. Hamilton, T.T. Wu, Frequent CpG island methylation in precursor lesions and early gastric adenocarcinomas, *Oncogene.* 23 (2004) 4646–4654. doi:10.1038/sj.onc.1207588.
- [117] X.P. Zou, B. Zhang, X.Q. Zhang, M. Chen, J. Cao, W.J. Liu, Promoter hypermethylation of multiple genes in early gastric adenocarcinoma and precancerous lesions, *Hum. Pathol.* 40 (2009) 1534–1542. doi:10.1016/j.humpath.2009.01.029.
- [118] H. Tomita, S. Takaishi, T.R. Menheniott, X. Yang, W. Shibata, G. Jin, K.S. Betz, K. Kawakami, T. Minamoto, C. Tomasetto, M. Rio, N. Lerkowit, A. Varro, A.S. Giraud, T.C. Wang, Inhibition of gastric carcinogenesis by the hormone gastrin is mediated by suppression of TFF1 epigenetic silencing, *Gastroenterology.* (2011). doi:10.1053/j.gastro.2010.11.037.
- [119] N. Padmanabhan, T. Ushijima, P. Tan, How to stomach an epigenetic insult: The gastric cancer epigenome, *Nat. Rev. Gastroenterol. Hepatol.* 14 (2017) 467–478. doi:10.1038/nrgastro.2017.53.
- [120] T. Niwa, T. Toyoda, T. Tsukamoto, A. Mori, M. Tatematsu, T. Ushijima, Prevention of helicobacter pylori-induced gastric cancers in gerbils by a DNA demethylating agent, *Cancer Prev. Res.* 6 (2013) 263–270. doi:10.1158/1940-6207.CAPR-12-0369.
- [121] T. Niwa, T. Tsukamoto, T. Toyoda, A. Mori, H. Tanaka, T. Maekita, M. Ichinose, M. Tatematsu, T. Ushijima, Inflammatory processes triggered by Helicobacter pylori infection cause aberrant DNA methylation in gastric epithelial cells, *Cancer Res.* 70 (2010) 1430–1440. doi:10.1158/0008-5472.CAN-09-2755.
- [122] N.Y. Chia, P. Tan, Molecular classification of gastric cancer, *Ann. Oncol.* 27 (2016) 763–769. doi:10.1093/annonc/mdw040.

- [123] T. Yoshida, S. Yamashita, T. Takamura-Enya, T. Niwa, T. Ando, S. Enomoto, T. Maekita, K. Nakazawa, M. Tatematsu, M. Ichinose, T. Ushijima, Alu and Sata hypomethylation in *Helicobacter pylori*-infected gastric mucosae, *Int. J. Cancer*. 128 (2011) 33–39. doi:10.1002/ijc.25534.
- [124] J.M. Bae, S.H. Shin, H.J. Kwon, S.Y. Park, M.C. Kook, Y.W. Kim, N.Y. Cho, N. Kim, T.Y. Kim, D. Kim, G.H. Kang, ALU and LINE-1 hypomethylations in multistep gastric carcinogenesis and their prognostic implications, *Int. J. Cancer*. 131 (2012) 1323–1331. doi:10.1002/ijc.27369.
- [125] F. Gao, G. Ji, Z. Gao, X. Han, M. Ye, Z. Yuan, H. Luo, X. Huang, K. Natarajan, J. Wang, H. Yang, X. Zhang, Direct ChIP-bisulfite sequencing reveals a role of H3K27me3 mediating aberrant hypermethylation of promoter CpG islands in cancer cells, *Genomics*. 103 (2014) 204–210. doi:10.1016/j.ygeno.2013.12.006.
- [126] L. Zhang, K. Zhong, Y. Dai, H. Zhou, Genome-wide analysis of histone H3 lysine 27 trimethylation by ChIP-chip in gastric cancer patients, *J. Gastroenterol.* 44 (2009) 305–312. doi:10.1007/s00535-009-0027-9.
- [127] L.-J. He, M.-Y. Cai, G.-L. Xu, J.-J. Li, Z.-J. Weng, D.-Z. Xu, G.-Y. Luo, S.-L. Zhu, D. Xie, Prognostic Significance of Overexpression of EZH2 and H3k27me3 Proteins in Gastric Cancer, *Asian Pacific J. Cancer Prev.* 13 (2012) 3173–3178. doi:10.7314/APJCP.2012.13.7.3173.
- [128] T.T. Yang, N. Cao, H.H. Zhang, J.B. Wei, X.X. Song, D.M. Yi, S.H. Chao, L. Da Zhang, L.F. Kong, S.Y. Han, Y.X. Yang, S.Z. Ding, *Helicobacter pylori* infection-induced H3Ser10 phosphorylation in stepwise gastric carcinogenesis and its clinical implications, *Helicobacter*. 23 (2018) 1–8. doi:10.1111/hel.12486.
- [129] C. Xie, L.-Y. Xu, Z. Yang, X.-M. Cao, W. Li, N.-H. Lu, Expression of γ H2AX in various gastric pathologies and its association with *Helicobacter pylori* infection, *Oncol. Lett.* 7 (2014) 159–163. doi:10.3892/ol.2013.1693.
- [130] H. Qi, Z. Yang, C. Dai, R. Wang, X. Ke, S. Zhang, X. Xiang, K. Chen, C. Li, J. Luo, J. Shao, J. Shen, STAT3 activates MSK1-mediated histone H3 phosphorylation to promote NFAT signaling in gastric carcinogenesis, *Oncogenesis*. 9 (2020). doi:10.1038/s41389-020-0195-2.
- [131] S. Ono, N. Oue, H. Kuniyasu, T. Suzuki, R. Ito, K. Matsusaki, T. Ishikawa, E. Tahara, W. Yasui, Acetylated histone H4 is reduced in human gastric adenomas and carcinomas, *J. Exp. Clin. Cancer Res.* (2002).
- [132] Y.S. Park, M.Y. Jin, Y.J. Kim, J.H. Yook, B.S. Kim, S.J. Jang, The global histone modification pattern correlates with cancer recurrence and overall survival in gastric adenocarcinoma, *Ann. Surg. Oncol.* 15 (2008) 1968–1976. doi:10.1245/s10434-008-9927-9.
- [133] Y. Li, D. Guo, R. Sun, P. Chen, Q. Qian, H. Fan, Methylation Patterns of Lys9 and Lys27 on Histone H3 Correlate with Patient Outcome in Gastric Cancer, *Dig. Dis. Sci.* 64 (2019)

- 439–446. doi:10.1007/s10620-018-5341-8.
- [134] Y.M. Pan, C.G. Wang, M. Zhu, R. Xing, J.T. Cui, W.M. Li, D.D. Yu, S. Bin Wang, W. Zhu, Y.J. Ye, Y. Wu, S. Wang, Y.Y. Lu, STAT3 signaling drives EZH2 transcriptional activation and mediates poor prognosis in gastric cancer, *Mol. Cancer*. 15 (2016) 1–14. doi:10.1186/s12943-016-0561-z.
- [135] K. Okuno, Y. Akiyama, S. Shimada, M. Nakagawa, T. Tanioka, M. Inokuchi, S. Yamaoka, K. Kojima, S. Tanaka, Asymmetric dimethylation at histone H3 arginine 2 by PRMT6 in gastric cancer progression, *Carcinogenesis*. (2019). doi:10.1093/carcin/bgy147.
- [136] L. Zhu, L. Zhu, J. Yang, J. Yang, L. Zhao, L. Zhao, X. Yu, X. Yu, L. Wang, L. Wang, F. Wang, F. Wang, Y. Cai, Y. Cai, J. Jin, J. Jin, Expression of hMOF, but not HDAC4, is responsible for the global histone H4K16 acetylation in gastric carcinoma, *Int. J. Oncol*. 46 (2015) 2535–2545. doi:10.3892/ijo.2015.2956.
- [137] Z.-J. Wang, J.-L. Yang, Y.-P. Wang, J.-Y. Lou, J. Chen, C. Liu, L.-D. Guo, Decreased histone H2B monoubiquitination in malignant gastric carcinoma., *World J. Gastroenterol*. 19 (2013) 8099–8107. doi:10.3748/wjg.v19.i44.8099.
- [138] W. Weichert, A. Röske, V. Gekeler, T. Beckers, M.P. Ebert, M. Pross, M. Dietel, C. Denkert, C. Röcken, Association of patterns of class I histone deacetylase expression with patient prognosis in gastric cancer: a retrospective analysis, *Lancet Oncol*. (2008). doi:10.1016/S1470-2045(08)70004-4.
- [139] K. Mutze, R. Langer, K. Becker, K. Ott, A. Novotny, B. Lubner, A. Hapfelmeier, M. Göttlicher, H. Höfler, G. Keller, Histone deacetylase (HDAC) 1 and 2 expression and chemotherapy in gastric cancer, *Ann. Surg. Oncol*. 17 (2010) 3336–3343. doi:10.1245/s10434-010-1182-1.
- [140] H. Takahashi, Y. Murai, K. Tsuneyama, K. Nomoto, E. Okada, H. Fujita, Y. Takano, Overexpression of phosphorylated histone H3 is an indicator of poor prognosis in gastric adenocarcinoma patients, *Appl. Immunohistochem. Mol. Morphol*. 14 (2006) 296–302. doi:10.1097/00129039-200609000-00007.
- [141] M.C. Phelan, Basic Techniques in Mammalian Cell Tissue Culture, *Curr. Protoc. Cell Biol*. (2007). doi:10.1002/0471143030.cb0101s36.
- [142] P. Pozarowski, Z. Darzynkiewicz, Analysis of cell cycle by flow cytometry., *Methods Mol. Biol*. (2004). doi:10.1385/1-59259-811-0:301.
- [143] K. Canene-Adams, Preparation of formalin-fixed paraffin-embedded tissue for immunohistochemistry, in: *Methods Enzymol.*, 2013. doi:10.1016/B978-0-12-420067-8.00015-5.
- [144] A.H. Fischer, K.A. Jacobson, J. Rose, R. Zeller, Hematoxylin and eosin staining of tissue and cell sections, *Cold Spring Harb. Protoc*. (2008). doi:10.1101/pdb.prot4986.
- [145] M. Verma, Cancer epigenetics: Risk assessment, diagnosis, treatment, and prognosis, *Cancer Epigenetics Risk Assessment, Diagnosis, Treat. Progn*. 1238 (2014) 1–799.

- doi:10.1007/978-1-4939-1804-1.
- [146] S. Miyamoto, R.C. Guzman, R.C. Osborn, S. Nandi, Neoplastic transformation of mouse mammary epithelial cells by in vitro exposure to N-methyl-N-nitrosourea, *Proc. Natl. Acad. Sci. U. S. A.* (1988). doi:10.1073/pnas.85.2.477.
- [147] J.S. Rhim, S. Jin, M. Jung, P.J. Thraves, M.R. Kuettel, M.M. Webber, B. Hukku, Malignant transformation of human prostate epithelial cells by N- nitroso-N-methylurea, *Cancer Res.* 57 (1997) 576–580.
- [148] W. Strober, Trypan Blue Exclusion Test of Cell Viability, *Curr. Protoc. Immunol.* (2015). doi:10.1002/0471142735.ima03bs111.
- [149] J.A. Plumb, Cell sensitivity assays: clonogenic assay., *Methods Mol. Med.* (2004). doi:10.1385/1-59259-687-8:17.
- [150] M.A. Booden, A.S. Ulku, C.J. Der, Cellular assays of oncogene transformation, in: *Cell Biol. Four-Volume Set*, 2006. doi:10.1016/B978-012164730-8/50042-3.
- [151] M.M. Sanders, F R A C T I O N A T I O N OF NUCLEOSOMES BY SALT E L U T I O N FROM M I C R O C O C C A L N U C L E A S E - D I G E S T E D N U C L E I distinguished from the pattern . A class of nucleosomes containing 13-17 % of the Purification of Rat Liver Nuclei Stepwise , October. 79 (1978).
- [152] E. Rocha, J.R. Davie, K.E. Van Holde, H. Weintraub, Differential salt fractionation of active and inactive genomic domains in chicken erythrocyte, *J. Biol. Chem.* 259 (1984) 8558–8563.
- [153] S.S. Teves, S. Henikoff, Salt fractionation of nucleosomes for genome-wide profiling, *Methods Mol. Biol.* (2012). doi:10.1007/978-1-61779-477-3_25.
- [154] D. Shechter, H.L. Dormann, C.D. Allis, S.B. Hake, Extraction, purification and analysis of histones, *Nat. Protoc.* (2007). doi:10.1038/nprot.2007.202.
- [155] C. Arndt, S. Koristka, A. Feldmann, H. Bartsch, M. Bachmann, Coomassie-brilliant blue staining of polyacrylamide gels, *Methods Mol. Biol.* (2012). doi:10.1007/978-1-61779-821-4_40.
- [156] J. Sassel, S.R. Gallagher, Staining proteins in gels, *Curr. Protoc. Mol. Biol.* (2009). doi:10.1002/0471142727.mb1006s85.
- [157] S. Alexander, W.S. Swatson, H. Alexander, Pharmacogenetics of Resistance to Cisplatin and Other Anticancer Drugs and the Role of Sphingolipid Metabolism, in: 2013. doi:10.1007/978-1-62703-302-2_10.
- [158] T.C. Chou, P. Talalay, Quantitative analysis of dose-effect relationships: the combined effects of multiple drugs or enzyme inhibitors, *Adv. Enzyme Regul.* (1984). doi:10.1016/0065-2571(84)90007-4.

- [159] T.C. Chou, Drug combination studies and their synergy quantification using the choutalalay method, *Cancer Res.* (2010). doi:10.1158/0008-5472.CAN-09-1947.
- [160] S.P. Khare, A. Sharma, K.K. Deodhar, S. Gupta, Overexpression of histone variant H2A.1 and cellular transformation are related in N-nitrosodiethylamine-induced sequential hepatocarcinogenesis, *Exp. Biol. Med.* (2011). doi:10.1258/ebm.2010.010140.
- [161] H.J. Fei, L.D. Zu, J. Wu, X.S. Jiang, J.L. Wang, Y.E. Chin, G.H. Fu, PCAF acts as a gastric cancer suppressor through a novel PCAF-p16-CDK4 axis, *Am. J. Cancer Res.* (2016).
- [162] M.Z. Ying, J.J. Wang, D.W. Li, G.Z. Yu, X. Wang, J. Pan, Y. Chen, M.X. He, The p300/CBP associated factor is frequently downregulated in intestinal-type gastric carcinoma and constitutes a biomarker for clinical outcome, *Cancer Biol. Ther.* 9 (2010) 312–320. doi:10.4161/cbt.9.4.10748.
- [163] T. Liu, X. Wang, W. Hu, Z. Fang, Y. Jin, X. Fang, Q.R. Miao, Epigenetically Down-Regulated Acetyltransferase PCAF Increases the Resistance of Colorectal Cancer to 5-Fluorouracil, *Neoplasia (United States)*. (2019). doi:10.1016/j.neo.2019.03.011.
- [164] J. Li, X. Liu, W. Wang, C. Li, X. Li, MSK1 promotes cell proliferation and metastasis in uveal melanoma by phosphorylating CREB, *Arch. Med. Sci.* (2019). doi:10.5114/aoms.2019.85810.
- [165] L.F. Johnson, H.T. Abelson, H. Green, S. Penman, Changes in RNA in relation to growth of the fibroblast. I. Amounts of mRNA, rRNA, and tRNA in resting and growing cells, *Cell.* (1974). doi:10.1016/0092-8674(74)90068-3.
- [166] M.A. McBrian, I.S. Behbahan, R. Ferrari, T. Su, T.W. Huang, K. Li, C.S. Hong, H.R. Christofk, M. Vogelauer, D.B. Seligson, S.K. Kurdistani, Histone Acetylation Regulates Intracellular pH, *Mol. Cell.* (2013). doi:10.1016/j.molcel.2012.10.025.
- [167] C. Herold, M. Ganslmayer, M. Ocker, M. Hermann, A. Geerts, E.G. Hahn, D. Schuppan, The histone-deacetylase inhibitor Trichostatin A blocks proliferation and triggers apoptotic programs in hepatoma cells, *J. Hepatol.* (2002). doi:10.1016/S0168-8278(01)00257-4.
- [168] W. Walter, D. Clynes, Y. Tang, R. Marmorstein, J. Mellor, S.L. Berger, 14-3-3 Interaction with Histone H3 Involves a Dual Modification Pattern of Phosphoacetylation, *Mol. Cell. Biol.* 28 (2008) 2840–2849. doi:10.1128/mcb.01457-07.
- [169] B. Schuettengruber, E. Simboeck, H. Khier, C. Seiser, Autoregulation of Mouse Histone Deacetylase 1 Expression, *Mol. Cell. Biol.* (2003). doi:10.1128/mcb.23.19.6993-7004.2003.
- [170] B. Drobic, B. Pérez-Cadahía, J. Yu, S.K.P. Kung, J.R. Davie, Promoter chromatin remodeling of immediate-early genes is mediated through H3 phosphorylation at either serine 28 or 10 by the MSK1 multi-protein complex, *Nucleic Acids Res.* 38 (2010) 3196–3208. doi:10.1093/nar/gkq030.

- [171] J.R. Davie, B. Drohic, B. Perez-Cadahia, S. He, P.S. Espino, J.M. Sun, H.Y. Chen, K.L. Dunn, L. Wark, S. Mai, D.H. Khan, S.N. Davie, S. Lu, C.P. Peltier, G.P. Delcuve, Nucleosomal response, immediate-early gene expression and cell transformation, *Adv. Enzyme Regul.* 50 (2010) 135–145. doi:10.1016/j.advenzreg.2009.10.008.
- [172] A. Sawicka, C. Seiser, Histone H3 phosphorylation - A versatile chromatin modification for different occasions, *Biochimie.* 94 (2012) 2193–2201. doi:10.1016/j.biochi.2012.04.018.
- [173] S.L. Chavez, S.L. McElroy, N.L. Bossert, C.J. De Jonge, M.V. Rodriguez, D.E. Leong, B. Behr, L.M. Westphal, R.A. Reijo Pera, Comparison of epigenetic mediator expression and function in mouse and human embryonic blastomeres, *Hum. Mol. Genet.* 23 (2014) 4970–4984. doi:10.1093/hmg/ddu212.
- [174] I. Nasa, S.F. Rusin, A.N. Kettenbach, G.B. Moorhead, Aurora B opposes PP1 function in mitosis by phosphorylating the conserved PP1-binding RVxF motif in PP1 regulatory proteins, *Sci. Signal.* (2018). doi:10.1126/scisignal.aai8669.
- [175] G. Xin, J. Fu, J. Luo, Z. Deng, Q. Jiang, C. Zhang, Aurora B regulates PP1 γ -Repo-Man interactions to maintain the chromosome condensation state, *J. Biol. Chem.* (2020). doi:10.1074/jbc.ac120.012772.
- [176] S.B. Baylin, P.A. Jones, Epigenetic determinants of cancer, *Cold Spring Harb. Perspect. Biol.* (2016). doi:10.1101/cshperspect.a019505.
- [177] Q.Y. Zhao, P.J. Lei, X. Zhang, J.Y. Zheng, H.Y. Wang, J. Zhao, Y.M. Li, M. Ye, L. Li, G. Wei, M. Wu, Global histone modification profiling reveals the epigenomic dynamics during malignant transformation in a Four-Stage breast cancer model, *Clin. Epigenetics.* (2016). doi:10.1186/s13148-016-0201-x.
- [178] Y.X. Song, Z.Y. Yue, Z.N. Wang, Y.Y. Xu, Y. Luo, H.M. Xu, X. Zhang, L. Jiang, C.Z. Xing, Y. Zhang, MicroRNA-148b is frequently down-regulated in gastric cancer and acts as a tumor suppressor by inhibiting cell proliferation, *Mol. Cancer.* 10 (2011) 1. doi:10.1186/1476-4598-10-1.
- [179] Y. Fujita, K. Kojima, R. Ohhashi, N. Hamada, Y. Nozawa, A. Kitamoto, A. Sato, S. Kondo, T. Kojima, T. Deguchi, M. Ito, MiR-148a attenuates paclitaxel resistance of hormone-refractory, drug-resistant prostate cancer PC3 cells by regulating MSK1 expression, *J. Biol. Chem.* 285 (2010) 19076–19084. doi:10.1074/jbc.M109.079525.
- [180] L. Graziosi, A. Mencarelli, C. Santorelli, B. Renga, S. Cipriani, E. Cavazzoni, G. Palladino, S. Laufer, M. Burnet, A. Donini, S. Fiorucci, Mechanistic role of p38 MAPK in gastric cancer dissemination in a rodent model peritoneal metastasis, *Eur. J. Pharmacol.* 674 (2012) 143–152. doi:10.1016/j.ejphar.2011.11.015.
- [181] Y. Hsieh, C. Shen, W. Huang, C. Chin, Y. Kuo, M.C. Hsieh, expression through Toll-like receptor 4 and activation of p38 MAPK / NF κ B signaling pathway in gastric cancer cells, (2014) 1–10.

- [182] X. Guo, N. Ma, J. Wang, J. Song, X. Bu, Y. Cheng, K. Sun, H. Xiong, G. Jiang, B. Zhang, M. Wu, L. Wei, Increased p38-MAPK is responsible for chemotherapy resistance in human gastric cancer cells, 9 (2008) 1–9. doi:10.1186/1471-2407-8-375.
- [183] W. Tan, H. Yu, H. Luo, W. Zhou, p38 mitogen-activated protein kinase regulates chemoresistance in human gastric cancer via epithelial mesenchymal transition, 11 (2018) 2059–2067.
- [184] Z. Liu, T. Li, K. Jiang, Q. Huang, Y. Chen, F. Qian, Induction of chemoresistance by all-trans retinoic acid via a noncanonical signaling in multiple myeloma cells, PLoS One. (2014). doi:10.1371/journal.pone.0085571.
- [185] J.Y. Zhou, Y. Liu, S.W. Gen, The role of mitogen-activated protein kinase phosphatase-1 in oxidative damage-induced cell death, Cancer Res. 66 (2006) 4888–4894. doi:10.1158/0008-5472.CAN-05-4229.
- [186] Y. Mitani, N. Oue, Y. Hamai, P.P. Aung, S. Matsumura, H. Nakayama, N. Kamata, W. Yasui, Histone H3 acetylation is associated with reduced p21WAF1/CIP1 expression by gastric carcinoma, J. Pathol. 205 (2005) 65–73. doi:10.1002/path.1684.
- [187] X. Fu, X. Fan, J. Hu, H. Zou, Z. Chen, Q. Liu, B. Ni, X. Tan, Q. Su, J. Wang, L. Wang, J. Wang, Overexpression of MSK1 is associated with tumor aggressiveness and poor prognosis in colorectal cancer, Dig. Liver Dis. 49 (2017) 683–691. doi:10.1016/j.dld.2017.02.009.
- [188] P.N.I. Lau, P. Cheung, Elucidating combinatorial histone modifications and crosstalks by coupling histone-modifying enzyme with biotin ligase activity, Nucleic Acids Res. 41 (2013). doi:10.1093/nar/gks1247.
- [189] S. Zhong, H. Goto, M. Inagaki, Z. Dong, Phosphorylation at serine 28 and acetylation at lysine 9 of histone H3 induced by trichostatin A, Oncogene. (2003). doi:10.1038/sj.onc.1206507.
- [190] A. Sawicka, D. Hartl, M. Goiser, O. Pusch, R.R. Stocsits, I.M. Tamir, K. Mechtler, C. Seiser, H3S28 phosphorylation is a hallmark of the transcriptional response to cellular stress, Genome Res. 24 (2014) 1808–1820. doi:10.1101/gr.176255.114.
- [191] C. Hauser, B. Schuettengruber, S. Bartl, G. Lagger, C. Seiser, Activation of the Mouse Histone Deacetylase 1 Gene by Cooperative Histone Phosphorylation and Acetylation, Mol. Cell. Biol. (2002). doi:10.1128/mcb.22.22.7820-7830.2002.
- [192] C. Bamia, P. Lagiou, G. Buckland, S. Grioni, C. Agnoli, A.J. Taylor, C.C. Dahm, K. Overvad, A. Olsen, , T. Norat, A. Trichopoulou, Mediterranean diet and colorectal cancer risk: Results from a European cohort, Eur. J. Epidemiol. (2013). doi:10.1007/s10654-013-9795-x.
- [193] M.G. Donovan, O.I. Selmin, T.C. Doetschman, D.F. Romagnolo, Mediterranean Diet: Prevention of Colorectal Cancer, Front. Nutr. (2017). doi:10.3389/fnut.2017.00059.

- [194] K.S. Bishop, H. Xu, G. Marlow, Epigenetic regulation of gene expression induced by butyrate in colorectal cancer: Involvement of microRNA, *Genet. Epigenetics*. (2017). doi:10.1177/1179237X17729900.
- [195] X. Tong, L. Yin, C. Giardina, Butyrate suppresses Cox-2 activation in colon cancer cells through HDAC inhibition, *Biochem. Biophys. Res. Commun.* (2004). doi:10.1016/j.bbrc.2004.03.066.
- [196] C. Crosio, G.M. Fimia, R. Loury, M. Kimura, Y. Okano, H. Zhou, S. Sen, C.D. Allis, P. Sassone-Corsi, Mitotic Phosphorylation of Histone H3: Spatio-Temporal Regulation by Mammalian Aurora Kinases, *Mol. Cell. Biol.* (2002). doi:10.1128/mcb.22.3.874-885.2002.
- [197] F. Hans, S. Dimitrov, Histone H3 phosphorylation and cell division, *Oncogene*. 20 (2001) 3021–3027. doi:10.1038/sj.onc.1204326.
- [198] R. Giet, D.M. Glover, *Drosophila* aurora B kinase is required for histone H3 phosphorylation and condensin recruitment during chromosome condensation and to organize the central spindle during cytokinesis, *J. Cell Biol.* (2001). doi:10.1083/jcb.152.4.669.
- [199] T.-H. Kang, D.-Y. Park, Y.H. Choi, K.-T.K.-J. Kim, H.S. Yoon, K.-T.K.-J. Kim, Mitotic Histone H3 Phosphorylation by Vaccinia-Related Kinase 1 in Mammalian Cells, *Mol. Cell. Biol.* 27 (2007) 8533–8546. doi:10.1128/mcb.00018-07.
- [200] M. Cargnello, P.P. Roux, Activation and Function of the MAPKs and Their Substrates, the MAPK-Activated Protein Kinases, *Microbiol. Mol. Biol. Rev.* (2011). doi:10.1128/mnbr.00031-10.
- [201] L. Ding, L. Yang, Y. He, B. Zhu, F. Ren, X. Fan, Y. Wang, M. Li, J. Li, Y. Kuang, S. Liu, W. Zhai, D. Ma, Y. Ju, Q. Liu, B. Jia, J. Sheng, Z. Chang, CREPT/RPRD1B associates with Aurora B to regulate Cyclin B1 expression for accelerating the G2/M transition in gastric cancer, *Cell Death Dis.* (2018). doi:10.1038/s41419-018-1211-8.
- [202] M.D. Rotelli, R.A. Policastro, A.M. Bolling, A.W. Killion, A.J. Weinberg, M.J. Dixon, G.E. Zentner, C.E. Walczak, M.A. Lilly, B.R. Calvi, A Cyclin A—Myb-MuvB—Aurora B network regulates the choice between mitotic cycles and polyploid endoreplication cycles, *PLoS Genet.* (2019). doi:10.1371/journal.pgen.1008253.
- [203] J.S. Ungerstedt, Y. Sowa, W.-S. Xu, Y. Shao, M. Dokmanovic, G. Perez, L. Ngo, A. Holmgren, X. Jiang, P.A. Marks, Role of thioredoxin in the response of normal and transformed cells to histone deacetylase inhibitors, *Proc. Natl. Acad. Sci.* 102 (2005) 673–678. doi:10.1073/pnas.0408732102.
- [204] P. Münster, D. Marchion, E. Bicaku, M. Schmitt, H.L. Ji, R. DeConti, G. Simon, M. Fishman, S. Minton, C. Garrett, A. Chiappori, R. Lush, D. Sullivan, A. Daud, Phase I trial of histone deacetylase inhibition by valproic acid followed by the topoisomerase II inhibitor epirubicin in advanced solid tumors: A clinical and translational study, *J. Clin. Oncol.* 25 (2007) 1979–1985. doi:10.1200/JCO.2006.08.6165.

- [205] F. Caponigro, E. Di Gennaro, F. Ionna, F. Longo, C. Aversa, E. Pavone, M.G. Maglione, A. Trotta, A.I. Zotti, F. Bruzzese, A. Daponte, E. Calogero, M. Montano, M. Pontone, G. De Feo, F. Perri, A. Budillon, Phase II clinical study of valproic acid plus cisplatin and cetuximab in recurrent and/or metastatic squamous cell carcinoma of Head and Neck-V-CHANCE trial, *BMC Cancer*. 16 (2016) 1–10. doi:10.1186/s12885-016-2957-y.
- [206] Z. Jiang, H. Yang, X. Zhang, Z. Wang, R. Rong, X. Wang, Histone deacetylase-1 as a prognostic factor and mediator of gastric cancer progression by enhancing glycolysis, *Hum. Pathol.* 85 (2019) 194–201. doi:10.1016/j.humpath.2018.10.031.

Chapter 10
Appendix

10.1 APPENDIX –I Clinicopathological Data of Patients used in the Study

S. No.	Type of Surgery	Sample code	Sex	Age (years)	WHO Classification	T stage	N stage	M stage	pTNM stage	NACT	Overall Survival (months) after DOS	Disease free survival (months) after DOS	Status at last followup (Dead/Alive)	Recurrence (Yes/No)	H score PRM	H Score Tumor
1	Distal	60	M	55	PD	T4	N3	M0	3	No	14	14	Alive	No	5	40
2	Distal	61	F	36	PD	T3	N0	M0	2	No	43	43	Alive	No	0	20
3	distal gastrectomy	70	F	38	SRC	T2	N0	M0	1	No	58	58	Alive	No	5	20
4	Subtotal gastrectomy	115	F	36	SRC	T1	N0	M0	1	No	41	41	Alive	No	5	5
5	Radical gastrec	78	M	46	SRC	T4	N2	M0	3	No	31	31	Dead	Yes	0	150
6	Distal gastrectomy	135	M	79	PD	T2	N0	M0	1	No	56	56	Alive	No	10	20
7	Proximal gastrectomy	131	M	61	SRC	T2	N1	M0	2	No	4	4	Dead	Yes	1	160
8	distal gastrectomy	91	F	62	SRC	T3	N1	M0	2	No	47	47	Alive	No	2	40
9	Distal gastrectomy	104	M	52	PD	T3	N0	M0	2	No	27	27	Dead	yes	50	85
10	Distal gastrectomy	112	F	63	PD	T4	N1	M0	3	No	11	11	Dead	yes	2	150
11	Distal gastrectomy	129	F	8	PD	T4	No	M0	3	No	19	19	Alive	Yes	5	15
12	Proximal gastrectomy	134	M	43	MD	T2	N1	M0	2	No	10	10	Dead	Yes	5	180
13	Subtotal	73	M	40	PD	T3	N1	M0	2	No	60	60	Alive	No	60	160
14	Total gastre	62	M	72	MD	T4	N1	M0	3	No	11	11	Dead	Yes	5	270
15	Distal radical gastrectomy	56	M	79	PD	T4	N2	M0	3	No	1	1	Dead	No	10	50
16	Subtotal gastrectomy	37	M	46	MD	T3	N2	M0	3	No	53	53	Alive	No	20	190
17	distal gastrectomy	53	M	41	PD	T3	N0	M0	2	No	45	45	Alive	No	10	120
18	distal gastrectomy	11	M	62	PD	T3	N2	M0	3	No	59	59	Alive	No	5	120
19	Total	9	F	54	SRC	T2	N2	M0	2	No	12	5	Dead	Yes	1	285
20	distal gsrectomy	39	M	56	PD	T3	N1	M0	2	No	54	40	Alive	yes	35	240
21	distal gastrectomy	21	M	71	PD	T2	N1	M0	2	No	34	34	Alive	No	10	180
22	distal gastrectomy	22	M	63	PD	T3	N3	M0	3	No	59	59	Alive	No	1	170
23	Subtotal gastrectomy	86	M	60	PD	T4	N0	M0	2	No	15	15	Alive	No	5	225
24	Total gastrectomy	122	M	60	MD	T1	N0	M0	1	No	42	42	Alive	No	10	30

10.2 APPENDIX-II – Buffer compositions, list of antibodies and primer sequence.

10.2.1 Composition of MNase Digestion Buffer

Sr No.	Component	Stock	Volume
1.	250 mM Sucrose	2M	625 μ l
2.	50 mM Tris-Cl pH 7.4	1M	250 μ l
3.	25 mM KCl	3M	42 μ l
4.	5mM MgCl ₂	1M	23 μ l
5.	50 mM Sodium Bisulfite	1M	250 μ l
6.	45 mM Sodium Butyrate	1M	225 μ l
7.	10 mM β -Mercaptoethanol	14.3M	3.5 μ l
8.	0.2% Triton X-100	25%	80 μ l
9.	0.15 mM Spermine	100 mM	15 μ l
10.	0.5 mM Spermidine	100 mM	50 μ l
11.	1 mM PMSF	100 mM	50 μ l
12.	1 mM Sodium Orthovanadate	0.5M	10 μ l
13.	10 mM β -Glycerophosphate	1M	50 μ l
14.	10 mM Sodium Fluoride	1M	50 μ l

Adjust final volume to 5 ml with MilliQ water

10.2.2 Composition of Salt Fractionation Buffer

Sr No.	Reagent	Stock	Volume
1.	10 mM Tris pH 7.4	1M	50 μ l
2.	250 mM Sucrose	2M	0.650 ml
3.	2 mM MgCl ₂	1M	10 μ l
4.	25 mM KCl	3M	42 μ l
5.	0.2 mM PMSF	100 mM	10 μ l
6.	10mM β -Glycerophosphate	1M	50 μ l
7.	10mM Sodium Fluoride	1M	50 μ l
8.	For 100 mM NaCl	5M	16 μ l/ml buffer
	For 400 mM NaCl		64 μ l/ml buffer

Adjust final volume to 5ml with MilliQ water

10.2.3 Composition of ChIP dilution Buffer

Sr No.	Reagent	Stock	Volume
1.	10 mM Tris pH 8.0	1M	50 μ l
2.	0.01% SDS	10 %	5 μ l
3.	1.% TritonX-100	1M	10 μ l
4.	1.2 mM EDTA	0.5 M	12 μ l
5.	140mM NaCl	5M	140 μ l

Adjust final volume to 5ml with MilliQ water

10.2.4 Composition of MKK Lysis buffer

Sr No.	Reagent	Stock	Volume
1.	10 mM Tris pH 7.4	1M	50 μ l
2.	0.27M Sucrose	2M	0.675 ml
3.	1mM EDTA	0.5M	10 μ l
4.	1mM EGTA	0.2M	25 μ l
5.	1% Triton X-100	25%	200 μ l
6.	10 μ g/ml Leupeptin	1mg/ml	50 μ l
7.	10 μ g/ml Aprotinin	5mg/ml	10 μ l
8.	1mM PMSF	100mM	50 μ l
9.	1mM Sodium Orthovanadate	0.5M	10 μ l
10.	10mM β -Glycerophosphate	1M	50 μ l
11.	10mM Sodium Fluoride	1M	50 μ l

Adjust final volume to 5ml with MilliQ water

10.2.5 Composition of Nuclei Isolation Buffer

Sr No.	Component	Stock	Volume
1.	250 mM Sucrose	2M	625 μ l
2.	50 mM Tris-Cl pH 7.4	1M	250 μ l
3.	25 mM KCl	3M	42 μ l
4.	5mM MgCl ₂	1M	23 μ l
5.	50 mM Sodium Bisulfite	1M	250 μ l
6.	45 mM Sodium Butyrate	1M	225 μ l
7.	10 mM β -Mercaptoethanol	14.3M	3.5 μ l
8.	25% Triton X-100	0.2%	80 μ l
9.	1 mM PMSF	100 mM	50 μ l
10.	1 mM Sodium Orthovanadate	0.5M	10 μ l
11.	10 mM β -Glycerophosphate	1M	50 μ l
12.	10 mM Sodium Fluoride	1M	50 μ l

Adjust final volume to 5 ml with MilliQ water

10.2.6 Composition of SDS-PAGE gels.

Sr. No	Components	18% Resolving	15% Resolving	10% Resolving	4% Stacking
1.	MilliQ Water	1.345 ml		4.076 ml	7.29 ml
2.	30% Acrylamide	6 ml		3.33 ml	1.3 ml
3.	1.5M Tris pH 8.8	2.5 ml	2.5 ml	2.5 ml	-
	1M Tris pH 6.8	-	-	-	1.25 ml
4.	10% SDS	100 µl	100 µl	100 µl	100 µl
5.	10% APS	50 µl	50 µl	50 µl	50 µl
6.	TEMED	5 µl	5 µl	5 µl	10 µl
Total Volume = 10 ml					

10.2.7 Composition of SDS-Running Buffer

Sr. No.	Component	Weight
1.	Glycine	14.2 g
2.	Tris	3.03 g
3.	SDS	1g
Make final volume to 1L with distilled water		

10.2.8 Composition of 1X Transfer buffer

Sr. No	Component	Weight
1.	Glycine	14.2 g
2.	Tris	3.03 g
3.	SDS	1g
4.	Methanol	200 ml
Make final volume to 1L with distilled water and chill buffer in -20°C until use.		

10.2.9 Composition of NP-40 Buffer

Sr No.	Reagent	Stock	Volume
1.	10 mM Tris pH 7.4	1M	50 μ l
2.	140 mM NaCl	5M	140 μ l
3.	1 mM EDTA	0.5 M	10 μ l
4.	0.5 mM EGTA	0.2 M	12.5 μ l
5	1% NP-40	100%	50 μ l
6.	1 mM PMSF	100 mM	100 μ l
7.	10 μ g/ml Leupeptin	1mg/ml	50 μ l
8.	10mM β -Glycerophosphate	1M	50 μ l
9.	1mM Sodium Orthovanadate	0.5M	10 μ l
10.	10mM Sodium Fluoride	1M	50 μ l
Adjust final volume to 5ml with MilliQ water			

10.2.10 List of antibodies and condition used

Sr. No	Antibody	Blocking condition	Primary antibody condition
1	H3 Upstate 05-499)	5% BSA in 0.01% TBST 60min RT	1:3000 1% BSA in 0.01% TBST O/N 4 $^{\circ}$ C
2	H3S10ph Millipore 06-570	5% BSA in 0.01% TBST 60min RT	1:3000 1% BSA in 0.01% TBST O/N 4 $^{\circ}$ C
3	H3S28ph Ab 5169	5% BSA in 0.01% TBST 60min RT	1:2000 1% BSA in 0.01% TBST O/N 4 $^{\circ}$ C (Western) 1:200 1% BSA TBST 2 hours(humid chamber) for IF
4	H3K9ac Millipore 06-570	5% BSA in 0.01% TBST 60min RT	1:5000 1% BSA in 0.01% TBST O/N 4 $^{\circ}$ C
5	H3K14ac Ab 52946	5% BSA in 0.01% TBST 60min RT	1:3000 1% BSA in 0.01% TBST O/N 4 $^{\circ}$ C
6	H3K18ac Millipore 07-354	5% BSA in 0.01% TBST 60min RT	1:5000 1% BSA in 0.01% TBST O/N 4 $^{\circ}$ C
7	H3K27ac Ab 4729	1% BSA in 0.01 TBST 60min RT	1:3000 1% BSA in 0.01% TBST O/N 4 $^{\circ}$ C
8	H3S10phK14ac Millipore 07-181	5% BSA in 0.01% TBST 60min RT	1:3000 1% BSA in 0.01% TBST O/N 4 $^{\circ}$ C

9	H3K56ac Ab 76309	1% BSA in 0.01 TBST 60min RT	1:2000 1% BSA in 0.01% TBST O/N 4 °C
10	H3K9me3 Ab 8898	5% BSA in 0.01% TBST 60min RT	1:2000 1% BSA in 0.01% TBST O/N 4 °C
11	H4K16ac Millipore 07-329	5% BSA in 0.01% TBST 60min RT	1:5000 1% BSA in 0.01% TBST O/N 4 °C
12	γH2AX Millipore 05-636	5% Milk in 0.01% TBST 60min RT	1:5000 1% BSA in 0.01% TBST O/N 4 °C
13	MSK1 Ab 99412	5% BSA in 0.01 TBST 60min RT	1:1000 1% BSA in 0.01% TBST O/N 4 °C
14	MSK2 Ab 99411	5% BSA in 0.01 TBST 60min RT	1:3000 1% BSA in 0.01% TBST O/N 4 °C
15	pMSK1 (S376) Millipore 04-384	5% BSA in 0.01 TBST 60min RT	1:5000 1% BSA in 0.01% TBST O/N 4 °C
16	ERK 1/2 Cell Signalling #9926	5% BSA in 0.01 TBST 60min RT	1:2000 1% BSA in 0.01% TBST O/N 4 °C
17	pERK1/2 Cell Signalling #9910	5% BSA in 0.01 TBST 60min RT	1:2000 1% BSA in 0.01% TBST O/N 4 °C
18	P38 Cell Signalling #9926	5% BSA in 0.01 TBST 60min RT	1:2000 1% BSA in 0.01% TBST O/N 4 °C
19	pP38 Cell Signalling #9910	5% BSA in 0.01 TBST 60min RT	1:2000 1% BSA in 0.01% TBST O/N 4 °C
20	GCN5/KAT2A Cell Signalling #8686	5% BSA in 0.01 TBST 60min RT	1:2000 1% BSA in 0.01% TBST O/N 4 °C
21	P300 Cell Signalling #8686	5% BSA in 0.01 TBST 60min RT	1:2000 1% BSA in 0.01% TBST O/N 4 °C
22	PCAF/KAT2B Cell Signalling #8686	5% BSA in 0.01 TBST 60min RT	1:2000 1% BSA in 0.01% TBST O/N 4 °C
23	HDAC1 Sigma SAB4501383	5% BSA in 0.01 TBST 60min RT	1: 5000 1% BSA in 0.01% TBST O/N 4 °C
24	K-Ras Sigma R3400	5% BSA in 0.01 TBST 60min RT	1:1000 1% BSA in 0.01% TBST O/N 4 °C
25	Cyclin B CB-69 Lab generated	1% BSA in 0.01 TBST 60min RT	1:50 1% BSA in 0.01 TBST O/N 4 °C
26	Cyclin D	1% BSA in 0.01 TBST 60min RT	1:1000 1% BSA in 0.01% TBST O/N 4 °C
27	MKP 1 SC-370	5% Milk in 0.01 TBST	1:3000 3% BSA in 0.01% TBST O/N 4 °C

		60min RT	
28	PP1 α Millipore 07-273	5% BSA in 0.01 TBST	1:3000 3% BSA in 0.01% TBST O/N 4°C
		60min RT	
29	Lamin B1 Ab26300	5% BSA in 0.01 TBST	1:2000 1% BSA in 0.01% TBST O/N 4°C
		60min RT	
30	Actin Sigma A-5316	5% Milk in 0.01 TBST	1:10000 1% BSA-TBST O/N 4°C
		60min RT	

10.2.11 List of primers used in the study

Sr No	Gene	Primer Sequence	Size (bp)	Purpose
1	HDAC1	F 5'ATATCGTCTTGGCCATCCTG 3' R 5'TGAAGCAACCTAACCGATCC 3'	361	RT-PCR
2	HDAC2	F 5'GGGAATACTTTCCTGGCACA3' R 5'ACGGATTGTGTAGCCACCTC3'	314	RT-PCR
3	HDAC3	F 5'TGGCATTGACCCATAGCCTG3' R 5'GCATATTGGTGGGGCTGACT3'	150	RT-PCR
4	HDAC4	F 5' TCGCTACTGGTACGGGAAAAC3' R 5'AGAGGGAAGTCATCTTTGGCG3'	126	RT-PCR
5	HDAC5	F 5'ACTGTTCTCAGATGCCAGC3' R 5'TGGTGAAGAGGTGCTTGACG3'	164	RT-PCR
6	HDAC6	F 5'AGTGGCCGCATTATCCTTATCC3' R 5'ATCTGCGATGGACTTGGATGG3'	178	RT-PCR
7	HDAC7	F 5'TTCCTGAGTGCAGGGGTAGT3' R 5'CATCGCCAGGAGGTTGATGT3'	167	RT-PCR
8	HDAC8	F 5'ATAACCTTGCCAACACGGCT3' R 5'CTTGGCGTGATTTCCAGCAC3'	136	RT-PCR
9	HDAC9	F 5'ACTGAAGCAACCAGGCAGTC3' R 5'TTCACAGCCCCAACTTGTCC3'	156	RT-PCR
10	HDAC10	F 5'CTGGCCTTTGAGGGGCAAAT3' R 5'CAGCAGCGTCTGTACTGTCA3'	162	RT-PCR
11	HDAC11	F 5'CCGGAAAATGGGGCAAAGTG3' R 5'TAAGATAGCGCCTCGTGTG3'	126	RT-PCR
12	c-Fos	F 5'CCGGGGATAGCCTCTCTTAC3' R 5'CCCTTCGATTCTCCTTTTC3'	366	RT-PCR
13	c-Jun	F 5'CCCCAAGATCCTGAAACAGA3' R 5'TCCTGCTCATCTGTCACGTT3'	233	RT-PCR
14	MSK1	F 5' TTCAGCTGTAAGCCACATGC3' R 5'TGAGATTGGAAGGGAACCTG3'	288	RT-PCR
15	RPS	F 5'GCTCTCCTTTCGTTGCCTGA3' F 5'ACTTCAACCAAGTGGGGACG3'	113	RT-PCR
16	MSK1 shRNA	5'CCGGAGCAACCTTCCACGCCTTAACT CGAGTTAAAGGCGTGGAAGGTTGCTTTT TTG-3' 5'AATTCAAAAAAGCAACCTTCCACGCC TTTAACTCGAGTTAAAGGCGTGGAAGG TTGCT-3'		Knock- down

17	CEBP- B HDAC1 promoter	F 5'AATTCACAGAAGTCTGAAC3' R 5' CCAATGTTATTTTCAGTTT3'	150	ChIP qPCR H3S10ph/ H3K14ac
18	CREB 3 HDAC1 promoter	F 5'TACTTGGCACACAGCAG3' R 5'CTACAGAAAAATAATTA3'	150	ChIP qPCR H3S10ph/ H3K14ac
19	FOS L1 HDAC1 promoter	F 5' TGTGCAAGTCACTTTTC3' R 5'CTCTGTAAACTTAACAGT3'	150	ChIP qPCR H3S10ph/ H3K14ac
20	FOS – FOSL HDAC1 promoter	F 5'CTTTATCCTGTCCTGTA3' R 5'GTACTGTGCGACACTTTAC3'	150	ChIP qPCR H3S10ph/ H3K14ac

10.2.12 Dose for combinatorial treatment of chemotherapy drugs and HDAC inhibitors in fixed constant ratio

		Dilution factor →						
		1/8 x IC50	1/4 x IC50	1/2 x IC50	IC50	2 x IC50	4 x IC50	8 x IC50
Dose of single agent (µM)	Cisplatin (Cis)	1.5	3	6	12	24	48	96
	Oxaliplatin (Oxa)	1.25	2.5	5	10	20	40	80
	Epirubicin (Epi)	0.025	0.05	0.1	0.2	0.4	0.8	1.6
	VPA	500	1000	2000	4000	8000	16000	32000
	TSA	0.25	0.5	1	2	4	8	16
	SAHA	0.00125	0.0025	0.005	0.01	0.02	0.04	0.08
Dose of combined agents (µM)	Cis and VPA	501.5	1003	2006	4012	8024	16048	32096
	Cis and TSA	1.75	3.5	7	14	28	54	112
	Cis and SAHA	1.50125	3.0025	6.005	12.01	24.02	48.04	112
	Oxa and VPA	501.25	1002.5	2005	4010	8020	16040	32080
	Oxa and TSA	1.5	3	6	12	24	46	96
	Oxa and SAHA	1.25125	2.5025	5.005	10.01	20.02	40.04	80.08
	Epi and VPA	500.025	1000.05	2000.1	4000.2	8000.4	16000.8	32001.6
	Epi and TSA	0.275	0.55	1.1	2.2	4.4	6.8	17.6
	Epi and SAHA	0.02625	0.0525	0.105	0.21	0.42	0.84	1.68

Basic Study

Histone deacetylase inhibitor pre-treatment enhances the efficacy of DNA-interacting chemotherapeutic drugs in gastric cancer

Ramchandra Vigay Amnekar, Shafqat Ali Khan, Mudasir Rashid, Bharat Khade, Rahul Thorat, Poonam Gera, Shailesh V Shrikhande, Duane T Smoot, Hassan Ashktorab, Sanjay Gupta

ORCID number: Ramchandra Vijay Amnekar (0000-0003-2644-4016); Shafqat Ali Khan (0000-0002-8573-792X); Mudasir Rashid (0000-0001-9342-6243); Bharat Khade (0000-0001-8099-2326); Rahul Thorat (0000-0001-5059-0342); Poonam Gera (0000-0001-7709-1594); Shailesh V Shrikhande (0000-0002-8036-4212); Duane T Smoot (0000-0002-8416-7419); Hassan Ashktorab (0000-0002-4048-4666); Sanjay Gupta (0000-0002-1209-189X).

Author contributions: Gupta S conceived the idea, designed the experiments, and edited the manuscript; Amnekar RV and Khan SA designed the experiments, performed the experiments, analyzed the data, and wrote the manuscript, they contributed equally to the work; Rashid M performed RT-PCR and TCGA data analysis; Khade B performed histone deacetylase and histone acetyltransferase assay; Thorat R and Khade B performed the animal experiments; Smoot DT and Ashktorab H provided the HFE145 cell line; Gera P performed the histopathology analysis; Shrikhande SV provided the tissue samples and clinical data; The paper was critically read by all the authors and approved for publication.

Supported by TMH-IRG (account number - 466/2012 and 164/2016); LTMT grant for project funding and ACTREC-TMC for funding to Gupta lab; Tumor Tissue Repository-ACTREC; and TTR-TMH-Indian Council Medical

Ramchandra Vigay Amnekar, Mudasir Rashid, Bharat Khade, Sanjay Gupta, Epigenetics and Chromatin Biology Group, Gupta Laboratory, Cancer Research Institute, Advanced Centre for Treatment Research and Education in Cancer, Tata Memorial Centre, Kharghar, Navi Mumbai, Maharashtra 410210, India

Ramchandra Vigay Amnekar, Mudasir Rashid, Sanjay Gupta, Homi Bhabha National Institute, Training School Complex, Anushakti Nagar, Mumbai, Maharashtra 400085, India

Shafqat Ali Khan, Department of Developmental Biology, School of Medicine, Washington University in St. Louis, Saint Louis, MO 63130, United States

Rahul Thorat, Animal House Facility, Cancer Research Institute, Advanced Centre for Treatment Research and Education in Cancer, Tata Memorial Centre, Kharghar, Navi Mumbai, Maharashtra 410210, India

Poonam Gera, Biorepository Lab, Advanced Centre for Treatment Research and Education in Cancer, Tata Memorial Centre, Kharghar, Navi Mumbai, Maharashtra 410210, India

Shailesh V Shrikhande, Gastrointestinal and Hepato-Pancreato-Biliary Service, Department of Surgical Oncology, Tata Memorial Hospital, Parel, Mumbai 400012, India

Duane T Smoot, Department of Medicine, Meharry Medical Center, Nashville, TN 37208, United States

Hassan Ashktorab, Department of Medicine and Cancer Center, College of Medicine, Howard University, Washington DC, WA 20060, United States

Corresponding author: Sanjay Gupta, PhD, Principal Investigator, Epigenetics and Chromatin Biology Group, Gupta Laboratory, Cancer Research Institute, Advanced Centre for Treatment Research and Education in Cancer, Tata Memorial Centre, Navi Mumbai, Maharashtra 410210, India. sgupta@actrec.gov.in

Abstract

BACKGROUND

The prognosis of gastric cancer continues to remain poor, and epigenetic drugs like histone deacetylase inhibitors (HDACi) have been envisaged as potential therapeutic agents. Nevertheless, clinical trials are facing issues with toxicity and efficacy against solid tumors, which may be partly due to the lack of patient stratification for effective treatments.

AIM

Research for providing tissue samples. Amnekar RV and Rashid M were supported by ACTREC fellowships.

Institutional review board

statement: The study was reviewed and approved by the Institutional Animal Ethics Committee in Kharghar, Navi Mumbai, India.

Institutional animal care and use

committee statement: All institutional and national guidelines for the care and use of laboratory animals were followed.

Conflict-of-interest statement: The authors declare that they have no competing interests.

Data sharing statement: No additional data are available.

ARRIVE guidelines statement:

The ARRIVE guidelines have been adopted. In vivo animal work has been carried out considering the ARRIVE guidelines.

Open-Access:

This article is an open-access article that was selected by an in-house editor and fully peer-reviewed by external reviewers. It is distributed in accordance with the Creative Commons Attribution NonCommercial (CC BY-NC 4.0) license, which permits others to distribute, remix, adapt, build upon this work non-commercially, and license their derivative works on different terms, provided the original work is properly cited and the use is non-commercial. See: <http://creativecommons.org/licenses/by-nc/4.0/>

Manuscript source: Invited Manuscript

Received: October 15, 2019

Peer-review started: October 15, 2019

First decision: December 4, 2019

Revised: December 20, 2019

Accepted: January 15, 2020

Article in press: January 15, 2020

Published online: February 14, 2020

P-Reviewer: Ebrahimifar M

S-Editor: Zhou JJ

L-Editor: Filipodia

E-Editor: Zhang YL



To study the need of patient stratification before HDACi treatment, and the efficacy of pre-treatment of HDACi as a chemotherapeutic drug sensitizer.

METHODS

The expression activity of class 1 HDACs and histone acetylation was examined in human gastric cancer cells and tissues. The potential combinatorial regime of HDACi and chemotherapy drugs was defined on the basis of observed drug binding assays, chromatin remodeling and cell death.

RESULTS

In the present study, the data suggest that the differential increase in HDAC activity and the expression of class 1 HDACs are associated with hypo-acetylation of histone proteins in tumors compared to normal adjacent mucosa tissue samples of gastric cancer. The data highlights for the first time that pre-treatment of HDACi results in an increased amount of DNA-bound drugs associated with enhanced histone acetylation, chromatin relaxation and cell cycle arrest. Fraction-affected plots and combination index-based analysis show that pre-HDACi chemo drug combinatorial regimes, including valproic acid with cisplatin or oxaliplatin and trichostatin A with epirubicin, exhibit synergism with maximum cytotoxic potential due to higher cell death at low combined doses in gastric cancer cell lines.

CONCLUSION

Expression or activity of class 1 HDACs among gastric cancer patients present an effective approach for patient stratification. Furthermore, HDACi therapy in pre-treatment regimes is more effective with chemotherapy drugs, and may aid in predicting individual patient prognosis.

Key words: Chemotherapy; Combinatorial index; Gastric cancer; Histone acetylation; Histone deacetylase inhibitor; Patient stratification

©The Author(s) 2020. Published by Baishideng Publishing Group Inc. All rights reserved.

Core tip: Our study suggests that pre-treatment with histone deacetylase inhibitors (HDACi) in a pre-clinical model of gastric cancer increases acetylation, opens chromatin and favors synergistic binding of DNA-interacting chemotherapeutic drugs. This enhances the cytotoxic potential of chemotherapeutic drugs at low therapeutic doses, and reduces toxicity. The dose response studies using Fa plots and median curve analysis proposes valproic acid as the most synergistic and effective HDACi in combination with platinum-based drugs. Furthermore, HDAC expression, or activity-based patient stratification prior to HDACi therapy, has been put forth for better clinical outcomes of chemotherapeutic drugs in solid tumors.

Citation: Amnekar RV, Khan SA, Rashid M, Khade B, Thorat R, Gera P, Shrikhande SV, Smoot DT, Ashktorab H, Gupta S. Histone deacetylase inhibitor pre-treatment enhances the efficacy of DNA-interacting chemotherapeutic drugs in gastric cancer. *World J Gastroenterol* 2020; 26(6): 598-613

URL: <https://www.wjgnet.com/1007-9327/full/v26/i6/598.htm>

DOI: <https://dx.doi.org/10.3748/wjg.v26.i6.598>

INTRODUCTION

Gastric cancer (GC) is the 3rd leading cause of cancer deaths, 5th in terms of incidence in the world, and the most lethal cancer in Asia^[1]. In India, it is one of the most aggressive cancers, ranking 5th in terms of incidence and mortality. The management of GC is multimodal, including surgical R0 resection, radiotherapy and chemotherapy. Based on multiple clinical trials, commonly used drug combinations for neoadjuvant and adjuvant chemotherapy (NACT and ACT) in GC involves drugs such as cisplatin, oxaliplatin and epirubicin, which exert their cytotoxic effects by binding to DNA^[2,3]. Earlier reports have shown that inhibitors of chromatin remodelers, such as valproic acid and butyric acid, increase the efficacy of

chemotherapeutic drugs^[4-6].

Post-translational modifications of histone proteins are one of the major epigenetic mechanisms regulating chromatin conformations^[7]. Acetylation of histones has been the most studied, and has been shown to positively correlate with chromatin relaxation. The dynamic equilibrium between histone acetyltransferases (HATs) and histone deacetylases (HDACs) dictates the acetylation levels and transcriptional status of chromatin^[8]. Alterations in the levels of several histone acetylation marks such as H3K12ac, H3K18ac, H3K9ac and H4K16ac have been reported in multiple cancers, such as liver, kidney, prostate, breast and stomach^[9]. Moreover, aberrant expression of HATs like CBP and p300, and HDACs like HDAC1 and HDAC2, has been observed in several malignancies^[9]. These findings have led to the exponential growth in research on HAT inhibitors (HATi) and HDAC inhibitors (HDACi), and their anti-cancer properties. HATi, like E-7438 and EPZ-5676, are in phase II and phase I clinical trials, respectively; also, sodium butyrate is in phase II, and panobinostat and valproic acid (VPA) are in phase III clinical trials. Additionally, HDACi, like vorinostat (SAHA) and romidepsin, is now FDA approved for cancer treatment^[10]. Importantly, studies have shown that HDACi can modulate cellular responses through different mechanisms, such as re-expression of tumor suppressors, transporters of chemotherapeutic drugs^[11], enzymes associated with drug metabolism^[12], and enhancing the levels of open chromatin^[13]. HDACis have shown to have potential therapeutic benefits, predominantly in advanced hematologic malignancies, more so as combinatorial chemotherapy than as single agents; however, clinical responses are disappointing in solid tumors^[14,15]. Marchio *et al*^[16]'s study suggested the use of HDACi (SAHA) as a chemo-sensitizer that increases the efficiency of epirubicin in breast cancer. To overcome the limitation of HDACi in solid tumors, the identification of synergistic combinations of selective HDACi with other chemotherapeutic drugs, along with patient stratification based on HDAC levels, is a must and would help to both minimize toxicity and predict the response to treatment.

In the present study, we show a strong association between global histone hypoacetylation with increased HDAC activity in human GC tissue samples and cell lines. Differential activity and expression levels of class 1 HDACs in patient samples and TCGA data highlight the importance of patient stratification for treatment with HDACi. Interestingly, the pre-treatment regime of HDACi followed by chemotherapeutic drugs exerts synergistic effects in GC cells and pre-clinical studies.

MATERIALS AND METHODS

Patient and tissue samples

Paired frozen tissue samples from normal adjacent gastric mucosa (negative resection margin) and tumors were collected from GC patients through the tumor tissue repository of ACTREC and the Tata Memorial Hospital, Mumbai, India. The protocol was reviewed and approved by the institutional review board and ethics committee. Written informed consent was undertaken from all patients. Based on histopathological analysis by a blinded pathologist, the tumor content was found to be > 60% in all tumor samples.

Cell lines and culture conditions

The AGS GC cell line (CRL 1739) was procured from ATCC, and the HFE145 cell line was provided by DTS and AH. The cell lines were cultured in RPMI1640 (Invitrogen) media with 10% fetal bovine serum and maintained at 37 °C with 5% CO₂ and 100 U/mL penicillin, 100 mg/mL streptomycin (Himedia).

Histone deacetylase inhibitors and chemotherapeutic drugs

HDACi, sodium valproate (VPA; Sigma, P4543), trichostatin A (TSA; Sigma, T8552) and suberoylanilide hydroxamic acid (SAHA; Sigma, SML0061) were dissolved in ethanol to prepare stock solutions. The chemotherapeutic drugs cisplatin (Calbiochem, 232120), oxaliplatin (Sigma, O9512) and epirubicin (Calbiochem, 324905) were dissolved in DMSO to prepare stock solutions. As per the experimental requirements, cells were treated with different concentrations of HDACi and chemotherapeutic drugs.

Cell viability assay

Cell viability was quantified by MTT assay (Sigma, M2128) as per the manufacturer's protocol. AGS cells (about 1000) were used for the assay, the absorbance was measured at 570 nm, and cell viability was expressed as the percentage of absorbance obtained compared to control cultures.

Analysis of histone post-translational modifications

Histones were extracted, resolved on an 18% SDS-PAGE gel and transferred to a PVDF membrane^[17]. Western blotting with the respective antibodies was carried out as per the manufacturer's protocol (H3, Millipore #05-499; H4, Millipore #07-108; H3K9ac, Millipore #06-599; H3K18ac, Millipore #07-354; H3K27ac, Abcam #4729; H3K16ac, Millipore #07-329; γ H2AX, Millipore #05-636; H3ac, Millipore #06-599; H4ac, Millipore #06-866). The signal was visualized using the ECL plus chemiluminescence kit (Millipore #WBKLS0500).

Histone acetyl-transferase and histone deacetylase assays

Nucleo-cytosolic fractions (NCF) from human GC tissues and cell lines were prepared as per the manufacturer's instructions (Biovision, K332-100 and K331-100). Protein lysates, cell lines (50 μ g) and tissues (100 μ g) were used for calorimetric-based assays. The absorbance was measured at A440 and A405 for HAT and HDAC, respectively, and the average absorbance was plotted.

Drug-DNA interaction assay

AGS cells treated with chemotherapeutic drugs with or without different combinations of HDAC inhibitors were washed in chilled PBS and lysed in nuclei isolation buffer (10 mmol/L HEPES pH 7.9, 1.5 mmol/L $MgCl_2$, 10 mmol/L KCl, 0.5 mmol/L DTT, 0.1% v/v NP-40, 2 mmol/L EDTA, 1 mmol/L EGTA, 0.15 mmol/L spermine, 0.5 mmol/L spermidine, 1 mmol/L sodium orthovanadate, 10 mmol/L sodium fluoride, 10 mmol/L β -Glycerophosphate, 0.2 mmol/L PMSF). The lysate was centrifuged at 5000 rpm for 10 min at 4 °C. The nuclear pellet obtained was lysed in 200 μ L 5 mol/L urea-2 mol/L NaCl solution to estimate the DNA concentration at 260 nm. DNA concentration was adjusted to 1 μ g/mL, and an equal volume was taken to measure the concentration of DNA-bound cisplatin, oxaliplatin and epirubicin at 220, 205 and 254 nm, respectively, as per European Pharmacopoeia 5.5^[18]. The absorbance was considered to be directly proportional to the amount of DNA bound to drug. The mean absorbance of three independent experiments was plotted for the chemotherapeutic drugs.

Fraction-affected curve analysis

Fraction-affected (FA) curves, a method for growth inhibition analysis, was carried out with cell survival percentage values obtained through three independent MTT assays. Fraction-affected values representing the percentages of cell death were calculated using the following formula:

FA value = $1 - (\% \text{ cell survival}/100)$. FA values ranged from 0.01 to 0.99; CompuSyn software was used to further assist in these calculations, which is based on the Chao Tally's algorithm^[19]. FA values and respective doses of the drugs were used to generate FA curves.

Median effect plot analysis

The median effect plot shows the combination index (CI) on the Y-axis and FA values on the X-axis. For a particular FA value, CI values range from 0 to 1; $CI < 0.8$, $CI = 0.8-1.2$, and $CI > 1.2$ represents the synergistic, additive or antagonistic nature of drug combinations, respectively. FA values and total doses of drug combinations (chemotherapeutic drugs and HDACi) were used to generate median effect plots with the help of CompuSyn software^[19].

Chromatin organization assay

Purified nuclei from control and VPA-treated AGS cells were subjected to micrococcal nuclease (MNase) digestion to analyze chromatin organization as per the published protocol^[20].

Expression of HDACs in GC cell lines

RNA was extracted by TRIzol method (Invitrogen, 5596026), and cDNA was synthesized as per the manufacturer's protocol (Thermo scientific, K1632). Quantitative PCR using SYBER green (Agilent Tech, 600882) was employed, and the primers used are listed in Table 1. Data analysis was performed using $\Delta\Delta Ct$ -based calculations, and fold changes were plotted for the different HDAC genes. The data were statistically analyzed by performing student *t*-tests.

Cell cycle analysis

Different phases of the cell cycle were determined by flow cytometry as previously described in^[20]. The data were analyzed using ModFit LN 2.0 software.

In vivo therapeutic potential of drug treatments in a tumor model

Table 1 List of primers used for carrying out real-time PCR on different genes

Gene	Forward primer, 5'-3'	Reverse primer, 5'-3'
<i>RPS13</i>	GCTCTCCTTTCGTTGCCTGA	ACTTCAACCAAGTGGGGACG
<i>HDAC1</i>	ATATCGTCTTGCCATCCTG	TGAAGCAACCTAACCGATCC
<i>HDAC2</i>	GGGAATACTTTCCTGGCACA	ACGGATTGTGTAGCCACCTC
<i>HDAC3</i>	TGGCATTGACCCATAGCCTG	GCATATTGGTGGGGCTGACT
<i>HDAC4</i>	TCGCTACTGGTACGGGAAAAC	AGAGGGAAGTCATCTTTGGCC
<i>HDAC5</i>	ACTGTTCTCAGATGCCCAGC	TGGTGAAGAGGTGCTTGACG
<i>HDAC6</i>	AGTGGCCGATTATCCTTATCC	ATCTGCGATGGACTTGGATGG
<i>HDAC7</i>	TTCTGAGTGCAGGGGTAGT	CATCGCCAGGAGGTGTATGT
<i>HDAC8</i>	ATAACCTTGCCAACACGGCT	CTTGGCGTGATTCCAGCAC
<i>HDAC9</i>	ACTGAAGCAACCAGGCAGTC	TTCACAGCCCCAACTTGTC
<i>HDAC10</i>	CTGGCCTTGGAGGGCAAAT	CAGCAGCGTCTGTACTGTCA
<i>HDAC11</i>	CCGGAAAATGGGGCAAAGTG	TAAGATAGCGCTCGTGTGC
<i>p27-CDKN1B</i>	TTGGGGCAAAAATCCGAGGT	TGTGTTACACAGCCCGAAGT
<i>p21-CDKN1A</i>	GCGACTGTGATGCGCTAATG	GAAGGTAGAGCTTGGGCAGG
<i>p16-CDKN2A</i>	ACTTCAGGGGTGCCACATTC	CGACCTGTCCCTCAAATCC

To study the *in vivo* therapeutic potential of a pre-treatment regime of VPA and cisplatin in an AGS cell-based xenograft model was developed after approval from the institutional animal ethics committee. AGS cells (approximately 5×10^6) were subcutaneously injected with matrigel (50 μ L) in NOD-SCID mice (4-6 wk). After one round of serial transplantation, the mice bearing tumors of approximately 6-10 mm maximum length were randomly divided into four groups: (1) Control; (2) VPA (300 mg/kg/d); (3) Cisplatin (2 mg/kg/d); and (4) Combinatorial pre-treatment group (VPA followed by cisplatin, with doses as mentioned above). Drugs or saline (control group) were administered intraperitoneally twice a week at an interval of 2 d for 6 wk. For the combinatorial regime, cisplatin was administered following 24 h of VPA treatment.

Tumor size and weight was monitored once a week by measuring two perpendicular tumor diameters with a caliper, and volume was calculated as $V = \pi / 6 \times \text{length} \times \text{width}^2$. The outcome of the different treatment regimens was statistically validated by performing unpaired *t*-tests. The animals were sacrificed, tissue was fixed in formalin, and 4-6 μ m sections were processed with hematoxylin and eosin staining for histopathological analysis.

***In silico* analysis of TCGA data for class1 HDACs in GC patients**

Normalized human gastric adenocarcinoma ($n = 415$) data (Z-score, cutoff > 1.5) of HDAC1, HDAC2, HDAC3 were downloaded from the cBioPortal website (<http://www.cbioportal.org/>)^[21,22]. The samples were categorized into high and low expression groups according to the Z-score, and then tabulated.

RESULTS

Hypo-acetylation associates with high histone deacetylase activity in GC patient samples

Histones were prepared from paired tumor and negative resection margin (RM) tissues, and subjected to immunoblot analysis to assess the level of acetylation using anti-acetyl lysine antibodies [Figure 1A(a)]. Immunoblot analysis showed low levels of histone H3 and H4 acetylation in the tumor tissues compared to RM tissues. This observed loss in acetylation levels of histone H3 and H4 could be the result of low histone acetyl-transferase (HAT) or high histone deacetylase (HDAC) activity in tumor tissues. Therefore, NCF was used to assess HAT and HDAC activity using calorimetric assays. Tumor and RM tissues showed differential levels of HAT and HDAC activity; however, all the tumor tissues showed high HDAC activity compared to their paired RM tissues, but HAT activity did not show any consistent pattern (Supplementary Figure 1). Further, statistical analysis showed a significantly higher level of HDAC activity in tumor compared to negative RM ($P < 0.001$) [Figure 1A(b)]; however, no significant difference was found in HAT activity. Taken together, our data suggested an inverse correlation between HDAC activity and histone acetylation

in GC.

The major reasons for HDACi failure in solid tumors may be attributed to expression or activity heterogeneity in class 1 HDACs of patients. To understand the need of patient stratification for HDACi therapy, we analyzed HDAC activity and found that it significantly differs among GC patients (Figure 1B). TCGA was analyzed for the expression of class 1 HDAC viz HDAC1, HDAC2 and HDAC3 in gastric adenocarcinoma patients ($n = 415$) versus control ($n = 35$), and categorized into high and low expression groups according to the Z-score. HDAC1, HDAC2 and HDAC3 were upregulated in only approximately 24% of gastric adenocarcinoma patients (Figure 1C). Further, in coherence with activity, expression levels also showed differentially increased levels of HDAC 1 and 3 compared to normal gastric tissue (Figure 1D). Altogether, these data provide evidence for patient stratification, and for tailoring the dose of HDACi for (re)sensitizing tumors to the anti-proliferative effects of chemotherapeutic drugs at reduced doses with minimal side effects.

Pre-treatment with HDACi enhances binding of chemotherapeutic drugs to chromatin

It has been hypothesized that HDACi mediates chromatin relaxation, which may enhance the amount of chemotherapeutic drugs bound to DNA. To understand this, histone acetylation and class 1 HDAC levels were determined in AGS and HFE145 cell lines. A decrease in site-specific histone acetylation at H3K9ac, H3K18ac, H3K27ac was observed [Figure 2A(a)], along with increased HDAC activity [Figure 2A(b)] and levels of class 1 HDACs 1, 2 and other HDACs 8, 10, 11 [Figure 2A(c)] in transformed AGS cells. The AGS cell line reflects the human gastric tumor state, and was therefore used for further studies. Dose response curves for chemotherapy drugs and HDACi showed IC50s of 12 $\mu\text{mol/L}$, 10 $\mu\text{mol/L}$ and 0.2 $\mu\text{mol/L}$ for cisplatin, oxaliplatin and epirubicin, respectively (Supplementary Figure 2A), whereas for HDACi, the IC50 concentrations of VPA, TSA and SAHA were found to be 4 mmol/L, 2 $\mu\text{mol/L}$ and 0.01 $\mu\text{mol/L}$, respectively (Supplementary Figure 2B). Further, we confirmed HDACi activity by treating AGS cells with IC50 doses for 24 h, and assessing HDAC activity and histone acetylation levels. A decrease in HDAC activity (Supplementary Figure 2C) with hyperacetylation of histones H3 and H4 (Supplementary Figure 2D) were observed upon HDACi treatment. Taken together, our data confirm that the HDACi used in our study is functionally active, and alters both HDAC activity and histone acetylation.

AGS cells treated with HDACi and chemotherapeutic drugs at IC50 values in three different combinations (Figure 2B): (1) Pre- (24 h HDACi treatment followed by 24 h chemotherapeutic drug treatment); (2) Concurrent (24 h HDACi and chemotherapeutic drug together); and (3) Post- (24 h chemotherapeutic drug treatment followed by 24 h HDACi treatment) showed that the quantity of DNA-bound chemotherapeutic drugs significantly increased with pre- followed by concurrent regimes. However, post-treatment did not show any significant increase compared to control for all three HDACis (Figure 2C).

HDACi-dependent sensitization of GC cells decreases the dose of chemotherapeutic drugs to attain maximum efficacy

The effect of regime-specific combinatorial treatment of HDACi and chemotherapeutic drugs on cell death was studied using FA plot analysis (Figure 3)^[23]. MTT assays were performed using a fixed constant ratio of chemotherapeutic drugs, and in three different combination regimes: Concurrent, pre- and post- (Supplementary Table 1). The data showed that pre-treatment with the three HDACis led to more cell death compared to concurrent or post-treatment in combination with cisplatin (Figure 3A), oxaliplatin (Figure 3B) and epirubicin (Figure 3C). Further, the combined doses of chemotherapeutic drugs and HDACi required to achieve FA values of 0.5, 0.75 and 0.95 was analyzed (Table 2). The pre-treatment regime of VPA with cisplatin required lesser combined doses to achieve FA 0.5, 0.75 and 0.95 compared to both concurrent and post-treatment regimes. However, pre-treatment of TSA or SAHA with cisplatin could only attain FA values of 0.5 and 0.75 at a lower combined dose than concurrent or post-treatment combinations. In the case of oxaliplatin, pre-treatment with only VPA attained FA values of 0.5, 0.75 and 0.95; whereas, TSA and SAHA achieved only FA values of 0.5 at lower combined doses than the concurrent or post-treatment regimes. In the case of epirubicin, pre-treatment with TSA was found to be most effective, achieving FA values of 0.5 and 0.75 at lesser doses, followed by SAHA. Overall, cell death by cisplatin and oxaliplatin is effectively enhanced with VPA, and epirubicin with TSA, in the pre-treatment combination regimes.

Synergistic interactions of combinatorial HDACi and chemotherapeutic drug

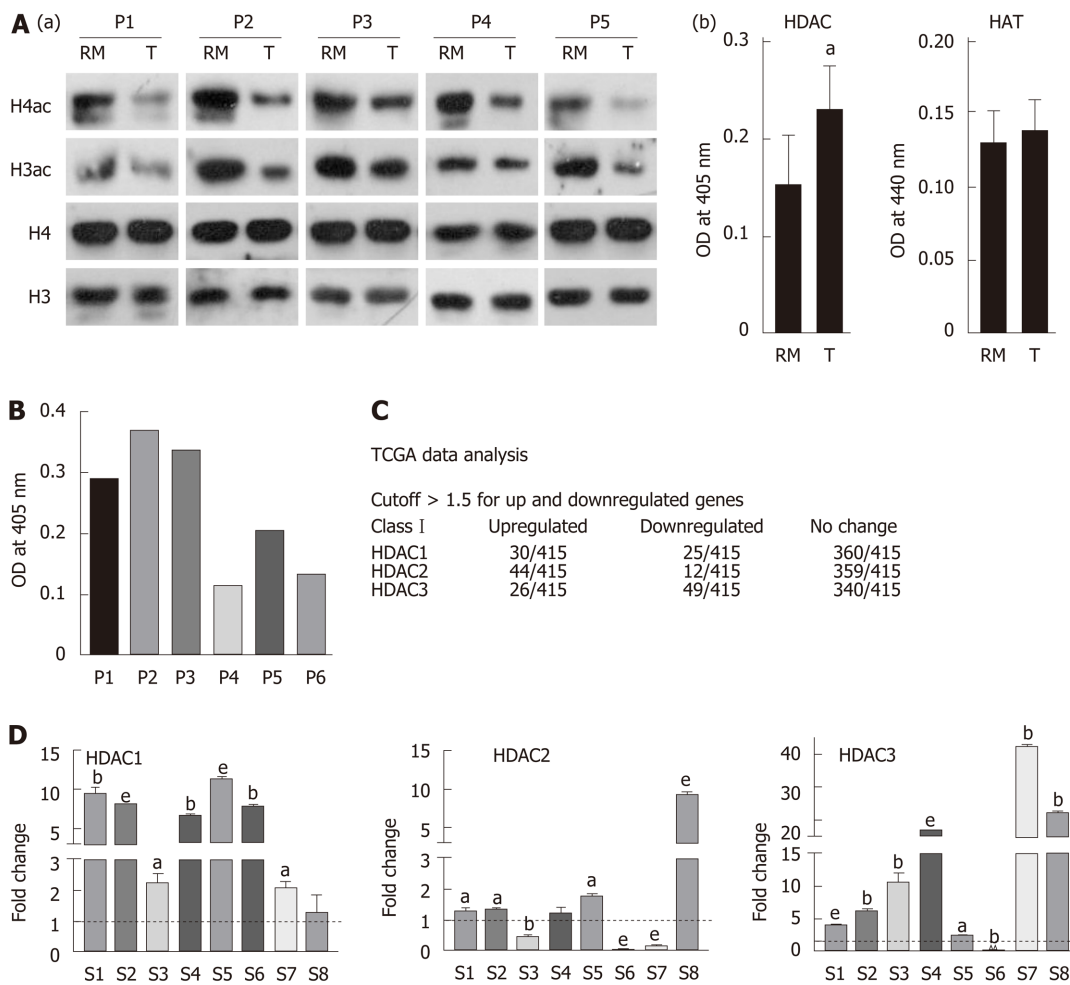


Figure 1 Hypo-acetylation in gastric cancer patient samples is associated with low histone deacetylase activity and transcripts. A: (a) Immunoblot analysis for the comparison of pan-acetyl levels of histone H3 and H4 between paired ($n = 5$) negative resection margins (RMs) and tumor (T) tissues, and (b) Nucleo-cytosolic fractions were used to compare histone deacetylase (HDAC) and histone acetyltransferase (HAT) levels in paired negative resection margins and tumor tissues using calorimetric assays; B: Differential HDAC activity amongst patients was studied calorimetrically; C: Analysis of The Cancer Genome Atlas data for class 1 HDAC transcript levels in gastric adenocarcinoma patients; D: Expression of Class I HDAC viz HDAC1, HDAC2 and HDAC3 in gastric cancer tumors compared to normal tissue (^a $P < 0.05$; ^b $P < 0.009$; ^e $P < 0.0009$). GC: Gastric cancer; HDAC: Histone deacetylase; HAT: Histone acetyltransferase; HDAC1: Histone deacetylase 1; HDAC2: Histone deacetylase 2; HDAC3: Histone deacetylase 3; RM: Resection margin; T: Tumor tissues.

treatments depend on regime

In order to assess which combination regimes of chemotherapeutic drugs and HDACi have a synergistic effect, median effect plot was generated using the combined doses of drugs and FA values. The data were quantitatively analyzed using CI at FA levels of 0.5, 0.75 and 0.95 (Figure 4 and Table 2). At an FA value of 0.5, concurrent and pre-combination regimes of VPA with cisplatin or oxaliplatin, pre-combination of TSA or SAHA with cisplatin, and pre-combination of TSA and epirubicin showed synergistic effects, whereas all other combination regimes showed antagonistic effects. In continuation, at an FA value of 0.75, pre-treatment and concurrent combination regimes of VPA or TSA with cisplatin or oxaliplatin showed synergistic effects; however, all other combinations showed additive or antagonistic effects. Further, at an FA level of 0.95, only pre-combination of VPA with cisplatin or oxaliplatin showed synergistic effects; however, all other combinations showed antagonistic effects. In conclusion, post-treatment with VPA, TSA or SAHA did not have any synergistic effect when combined with cisplatin, oxaliplatin or epirubicin. VPA was found to have a more synergistic effect in the pre-treatment combination regime with cisplatin and oxaliplatin.

VPA followed by cisplatin leads to induction of histone acetylation and chromatin re-organization, favoring higher drug binding that leads to cell death

The synergistic effect of the pre-treatment combination regime on DNA damage, histone acetylation and cell cycle was investigated following treatment of AGS cells with IC25 doses of VPA and cisplatin either alone or in combination. MNase assays

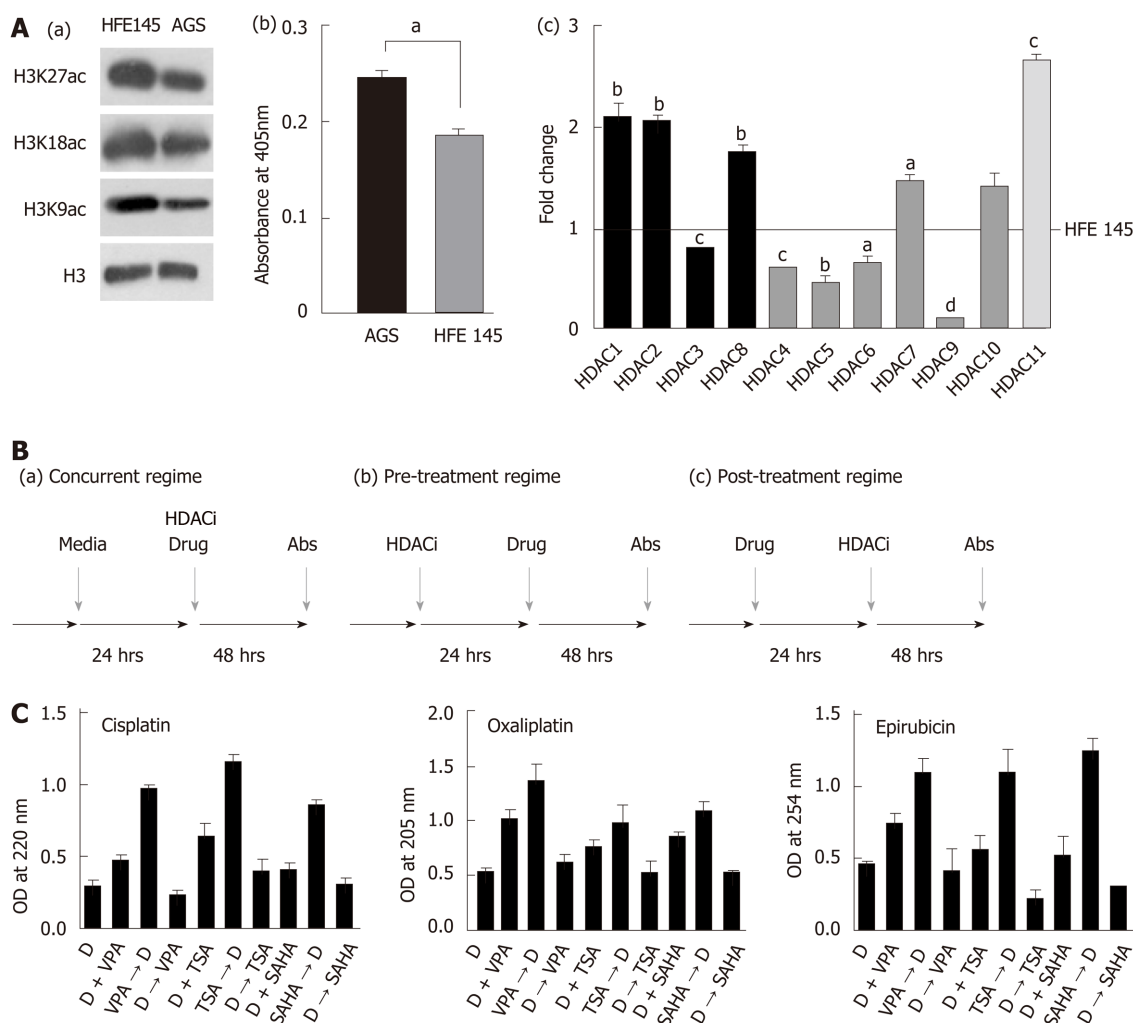


Figure 2 Pre-treatment regime with histone deacetylase inhibitor maximally enhances binding of chemotherapeutic drugs to chromatin. A: (a) Immunoblot analysis for the comparison of site-specific histone acetylation levels between gastric cancer (GC) cell lines, transformed AGS and untransformed HFE145; (b) Nucleo-cytosolic fractions were used to compare HDAC levels in GC cell lines using calorimetric assays; and (c) Real time PCR data of Class I to Class IV HDAC levels in the AGS cell line compared to HFE145 (^a $P < 0.05$; ^b $P < 0.009$; ^c $P < 0.0009$; ^d $P < 0.0001$); B: Schematic representation of three different combination regimes: (a) concurrent [histone deacetylase inhibitor (HDACi) + Drug], (b) pre- (HDACi Drug) and (c) post- (Drug HDACi); C: AGS cells were treated with chemotherapeutic drugs and HDACi at their inhibitory concentration (IC)50 concentration for 24 h in three different combinations as mentioned above. Experiment was performed in triplicate, absorbance was taken, normalized with blank, and mean absorbance was incorporated into a bar graph. HDACi: Histone deacetylase inhibitor; HDAC: Histone deacetylase; Drug: Chemotherapy drugs; VPA: Valproic acid; SAHA: Suberoylanilide hydroxamic acid; TSA: Trichostatin A; IC: Inhibitory concentration.

after VPA treatment suggested an increased intensity of mono- and di-nucleosomes, with a decrease in high molecular weight DNA, indicating chromatin relaxation in VPA-treated cells compared to control (Figure 5A). In coherence, levels of H3Kac and H4K16ac increase after VPA treatment (Figure 5B). H4K16ac is reported to prevent higher order chromatin organization, and therefore its increase indicated open chromatin^[24]. The increased acetylation and relaxation of chromatin further correlated with an increased level of γ H2AX after combinatorial treatment compared to VPA and cisplatin alone (Figure 5B). Interestingly, H4K16ac decreased after cisplatin treatment alone, indicating the compaction of chromatin. This was likely an outcome of G2/M arrest post-cisplatin treatment, which may lead to poor drug binding to chromatin. VPA treatment, on the other hand, arrests the cells in G1 phase, leading to an open chromatin conformation to enhance drug binding (Figure 5C).

Gatekeeper tumor suppressor genes are known to be repressed in GC by an HDAC-mediated mechanism^[25,26]. Levels of tumor suppressors were assessed after IC25 and IC50 treatment of VPA for 24 h. A two-fold increase in p16, p21 and p27 was observed, suggesting the involvement of tumor suppressor-mediated cell cycle arrest, and the observed effects of cell death (Figure 5D). Taken together, results indicate that the pre-treatment regime of VPA opens chromatin, increases the expression of tumor suppressor genes, and enhances cisplatin binding to chromatin, ultimately leading to more cell death.

Table 2 Regime-specific synergistic, additive or antagonistic effects of chemotherapeutic drugs and histone deacetylase inhibitors

Drugs	Treatment sequence and result of FA and median effect plot analysis		FA		
			0.5	0.75	0.95
Cisplatin and VPA	Pre	Dose of Cis, VPA ($\mu\text{mol/L}$)	0.965, 386.359	2.711, 1084.65	15.361, 6144.61
		CI	0.352	0.471	0.784
	Concurrent	Dose of Cis, VPA ($\mu\text{mol/L}$)	0.705, 282.387	3.874, 1549.74	67.690, 27076.0
		CI	0.257	0.673	3.454
	Post	Dose of Cis, VPA ($\mu\text{mol/L}$)	3.254, 1301.90	9.362, 3745.16	55.260, 22104.1
		CI	1.188	1.627	2.820
Oxaliplatin and VPA	Pre	Dose of Oxa, VPA ($\mu\text{mol/L}$)	0.788, 394.469	2.094, 1047.04	10.796, 5398.39
		CI	0.404	0.453	0.552
	Concurrent	Dose of Oxa, VPA ($\mu\text{mol/L}$)	1.533, 766.633	4.305, 2152.92	24.406, 12203.2
		CI	0.786	0.933	1.249
	Post	Dose of Oxa, VPA ($\mu\text{mol/L}$)	2.362, 1181.47	8.451, 4225.64	71.917, 35958.6
		CI	1.211	1.83182	3.68265
Epirubicin and TSA	Pre	Combined dose (μg)	0.030, 0.300	0.093, 0.931	0.623, 6.231
		CI	0.645	0.727	1.222
	Concurrent	Combined dose (μg)	0.129, 1.299	0.410, 4.105	2.835, 28.356
		CI	2.789	3.207	5.563
	Post	Combined dose (μg)	0.137, 1.375	0.301, 3.010	1.122, 11.220
		CI	2.952	2.351	2.201

FA: Fraction affected; Pre: Pre-treatment; Post: Post-treatment; TSA: Trichostatin A; Cis: Cisplatin; VPA: Valproic acid; Oxa: Oxaliplatin; CI: Combination index. Dose at Fa-0.5 for VPA- 1827.79, TSA-1.50, Cisplatin-6.84, Oxaliplatin-4.18 and Epirubicin- 0.07; Dose at Fa-0.75 for VPA- 4165.97, TSA-2.61, Cisplatin-12.85, Oxaliplatin-10.33 and Epirubicin- 0.25; Dose at Fa 0.95 for VPA- 16628.5, TSA-6.56, Cisplatin-37.06, Oxaliplatin-47.30, and Epirubicin- 2.29.

Monitoring of tumor growth and drug efficacy in GC xenografts

The pre-treatment regime of HDACi, VPA alone or combined with cisplatin was further explored *in vivo* with a xenograft tumor model using AGS cells (Figure 6A and B). After 3 wk of treatment, a change in tumor volume was observed in VPA, cisplatin, and VPA followed by cisplatin-treated groups. *In vivo*, cisplatin and VPA alone showed a similar decrease in tumor volume, however a 3X decrease in tumor volume was observed in the combinatorial treatment group at the end of 5 wk (Figure 6C). Thus, the pre-treatment regime showed a synergistic anticancer effect in the xenograft tumor model. Drug toxicity, as assessed by a decrease in weight, was minimal, with a 15% weight loss in the combination group, indicating better drug tolerance (Figure 6D). Histopathological examination of different tumor tissues showed decreased levels of viable cells (20%-55%) in the case of the combinatorial treatment group compared to the control group (70%-90%). Interestingly, infiltration of inflammatory cells was also observed in the combination group. Also, a greater number of mitotic cells was observed in cisplatin alone and the combinatorial group. Moreover, pleomorphic, hyperchromatic nuclei were observed in the combinatorial-treated group compared to control, suggesting chromatin-associated alterations after drug treatments (Figure 6E). The preclinical study warrants use of the pre-treatment regime in clinical trials for better HDACi therapy success in solid tumors.

DISCUSSION

Histone acetylation has a significant effect in modulating chromatin architecture and transcription^[8]. Thus, acetylation marks and their modifiers have been studied in cancer for their diagnostic, prognostic and therapeutic potential^[9]. The clinical application of HDACi has been disappointing in solid tumors, and the major factor for failure in diverse clinical trials is the concurrent treatment regime, limited combination chemotherapeutic studies, and no patient stratification.

Our data suggest that sensitizing GC cells or *in vivo* xenografts containing increased levels of Class 1 HDACs with pre-HDACi treatment results in histone hyperacetylation and relaxed chromatin organization. Increased accessibility of chromatin to DNA-interacting drugs induces DNA damage and cell death. Increases in cell death upon combination of two or more drugs do not form the basis of pre-clinical or

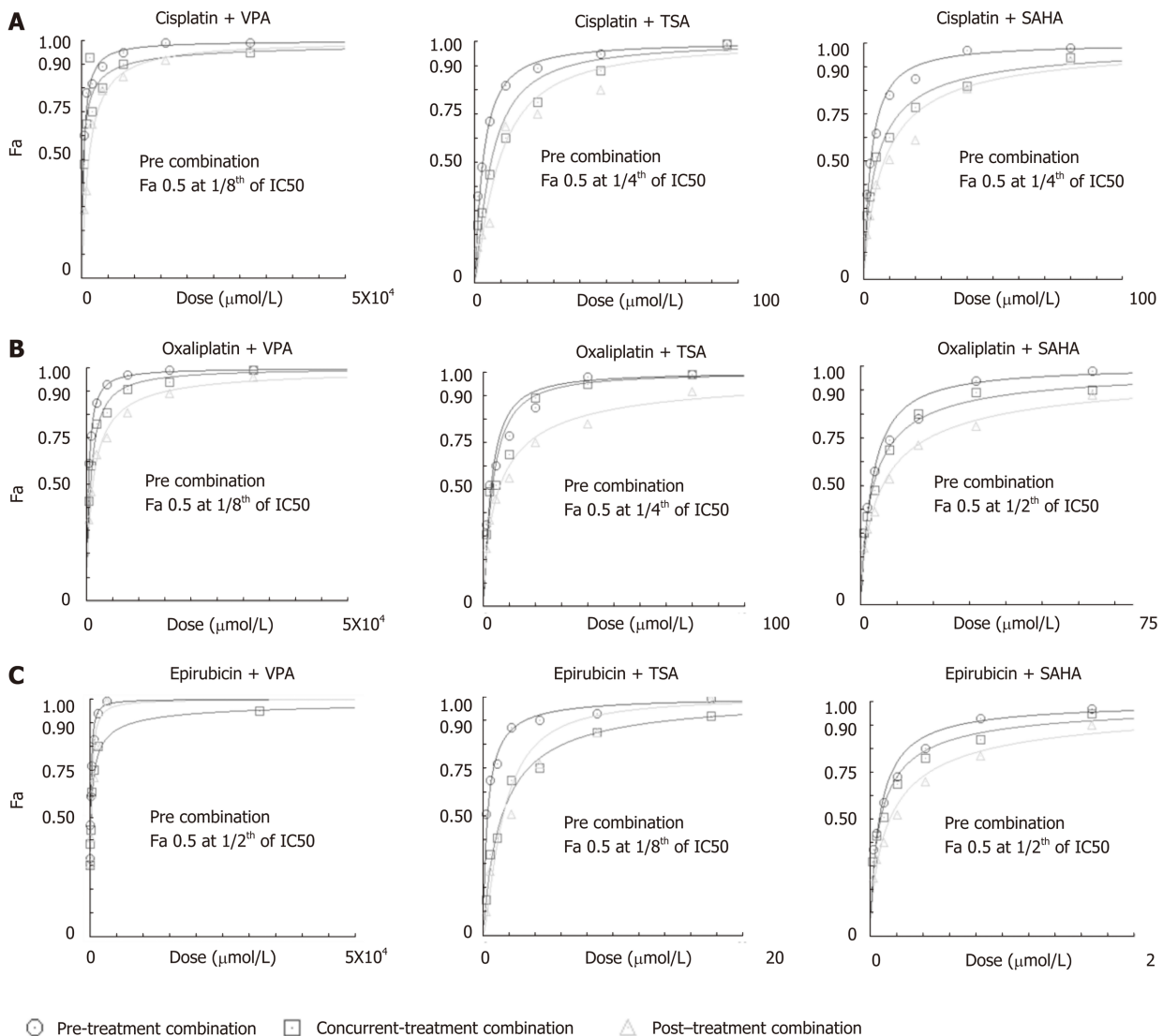


Figure 3 Histone deacetylase inhibitor-dependent sensitization of gastric cancer cells decreases the dose of chemotherapeutic drugs to attain maximum efficacy. AGS cells were treated with chemotherapeutic drugs (cisplatin, oxaliplatin and epirubicin) and histone deacetylase (HDAC) inhibitors [valproic acid (VPA), trichostatin A (TSA) and suberoylanilide hydroxamic acid (SAHA)] for 24 h each in three different combinations: (i) concurrent (HDACi + Drug), (ii) pre- (HDACi Drug) and (iii) post- (Drug HDACi) at the combined dose (as mentioned in Supplementary Table 1), and : 3-(4,5-Dimethylthiazol-2-yl)-2,5-diphenyltetrazolium bromide (MTT) assays were performed. Fraction-affected dose response curve of A: Cisplatin; B: Oxaliplatin; and C: Epirubicin in different combinations with VPA, TSA or SAHA. TSA: Trichostatin A; VPA: Valproic acid; SAHA: Suberoylanilide hydroxamic acid.

clinical studies until the combination shows synergistic effects. All pre-treatment combinations of HDACi and chemotherapeutic drugs showed higher percentages of cell death at low combined doses; however, only VPA with oxaliplatin or cisplatin was found to be best, due to their synergistic effects across FA values from 0.5 to 0.95. Thus, in pre-clinical and clinical settings, the pre-treatment approach with HDACi would allow for a low dosage of chemotherapeutic drugs with similar dose-related cell toxicities. Earlier, Mutze *et al*^[27] showed the importance of HDACi-SAHA pre-treatment to sensitize GC cell lines. The synergistic effect was further recapitulated in a pre-clinical *in vivo* model, wherein a decrease in tumor volume was observed in the pre-treatment group with low toxicity compared to the cisplatin only and VPA groups. Body weight in the VPA-treated group was not altered compared to the VPA/cisplatin-treated group. This suggests that VPA alone as a sensitizer has no appreciable side effects in the pre-clinical study. Earlier studies have shown that thioredoxin (Trx) levels play an important role in determining HDACi-induced cell death in cancer cells^[28]. Normal cells have relatively higher levels of Trx, and therefore could account, in part, for the low toxicity observed in the pre-clinical protocol. Moreover, the cells are arrested in the G1 phase as opposed to the G2/M phase in the case of cisplatin treatment; the G1 phase with more open chromatin thus favors enhanced cisplatin binding and more cell death as suggested by increased γ H2AX

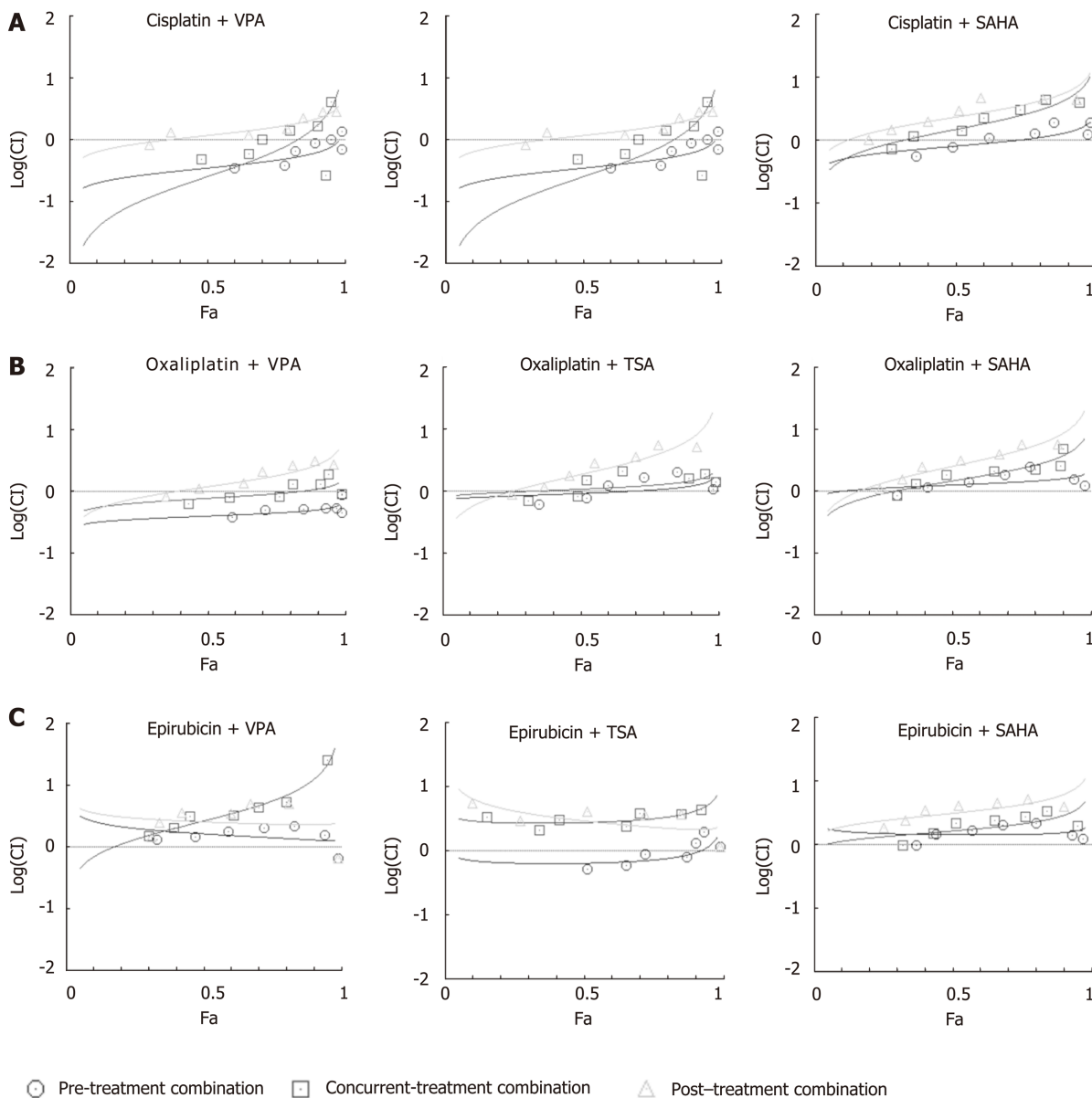


Figure 4 Median effect plot analysis for drug combinations (chemotherapeutic drugs and histone deacetylase inhibitors) as synergistic, additive or antagonistic. AGS cells were treated with chemotherapeutic drugs (cisplatin, oxaliplatin and epirubicin) and histone deacetylase inhibitors (HDACi) [valproic acid (VPA), trichostatin A (TSA) and suberoylanilide hydroxamic acid (SAHA)] for 24 h each in three different combinations - concurrent (HDACi + Drug), pre- (HDACi Drug) and post- (Drug HDACi) at the combined dose (as mentioned in [Supplementary Table 1](#)), and 3-(4,5-Dimethylthiazol-2-yl)-2,5-diphenyltetrazolium bromide assays were performed. Median effect plot shows the combination index (CI) on the Y-axis and fraction-affected values on the X-axis; A: Cisplatin; B: Oxaliplatin; and C: Epirubicin in different combinations with VPA (left panel), TSA (middle panel) and SAHA (right panel). For a particular fraction affected value, the combination index values range from 0 to 1; $CI < 0.8$, $CI = 0.8-1.2$, and $CI > 1.2$ represents the synergistic, additive or antagonistic nature of drug combinations, respectively. GC: Gastric cancer; HDACi: Histone deacetylase inhibitor; HDAC: Histone deacetylase; Drug: Chemotherapy drugs; VPA: Valproic acid; SAHA: Suberanilohydroxamic acid; TSA: Trichostatin A; MTT: 3-(4,5-Dimethylthiazol-2-yl)-2,5-diphenyltetrazolium bromide; CI: Combination index.

levels. A recent phase II study in GC with vorinostat as a first-line therapy with capecitabine and cisplatin did not meet its expected outcome^[29]. In this study, vorinostat was administered concurrent with chemotherapeutic drugs, suggesting vorinostat had insufficient time to enforce a chromatin modulatory effect, leading to weak drug binding. The prerequisite for changing chromatin organization by HDACi in the case of multiple solid tumors is strengthened by phase I clinical trials with VPA and the topoisomerase II inhibitor epirubicin^[30]. In this study, a 48 h pre-exposure of VPA was found to be essential to obtain synergistic outcomes with epirubicin. The pre-treatment combinatorial chemotherapy approach could achieve a positive outcome with acceptable toxicities in heavily treated and previously anthracycline-resistant tumors.

Decades of research involving HDACi and chemotherapeutic drugs have failed to take into account the HDAC levels or activity status of patients, resulting in inappropriate HDACi dose administration. The Neck-V-CHANCE trial will be the

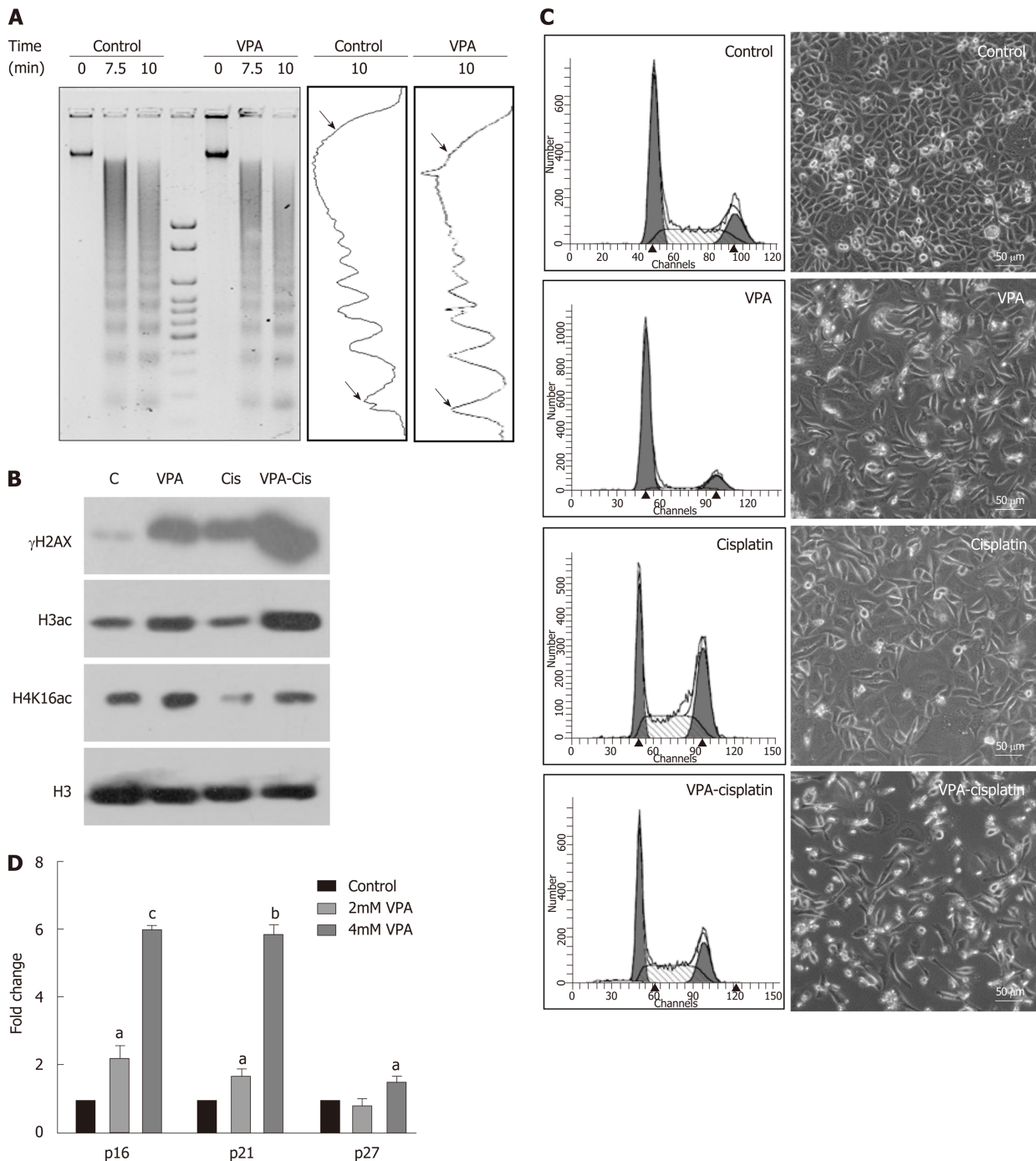


Figure 5 Pretreatment regime is associated with chromatin relaxation, enhanced DNA damage and re-expression of tumor suppressors. **A:** Chromatin organization in the AGS cell line by micrococcal nuclease (MNase) assays with time-dependent kinetics was studied following 24 h treatment with valproic acid (VPA) (2 mmol/L). AGS cells were treated with an inhibitory concentration (IC)25 concentration of cisplatin and VPA alone or in combination for 24 h, and the following parameters were analyzed: **B:** Histone post-translational modifications; **C:** Cell cycle profile and morphology; and **D:** Effect of VPA on re-expression of tumor suppressors was studied by treating AGS cells with the IC25 and IC50 concentrations of VPA for 24 h, followed by real time PCR for the *p16*, *p21* and *p27* genes (^a $P < 0.02$; ^b $P < 0.0009$; ^c $P < 0.0001$). MNase: Micrococcal nuclease; HDACi: Histone deacetylase inhibitor; PTMs: Post-translational modifications; VPA: Valproic acid; IC: Inhibitory concentration; PCR: Polymerase chain reaction.

first clinical trial to test the efficacy of HDACi pre-treatment. In this ongoing head and neck cancer trial, valproic acid will be administered 2 wk prior to the administration of cisplatin and cetuximab. However, this trial also does not stratify patients based on HDAC levels^[31]. Our HDAC activity correlative data linking HDAC expression with histone acetylation, and the presence of heterogeneous HDAC activity and transcript levels in patients, provides sufficient evidence for categorizing the patients for HDACi therapy. Weichert *et al*^[32] showed that approximately 71% (209/293) of GC patients are positive for the expression of either all three or one of the three class 1 HDAC isoforms. Also, Mutze *et al*^[27] highlights that high expression of HDAC1/2 in

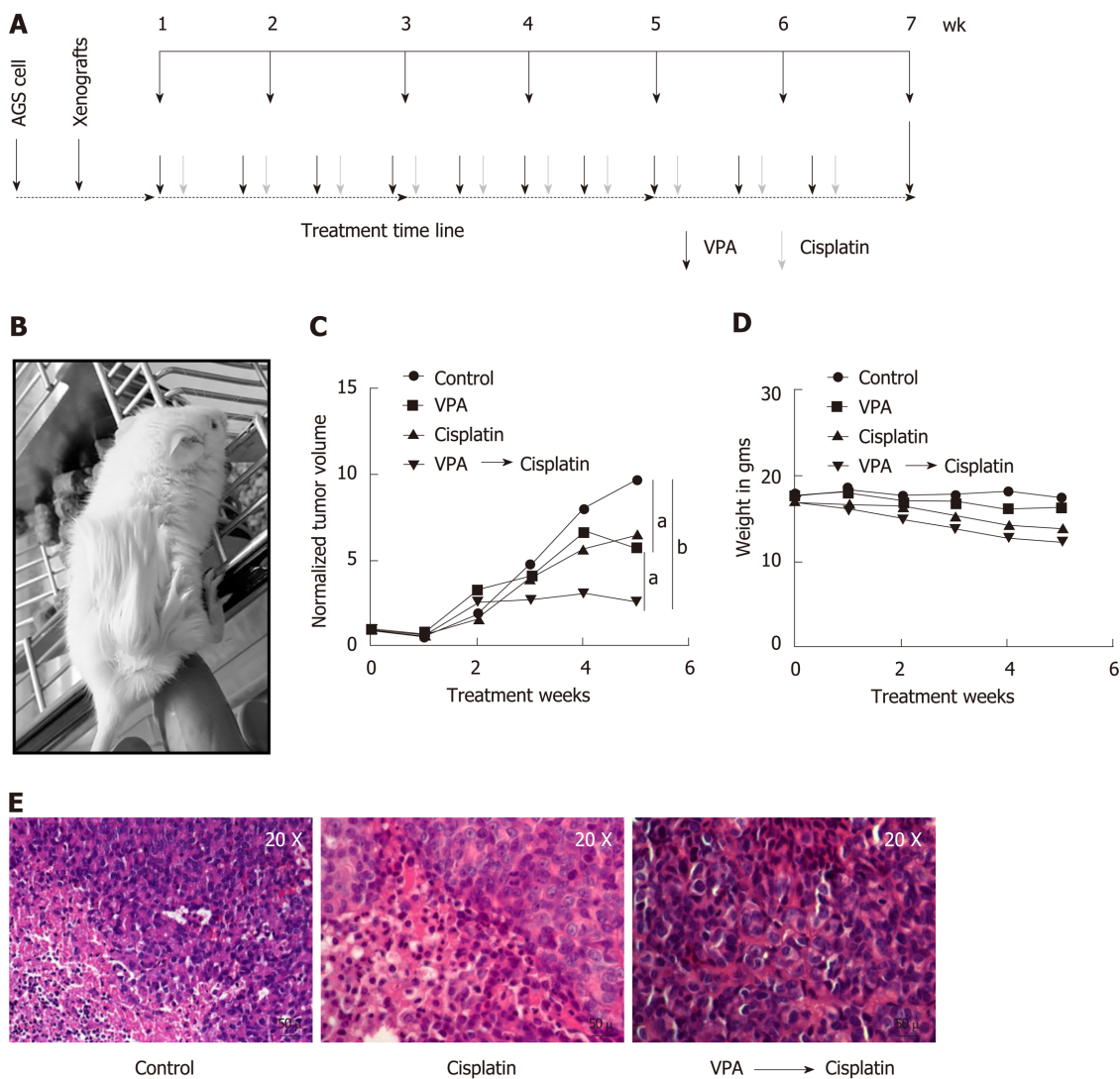


Figure 6 Valproic sensitizes AGS cell xenografts to cisplatin in an *in vivo* mice model. **A:** Schematic diagram depicting timeline of *in vivo* drug administration. AGS cells were injected into NOD-SCID mice. After tumors reached approximately 100 mm³; **B:** Mice were divided into four groups ($n = 3$), (1) control, (2) valproic acid (300 mg/kg/d), (3) cisplatin (2 mg/kg/d), and (4) combinatorial treatment of valproic acid followed by cisplatin at the same dose mentioned above; **C:** Average tumor volumes of groups normalized to the initial tumor volumes (before treatment) are plotted over a period of 5 wk of drug treatment. The outcome of the different treatment regimens was statistically validated by performing unpaired *t*-tests (^a $P < 0.05$; ^b $P < 0.005$); **D:** Mean weight of animals in a group measured over the treatment period to assess toxicity; **E:** Histopathology of tumor sections by hematoxylin and eosin staining of different groups following 5 wk of treatment. VPA: Valproic acid.

GC does not relate to response and overall survival. The latest publication by Jiang *et al*^[33] showed an association between high HDAC1 (60% patients) with larger tumor size, tumor grade, lymph node metastasis and lymphovascular invasion, making it an independent prognostic factor for GC. Our *in silico* TCGA data analysis suggests that 24% of GC patients have higher expression levels of class 1 HDACs. This explains the need for prior assessment of class 1 HDAC levels HDACi therapy patient stratification. This will also assist in defining the dose of HDACi in pre-treatment regimes with DNA-interacting chemotherapeutic drugs for better therapeutic potential.

In conclusion, our results establish a strong rationale for exploring pre-treatment regimes in stratified patients groups with HDACi in clinical trials. The proposed mechanism is through the attainment of open chromatin architecture, and the accumulation of activating histone marks for enhanced binding of DNA-interacting chemotherapeutic drugs (graphical abstract, **Figure 7**). This worthwhile strategy may become more successful in overcoming the limitations of epi-drugs in solid tumor treatment, and may increase therapeutic outcomes with minimal chemotherapeutic toxicity in the clinic.

Graphical abstract

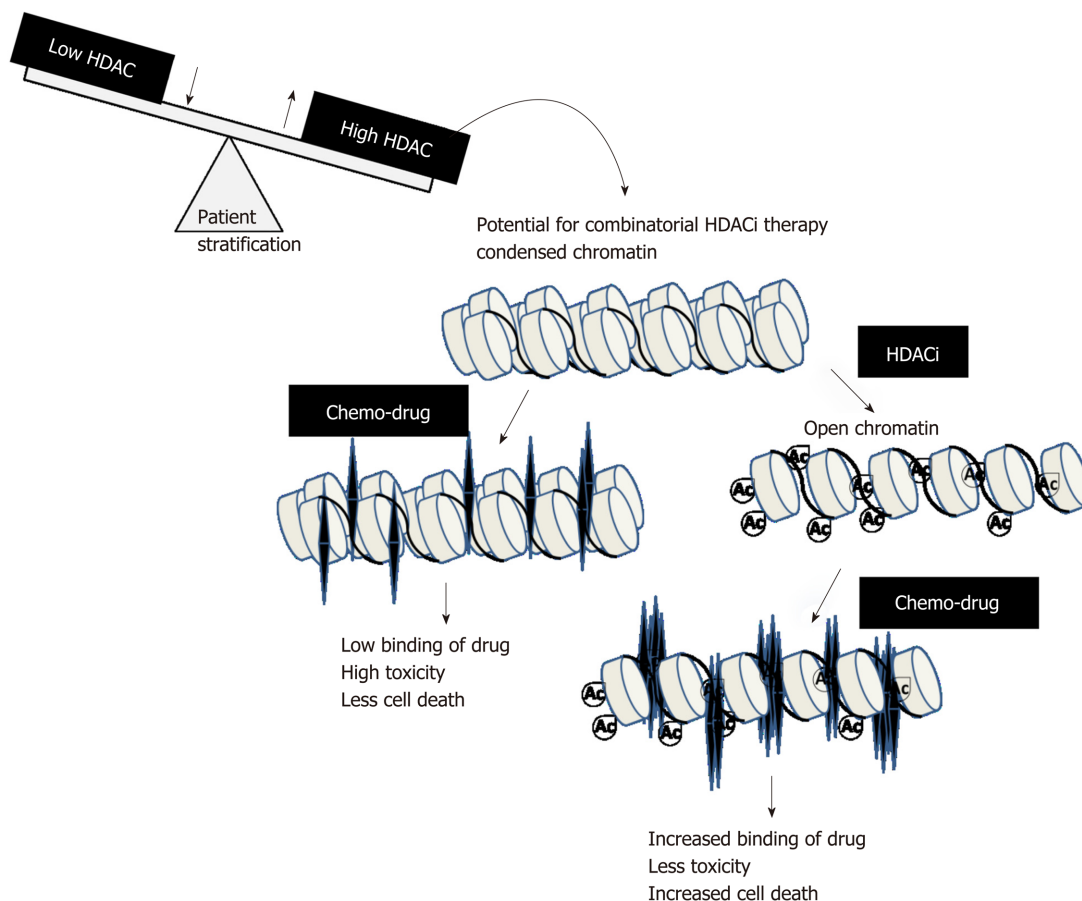


Figure 7 Graphical abstract: Model depicting stratification of patients with high histone deacetylase activity/levels of histone deacetylase inhibitor therapy. A prior treatment of histone deacetylase inhibitors would relax the condensed chromatin of a stratified patient group, making it more accessible and increasing its interaction with chemotherapeutic drugs compared to only first-line chemo treatment. This would enhance the number of cells killed at lower drug concentrations with a decrease in side-effects and toxicity. HDAC: Histone deacetylase; HAT: Histone acetyl transferase.

ARTICLE HIGHLIGHTS

Research background

Alterations of the epigenome play an important role during the process of gastric carcinogenesis. Therefore, drugs like histone deacetylase inhibitors (HDACi) are being explored for their anti-tumor activity.

Research motivation

Identify alterations in the epigenetic milieu of gastric cancer, and check whether the concomitant usage of HDACi with chemotherapeutic drugs increases the drug's efficacy.

Research objectives

This study aimed to reveal the most optimal combination of chemotherapeutic drugs, as well as HDACi type, dose and regime (pre, post and concurrent). The biochemical mechanism of action was investigated, and the combination was tested in an *in vivo* system.

Research methods

This study utilized paired gastric cancer human samples, along with the gastric adenocarcinoma cell line AGS and immortalized normal counterpart HFE145. The efficacy of several chemotherapeutic agents and HDACi was tested in the AGS cell line, and the final combination was tested in an animal model of gastric cancer.

Research results

Gastric cancer patients showed differential HDAC activity and levels. Furthermore, pretreatment of valproic acid followed by cisplatin favors an open chromatin conformation *via* increased histone acetylation. These changes increase the binding of cisplatin to DNA at lower concentrations. *In vivo* studies suggest a better response with pretreatment regimes that do not cause toxicity.

Research conclusions

This study described that decreased histone acetylation in human gastric cancer tumor samples may be attributed to differential/elevated histone deacetylase activity and expression. Additionally, pre-treatment with HDACi was the most optimal regime that maximally enhanced the cell killing potential of chemotherapeutic drugs. This was achieved by increased intercalation of the drug in chromatin post-HDACi treatment. The pre-treatment of HDACi valproic acid and cisplatin was able to decrease tumor volume *in vivo* compared to cisplatin alone.

Research perspectives

This pre-clinical study provides evidence that pre-treatment of HDACi followed by standard chemotherapeutic agents enhances the effectiveness of the drug. Hence, clinical testing of such combinations may be explored for better management of gastric cancer.

ACKNOWLEDGEMENTS

The authors are thankful to departments of Flow Cytometry and Mr. Mahesh Pawar, Laboratory Animal Facility, ACTREC, Ms. Kanchan Hariramani and Mr. Narendra Varma, trainees at Gupta laboratory for their assistance during experimental work. The authors are also thankful to members of Gupta laboratory for critical reading of the manuscript.

REFERENCES

- 1 **Bray F**, Ferlay J, Soerjomataram I, Siegel RL, Torre LA, Jemal A. Global cancer statistics 2018: GLOBOCAN estimates of incidence and mortality worldwide for 36 cancers in 185 countries. *CA Cancer J Clin* 2018; **68**: 394-424 [PMID: 30207593 DOI: 10.3322/caac.21492]
- 2 **Denny WA**. DNA-intercalating ligands as anti-cancer drugs: prospects for future design. *Anticancer Drug Des* 1989; **4**: 241-263 [PMID: 2695099]
- 3 **Martínez R**, Chacón-García L. The search of DNA-intercalators as antitumoral drugs: what it worked and what did not work. *Curr Med Chem* 2005; **12**: 127-151 [PMID: 15638732 DOI: 10.2174/0929867053363414]
- 4 **Catalano MG**, Fortunati N, Pugliese M, Poli R, Bosco O, Mastrocola R, Aragno M, Boccuzzi G. Valproic acid, a histone deacetylase inhibitor, enhances sensitivity to doxorubicin in anaplastic thyroid cancer cells. *J Endocrinol* 2006; **191**: 465-472 [PMID: 17088416 DOI: 10.1677/joe.1.06970]
- 5 **Niitsu N**, Kasukabe T, Yokoyama A, Okabe-Kado J, Yamamoto-Yamaguchi Y, Umeda M, Honma Y. Anticancer derivative of butyric acid (Pivalyloxymethyl butyrate) specifically potentiates the cytotoxicity of doxorubicin and daunorubicin through the suppression of microsomal glycosidic activity. *Mol Pharmacol* 2000; **58**: 27-36 [PMID: 10860924 DOI: 10.1124/mol.58.1.27]
- 6 **Wittenburg LA**, Bisson L, Rose BJ, Korch C, Thamm DH. The histone deacetylase inhibitor valproic acid sensitizes human and canine osteosarcoma to doxorubicin. *Cancer Chemother Pharmacol* 2011; **67**: 83-92 [PMID: 20306194 DOI: 10.1007/s00280-010-1287-z]
- 7 **Bannister AJ**, Kouzarides T. Regulation of chromatin by histone modifications. *Cell Res* 2011; **21**: 381-395 [PMID: 21321607 DOI: 10.1038/cr.2011.22]
- 8 **Yang XJ**, Seto E. HATs and HDACs: from structure, function and regulation to novel strategies for therapy and prevention. *Oncogene* 2007; **26**: 5310-5318 [PMID: 17694074 DOI: 10.1038/sj.onc.1210599]
- 9 **Füllgrabe J**, Kavanagh E, Joseph B. Histone onco-modifications. *Oncogene* 2011; **30**: 3391-3403 [PMID: 21516126 DOI: 10.1038/onc.2011.121]
- 10 **Dhanak D**, Jackson P. Development and classes of epigenetic drugs for cancer. *Biochem Biophys Res Commun* 2014; **455**: 58-69 [PMID: 25016182 DOI: 10.1016/j.bbrc.2014.07.006]
- 11 **Chen JH**, Zheng YL, Xu CQ, Gu LZ, Ding ZL, Qin L, Wang Y, Fu R, Wan YF, Hu CP. Valproic acid (VPA) enhances cisplatin sensitivity of non-small cell lung cancer cells via HDAC2 mediated down regulation of ABCA1. *Biol Chem* 2017; **398**: 785-792 [PMID: 28002023 DOI: 10.1515/hsz-2016-0307]
- 12 **Terranova-Barberio M**, Roca MS, Zotti AI, Leone A, Bruzzese F, Vitagliano C, Scogliamiglio G, Russo D, D'Angelo G, Franco R, Budillon A, Di Gennaro E. Valproic acid potentiates the anticancer activity of capecitabine in vitro and in vivo in breast cancer models via induction of thymidine phosphorylase expression. *Oncotarget* 2016; **7**: 7715-7731 [PMID: 26735339 DOI: 10.18632/oncotarget.6802]
- 13 **Marchion DC**, Bicaku E, Daud AI, Sullivan DM, Munster PN. Valproic acid alters chromatin structure by regulation of chromatin modulation proteins. *Cancer Res* 2005; **65**: 3815-3822 [PMID: 15867379 DOI: 10.1158/0008-5472.CAN-04-2478]
- 14 **Oronsky B**, Oronsky N, Scicinski J, Fanger G, Lybeck M, Reid T. Rewriting the epigenetic code for tumor resensitization: a review. *Transl Oncol* 2014; **7**: 626-631 [PMID: 25389457 DOI: 10.1016/j.tranon.2014.08.003]
- 15 **Ahuja N**, Easwaran H, Baylin SB. Harnessing the potential of epigenetic therapy to target solid tumors. *J Clin Invest* 2014; **124**: 56-63 [PMID: 24382390 DOI: 10.1172/JCI69736]
- 16 **Marchion DC**, Bicaku E, Daud AI, Richon V, Sullivan DM, Munster PN. Sequence-specific potentiation of topoisomerase II inhibitors by the histone deacetylase inhibitor suberoylanilide hydroxamic acid. *J Cell Biochem* 2004; **92**: 223-237 [PMID: 15108350 DOI: 10.1002/jcb.20045]
- 17 **Khan SA**, Amnekar R, Khade B, Barreto SG, Ramadwar M, Shrikhande SV, Gupta S. p38-MAPK/MSK1-mediated overexpression of histone H3 serine 10 phosphorylation defines distance-dependent prognostic value of negative resection margin in gastric cancer. *Clin Epigenetics* 2016; **8**: 88 [PMID: 27588146 DOI: 10.1186/s13148-016-0255-9]
- 18 **Alexander S**, Swatson WS, Alexander H. Pharmacogenetics of resistance to Cisplatin and other anticancer drugs and the role of sphingolipid metabolism. *Methods Mol Biol* 2013; **983**: 185-204 [PMID: 23494308 DOI: 10.1007/978-1-62703-302-2_10]

- 19 **Chou TC.** Drug combination studies and their synergy quantification using the Chou-Talalay method. *Cancer Res* 2010; **70**: 440-446 [PMID: 20068163 DOI: 10.1158/0008-5472.CAN-09-1947]
- 20 **Sharma AK,** Bhattacharya S, Khan SA, Khade B, Gupta S. Dynamic alteration in H3 serine 10 phosphorylation is G1-phase specific during ionization radiation induced DNA damage response in human cells. *Mutat Res* 2015; **773**: 83-91 [PMID: 25847424 DOI: 10.1016/j.mrfmmm.2015.01.017]
- 21 **Cerami E,** Gao J, Dogrusoz U, Gross BE, Sumer SO, Aksoy BA, Jacobsen A, Byrne CJ, Heuer ML, Larsson E, Antipin Y, Reva B, Goldberg AP, Sander C, Schultz N. The cBio cancer genomics portal: an open platform for exploring multidimensional cancer genomics data. *Cancer Discov* 2012; **2**: 401-404 [PMID: 22588877 DOI: 10.1158/2159-8290.CD-12-0095]
- 22 **Gao J,** Aksoy BA, Dogrusoz U, Dresdner G, Gross B, Sumer SO, Sun Y, Jacobsen A, Sinha R, Larsson E, Cerami E, Sander C, Schultz N. Integrative analysis of complex cancer genomics and clinical profiles using the cBioPortal. *Sci Signal* 2013; **6**: p11 [PMID: 23550210 DOI: 10.1126/scisignal.2004088]
- 23 **Chou TC,** Talalay P. Quantitative analysis of dose-effect relationships: the combined effects of multiple drugs or enzyme inhibitors. *Adv Enzyme Regul* 1984; **22**: 27-55 [PMID: 6382953 DOI: 10.1016/0065-2571(84)90007-4]
- 24 **Shogren-Knaak M,** Ishii H, Sun JM, Pazin MJ, Davie JR, Peterson CL. Histone H4-K16 acetylation controls chromatin structure and protein interactions. *Science* 2006; **311**: 844-847 [PMID: 16469925 DOI: 10.1126/science.1124000]
- 25 **Richon VM,** Sandhoff TW, Rifkind RA, Marks PA. Histone deacetylase inhibitor selectively induces p21WAF1 expression and gene-associated histone acetylation. *Proc Natl Acad Sci USA* 2000; **97**: 10014-10019 [PMID: 10954755 DOI: 10.1073/pnas.180316197]
- 26 **Herold C,** Ganslmayer M, Ocker M, Hermann M, Geerts A, Hahn EG, Schuppan D. The histone-deacetylase inhibitor Trichostatin A blocks proliferation and triggers apoptotic programs in hepatoma cells. *J Hepatol* 2002; **36**: 233-240 [PMID: 11830335 DOI: 10.1016/S0168-8278(01)00257-4]
- 27 **Mutze K,** Langer R, Becker K, Ott K, Novotny A, Luber B, Hapfelmeier A, Göttlicher M, Höfler H, Keller G. Histone deacetylase (HDAC) 1 and 2 expression and chemotherapy in gastric cancer. *Ann Surg Oncol* 2010; **17**: 3336-3343 [PMID: 20585871 DOI: 10.1245/s10434-010-1182-1]
- 28 **Ungerstedt JS,** Sowa Y, Xu WS, Shao Y, Dokmanovic M, Perez G, Ngo L, Holmgren A, Jiang X, Marks PA. Role of thioredoxin in the response of normal and transformed cells to histone deacetylase inhibitors. *Proc Natl Acad Sci USA* 2005; **102**: 673-678 [PMID: 15637150 DOI: 10.1073/pnas.0408732102]
- 29 **Yoo C,** Ryu MH, Na YS, Ryoo BY, Lee CW, Kang YK. Vorinostat in combination with capecitabine plus cisplatin as a first-line chemotherapy for patients with metastatic or unresectable gastric cancer: phase II study and biomarker analysis. *Br J Cancer* 2016; **114**: 1185-1190 [PMID: 27172248 DOI: 10.1038/bjc.2016.125]
- 30 **Münster P,** Marchion D, Bicaku E, Schmitt M, Lee JH, DeConti R, Simon G, Fishman M, Minton S, Garrett C, Chiappori A, Lush R, Sullivan D, Daud A. Phase I trial of histone deacetylase inhibition by valproic acid followed by the topoisomerase II inhibitor epirubicin in advanced solid tumors: a clinical and translational study. *J Clin Oncol* 2007; **25**: 1979-1985 [PMID: 17513804 DOI: 10.1200/JCO.2006.08.6165]
- 31 **Caponigro F,** Di Gennaro E, Ionna F, Longo F, Aversa C, Pavone E, Maglione MG, Di Marzo M, Muto P, Cavalcanti E, Petrillo A, Sandomenico F, Maiolino P, D'Aniello R, Botti G, De Cecio R, Losito NS, Scala S, Trotta A, Zotti AI, Bruzzese F, Daponte A, Calogero E, Montano M, Pontone M, De Feo G, Perri F, Budillon A. Phase II clinical study of valproic acid plus cisplatin and cetuximab in recurrent and/or metastatic squamous cell carcinoma of Head and Neck-V-CHANCE trial. *BMC Cancer* 2016; **16**: 918 [PMID: 27884140 DOI: 10.1186/s12885-016-2957-y]
- 32 **Weichert W,** Röske A, Gekeler V, Beckers T, Ebert MP, Pross M, Dietel M, Denkert C, Röcken C. Association of patterns of class I histone deacetylase expression with patient prognosis in gastric cancer: a retrospective analysis. *Lancet Oncol* 2008; **9**: 139-148 [PMID: 18207460 DOI: 10.1016/S1470-2045(08)70004-4]
- 33 **Jiang Z,** Yang H, Zhang X, Wang Z, Rong R, Wang X. Histone deacetylase-1 as a prognostic factor and mediator of gastric cancer progression by enhancing glycolysis. *Hum Pathol* 2019; **85**: 194-201 [PMID: 30500418 DOI: 10.1016/j.humpath.2018.10.031]



Published By Baishideng Publishing Group Inc
7041 Koll Center Parkway, Suite 160, Pleasanton, CA 94566, USA
Telephone: +1-925-3991568
E-mail: bpgoffice@wjgnet.com
Help Desk: <http://www.f6publishing.com/helpdesk>
<http://www.wjgnet.com>



HDAC Inhibitors in Solid Tumors: An Incomplete Story

Ramchandra V Amnekar^{1, 2}
and Sanjay Gupta^{1, 2*}

Received: March 19, 2018; Accepted: March 22, 2018; Published: March 26, 2018

In the Field of Observation, Chances Favor the Prepared Minds – Louis Pasteur

With the vast experience of the last several decades, now it has become clear that epigenetic changes like post-translational histone modifications (PTMs) define the hallmarks of cancer. Histone acetylation, a well-studied PTM in cancer, is controlled by the opposing activities of histone acetyltransferases (HATs) and histone deacetylases (HDACs) [1]. In 1971, Charlotte Friend's serendipitous voyage to decipher the mechanism of DMSO induced erythroid differentiation in murine erythroblastic leukemia, paved the way for development of SAHA: a potent inhibitor of cell proliferation and inducer of cell death. By 1998, HDACs were found to be the target of SAHA and by 2006 FDA approved SAHA (Vorinostat) for the treatment of cutaneous T cell lymphoma, making it one of the first generation epi-drug along with 5'-azacytidine. HDAC's are NAD⁺ or Zn²⁺ dependent enzymes catalyzing deacetylation of histones and non-histone proteins. Depending on their substrate specificity and cellular localization they have been classified under four classes [2].

Acetylation of histones on cis-acting regulatory elements like enhancer and promoters and the associated chromatin changes is at the heart of transcription and gene reprogramming. The prognostic utility of site specific histone acetylations *viz* H3K9ac, H3K18ac, H4K12ac, H4K16ac has been demonstrated through their correlation with clinicopathological parameters in case of breast, lung, prostate and gastric cancer [3]. This hypoacetylation could be an outcome of decreased levels of HATs or inactivation as in case of hMOF or conversely an increase in HDAC's or HDAC activity [4]. Infact, increased Class I and Class II HDACs has been demonstrated to be an indicator in case of colon, pancreatic, gastric and ovarian cancers for tumor aggressiveness, impact on survival, invasive potential and dedifferentiated state of tumors [5].

Epigenetic processes being reversible, epi-drugs like HDACi are envisaged as the new arsenal to combat the altered epigenome and gene expression in cancer. The effects of HDACi may range from hyperacetylation of histones/non-histone proteins to re-expression of tumor suppressors like p21, p16 leading to apoptosis or cell cycle arrest or by induction of differentiation as in case of chondrosarcomas [6] and colon cancer cells [7]. Today, pan HDAC inhibitors like Vorinostat and Romidepsin have shown promising results as single agents in hematological malignancies and also in cell line studies on breast, prostate and

- 1 Epigenetics and Chromatin Biology Group, Gupta Laboratory, Cancer Research Centre, Advanced Centre for Treatment Research and Education in Cancer, Tata Memorial Centre, Kharghar, Navi Mumbai, MH, 410210, India
- 2 Homi Bhabha National Institute, Training School Complex, Anushakti Nagar, Mumbai, MH, 400085, India

*Corresponding author: Sanjay Gupta

✉ sgupta@actrec.gov.in

Homi Bhabha National Institute, Training School Complex, Anushakti Nagar, Mumbai, MH, 400085, India.

Citation: Amnekar RV, Gupta S (2018) HDAC Inhibitors in Solid Tumors: An Incomplete Story. J Clin Epigenet Vol.4 No.2:8

gastric cancers [8]. However, the translation of these *in vitro* and pre-clinical studies into clinics in case of solid tumors has been abortive owing to their ineffectiveness and toxicities involved. This warrants the need to investigate the confounding factors.

Pleiotropic function of HDAC's in different physiological processes warrants the use of selective inhibitors, minimizing off target effect. This has been a major concern for the FDA approved HDACi which cannot discriminate between the different classes of HDACs. Further, the trials carried out during the last few decades are on terminally ill patients or patient who has received prior chemotherapy, thus having less tolerability to epi-drugs. Also, trials failed to sub-categorize the patients on the basis of their HDAC or the histone acetylation status. This need of patient stratification is further supported by the fact that colon and endometrial cells with inactivating HDAC1 mutation failed to respond to TSA treatment [9]. In 2008, Weichert et al. conducted a retrospective analysis in a 143 patient training cohort and 150 patient validation cohort, wherein expression of Class I HDACs was evaluated for gastric cancer. Around 78% and 65% patients in the training and validation cohort showed high expression of either all three or one of the Class I HDACs respectively. Further,

this high expression co-related with lymph node metastasis and poor survival of patients. It would be imperative to consider the high HDAC expression group for HDACi treatment, rather considering all patients [10]. Thus, efforts should be envisaged in selecting the right targetable tumors as HDACi might be useful only in those tumors where HDAC's are the key players in pathogenesis.

The outcome of HDACi treatment is also dependent on the levels of thioredoxin (TRX) gene or other ROS scavenging agents like superoxide dismutase. HDACi treatment is associated with increased reactive oxygen species specifically in tumor cells. This has been attributed to the biased role of HDACi, wherein they induces expression of TRX gene in normal cells, mitigating the increased ROS generated. However, in tumor cells they induce the expression of TRX binding protein: a negative regulator of TRX, making tumor cells susceptible to ROS mediated cell death [11]. A high level of TRX or other ROS scavenging agents like superoxide dismutase which is observed in certain cancer may predispose the tumor to HDACi resistance [11]. Thus, additional determinants need to be studied and validated before stratification.

References

- 1 Cohen I, Poręba E, Kamieniarz K, Schneider R (2011) Histone modifiers in cancer: Friends or foes. *Genes Cancer* 2: 631-647.
- 2 Marks PA, Breslow R (2007) Dimethyl sulfoxide to vorinostat: Development of this histone deacetylase inhibitor as an anticancer drug. *Nat Biotechnol* 25: 84-90.
- 3 Khan SA, Reddy D, Gupta S (2015) Global histone post-translational modifications and cancer: Biomarkers for diagnosis, prognosis and treatment. *World J Biol Chem* 6: 333-345.
- 4 Wang Y, Zhang R, Wu D, Lu Z, Sun W, et al. (2013) Epigenetic change in kidney tumor: Downregulation of histone acetyltransferase MYST1 in human renal cell carcinoma. *J Exp Clin Cancer Res* 32: 8.
- 5 Moradzadeh M, Tabarraei A, Sadeghnia HR (2015) The role of histone deacetylase (HDAC) as a biomarker in cancer. *J Mol Biomark Diagn* 5: 240.
- 6 Sakimura R, Tanaka K, Yamamoto S, Matsunobu T, Li X, Hanada M et al. (2007) Epigenetic change in kidney tumor: Downregulation of histone acetyltransferase MYST1 in human renal cell carcinoma. The effects of histone deacetylase inhibitors on the induction of differentiation in chondrosarcoma cells. *Clin Cancer Res* 32: 8.
- 7 Lea MA, Ibeh C, Shah N, Moyer MP (2007) Induction of differentiation of colon cancer cells by combined inhibition of kinases and histone deacetylase. *Anticancer Res* 27: 741-748.
- 8 Nervi C, De Marinis E, Codacci-Pisanelli G (2015) Epigenetic treatment of solid tumours: A review of clinical trials. *Clinical Epigenetics* 7: 127.
- 9 Ropero S, Fraga MF, Ballestar E, Hamelin R, Yamamoto H, et al. (2006) A truncating mutation of HDAC2 in human cancers confers resistance to histone deacetylase inhibition. *Nat Genet* 38: 566-569.
- 10 Weichert W, Röske A, Gekeler V, Beckers T, Ebert MP, et al. (2008) Association of patterns of class I histone deacetylase expression with patient prognosis in gastric cancer: A retrospective analysis. *Lancet Oncol* 9: 139-148.
- 11 Marks PA (2006) Thioredoxin in cancer -Role of histone deacetylase inhibitors. *Semin Cancer Biol* 16: 436-443.
- 12 Wawruszak A, Luszczki JJ, Grabarska A, Gumbarewicz E, Dmoszynska-Graniczka M, et al. (2015) Assessment of interactions between cisplatin and two histone deacetylase inhibitors in MCF7, T47D and MDA-MB-231 human breast cancer cell lines: An isobolographic analysis. *PLoS One* 10: e0143013.
- 13 Mutze K, Langer R, Becker K, Ott K, Novotny A, et al. (2010) Histone deacetylase (HDAC) 1 and 2 expression and chemotherapy in gastric cancer. *Ann Surg Oncol* 17: 3336-3343.
- 14 To KK, Tong WS, Fu LW (2017) Reversal of platinum drug resistance by the histone deacetylase inhibitor belinostat. *Lung Cancer* 103: 58-65.
- 15 Reddy D, Khade B, Pandya R, Gupta S (2017) A novel method for isolation of histones from serum and its implications in therapeutics and prognosis of solid tumours. *Clin Epigenetics* 9: 30.

RESEARCH

Open Access



p38-MAPK/MSK1-mediated overexpression of histone H3 serine 10 phosphorylation defines distance-dependent prognostic value of negative resection margin in gastric cancer

Shafqat Ali Khan^{1,2}, Ramchandra Amnekar^{1,2}, Bharat Khade¹, Savio George Barreto³, Mukta Ramadwar⁴, Shailesh V. Shrikhande⁵ and Sanjay Gupta^{1,2*}

Abstract

Background: Alterations in histone modifications are now well known to result in epigenetic heterogeneity in tumor tissues; however, their prognostic value and association with resection margins still remain poorly understood and controversial. Further, histopathologically negative resection margins in several cancers have been associated with better prognosis of the disease. However, in gastric cancer, despite a high rate of R0 resection, a considerably high incidence of loco-regional recurrence is observed. We believe alterations of global histone post-translational modifications could help in identifying molecular signatures for defining the true negative surgical resection margins and also the prognosis of gastric cancer patients.

Results: The present study compares the level of H3S10ph among paired tumor and histopathologically confirmed disease-free (R0) proximal and distal surgical resection margin (PRM and DRM) tissue samples of GC patients ($n = 101$). Immunoblotting and immune-histochemical analysis showed a significantly ($p < 0.01$) higher level of H3S10ph in tumor compared to R0 surgical resection margins. Along with tumor, high H3S10ph levels in both PRM and DRM correlated with clinical parameters and poor survival. Interestingly, in the case of PRM and DRM, the association of H3S10ph with poor survival was only found in a patient group with the resection margin distance < 4 cm. Further investigations revealed that the increase of H3S10ph in tumor tissues is not due to the change in cell cycle profile but rather an interphase-associated phenomenon. Moreover, an increase in ph-MSK1 and ph-p38 levels in tumor tissues and the decrease in ph-MSK1 and H3S10ph on p38 inhibition in gastric cancer cells confirmed p38-MAPK/MSK1 pathway-mediated regulation of H3S10ph in gastric cancer.

Conclusions: Our study provides the first evidence that p38-MAPK/MSK1-regulated increase of H3S10ph in GC is predictive of a more aggressive cancer phenotype and could help in defining true negative surgical resection margin. Importantly, our data also gave a new rationale for exploration of the use of MSK1 inhibitor in gastric cancer therapy and the combination of histone post-translational modifications, H4K16ac and H4K20me3 along with H3S10ph as epigenetic prognostic markers.

(Continued on next page)

* Correspondence: sgupta@actrec.gov.in

¹Epigenetics and Chromatin Biology Group, Gupta Laboratory, Cancer Research Centre, Advanced Centre for Treatment Research and Education in Cancer, Tata Memorial Centre, Kharghar, Navi Mumbai, MH 410210, India

²Homi Bhabha National Institute, Training School Complex, Anushakti Nagar, Mumbai, MH 400085, India

Full list of author information is available at the end of the article



(Continued from previous page)

Keywords: Gastric cancer, Histone post-translational modification, H3S10 phosphorylation, Resection margin, Prognosis, p38 MAPK/MSK1 pathway

Abbreviations: DFS, Disease-free survival; DRM, Distal surgical resection margin; FFPE, Formalin-fixed paraffin-embedded; GC, Gastric cancer; H3S10ph, Histone H3 serine 10 phosphorylation; IE, Immediate early genes; MSK1, Mitogen- and stress-activated protein kinase-1; NACT, Neoadjuvant chemotherapy; OS, Overall survival; PRM, Proximal surgical resection margin; PTMs, Post-translational modifications; R0, Disease-free surgical resection margin

Background

Gastric cancer (GC) is one of the most common malignancies worldwide. Globally, GC ranks fourth and third in terms of incidence and mortality, respectively [1]. In India, it is one of the most aggressive cancers ranking third and second in terms of incidence and mortality, respectively [2]. Surgery remains the mainstay for cure especially in early cancers, while in locally advanced GC the addition of perioperative/neoadjuvant chemotherapy (NACT) affords a better survival advantage [3]. The current standard practice in GC is to submit the resected stomach for pathological examination to confirm the diagnosis and stage of the tumor as well as to assess the margins of resection using hematoxylin and eosin (H&E) staining. A pathologically negative resection/R0 margin affords the best chance of cure in GC with 5-year survival rates of 13 versus 35 % for positive and negative resection margins, respectively [4]. However, despite an apparently curative surgery, loco-regional recurrence has still been encountered in 87 % of GC patients [5]. Thus, raising the doubt on current pathological techniques used in day to day practice to truly confirm the adequacy of the R0 surgical resection margins. Therefore, there is an urgent need to identify molecular markers and investigate their expression in not only the cancerous tissues but also the surrounding resected (margin) tissue that is apparently free from disease (R0) based on histopathology.

Over the past decade, accumulated evidence indicates towards the association of aberrant covalent histone post-translational modifications (PTMs) with cancer such as loss of acetylation of histone H4 at lysine 16 (H4K16ac) and tri-methylation of histone H4 at lysine 20 (H4K20me3), defined as “histone onco-modifications” [6, 7]. In GC, a high level of tri-methylation of histone H3 at lysine 9 (H3K9me3) was found to be correlated with lympho-vascular invasion, recurrence, poor survival rate, and as an independent prognostic marker [8]. In addition to their role in disease prognosis, epigenetic alterations, specifically DNA methylation, are also reported in field cancerization/defects in various types of cancer, including stomach, liver, colon, lung, breast, kidney, and esophageal [9]. However, the relation of histone

PTMs between tumor and resection margin and the regulatory mechanism for their alteration is poorly understood in cancer.

In this study on human GC, we identified phosphorylation of histone H3 at serine 10 (H3S10ph) as a histone PTM with most consistent and significant difference between tumor and negative resection margin. For the first time, our results demonstrate a distance-dependent (≤ 4 vs >4 cm) relation of H3S10ph of the tumor with both PRM and DRM and also it correlates with the prognosis of GC patients. Further, we report that phosphorylation of H3S10 in GC is mediated by mitogen- and stress-activated protein kinase-1 (MSK1) through the p38-MAPK pathway.

Methods

Tissue samples and histopathological analysis

Frozen tissue sections ($n = 36$) and formalin-fixed paraffin-embedded (FFPE) tissue blocks ($n = 115$) of the tumor (T), PRM, and DRM from each gastric adenocarcinoma patients were obtained. All the patients were operated between 2009 and 2012 at Tata Memorial Hospital, Mumbai, India. Histopathological analysis including determination of tumor content (% of tumor cells) was done by a blinded gastrointestinal pathologist. Based on the histopathological analysis, frozen tumor tissues with ≥ 70 % tumor content, FFPE tumor tissues with ≥ 10 % tumor content, and negative resection margins (without any tumor cell) were included in the study. Finally, the study was conducted on paired tumor, PRM, and DRM frozen tissues ($n = 10$), and FFPE tissue blocks ($n = 101$). The protocol of the study was reviewed and approved by the Institutional Review Board and Ethics Committee (project number-466). All patients provided a written informed consent.

Immunohistochemistry

Immunohistochemical (IHC) staining was performed using VECTASTAIN® ABC kit (Vector Lab-P6200). FFPE tissue blocks were sectioned at a thickness of 4 μ m and mounted on poly-L-lysine-coated glass slides. The sections were deparaffinized through a graded series of xylene and rehydrated through a graded series of absolute ethanol to

distilled water. Endogenous peroxidase was quenched with 3 % hydrogen peroxide in methanol at room temperature for 30 min in the dark. Microwave antigen retrieval was carried out with 0.01 M Sodium citrate buffer (pH 6). Anti H3S10ph (Abcam-1776), H3K16ac (Millipore-07-329), H4K20me3 (Abcam-9053), and ph-MSK1 (Abcam-32190) antibodies were applied for 16 h at 4 °C at the dilution of 1:100. Immunoreactive proteins were chromogenically detected with diaminobenzidine (DAB; Sigma-D5537). The sections were counterstained with Harris's hematoxylin, dehydrated, and mounted. In parallel, control staining was performed without adding a primary antibody.

Evaluation of immunohistochemistry

The nuclear IHC staining for all the antibodies were scored using H-score which is based on intensity of staining (ranges from zero to three) and percentage of stained cells using the following formula: $H\text{-score} = [(0 \times \% \text{ of cells with staining intensity of zero}) + (1 \times \% \text{ of cells with staining intensity of one}) + (2 \times \% \text{ of cells with staining intensity one}) + (3 \times \% \text{ of cells with staining intensity two})]$. H-score was further divided into three groups: (i) 0–100: low level, (ii) 100–200: intermediate level, and (iii) 200–300: high level. The IHC staining was examined by two independent researchers (SAK and MR), one of whom is a senior consultant pathologist (MR). Both the researchers were blinded to all clinicopathological and outcome variables.

Cell culture, transfection, and treatment

GC cell lines, AGS (CRL-1739) and KATOIII (HTB-103), were procured from ATCC. AGS and KATOIII were cultured in RPMI1640 (Invitrogen) and F12K (Himedia) media, respectively, at 37 °C with 5 % CO₂ supplemented with 10 % FBS, 100 U/ml penicillin, and 100 mg/ml streptomycin (Sigma). AGS cells were transfected using CaCl₂ method with 10 µg of the pCMV-flag-MSK1 construct. AGS and KATOIII cells were treated for 1 h with chemical inhibitors against ph-p38 (SB203580, Calbiochem), ph-ERK (PD98059, Calbiochem), and ph-MSK1 (H89, Millipore) at 10 and 20 µM concentrations for 1 h, respectively.

Total RNA isolation and RT-PCR

Total RNA was extracted (Thermo scientific-0731) from 25 mg of the frozen tumor and resection margin (PRM or DRM) tissues with the maximum distance from the site of the tumor. Total RNA (1 µg) was used for cDNA synthesis (Fermentas-K1632) using random hexamers. RT-PCR amplification was done using specific primers for *c-Jun* (F:CCCCAAGATCCTGAAACAGA, R:TCCTGCTCATCTGTACGTT), *c-Fos* (F:CGGGGATAGCC TCTCTTAC, R:CCCTTCGGATTCTCCTTTTC), cyclin-E1 (F:AGCGGTAAGAAGCAGAGCAG, R:TTTGATG

CCATCCACA GAAA), cyclin-B1 (F:CGGGAAGTCAC TGGAAACAT, R:CCGACCCAGACCAAAGTTTA), cyclin-D1 (F:GATCAAGTGTGACCCGGACT, R:AGAGATGGAAGGGGGAAAGA), and 18S rRNA (F:AAACGGCTACCACATCCAAG, R:CCTCCAATGGATC CTCGTTA) with an initial denaturation step at 95 °C for 2 min, followed by 15 cycles of denaturation at 95 °C for 45 s, primer annealing at 55 °C for 30 s, primer extension at 72 °C for 30 s, and a final extension at 72 °C for 10 min. Amplified products were resolved on 1.5 % agarose gels and visualized by EtBr staining.

Preparation of total cell lysate, nucleo-cytosolic fraction, and histones

Cells were harvested from 90-mm plates and lysed in 200 µl of Laemmli buffer to prepare the total cell lysate (TCL). Nucleo-cytosolic fraction (NCF) was prepared by homogenizing 100 mg of frozen tissue in 2 ml of ice-cold lysis buffer (20 mM Tris-Cl pH 8, 2 mM EDTA pH 8, 10 mM EGTA, 5 mM MgCl₂, 0.1 % TritonX-100, 1 mM sodium orthovanadate, 1 mM sodium fluoride, 20 mM β-glycerophosphate, 1 mM DTT, 1 mM PMSE, 10 µg/ml leupeptin, 10 µg/ml aprotinin), and for cell lines, 2 ml of ice-cold MKK lysis buffer (10 mM Tris-Cl, 1 mM EDTA, 1 mM EGTA, 1 % Triton X-100, 10 µg/ml leupeptin, 10 µg/ml aprotinin, 1 mM PMSE, 1 mM sodium orthovanadate, 10 mM sodium fluoride, 10 mM β-glycerophosphate) [10] was used for cells harvested from a 90-mm plate. Both the homogenates were then kept at 4 °C for 30 min with intermittent mixing and then was clarified by centrifugation at 16,000 rpm for 30 min. The supernatant was collected as NCF and stored at –20 °C until it is required, and the pellet was used for histone isolation by acid extraction method [11]. For the preparation of NCF and histones, along with tumor, resection margin (PRM or DRM) tissues with the maximum distance from the site of the tumor were used.

Electrophoresis and immunoblotting

TCL and NCF, and histones were resolved on 10 and 18 % polyacrylamide SDS-PAGE, respectively, and transferred to PVDF membrane. Proteins on PVDF membrane were hybridized with anti-H3 (Upstate-06-755; 1:2000 dilution), H4 (Millipore-07-108; 1:4000 dilution), H3S10ph (Millipore-06-570; 1:7000 dilution), H4K16ac (Millipore-07-329; 1:8000 dilution), H4K20me3 (Abcam-9053; 1:4000 dilution), β-actin (Sigma-A5316; 1:10,000 dilution), MSK1 (Santacruz-9392; 1:2000 dilution), ph-MSK1 (Abcam-31190; 1:3000 dilution), ERK1/2 (Santacruz-292838; 1:2000 dilution), ph-ERK (Cell signaling-9910; 1:2000 dilution), p38 (Santacruz-728; 1:2000 dilution), ph-p38 (Cell signaling-9910; 1:2000 dilution), and anti-flag (Sigma-F3165; 1:5000 dilution). Signal was visualized using horseradish peroxidase-conjugated anti-rabbit/mouse secondary

antibody and ECL plus chemiluminescence kit (Amersham). Wherever required, the densitometry analysis was done on immunoblot and membrane to determine their mean intensities using ImageJ software. For native proteins, mean intensity of immunoblot was normalized with the stained PVDF membrane; for phosphorylated forms, mean intensity of immunoblot was normalized with immunoblot of native proteins. The resulted value was used to express their mean relative levels in resection margin and tumor.

Immunofluorescence microscopy

Cells grown on glass coverslips were fixed with 4 % paraformaldehyde for 20 min. Cells were then permeabilized in PBS containing 0.5 % Triton X-100 for 20 min at RT and then blocked with PBS containing 3 % BSA and 0.1 % NP-40 for 1 h. Next, cells were incubated with a primary antibody against H3S10ph (Millipore-06-570) and ph-MSK1 (Abcam-31190) and appropriate secondary antibodies for 2 h each. Dilution of primary (1:100) and secondary antibodies (Alexa-568 or Alexa-488; Cell signaling; 1:300 dilution) was made in blocking buffer. After the addition of secondary antibody, all the steps were performed in the dark and at room temperature. Finally, coverslips were mounted in VECTASHIELD (Vector lab). Fluorescence intensity was analyzed using a fluorescence microscope (IX81; Olympus, Japan).

Cell cycle analysis

Frozen tissue (50 mg) was powdered using mortar and pestle in liquid nitrogen. The powder was homogenized in 2 ml of nuclear buffer A (15 mM Tris-Cl pH 7.5, 60 mM KCl, 15 mM NaCl, 2 mM EDTA, 0.5 mM EGTA, 0.34 M sucrose, 0.15 mM β -ME, 0.15 mM spermine, and 0.5 mM spermidine) using a Dounce homogenizer. In the case of cell lines, cells were trypsinized and harvested in PBS. Tissue homogenate and cells were then centrifuged (5000 rpm for 15 min at 4 °C) to pellet nuclei and cells, respectively; the supernatant was discarded. The pellet was then fixed with 70 % chilled ethanol and stored at -20 °C. When required, tissue nuclei/cells were washed with PBS and suspended in 500 μ l of PBS containing 0.1 % TritonX-100 and 100 μ g/ml of RNaseA and incubated at 37 °C for 30 min. After incubation, propidium iodide (25 μ g/ml) was added and nuclei were incubated at 37 °C for 30 min. DNA content analysis was carried out in a FACSCalibur flow cytometer (BD Biosciences). Cell cycle analysis was performed using the Mod-fit software.

Mitotic index analysis

Based on the morphology of nuclei, mitotic cells were counted in 10 consecutive high power fields (HPF; $\times 40$) of H&E-stained tissue (tumor and resection margin) section slides. Average of mitotic cells from 10 HPF was

represented as mitotic index. H&E staining was done as per the standard protocol on 4- μ m-thick FFPE tissue sections.

Statistical analysis

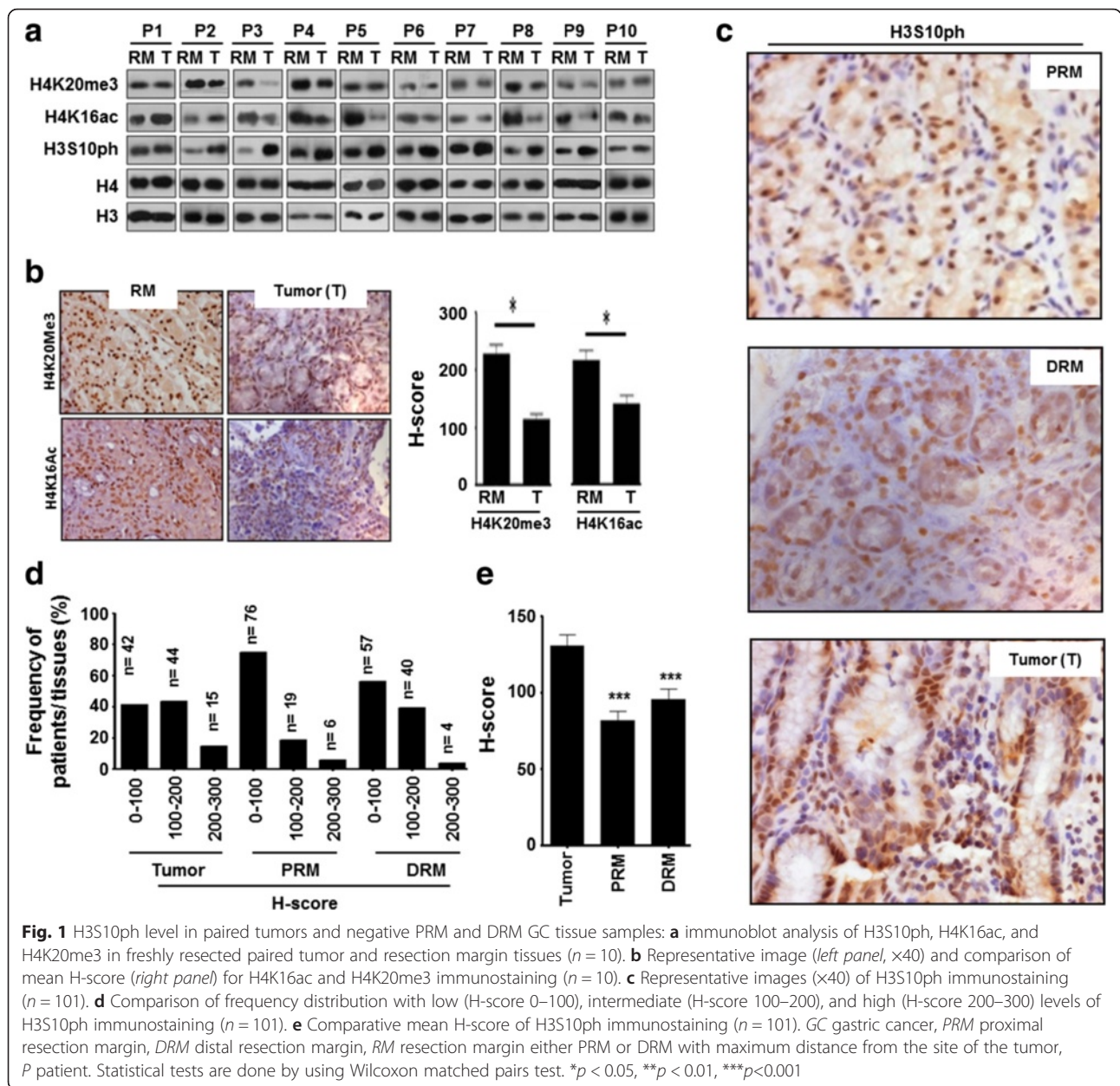
To test the statistical significance of paired and unpaired resection margin and tumor tissues, Wilcoxon matched pair and Mann-Whitney test were used, respectively. To test whether variables differed across groups, we used the chi-square test. Chi-square analysis was used to find the correlation between H3S10ph levels of the tumor, PRM, and DRM tissues and clinical parameters. Survival curves were plotted using the Kaplan-Meier method, and the significance of the differences between the survival curves was determined using a univariate log-rank test. To test the statistical independence and significance of predictors, a multivariate survival analysis was performed using the Cox proportional hazard regression model. All p values were two-sided, and $p < 0.05$ was considered significant. All statistical analyses were performed with GraphPad and/or SPSS software.

Results

Level of H3S10ph in tumor and resection margin tissues of GC

Histones were prepared from freshly resected paired ($n = 10$) tumor and R0 resection margin (RM) tissues of GC patients, for a pilot study. Histones and their respective paraffin blocks were subjected to immunoblotting and IHC analysis with site-specific acetylation, methylation, and phosphorylation marks of histone H3 and H4 (data not shown). H3S10ph showed a most consistent (9/10 patients) increase in tumor compared to resection margin tissues in immunoblot analysis (Fig. 1a). Further, the loss of H4K16ac and H4K20me3 is a hallmark of the tumor [7]; however, it was not reported in paired GC tissue samples. Our immunoblot and IHC analysis in the paired tissues confirmed the decrease of H4K16ac (8/10 patients) and H4K20me3 (8/10 patients) in GC as well (Fig. 1a, b and Additional file 1: Figure S1).

The status of H3S10ph was further studied in a validation set ($n = 101$) among tumor and histopathologically negative PRM and DRM tissues using IHC. IHC analysis showed a high level of H3S10ph in tumor compared to both the resection margins (Fig. 1c). H-score-based analysis of frequency distribution of tumor and PRM and DRM tissue samples of GC patients showed 76, 57, and 42; 19, 40, and 44; and 6, 4, and 15 samples with a low, intermediate and high level of H3S10ph, respectively (Fig. 1d). Further, comparison of H-score showed a significant high level of H3S10ph in tumor compared to PRM ($p < 0.001$) and DRM ($p < 0.001$) tissues (Fig. 1e).



Correlation of H3S10ph levels of tumor, PRM, and DRM with clinicopathological variable of GC patients

Chi-square analysis was used to find a correlation between H3S10ph levels of the tumor, PRM, and DRM tissues, and clinical parameters (Table 1). H3S10ph levels of tumor tissues showed a significant positive correlation with the World Health Organization (WHO) classification ($p = 0.0001$), T stage ($p = 0.005$), pTNM stage ($p = 0.016$), and recurrence ($p = 0.034$). Interestingly, except recurrence, H3S10ph levels of PRM and DRM tissues also showed a significant positive correlation with the same clinical parameters as tumor tissues; WHO classification ($p = 0.008$ and

0.0001 for PRM and DRM, respectively), T stage ($p = 0.001$ and 0.003 for PRM and DRM, respectively), and pTNM stage ($p = 0.015$ and 0.037 for PRM and DRM, respectively). Only DRM showed a significant correlation with recurrence ($p = 0.012$).

Correlation of H3S10ph levels of tumor and resection margins with survival of GC patients

Overall survival (OS) and disease-free survival (DFS) rate among groups with the low, intermediate, and high level of H3S10ph was compared by log-rank test/Kaplan-Meier survival analysis (Fig. 2). Analysis showed a significant negative correlation of H3S10ph

Table 1 Correlation between H3S10 phosphorylation levels of tumor, PRM, and DRM with clinicopathological variables

Total (n = 101)	H3S10 phosphorylation level of tumor			p value	H3S10 phosphorylation level of PRM			p value	H3S10 phosphorylation level of DRM			p value
	Low (%), n = 42	Inter. (%), n = 44	High (%), n = 15		Low (%), n = 76	Inter. (%), n = 19	High (%), n = 6		Low (%), n = 57	Inter. (%), n = 40	High (%), n = 4	
Age (years)												
≤50	15 (35.7)	18 (40.9)	6 (40.0)	0.879 [†]	31 (40.8)	6 (31.6)	2 (33.3)	0.734 [†]	21 (36.8)	16 (40.0)	2 (50.0)	0.849 [†]
>50	27 (64.3)	26 (59.1)	9 (60.0)		45 (59.2)	13 (68.4)	4 (66.7)		36 (63.2)	24 (60.0)	2 (50.0)	
Sex												
Male	29 (69.0)	32 (72.7)	9 (60.0)	0.652 [†]	53 (69.7)	11 (57.9)	6 (100.0)	0.148 [†]	40 (70.2)	26 (65.0)	4 (100.0)	0.343 [†]
Female	13 (31.0)	12 (27.7)	6 (40.0)		23 (30.3)	8 (42.1)	0 (0.0)		17 (29.8)	14 (35.0)	0 (0.0)	
WHO classification												
WD	2 (4.8)	0 (0.0)	0 (0.0)	0.0001 [†]	2 (2.6)	0 (0.0)	0 (0.0)	0.008 [†]	2 (3.5)	0 (0.0)	0 (0.0)	0.0001 [†]
MD	22 (52.4)	3 (6.8)	0 (0.0)		24 (31.6)	1 (5.3)	0 (0.0)		23 (40.4)	2 (5.0)	0 (0.0)	
PD	16 (38.1)	40 (40.9)	7 (46.7)		44 (57.9)	16 (84.2)	3 (50.0)		29 (50.9)	33 (82.5)	1 (25.0)	
SRC	2 (4.8)	1 (2.3)	8 (53.3)		6 (7.9)	2 (10.5)	3 (50.0)		3 (5.3)	5 (12.5)	3 (75.0)	
T stage												
T1	9 (21.4)	4 (9.1)	1 (6.7)	0.005 [†]	13 (17.1)	1 (5.3)	0 (0.0)	0.001 [†]	11 (19.3)	3 (7.5)	0 (0.0)	0.003 [†]
T2	11 (26.2)	10 (22.7)	3 (20.0)		22 (28.9)	2 (10.5)	0 (0.0)		14 (24.6)	10 (25.0)	0 (0.0)	
T3	16 (38.1)	20 (45.5)	2 (13.3)		26 (34.2)	10 (52.6)	2 (33.3)		23 (40.4)	15 (37.5)	0 (0.0)	
T4	6 (14.3)	10 (22.7)	9 (60.0)		15 (19.7)	6 (31.6)	4 (66.7)		9 (15.8)	12 (30.0)	4 (0.0)	
Lymph node metastasis												
Absent	20 (47.6)	27 (61.4)	10 (66.7)	0.136 [†]	42 (55.3)	10 (52.6)	5 (83.3)	0.385 [†]	30 (52.6)	24 (60.0)	3 (75.0)	0.311 [†]
Present	22 (52.4)	17 (38.6)	5 (33.3)		34 (44.7)	9 (47.4)	1 (16.7)		27 (47.4)	16 (40.0)	1 (25.0)	
pTNM stage												
I	14 (33.3)	7 (15.9)	1 (6.7)	0.016 [†]	20 (26.3)	2 (10.5)	0 (0.0)	0.015 [†]	17 (29.8)	5 (12.5)	0 (0.0)	0.037 [†]
II	15 (35.7)	22 (50.0)	6 (40.0)		33 (43.4)	8 (42.1)	2 (33.3)		22 (38.6)	20 (50.0)	1 (25.0)	
III	13 (31.0)	14 (31.8)	7 (46.7)		22 (28.9)	8 (42.1)	4 (66.7)		17 (29.8)	14 (35.0)	3 (75.0)	
IV	0 (0.0)	1 (2.3)	1 (6.7)		1 (1.3)	1 (5.3)	0 (0.0)		1 (1.8)	1 (2.5)	0 (0.0)	
Recurrence												
Absent	32 (76.2)	28 (63.6)	7 (46.7)	0.034 [†]	54 (71.1)	8 (42.1)	5 (83.3)	0.351 [†]	43 (75.4)	23 (57.5)	1 (25.0)	0.012 [†]
Present	10 (23.8)	16 (36.4)	8 (53.3)		22 (28.9)	11 (57.9)	1 (16.7)		14 (24.6)	17 (42.5)	3 (75.0)	
Treatment modality												
Surgery	24 (57.1)	21 (47.7)	12 (80.0)	0.093 [†]	43 (56.6)	11 (57.9)	3 (50.0)	0.943 [†]	28 (49.1)	26 (65.0)	3 (75.0)	0.087 [†]
NACT + Surgery	18 (42.9)	23 (52.3)	3 (20.0)		33 (43.4)	8 (42.1)	3 (50.0)		29 (50.9)	14 (35.0)	1 (25.0)	

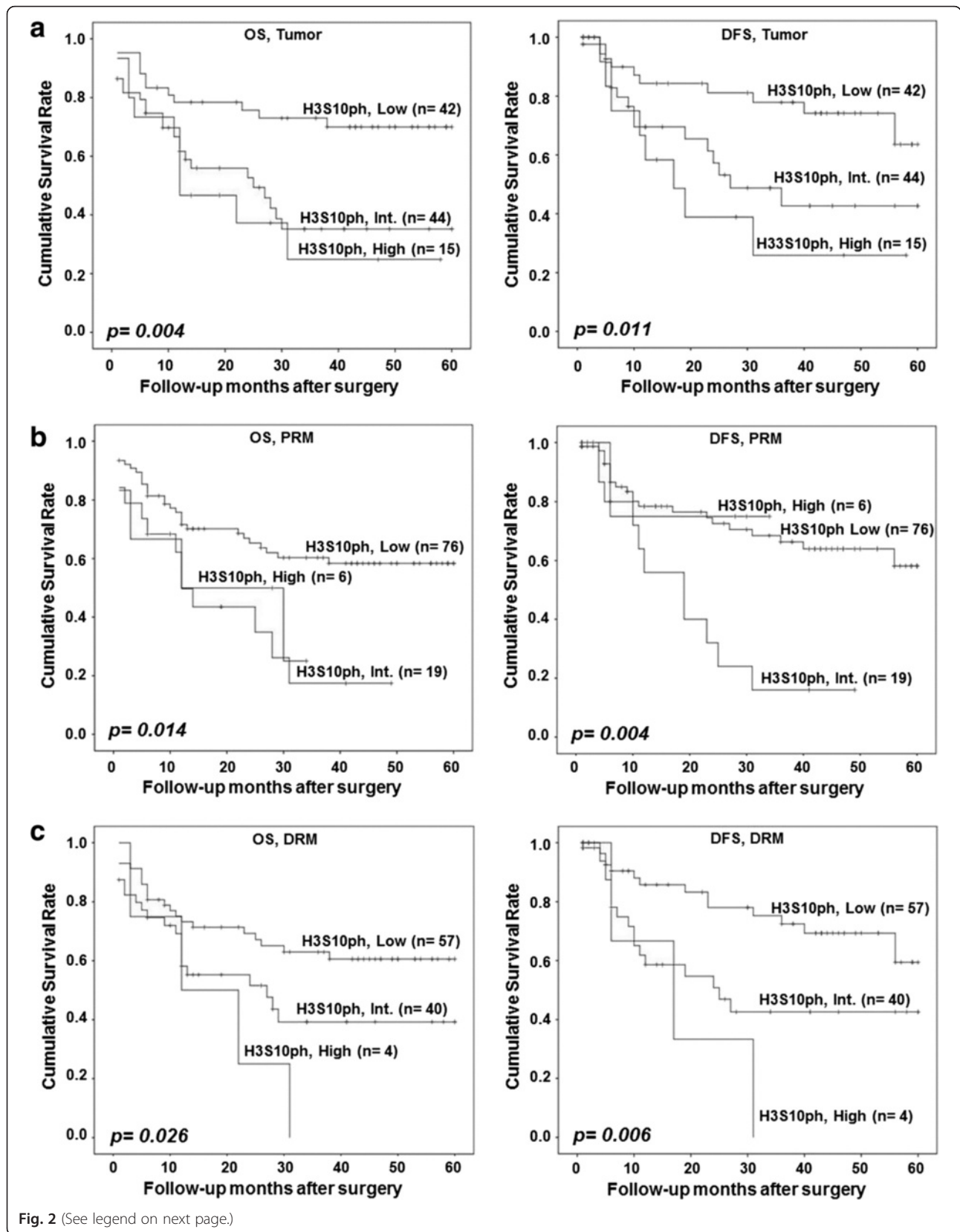
All three columns are compared in each category: [†]chi-square test by two-sided linear-by-linear association; [‡]chi-square test by two-sided Fisher's exact test. Italics indicates values that are statistically significant (<0.05)

Int. intermediate, PRM proximal resection margin, DRM distal resection margin

levels of tumor ($p = 0.004$ and 0.011), PRM ($p = 0.014$ and 0.004), and DRM ($p = 0.026$ and 0.006) with OS and DFS, respectively (Fig. 1a–c). Moreover, H3S10ph levels of the tumor, but not the PRM and DRM, were found to be independent predictors of overall survival (Additional file 2: Table S1). Therefore, together, data of this and previous sections confirm the association of a high level of H3S10ph of resection margins along with tumor tissues with poor prognosis of GC.

Relation of H3S10ph levels of resection margins and their distance from the site of the tumor in GC

Our observation of the low level of H3S10ph in resection margin compared to tumor tissues led us to examine whether the decrease had any relation with the distance of resection margin from the site of the tumor. To answer this, we first grouped the resection margin samples as per their distance from the tumor site and compared the mean H-score of H3S10ph immunostaining of each group with



(See figure on previous page.)

Fig. 2 Effect of H3S10ph levels of tumor, PRM, and DRM on GC patients' survival. Kaplan-Meier survival analysis was done according to H3S10ph staining H-score: low (0–100), intermediate (100–200), and high (200–300). High level of H3S10P of tumor and PRM and DRM is associated with both poor overall survival (OS) and disease-free survival (DFS). **a** OS and DFS based on H3S10P levels of tumor tissues, **b** OS and DFS based on H3S10P levels of PRM tissues, **c** OS and DFS based on H3S10P levels of DRM tissues. GC gastric cancer, PRM proximal resection margin, DRM distal resection margin, *Int.* intermediate. Comparison was done by log-rank test. $p < 0.05$ was considered as significant

the mean H-score of tumor samples (Fig. 3). For both PRM and DRM, a significant reduction in H3S10ph ($p < 0.05$) was observed for patient's group with resection margin distance >4 cm (Fig. 3a, b, left panel). Further, patients were divided into two groups based on the distance of resection margin ≤ 4 or >4 cm and their mean H-scores were compared with the tumor tissues. Interestingly, further analysis showed H3S10ph levels of

resection margins with the distance ≤ 4 cm were almost equal to those of the tumor tissues; however, resection margins with >4 cm showed a significant ($p < 0.001$) reduction in both PRM and DRM (Fig. 3a, b, middle panel). Additionally, immunoblot analysis also confirmed the reduction of H3S10ph levels of resection margins if the distance is >4 cm from the site of the tumor (Fig. 3a, b, right panel).

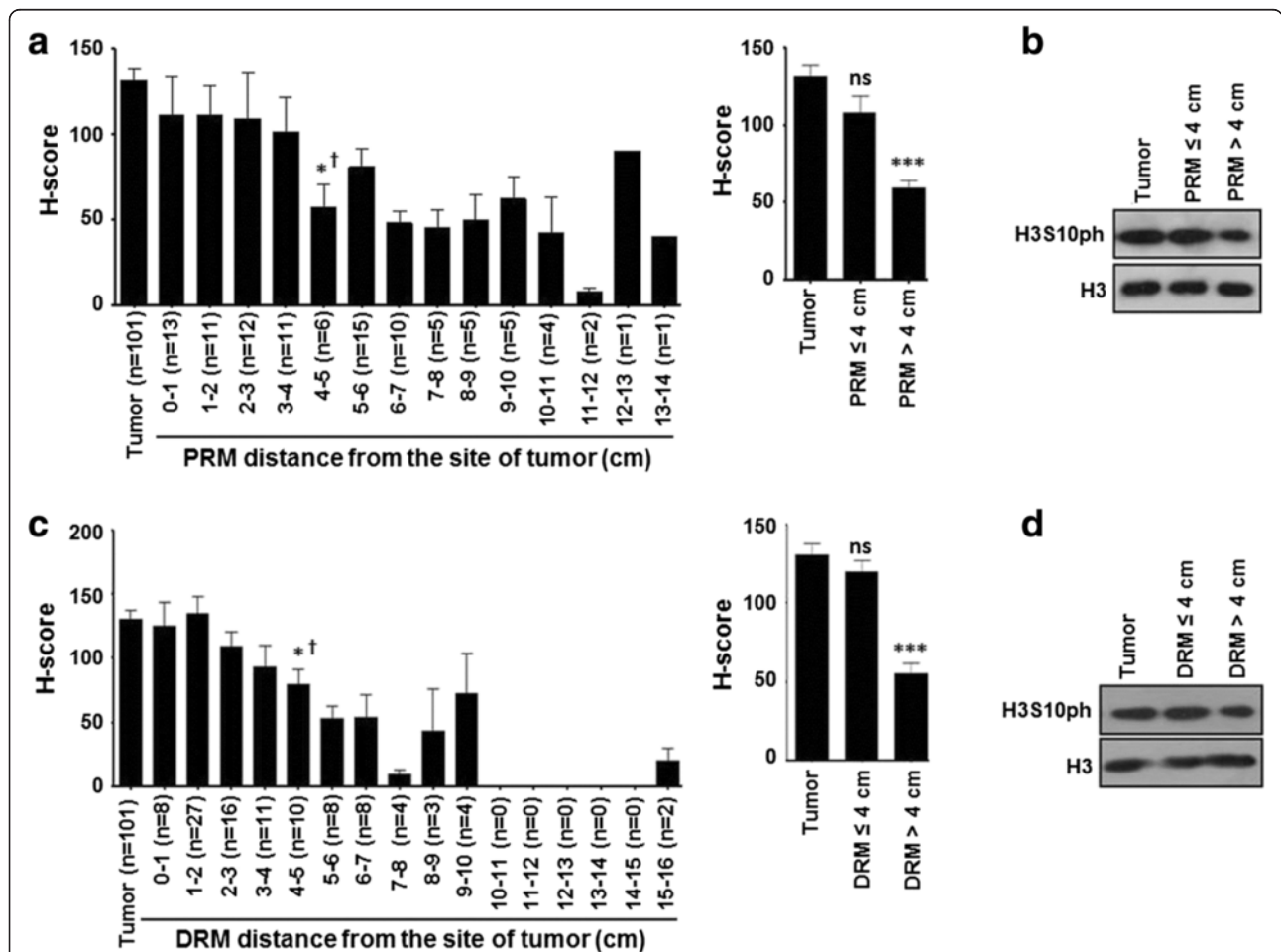


Fig. 3 Association of H3S10ph with the distance of negative resection margins in GC. **a, c** Resection margins were grouped as per their distance from the site of the tumor with 1 cm interval and mean H-score of H3S10ph immunostaining of each group was compared with tumor (*left panel*). In case of both PRM and DRM, analysis showed a significant decrease in H3S10ph levels as the margin length reaches more than 4 cm (*left panel*). Comparison of mean H-score of H3S10ph immunostaining of all resection margins with a margin distance ≤ 4 and >4 cm with tumor confirms the significant reduction of H3S10ph if the margin distance is >4 cm (*right panel*). **b, d** Confirmation of reduction of H3S10ph, if the margin length is >4 cm by immunoblotting. GC gastric cancer, PRM proximal resection margin, DRM distal resection margin. Statistical tests are done by using Mann-Whitney test (\dagger) and Wilcoxon matched pairs test. $*p < 0.05$, $**p < 0.01$, $***p < 0.001$

Effect of resection margin distance on prognostic value of H3S10ph in GC

To investigate the effect of resection margin distance from the site of the tumor on the prognostic value of

H3S10ph, its association with clinicopathological variables and survival was compared between the group with the resection margin ≤ 4 and >4 cm. Chi-square analysis (Table 2) showed a positive correlation of

Table 2 Correlation between H3S10ph levels of PRM and DRM, ≤ 4 vs >4 cm

Total (n = 101)	H3S10 phosphorylation level of PRM ≤ 4 cm (n = 48)			p value	H3S10 phosphorylation level of PRM >4 cm (n = 53)			p value	
	Low (%), n = 28	Int. (%), n = 14	High (%), n = 6		Low (%), n = 48	Int. (%), n = 5	High (%), n = 0		
WHO classification									
WD	1 (3.6)	0 (0.0)	0 (0.0)	<i>0.001[†]</i>	1 (2.1)	0 (0.0)	0 (0.0)	0.632 [‡]	
MD	14 (50.0)	1 (7.1)	0 (0.0)		10 (20.8)	0 (0.0)	0 (0.0)		
PD	12 (42.9)	12 (85.7)	3 (50.0)		32 (66.7)	4 (80.0)	0 (0.0)		
SRC	1 (3.6)	1 (7.1)	3 (50.0)		5 (10.4)	1 (20.0)	0 (0.0)		
T stage									
T1	6 (21.4)	1 (7.1)	0 (0.0)	<i>0.002[†]</i>	7 (14.6)	0 (0.0)	0 (0.0)	0.121 [†]	
T2	10 (35.7)	2 (14.3)	0 (0.0)		12 (25.0)	0 (0.0)	0 (0.0)		
T3	8 (28.6)	7 (50.0)	2 (33.3)		18 (37.5)	3 (60.0)	0 (0.0)		
T4	4 (14.3)	4 (28.6)	4 (66.7)		11 (22.9)	2 (40.0)	0 (0.0)		
pTNM stage									
I	10 (35.7)	2 (14.3)	0 (0.0)	<i>0.023[†]</i>	10 (20.8)	0 (0.0)	0 (0.0)	0.068 [†]	
II	10 (35.7)	6 (42.9)	2 (33.3)		23 (47.9)	2 (40.0)	0 (0.0)		
III	8 (28.6)	6 (42.9)	4 (66.7)		14 (29.2)	2 (40.0)	0 (0.0)		
IV	0 (0.0)	0 (0.0)	0 (0.0)		1 (2.1)	1 (10.0)	0 (0.0)		
Recurrence									
Absent	20 (71.4)	8 (57.1)	5 (57.1)	<i>0.956[†]</i>	34 (70.8)	2 (40.0)	0 (0.0)	0.193 [†]	
Present	8 (28.6)	6 (42.9)	1 (16.7)		14 (29.2)	3 (50.0)	0 (0.0)		
Total (n = 101)									
		H3S10 phosphorylation level of DRM ≤ 4 cm (n = 62)			p value	H3S10 phosphorylation level of DRM >4 cm (n = 39)			p value
		Low (%), n = 24	Int. (%), n = 34	High (%), n = 4		Low (%), n = 33	Int. (%), n = 6	High (%), n = 0	
WHO classification									
WD	1 (4.2)	0 (0.0)	0 (0.0)	<i>0.0001[†]</i>	1 (3.0)	0 (0.0)	0 (0.0)	0.6 [‡]	
MD	10 (41.7)	1 (2.9)	0 (0.0)		13 (39.4)	1 (16.7)	0 (0.0)		
PD	12 (4.2)	29 (85.3)	1 (25.0)		17 (51.5)	4 (66.7)	0 (0.0)		
SRC	1 (4.2)	4 (11.8)	3 (75.0)		2 (6.1)	1 (16.7)	0 (0.0)		
T stage									
T1	5 (20.8)	3 (8.8)	0 (0.0)	<i>0.009</i>	6 (18.2)	0 (0.0)	0 (0.0)	0.287 [†]	
T2	6 (25.0)	8 (23.5)	1 (25.0)		8 (24.2)	2 (33.3)	0 (0.0)		
T3	9 (37.5)	13 (38.2)	3 (75.0)		14 (42.4)	2 (33.3)	0 (0.0)		
T4	4 (16.7)	10 (29.4)	0 (0.0)		5 (15.2)	2 (33.3)	0 (0.0)		
pTNM stage									
I	5 (20.8)	5 (14.7)	0 (0.0)	<i>0.361[†]</i>	12 (36.4)	0 (0.0)	0 (0.0)	0.107 [†]	
II	9 (37.5)	17 (50.0)	1 (25.0)		13 (39.4)	3 (50.0)	0 (0.0)		
III	10 (41.7)	11 (32.4)	3 (75.0)		7 (21.2)	3 (50.0)	0 (0.0)		
IV	0 (0.0)	1 (2.9)	0 (0.0)		1 (3.0)	0 (0.0)	0 (0.0)		
Recurrence									
Absent	19 (79.2)	13 (38.2)	1 (25.0)	<i>0.031[†]</i>	24 (72.7)	4 (66.7)	0 (0.0)	0.063 [†]	
Present	5 (20.8)	21 (61.8)	3 (75.0)		9 (27.3)	2 (33.3)	0 (0.0)		

All three columns are compared in each category: [†]chi-square test by two-sided linear-by-linear association; [‡]chi-square test by two-sided Fisher's exact test. Italics indicates values that are statistically significant (<0.05)

H3S10ph levels with WHO classification ($p = 0.001$), T stage ($p = 0.002$), and TNM stage ($p = 0.023$) for the patients with resection margin ≤ 4 cm. In case of DRM, chi-square analysis showed a positive correlation of H3S10ph levels with WHO classification ($p = 0.0001$) and T stage ($p = 0.009$) and recurrence ($p = 0.031$) for the patients with resection margins ≤ 4 cm. For both the resection margins, no correlation was found for patients with >4 cm resection margin distance.

In the case of OS, patients with PRM ≤ 4 cm showed a significant ($p = 0.003$) difference among the group of high, intermediate, and low levels of H3S10ph (Additional file 3: Figure S2A) and no difference was observed in the case of DRM (Additional file 2: Figure S1C). However, in the case of DFS, distance seems to have no effect as patients with both ≤ 4 or >4 cm resection showed significant difference in survival among the group of high, intermediate, and low levels of H3S10ph for both PRM ($p = 0.028$ vs 0.006) and DRM ($p = 0.041$ vs 0.005). Moreover, when the patients were grouped just based on the distance of the resection margin from the site of the tumor (≤ 4 or >4 cm), no significant difference was observed in the case of both OS and DFS (Additional file 4: Figure S3).

Taken together, these data indicate that the distance of resection margin is an important factor in GC prognosis and H3S10ph could be a potential biomarker in predicting the association between distance of resection margin and clinical parameters. However, H3S10ph cannot be used to predict the survival difference based on the distance of the resection margin for both PRM and DRM.

Association of an increase of H3S10ph with the phase of cell cycle in GC

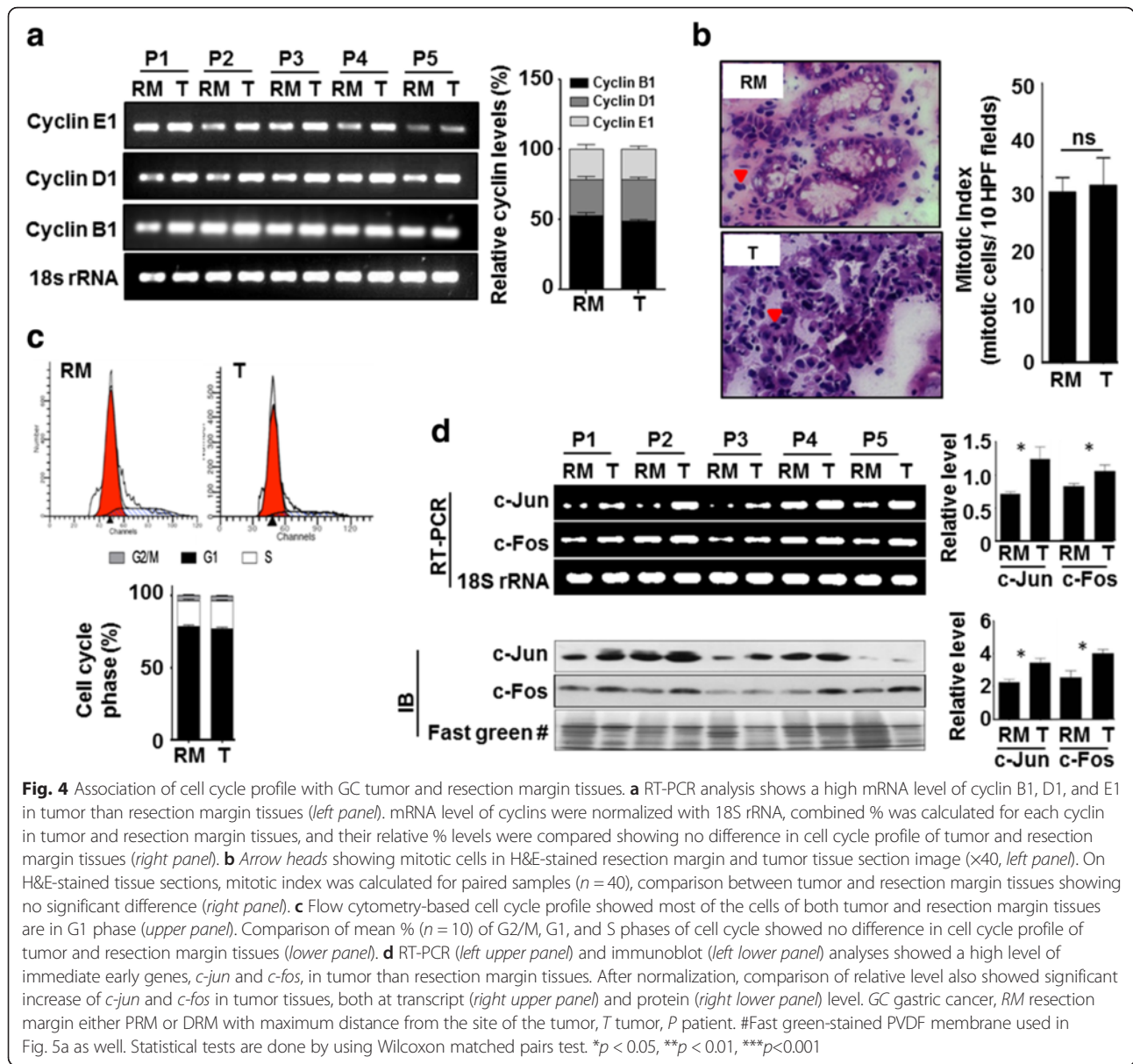
H3S10ph is a very dynamic histone mark and its level changes throughout the cell cycle with the highest level in mitotic phase and the lowest level in the interphase of the cell cycle [12, 13]. Therefore, to determine whether the increase of H3S10ph in GC is dependent on the cell cycle profile of the tissues samples, cyclin levels, mitotic index, and cell cycle profile of the tumor and resection margin tissues were studied (Fig. 4). Cyclin B1, D1, and E1 levels are known to peak at the time of G2/M phase transition, mid-S phase, and G1/S phase transition, respectively. RT-PCR analysis showed the increase in the messenger RNA (mRNA) levels of all the cyclins in tumor than the resection margin tissues; however, no changes were observed in their ratios between the tumor and resection margin tissues (Fig. 4a). The mitotic index also did not show any significant increase in mitotic cells in tumor compared to resection margin tissues (Fig. 4b). Flow cytometry-based cell cycle analysis of tissue samples showed an equal percentage of G1, S, and G2/M cells in the tumor and resection margin tissues with a

maximum population of cells in the G1 phase (Fig. 4c). These results indicate that the observed increase of H3S10ph in GC is not because of the enrichment of cells in any cell cycle phase in tumor compared to resection margin tissues.

In the mitotic phase, H3S10ph is associated with chromatin condensation and transcription silencing while in the interphase of cell cycle an increase of H3S10ph is associated with chromatin relaxation and transcription up-regulation of mainly immediate early (IE) genes [12, 13]. Cell cycle analysis revealed about 80 % cells of the tumor and resection margin tissues were in G1 phase (Fig. 4c). Therefore, to determine whether the increase in H3S10ph in GC is an interphase-associated phenomenon or not, we checked the levels of IE genes (*c-jun* and *c-fos*) using RT-PCR and immunoblotting. The data showed an increase in the levels of *c-jun* and *c-fos* in tumor compared to resection margin tissues (Fig. 4d). Therefore, taken together, these data confirm that increase in H3S10ph levels in GC is not due to the alteration in the cell cycle phase, but an interphase-associated phenomenon.

MSK1 phosphorylates H3S10 through p38-MAPK pathway in GC

Several kinases are known to phosphorylate H3S10 [12]; however, only mitogen- and stress-activated protein kinase-1 (MSK1)-mediated phosphorylation of H3S10 is known to be involved in cellular transformation [11] which is activated through p38 and/or ERK1/2 MAP kinase pathway [14]. In addition, overexpression of *c-jun* and *c-fos* as observed in our experiments (Fig. 4d) has also been linked to MSK1-mediated phosphorylation of H3S10 at their promoters [15]. Therefore, ph-MSK1, ph-p38, and ph-ERK1/2 levels in tumor and resection margin tissues of GC patients were analyzed. Immunoblot (Fig. 5a, upper panel) as well as its densitometry analysis (Fig. 5a, lower panel) showed the significant increase of ph-MSK1 ($p < 0.001$), p38 ($p < 0.01$), and ph-p38 ($p < 0.001$), while ph-ERK1/2 ($p < 0.001$) levels significantly decrease in tumor compared to resection margin tissues, thus, indicating p38-mediated activation of MSK1 in GC. The increase of ph-MSK1 levels in GC was further confirmed by IHC analysis of the same tissues (Fig. 5b). The observed increase of H3S10ph on the overexpression of MSK1 in AGS cells by immunoblot (Fig. 5c and Additional file 5: Figure S4A) and, moreover, decrease of H3S10ph- on H89-mediated biochemical inhibition of MSK1 by immunoblot studies in AGS and KATOIII cell lines (Fig. 5d and Additional file 5: Figure S4B) and immunofluorescence studies in AGS cells (Fig. 5e) confirmed MSK1-mediated phosphorylation of H3S10 in GC. Further, immunoblot analysis with specific antibodies showed a decrease of ph-MSK1 and H3S10ph only on the treatment of p38 inhibitor (SB203580) in AGS and KATOIII cells but not on the treatment of ERK1/2



inhibitor (PD89059) (Fig. 5f). And immunofluorescence studies on inhibitor-treated AGS cells validated that p38 is responsible for phosphorylation of MSK1 in GC (Fig. 5g), thus, confirming p38-MAPK/MSK1-mediated increase of H3S10ph in GC.

Discussion

In this study on human GC, comparison of several histone PTMs (data not shown) between the tumor and R0 resection margin tissues using immunoblot and IHC resulted H3S10ph with most consistent and significant difference (Fig. 1a, b and Additional file 2: Figure S1). Therefore, H3S10ph was taken for detailed study. To the best of our knowledge, several cell line- and animal model-based studies have shown increase in H3S10ph, as the only

histone mark involved in carcinogenesis and cellular transformation [11, 16–18]. However, there is no report on its relative level (tumor vs resection margin) and regulatory pathway in GC. Our IHC analysis in paired samples ($n = 101$), for the first time, demonstrated an increase of H3S10ph in gastric tumor compared to both negative resection margins, PRM and DRM (Fig. 1c–e). This observation also corroborated earlier study in nasopharyngeal carcinoma (NPC) where H3S10ph was found to be significantly higher in the poorly differentiated NPC tissues than normal nasopharynx tissues [17]. On further analysis with clinical parameters, we identified that an increase of H3S10ph in tumor tissues is a marker of poor prognosis and independent prognostic marker for OS in GC (Table 1, Additional file 1: Table S1 and Fig. 2a).

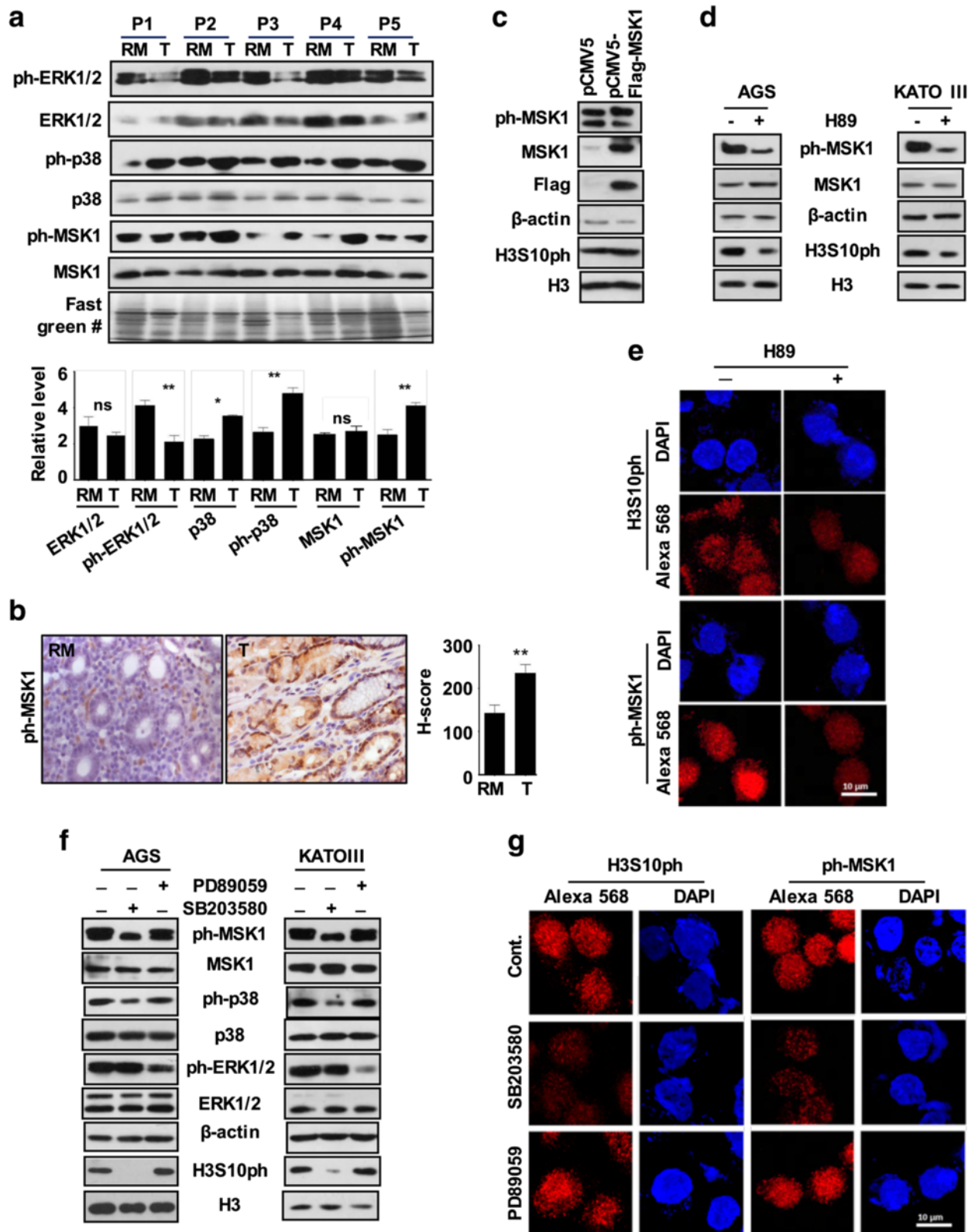


Fig. 5 (See legend on next page.)

(See figure on previous page.)

Fig. 5 Regulatory mechanism for differential levels of H3S10ph in GC. **a** Immunoblot analysis (*upper panel*) of paired tissue ($n = 5$) and densitometry-based analysis of relative levels (*lower panel*) showed a significant increase in ph-MSK1 and ph-p38 levels and decrease in ph-ERK1/2 levels in tumor compared to resection margin tissues. **b** Representative image of immunohistochemistry ($\times 40$) (*left panel*) analysis in paired tissue samples ($n = 10$) and comparison of their relative H-score (*right panel*) showed high ph-MSK1 levels in tumor than resection margin tissues. **c** Immunoblot analysis of AGS cells transiently over-expressing MSK1 showed moderate increase of ph-MSK1 and H3S10ph in corresponding lanes. **d, e** Immunoblot analysis of AGS and KATOIII cells and immunofluorescence analysis of AGS cells after 6-h treatment with MSK1 inhibitor, H89 (20 μM) showed loss of ph-MSK1 and H3S10ph. **f, g** Immunoblot analysis of AGS and KATOIII cells and immunofluorescence analysis of AGS cells showed loss of ph-MSK1 and H3S10ph only after 1-h treatment of p38 inhibitor SB203580 (10 μM), but not for ERK1/2 inhibitor PD98059 (10 μM) treatment. GC gastric cancer, RM resection margin either PRM or DRM with maximum distance from the site of the tumor, T tumor, P patient. #Fast green-stained PVDF membrane used in Fig. 4d as well. Statistical tests are done by using Wilcoxon matched pairs test. * $p < 0.05$, ** $p < 0.01$, *** $p < 0.001$

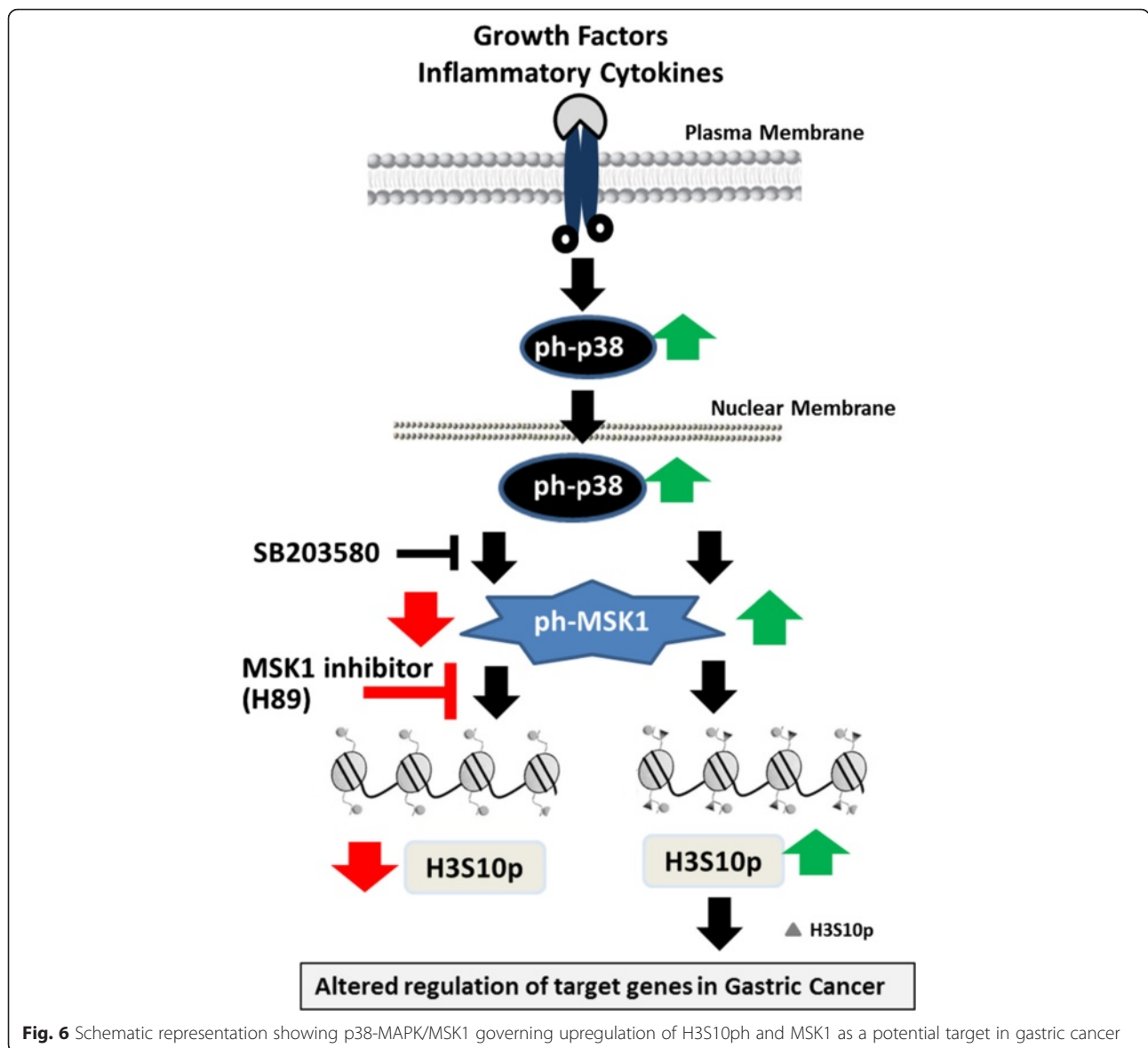
Currently, surgery is the main treatment modality for GC and achieving adequate margin length for R0 resection is a major challenge. With 9–21 % false negative results, palpation, gross inspection, and even assessment of tumor and resection margin by frozen section examination are seemingly unreliable methods to judge the adequacy of resection [19, 20]. Studies in esophageal, pancreatic, rectal, and oral cancer and soft tissue sarcoma have demonstrated that a negative resection margin does not have any prognostic value; however, a positive resection margin and its length affect recurrence and survival of patients [21–25]. The alarmingly high loco-regional recurrence rate in GC patients with R0 resection [26] points towards the fact that a defined negative resection margin is not a “true” negative resection margin. In our study, H3S10ph of both PRM and DRM showed association with clinical parameters and poorly affects OS and DFS (Table 1; Fig. 2b, c). Additionally, H3S10ph levels of DRM showed a positive correlation with recurrence where disease reverted back in 75 % patients in the high-level H3S10ph group compared to 42.5 and 24.6 % in the intermediate and low level H3S10ph groups, respectively. Thus, this study for the first time identified H3S10ph as a potential molecular marker for predicting prognosis of R0 resected GC patients using their histopathologically confirmed negative resection margins. Further, distance-dependent association of H3S10ph with clinical parameters (Table 2) could be utilized in determining the “true” negative resection margin in GC. Demarcation of 4 cm as an optimal margin length in our study rationalizes the recommendations of the National Comprehensive Cancer Network at the molecular level, which state that “the resection margin of more than 4 cm is necessary to achieve a negative microscopic margin” [27]. Therefore, H3S10ph could be helpful in limiting the extent of resection and thereby preventing post-surgery loco-regional recurrence of disease.

The distance-dependent relation of H3S10ph with clinical parameters (Table 2) strongly suggests its association with field cancerization defects. Moreover, various epigenetic factors like chromatin state, histone deacetylase, microRNA, DNA methylation, and chromatin

remodeling factors have shown their involvement in field cancerization in a number of cancers including GC [28–31]. Further, earlier *in vitro* studies have shown that a higher level of H3S10ph alone is directly involved in cellular transformation [11]. Therefore, the occurrence of such epigenetic field defects may facilitate a more permissive chromatin environment for the growth of newly transformed cells. Hence, analysis of high H3S10ph levels in resection margins could predispose the tissue for a high rate GC recurrence after R0 resection.

Most of the earlier reports have shown H3S10ph as a better marker for assessing proliferation and mitotic index than Ki-67 and have also shown increase of H3S10ph as a marker for poor prognosis in several cancers including GC [32–37]. However, except glioblastoma study, none of the cancer studies have used paired normal mucosa or negative resection margin along with tumor tissues; therefore, it is difficult to comment on whether the high proliferation and/or mitotic index or G2/M phase cells is the reason for the increased level of H3S10ph in cancer. H3S10ph is known to regulate protein-protein interactions to favor chromatin condensation as cells enter the M phase, whereas it favors expression of immediate early genes in G1 phase of cell cycle. In light of these cell cycle-specific functions, our data (Fig. 4a–c) have shown no difference in the relative level of cyclins, mitotic index, and cell cycle profile between tumor and paired negative resection margin tissues, thus strongly suggesting that an increase of H3S10ph is independent of G2/M cell cycle phase in GC. A recent report has also shown a cell cycle-independent cigarette side-stream smoke-induced increase of H3S10ph leading to the overexpression of proto-oncogenes, *c-jun* and *c-fos*, and tumor promotion [18]. Further, our study also showed the presence of maximum percentage of cells in the G1 phase of the cell cycle (Fig. 4c), and overexpression of *c-jun* and *c-fos* in tumor compared to paired negative resection margin tissues lead us to believe that the increase of H3S10ph is associated with G1 phase-specific alterations in GC.

Interestingly, global H3S10ph modification levels were lower in “true” negative resection margin tissue and increased significantly in GC. This indicates that the



action of the histone-modifying enzymes differs in the resection margin as compared to GC tissues. In our study, a G1 phase-associated increase of H3S10p and high expression of IE genes, *c-jun* and *c-fos* (Fig. 4), suggest that G1-specific kinase and MSK1 may be phosphorylating H3S10 [12]. Moreover, MSK1 is the only known kinase of H3S10 whose direct role has been implicated in cellular transformation [11, 38]. This notion was further strengthened by the observed high level of ph-MSK1 (an active form of MSK1) in GC tumor tissues (Fig. 5a, b). MSK1 is phosphorylated by MAP kinases, ERK1/2, or p38 in a context-dependent manner [14, 39]. In GC, ph-ERK1/2 has been reported to have no association with clinical parameters [40]. On the other hand, several studies in different cancer like prostate, breast, bladder, liver, lung, transformed follicular lymphoma,

and leukemia have suggested a direct role of p38 MAPK in cancer patho-physiological characteristics like proliferation, metastasis, and angiogenesis [41–47]. Further, p38 MAPK being a key regulator of inflammatory response and chronic inflammation is a characteristic of GC which manifests itself by overexpression of pro-inflammatory cytokines like IL-1 and IL-6 [48–50]. Therefore, along with above stated facts, our findings conclude that p38-MAPK/MSK1, but not ERK1/2-MAPK/MSK1, pathway is regulating the H3S10p in GC (Fig. 5).

Conclusions

In summary, to the best of our knowledge, this study provides the first evidence of a p38-MAPK/MSK1 pathway-regulated increase in H3S10p with a strong prognostic

value in survival as well as in defining the “true” resection margin in GC (Fig. 6). The central role of MSK1-mediated nucleosomal response via H3S10ph in GC might be associated with the induction of aberrant gene expression. Further, the coherence of H3S10ph in GC with two well-known reported altered histone modifications in human cancers, H4K16ac and H3K20me3, suggests that combination of epigenetic modifications may serve as molecular biomarkers for GC. Importantly, our data gave new rationales for using MSK1 as a molecular target along with other epi-drugs to alter the epigenetic landscape in GC for better patient care.

Additional files

Additional file 1: Figure S1. Densitometry analysis of immunoblot of Figure 1a. Immunoblot was done for indicated antibodies using histone isolated from tumor (T) and negative resection margin (RM) of gastric cancer patients ($n = 10$). Mean intensities of H4K20me3 and H4K16ac were normalized with mean intensity of H4; similarly H3S10ph with H3. Normalized values were represented as relative levels in the form of bar graphs. Statistical tests are done by using Wilcoxon matched pairs test. * $p < 0.05$, ** $p < 0.01$, *** $p < 0.001$. (JPG 64 kb)

Additional file 2: Table S1. Survival analysis of variables predicting the risk of death for patients with gastric cancer. (DOCX 30 kb)

Additional file 3: Figure S2. Effect of distance of resection margin-dependent H3S10ph levels on GC patients' survival. Kaplan-Meier survival analysis was done according to H3S10ph staining H-score; low (0–100), intermediate (100–200), and high (200–300). (A) and (B) Low level of H3S10ph associates with better overall survival (OS) of the patients with PRM ≤ 4 cm; however it does not affect disease-free survival (DFS). (C) and (D) Low level of H3S10ph associates with better OS and DFS, however, distance does not affect this association. GC-gastric cancer; PRM-proximal resection margin; DRM-distal resection margin; Int. - Intermediate. Comparison was done by log-rank test. $p < 0.05$ was considered as significant. (TIF 1036 kb)

Additional file 4: Figure S3. Effect of 4 cm resection margin distance on GC patients' survival. Kaplan-Meier survival analysis according to H3S10ph staining H-score: low (0–100), intermediate (100–200), and high (200–300). High level of H3S10P of tumor, PRM, and DRM is associated with both poor overall survival (OS) and disease-free survival (DFS). (A) OS and DFS based on H3S10P levels of tumor tissues (B) OS and DFS based on H3S10P levels of PRM tissues (C) OS and DFS based on H3S10P levels of DRM tissues. Int. - Intermediate. Comparison was done by log-rank test. $p < 0.05$ was considered as significant. (TIF 649 kb)

Additional file 5: Figure S4. Cell cycle analysis of AGS cells. Flow cytometry-based cell cycle profile after transfection (A) and H89 treatment (B) showed identical cell cycle profile with negligible apoptosis or cell death. (TIF 311 kb)

Acknowledgements

We acknowledge the Tumor Tissue Repository of Indian Council Medical Research for providing tissue samples and related clinical data and the senior residents of the Gastrointestinal and Hepato-Pancreato-Biliary Service, Department of Surgical Oncology, Tata Memorial Hospital, Mumbai, India, for taking patients' consent and providing their clinical information. SAK and RA thank DBT and ACTREC, respectively, for the doctorate fellowship.

Funding

The authors would like to thank Tata Memorial Hospital - Intramural Research Grant for partially funding (A/C number: 466) the project and Advanced Center for Treatment Research and Education in Cancer (ACTREC), India, for funding Gupta Laboratory.

Authors' contributions

SG, SGB, and SVS conceived the idea; SG and SAK designed the experiments in-depth; SAK, BK, and RA performed the experiments; SVS provided tissue samples and related clinical data; SAK, MR, and SG analyzed the data; SAK, SGB, and SG contributed to the figure and analysis tools; SAK and SG wrote the paper. The paper was critically read by all the authors and approved for publication.

Availability of data and supporting materials

The protocols are detailed in the manuscript for scientists wishing to use them for their research work. Also, the supporting data will be made available to editors and peer-reviewers, if required for the purposes of evaluating the manuscript.

Competing interests

Authors declare that they have no competing interests.

Ethics approval and consent to participate

The protocol was reviewed and approved by the Institutional Review Board and Ethics Committee of Tata Memorial Centre, Mumbai. The project number-466 is assigned to the approved study. All patients provided a written informed consent.

Author details

¹Epigenetics and Chromatin Biology Group, Gupta Laboratory, Cancer Research Centre, Advanced Centre for Treatment Research and Education in Cancer, Tata Memorial Centre, Kharghar, Navi Mumbai, MH 410210, India. ²Homi Bhabha National Institute, Training School Complex, Anushakti Nagar, Mumbai, MH 400085, India. ³Medanta – The Medicity, Gurgaon, Haryana 122001, India. ⁴Department of Pathology, Tata Memorial Hospital, Mumbai, MH 400012, India. ⁵Department of Surgical Oncology, Gastrointestinal and Hepato-Pancreato-Biliary Service, Tata Memorial Hospital, Mumbai, MH 400012, India.

Received: 23 May 2016 Accepted: 21 August 2016

Published online: 31 August 2016

References

- Siegel R, Naishadham D, Jemal A. Cancer statistics, 2013. *CA Cancer J Clin*. 2013;63(1):11–30.
- Dikshit RP, Mathur G, Mhatre S, Yeole BB. Epidemiological review of gastric cancer in India. *Indian J Med Paediatr Oncol*. 2011;32(1):3–11.
- Shrikhande SV, Barreto SG, Talole SD, Vinchurkar K, Annaiah S, Suradkar K, Mehta S, Goel M. D2 lymphadenectomy is not only safe but necessary in the era of neoadjuvant chemotherapy. *World J Surg Oncol*. 2013;11:31.
- Wanebo HJ, Kennedy BJ, Chmiel J, Steele Jr G, Winchester D, Osteen R. Cancer of the stomach. A patient care study by the American College of Surgeons. *Ann Surg*. 1993;218(5):583–92.
- Gunderson LL, Sosin H. Adenocarcinoma of the stomach: areas of failure in a re-operation series (second or symptomatic look) clinicopathologic correlation and implications for adjuvant therapy. *Int J Radiat Oncol Biol Phys*. 1982;8(1):1–11.
- Fullgrabe J, Kavanagh E, Joseph B. Histone onco-modifications. *Oncogene*. 2011;30(31):3391–403.
- Fraga MF, Ballestar E, Villar-Garea A, Boix-Chornet M, Espada J, Schotta G, Bonaldi T, Haydon C, Ropero S, Petrie K, et al. Loss of acetylation at Lys16 and trimethylation at Lys20 of histone H4 is a common hallmark of human cancer. *Nat Genet*. 2005;37(4):391–400.
- Park YS, Jin MY, Kim YJ, Yook JH, Kim BS, Jang SJ. The global histone modification pattern correlates with cancer recurrence and overall survival in gastric adenocarcinoma. *Ann Surg Oncol*. 2008;15(7):1968–76.
- Ushijima T. Epigenetic field for cancerization. *J Biochem Mol Biol*. 2007;40(2): 142–50.
- Staples CJ, Owens DM, Maier JV, Cato AC, Keyse SM. Cross-talk between the p38alpha and JNK MAPK pathways mediated by MAP kinase phosphatase-1 determines cellular sensitivity to UV radiation. *J Biol Chem*. 2010;285(34): 25928–40.
- Choi HS, Choi BY, Cho YY, Mizuno H, Kang BS, Bode AM, Dong Z. Phosphorylation of histone H3 at serine 10 is indispensable for neoplastic cell transformation. *Cancer Res*. 2005;65(13):5818–27.
- Prigent C, Dimitrov S. Phosphorylation of serine 10 in histone H3, what for? *J Cell Sci*. 2003;116(Pt 18):3677–85.

13. Nowak SJ, Corces VG. Phosphorylation of histone H3: a balancing act between chromosome condensation and transcriptional activation. *Trends Genet.* 2004;20(4):214–20.
14. Deak M, Clifton AD, Lucocq LM, Alessi DR. Mitogen- and stress-activated protein kinase-1 (MSK1) is directly activated by MAPK and SAPK2/p38, and may mediate activation of CREB. *EMBO J.* 1998;17(15):4426–41.
15. Drohic B, Perez-Cadahia B, Yu J, Kung SK, Davie JR. Promoter chromatin remodeling of immediate-early genes is mediated through H3 phosphorylation at either serine 28 or 10 by the MSK1 multi-protein complex. *Nucleic Acids Res.* 2010;38(10):3196–208.
16. Chadee DN, Hendzel MJ, Tylipski CP, Allis CD, Bazett-Jones DP, Wright JA, Davie JR. Increased Ser-10 phosphorylation of histone H3 in mitogen-stimulated and oncogene-transformed mouse fibroblasts. *J Biol Chem.* 1999;274(35):24914–20.
17. Li B, Huang G, Zhang X, Li R, Wang J, Dong Z, He Z. Increased phosphorylation of histone H3 at serine 10 is involved in Epstein-Barr virus latent membrane protein-1-induced carcinogenesis of nasopharyngeal carcinoma. *BMC Cancer.* 2013;13:124.
18. Ibuki Y, Toyooka T, Zhao X, Yoshida I. Cigarette sidestream smoke induces histone H3 phosphorylation via JNK and PI3K/Akt pathways, leading to the expression of proto-oncogenes. *Carcinogenesis.* 2014;35(6):1228–37.
19. Papachristou DN, Agnanti N, D'Agostino H, Fortner JG. Histologically positive esophageal margin in the surgical treatment of gastric cancer. *Am J Surg.* 1980;139(5):711–3.
20. Eker R. Carcinomas of the stomach; investigation of the lymphatic spread from gastric carcinomas after total and partial gastrectomy. *Acta Chir Scand.* 1951;101(2):112–26.
21. Pultrum BB, Honing J, Smit JK, van Dullemen HM, van Dam GM, Groen H, Hollema H, Plukker JT. A critical appraisal of circumferential resection margins in esophageal carcinoma. *Ann Surg Oncol.* 2010;17(3):812–20.
22. Reid TD, Chan DS, Roberts SA, Crosby TD, Williams GT, Lewis WG. Prognostic significance of circumferential resection margin involvement following oesophagectomy for cancer and the predictive role of endoluminal ultrasonography. *Br J Cancer.* 2012;107(12):1925–31.
23. Nagtegaal ID, Quirke P. What is the role for the circumferential margin in the modern treatment of rectal cancer? *J Clin Oncol.* 2008;26(2):303–12.
24. Novais EN, Demiralp B, Alderete J, Larson MC, Rose PS, Sim FH. Do surgical margin and local recurrence influence survival in soft tissue sarcomas? *Clin Orthop Relat Res.* 2010;468(11):3003–11.
25. Priya SR, D'Cruz AK, Pai PS. Cut margins and disease control in oral cancers. *J Cancer Res Ther.* 2012;8(1):74–9.
26. D'Angelica M, Gonen M, Brennan MF, Turnbull AD, Bains M, Karpeh MS. Patterns of initial recurrence in completely resected gastric adenocarcinoma. *Ann Surg.* 2004;240(5):808–16.
27. Ajani JA, Barthel JS, Bekaii-Saab T, Bentrem DJ, D'Amico TA, Das P, Denlinger C, Fuchs CS, Gerdes H, Hayman JA, et al. Gastric cancer. *J Natl Compr Canc Netw.* 2010;8(4):378–409.
28. Ando T, Yoshida T, Enomoto S, Asada K, Tatematsu M, Ichinose M, Sugiyama T, Ushijima T. DNA methylation of microRNA genes in gastric mucosae of gastric cancer patients: its possible involvement in the formation of epigenetic field defect. *Int J Cancer.* 2009;124(10):2367–74.
29. Stypula-Cyrus Y, Damania D, Kunte DP, Cruz MD, Subramanian H, Roy HK, Backman V. HDAC up-regulation in early colon field carcinogenesis is involved in cell tumorigenicity through regulation of chromatin structure. *PLoS One.* 2013;8(5):e64600.
30. Cherkezyan L, Stypula-Cyrus Y, Subramanian H, White C, Dela Cruz M, Wali RK, Goldberg MJ, Bianchi LK, Roy HK, Backman V. Nanoscale changes in chromatin organization represent the initial steps of tumorigenesis: a transmission electron microscopy study. *BMC Cancer.* 2014;14:189.
31. Takeshima H, Niwa T, Takahashi T, Wakabayashi M, Yamashita S, Ando T, Inagawa Y, Taniguchi H, Katai H, Sugiyama T, et al. Frequent involvement of chromatin remodeler alterations in gastric field cancerization. *Cancer Lett.* 2015;357(1):328–38.
32. Tetzlaff MT, Curry JL, Ivan D, Wang WL, Torres-Cabala CA, Bassett RL, Valencia KM, McLemore MS, Ross MI, Prieto VG. Immunodetection of phosphohistone H3 as a surrogate of mitotic figure count and clinical outcome in cutaneous melanoma. *Mod Pathol.* 2013;26(9):1153–60.
33. Ladstein RG, Bachmann IM, Straume O, Akslen LA. Prognostic importance of the mitotic marker phosphohistone H3 in cutaneous nodular melanoma. *J Invest Dermatol.* 2012;132(4):1247–52.
34. Pacaud R, Cheray M, Nadaradjane A, Vallette FM, Cartron PF. Histone H3 phosphorylation in GBM: a new rationale to guide the use of kinase inhibitors in anti-GBM therapy. *Theranostics.* 2015;5(1):12–22.
35. Takahashi H, Murai Y, Tsuneyama K, Nomoto K, Okada E, Fujita H, Takano Y. Overexpression of phosphorylated histone H3 is an indicator of poor prognosis in gastric adenocarcinoma patients. *Appl Immunohistochem Mol Morphol.* 2006;14(3):296–302.
36. Uguen A, Conq G, Doucet L, Talagas M, Costa S, De Braekeleer M, Marcorettes P. Immunostaining of phospho-histone H3 and Ki-67 improves reproducibility of recurrence risk assessment of gastrointestinal stromal tumors. *Virchows Arch.* 2015;467(1):47–54.
37. Nielsen PS, Riber-Hansen R, Jensen TO, Schmidt H, Steiniche T. Proliferation indices of phosphohistone H3 and Ki67: strong prognostic markers in a consecutive cohort with stage I/II melanoma. *Mod Pathol.* 2013;26(3):404–13.
38. Kim HG, Lee KW, Cho YY, Kang NJ, Oh SM, Bode AM, Dong Z. Mitogen- and stress-activated kinase 1-mediated histone H3 phosphorylation is crucial for cell transformation. *Cancer Res.* 2008;68(7):2538–47.
39. Soloaga A, Thomson S, Wiggin GR, Rampersaud N, Dyson MH, Hazzalin CA, Mahadevan LC, Arthur JS. MSK2 and MSK1 mediate the mitogen- and stress-induced phosphorylation of histone H3 and HMG-14. *EMBO J.* 2003;22(11):2788–97.
40. Fujimori Y, Inokuchi M, Takagi Y, Kato K, Kojima K, Sugihara K. Prognostic value of RKP and p-ERK in gastric cancer. *J Exp Clin Cancer Res.* 2012;31:30.
41. Maroni PD, Koul S, Meacham RB, Koul HK. Mitogen activated protein kinase signal transduction pathways in the prostate. *Cell Commun Signal.* 2004;2(1):5.
42. Tsai PW, Shiah SG, Lin MT, Wu CW, Kuo ML. Up-regulation of vascular endothelial growth factor C in breast cancer cells by heregulin-beta 1. A critical role of p38/nuclear factor-kappa B signaling pathway. *J Biol Chem.* 2003;278(8):5750–9.
43. Kumar B, Koul S, Petersen J, Khandrika L, Hwa JS, Meacham RB, Wilson S, Koul HK. p38 mitogen-activated protein kinase-driven MAPKAP2 regulates invasion of bladder cancer by modulation of MMP-2 and MMP-9 activity. *Cancer Res.* 2010;70(2):832–41.
44. Iyoda K, Sasaki Y, Horimoto M, Toyama T, Yakushiji T, Sakakibara M, Takehara T, Fujimoto J, Hori M, Wands JR, et al. Involvement of the p38 mitogen-activated protein kinase cascade in hepatocellular carcinoma. *Cancer.* 2003;97(12):3017–26.
45. Greenberg AK, Basu S, Hu J, Yie TA, Tchou-Wong KM, Rom WN, Lee TC. Selective p38 activation in human non-small cell lung cancer. *Am J Respir Cell Mol Biol.* 2002;26(5):558–64.
46. Elenitoba-Johnson KS, Jenson SD, Abbott RT, Palais RA, Bohling SD, Lin Z, Tripp S, Shami PJ, Wang LY, Coupland RW, et al. Involvement of multiple signaling pathways in follicular lymphoma transformation: p38-mitogen-activated protein kinase as a target for therapy. *Proc Natl Acad Sci U S A.* 2003;100(12):7259–64.
47. Liu RY, Fan C, Liu G, Olshaw NE, Zuckerman KS. Activation of p38 mitogen-activated protein kinase is required for tumor necrosis factor-alpha-supported proliferation of leukemia and lymphoma cell lines. *J Biol Chem.* 2000;275(28):21086–93.
48. Kumar S, Boehm J, Lee JC. p38 MAP kinases: key signalling molecules as therapeutic targets for inflammatory diseases. *Nat Rev Drug Discov.* 2003;2(9):717–26.
49. Fox JG, Wang TC. Inflammation, atrophy, and gastric cancer. *J Clin Invest.* 2007;117(1):60–9.
50. Kabir S, Daar GA. Serum levels of interleukin-1, interleukin-6 and tumour necrosis factor-alpha in patients with gastric carcinoma. *Cancer Lett.* 1995;95(1-2):207–12.

List of Publications arising from the thesis

Journal

- 1) **Ramchandra Vijay Amnekar**, Shafqat Ali Khan, Mudasir Rashid, Bharat Khade, Rahul Thorat, Poonam Gera, Shailesh V Shrikhande, Duane T Smoot, Hassan Ashktorab, Sanjay Gupta. Histone deacetylase inhibitor pre-treatment enhances the efficacy of DNA-interacting chemotherapeutic drugs in gastric cancer. *World J Gastroenterol* 2020 February 14; 26(6): 598-613. DOI: 10.3748/wjg.v26.i6.598
- 2) Shafqat Ali Khan, **Ramchandra Amnekar**, Bharat Khade¹, Savio George Barreto, Mukta Ramadwar, Shailesh V. Shrikhande and Sanjay Gupta. p38-MAPK/MSK1 mediated overexpression of histone H3 serine 10 phosphorylation defines distance-dependent prognostic value of negative resection margin in gastric cancer. *Clinical Epigenetics* (2016) 8:88 . DOI 10.1186/s13148-016-0255-9

Chapters in books and lectures notes

1. Asmita Sharda, **Ramchandra Vijay Amnekar**, Abhiram Natu, Sukanya, Sanjay Gupta. Histone posttranslational modifications: Potential role in diagnosis, prognosis, and therapeutics of cancer. *Prognostic Epigenetics. Vol.15, Translational Epigenetics. Academic Press, London:351-373, 2019.*

Conferences

1. 16th Asian Forum of Chromosome and Chromatin Biology, CCMB Hyderabad, 2017. Poster presented entitled “Phosphoacetylation of histones in gastric cancer and their clinical relevance”.
2. 4th Annual Conference of Environmental Mutagen Society of India, BARC, Mumbai, 2018. Poster presented entitled “Epigenetic alterations during cellular transformation of gastric epithelial cells “.
3. “Chromatin Dynamics and Nuclear Organization in Genome Maintenance”, EMBO Workshop, Illkirch, France in 2018. Poster presented entitled “Chromatin Dynamics at the interface of cellular transformation”*

4. 17th Asian Forum of Chromatin and Chromosome Biology, JNCASR Bangalore, 2018. Poster presented entitled “Chromatin Dynamics at the interface of cellular transformation”.

Others

1. **Ramchandra V Amnekar** and Sanjay Gupta. HDAC Inhibitors in Solid Tumors: An Incomplete Story. Journal of Clinical Epigenetics (2018) 4; 2:8. DOI: 10.21767/2472-1158.100093



Mr. Ramchandra V Amnekar

Thesis Highlight

Name : Mr Ramchandra Amnekar

Name of the CI/OCC: TMC-ACTREC

Enrollment Number: LIFE09201304005

Thesis Title: Phosphoacetylation of histones during cellular transformation in mammalian cells

Discipline: Life Sciences **Sub-area of Discipline:** Epigenetics and Chromatin Biology

Date of Viva-voce: 4th February, 2021

The present study highlights the significant role played by histone modifications and their dysregulation through chromatin modifiers during cellular transformation which could be explored for therapeutic intervention in combination with chemotherapy drugs. A specific context-dependent crosstalk between histone H3S10 phosphorylation and H3K14 acetylation, regulated by an intricate balance between MSK1, HDAC and HATs, was observed upon cellular transformation. MSK-mediated HDAC1 expression alongwith PCAF downregulation led to hypoacetylation of histones. This together with increased phosphoacetylation constitutes a code that at least in part determines epigenetic landscape of transformed cells. Another interesting and novel finding was the inverse association between H3 phosphorylation and acetylation in mitosis that was partly regulated by MSK and was essential for immaculate completion of cell division. Further perturbation of the histone acetylation status by pre-treatment of histone deacetylase inhibitor was found to enhance the efficacy of DNA interacting chemotherapeutic drugs in gastric cancer. Overall, the work emphasizes the therapeutic utility of epigenetic alterations that could be translated into useful therapeutic potential for better management of gastric cancer.